

Some pages of this thesis may have been removed for copyright restrictions.

If you have discovered material in Aston Research Explorer which is unlawful e.g. breaches copyright, (either yours or that of a third party) or any other law, including but not limited to those relating to patent, trademark, confidentiality, data protection, obscenity, defamation, libel, then please read our [Takedown policy](#) and contact the service immediately (openaccess@aston.ac.uk)

**Surface Pressure Measurements
of Ex-vivo Tear Lipids**

Application of the Langmuir Technique in Lipid-Aqueous Interfacial Studies

Marc Philip Broadbent
Doctor of Philosophy

Aston University
November 2013

©Marc Philip Broadbent, 2013

Marc Philip Broadbent asserts his moral right to be identified as the author of this thesis.

This copy of the thesis has been supplied on condition that anyone who consults it is understood to recognise that its copyright rests with its author and that no quotation from the thesis and no information derived from it may be published without proper acknowledgement.

Aston University

Surface Pressure Measurements of Ex-Vivo Tear Lipids

Application of the Langmuir Technique in Lipid-Aqueous Interfacial Studies

Marc Philip Broadbent

Submitted for the Degree
of Doctor of Philosophy

November 2013

Summary

This thesis extends previous work utilising the Langmuir trough technique to study tear film lipids towards a new and important area - the effect of contact lens wear on the nature and fate of the lipid layer in the lens-wearing eye. The lipid layer plays a vital part in maintaining tear film stability and the contact lens has a marked influence on the ocular environment. Surface behaviour studies are of particular importance in understanding the physicochemical factors that affect comfort and the occurrence of adverse responses accompanied by the use of this biomaterial device.

The measured surface activity (i.e. surface pressure) of individual tear lipids has highlighted the importance of lipid polarity and fatty acid content on the compression and spreading behaviour of the molecule. From this basis, understanding of the behaviour of the whole lipid layer during a blink can be inferred from subsequent studies of ex-vivo tear samples obtained from tear films of individual lens wearers.

A particular point of interest in this work is the use of the lens as a probe or carrier to remove lipid from the eye. Differences in key π -A isotherm data were observed due to changes in the collected lipids as a function of lens material and wear modality. It was observed that greater quantities of lipid are deposited as lens hydrophobicity increases. Lipid samples obtained from daily wear and daily disposable lenses showed increased π_{\max} at lower surface concentrations than lipid samples obtained from continuous wear lenses.

The potential value of using phospholipids as a supplementary compound in order to increase the surface pressure and stability of native lipid layer. This was examined using a commercial contact lens modified to include an extractable phospholipid.

This thesis has examined the use of the Langmuir trough technique to evaluate a variety of factors involved in contact lens wear such as wear schedule, cleaning regimes, lens material and potential phospholipid delivery techniques. These all have potential effects on the surface behaviour and stability of the tear film lipid layer in the lens-wearing eye.

Keywords: tear lipids, tear film, Langmuir trough, Brewster angle, surface pressure.

To my family.

Acknowledgements

Without this sounding too much like a soppy Oscar acceptance speech, there are many people that I would like to thank profusely for their part, however large or small, over the course of this thesis and its research.

First and foremost, I would like to thank my supervisor, Professor Brian Tighe, for all of his aid, his suggestions and his patience throughout the course of writing this thesis.

I would also like to thank all of the members of the Biomaterials Research Unit, past or present. I have made some great friends in this research group and I am eternally thankful to them for being a source of information (for the work side) and entertainment (for the social side). So huge thanks to Russ, Manpreet, Aman, Tom, Tarnveer, Ais, Darren, Anisa, Fiona, Val, Gareth, Jane, Dan and especially to Sarah and Nilla, who were there at the start and the end.

I'd also like to thank my family, who have been supportive throughout my life and my choice of career, and my friends, who have understood when I have gone AWOL for birthdays and other gatherings.

Last, but by certainly no means least, my heartfelt thanks to my partner Carrie, without whom I may have long gone insane writing this thesis. She has been a constant source of calm and understanding whenever I have been stressed, supplying many cups of tea along the way. I don't think I would have got this far without her support.

List of Contents

Contents	Page
Title Page	1
Summary	2
Dedication	3
Acknowledgments	4
List of Contents	5
List of Figures	10
List of Tables	16
List of Symbols and Abbreviations	18
1. Introduction	21
1.1. The Tear Film	21
1.1.1. Structure of the Tear Film	22
1.1.2. Role of the Tear Film	23
1.2. The Lipid-Aqueous Interface	23
1.2.1. The Lipid Layer	23
1.2.1.1. The Role of Lipid Layer	24
1.2.1.2. Tear Film Lipid Layer Composition	26
1.2.1.3. Structure of the Lipid Layer	34
1.2.2. The Aqueous Layer	35
1.2.2.1. Tear Proteins	35
1.2.2.2. Surfactant Proteins	36
1.2.2.3. Metabolites	37
1.2.2.4. Electrolytes	37
1.2.2.5. Mucin	38
1.3. Surface Chemistry	39
1.3.1. Defining The Interfacial Region	39
1.3.2. Surface and Interfacial Tension	40
1.3.3. Adsorption	42
1.3.4. Wetting and Spreading	43
1.4. Interfaces in Biological Systems	44
1.5. Stability of the Lipid-Aqueous Interface	45
1.5.1. Tear Film Stability as a Function of Surface Tension	45
1.5.2. Physicochemical Structure of the Lipid Layer	46
1.5.3. Lipid Layer Spreading	46
1.5.4. The Role of Protein and Aqueous Layer Components	47
1.6. Degradation of Tear Film Stability	48
1.6.1. Ocular Diseases	48
1.6.2. Degradation of Tear Lipids - Oxidation and Hydrolysis	49
1.6.2.1. Hydrolysis	49
1.6.2.2. Oxidation	50

Contents	Page
1.6.3. Contact Lens Wear	53
1.6.3.1. Development of Contact Lenses	53
1.6.3.2. Biocompatibility	54
1.6.3.3. Lipid Degradation during Contact Lens Wear	55
1.6.3.4. Tear Breakup and Contact Lens-related Dry Eye Disease	56
1.7. Langmuir Trough Method	57
1.7.1. Measurement of Surface Pressure	58
1.7.2. Surface Pressure-Area Isotherms	59
1.8. Scope of Research	61
1.9. Aims of Research	62
2. Methodology	63
2.1. Langmuir Trough	63
2.1.1. Instrumentation	63
2.1.2. Materials	64
2.1.2.1. Solvents	64
2.1.2.2. Subphase Solutions	64
2.1.3. Surface Pressure-Area (π -A) Isotherm	65
2.1.3.1. Reversibility	66
2.1.4. Surface Pressure-Time (π -t) Isotherms	69
2.2. Brewster Angle Microscopy	70
2.2.1. Principles	70
2.2.2. Instrumentation	71
2.2.3. Imaging Procedure	72
3. Preliminary Study: Understanding the Surface Chemistry of Individual Tear Film Components	73
3.1. Condition Testing	73
3.1.1. Objective	73
3.1.2. Experimental design	73
3.1.3. Results	74
3.1.3.1. Subphase Composition	75
3.1.3.2. Temperature	78
3.1.3.3. Surface Concentration	79
3.2. Lipid Components	81
3.2.1. Objective	81
3.2.2. Experimental Design	81
3.2.3. Results	82
3.2.3.1. Fatty Acids	82
3.2.3.2. Fatty Alcohols	87
3.2.3.3. Cholesterol Esters	88
3.2.3.4. Wax Esters	90
3.2.3.5. Phospholipids	91

Contents	Page
3.2.3.6. Acylglycerides	94
3.3. Protein and Mucin Components	95
3.3.1. Objective	95
3.3.2. Experimental design	96
3.3.2.1. π -A Isotherms	96
3.3.2.2. Adsorption of Tear Protein and Mucin Analogues to Interface	96
3.3.3. Results	97
3.3.3.1. π -A Isotherms	97
3.3.3.2. π -t Adsorption Isotherms	98
3.4. Discussion	102
3.4.1. Lipid Structure and Interaction	102
3.4.2. Interactions with Proteins and Mucins	103
3.4.3. Experimental Considerations	104
3.5. Summary	105
4. In-vitro Study of Tear Film Samples: Preliminary Evaluation of Collection Methodology	106
4.1. Objectives	106
4.2. Experimental Design	106
4.2.1. Microcapillary Tube Collection	107
4.2.2. Schirmer Strip Collection	108
4.2.3. Sponge Collection	109
4.2.4. Contact Lenses	109
4.3. Results	110
4.3.1. Microcapillary Tubes	110
4.3.2. Schirmer Strip Collection	112
4.3.2.1. Inter- and Intra-subject Variability	112
4.3.2.2. Extraction Solvent: Hexane vs. Chloroform	119
4.3.2.3. Trough B π -A Isotherm Study	123
4.3.3. Visispear™ Ophthalmic Sponges	123
4.3.3.1. Trough A π -A Isotherms	123
4.3.3.2. Extraction Solvent: Hexane vs. Chloroform	127
4.3.3.3. Trough B π -A Isotherms	130
4.3.3.4. Brewster Angle Microscopy	133
4.3.4. Contact Lens Extraction	136
4.3.4.1. Inter- and Intra-subject Variability	136
4.3.4.2. Comparison of Extraction Solvents	138
4.3.4.3. Trough B π -A Isotherms	143
4.3.4.4. Brewster Angle Microscopy	146
4.4. Discussion	147
4.5. Summary	151

Contents	Page
5. In-vitro Study of Tear Film Samples: Fate of Lipids on Extended Wear Silicone Hydrogel Contact Lenses	152
5.1. Objectives	152
5.2. Experimental Design	152
5.3. Results	154
5.3.1. Focus Night+Day Contact Lenses	154
5.3.1.1. Chloroform : Methanol (1:1 w/w) Extraction	154
5.3.1.2. Hexane Extraction	158
5.3.1.3. Hexane : Methanol (9:1 w/w) Extraction	162
5.3.2. PureVision Contact Lenses	166
5.3.2.1. Chloroform : Methanol (1:1 w/w) Extraction	166
5.3.2.2. Hexane Extraction	170
5.3.2.3. Hexane : Methanol (9:1 w/w) Extraction	174
5.4. Discussion	178
5.5. Summary	184
6. Effect of Daily Disposable Contact Lens Wear on the Tear Film Lipid Layer	185
6.1. Comparison of Daily Disposable SiHy Contact Lenses	185
6.1.1. Objectives	185
6.1.2. Experimental Design	185
6.1.3. Results	187
6.1.3.1. Clariti 1day Contact Lenses	187
6.1.3.2. 1-Day Acuvue TruEye Contact Lenses	201
6.2. Focus Dailies Total-1 Contact Lenses	217
6.2.1. Objective	217
6.2.2. Experimental Design	217
6.2.2.1. Pre-production Lenses	217
6.2.2.2. Clinical Samples	218
6.2.2.3. Tear Samples from Lens-wearing Eye	218
6.2.2.4. π -A Isotherm Measurement	218
6.2.3. Results	219
6.3.3.1. Pre-production Lenses	219
6.3.3.2. Clinical Lens Trials	222
6.3. Discussion	227
6.3.1. Effect of Daily Disposable SiHy Lens Wear on the Tear Film	227
6.3.2. Hildebrand Solubility Parameters	228
6.3.3. DMPC Release from Focus Dailies Total-1 Lenses	231
6.4. Summary	232

Contents	Page
7. Summary, Conclusions and Suggestions for Future Work	234
7.1. Summary and Conclusions	234
7.1.1. Tear Film Lipid Component Behaviour	234
7.1.2. Tear Film Protein Component Behaviour	235
7.1.3. Tear Sampling Methodology	236
7.1.4. The Fate of Lipids on Contact Lenses	238
7.1.5. Tear Film Supplementation	240
7.2. Suggestions for Future Work	241
References	245
Appendices	263

List of Figures

Figure	Title	Page
Fig 1.1	Structure of the tear film: (a) Traditional three-layer representation; (b) six-layer representation of the tear film	22
Fig 1.2	General structures of saturated, unsaturated and branched fatty acids.	27
Fig 1.3	General structures of fatty alcohols showing straight chain, iso- and anteiso-isomeric forms	28
Fig 1.4	Structure of a cholesterol molecule	28
Fig 1.5	General structure of a wax ester and examples of TFL WE species.	29
Fig 1.6	General structure of a cholesterol ester (cholesterol 9-octadecenoate (Ch-18:1 ^{Δ9}))	29
Fig 1.7	General structure of a phospholipid molecule with examples of common alcohol functional groups.	30
Fig 1.8	General structure of sphingolipids (R = H - ceramide; PC/PE - sphingomyelin; sugar - glycosphingolipids)	31
Fig 1.9	General structure of OAHFA (R ₁ , R ₂ and R ₃ represent saturated hydrocarbon chains of varying lengths).	32
Fig 1.10	Formation of monoacylglyceride (MAG), diacylglyceride (DAG) and triacylglyceride (TAG) from glycerol and fatty acids.	33
Fig 1.11	Biphasic representation of the lipid layer	34
Fig 1.12	Example interfacial system	39
Fig 1.13	Attractive forces between water molecules within the bulk and at the surface	40
Fig 1.14	Attractive forces between molecules at the interface between two immiscible liquids	42
Fig 1.15	The triple interface between gas, liquid and solid phases	43
Fig 1.16	Behaviour of oil molecules on the surface of water: (a) lens formation; (b) surface spreading.	44
Fig 1.17	Hydrolysis of non-polar lipids: (a) wax esters and cholesterol esters (R = FAlc / Ch); (b) triacylglycerides (R = FA)	49
Fig 1.18	Enzymatic hydrolysis by phospholipases on phospholipid molecules	50
Fig 1.19	Oxidation of unsaturated fatty acids.	52
Fig 1.20	Formation of malondialdehyde (MDA) from oxidation of a polyunsaturated fatty acid (PUFA).	52
Fig 1.21	Position of contact lens in the tear film	55
Fig 1.22	Schematic of the Langmuir trough apparatus	57
Fig 1.23	Wilhelmy plate diagram	58
Fig 1.24	Example π -A isotherm for a fatty acid with diagrammatic representation of the behaviour of lipid molecules during compression.	60
Fig 1.25	Collapse of a surfactant monolayer as surface area is decreased	61

Figure	Title	Page
Fig 2.1	Example π -A isotherms for stearic acid (a) and a tear sample (b) showing the key characteristics recorded for the isocycle.	65
Fig 2.2	Calculating the area between two adjacent data points	66
Fig 2.3	Sample π -A isocycle showing the compression isotherm (blue) and expansion isotherm (red).	68
Fig 2.4	Experimental procedure for obtaining surface pressure-time adsorption isotherms	69
Fig 2.5	Example surface pressure-time (π -t) isotherm	70
Fig 2.6	The Brewster angle and the changes in reflection from a clean surface to one with an adsorbed monolayer at various stages of compression.	71
Fig 2.7	MicroBAM2 Instrument: (a) MicroBAM2 instrument schematic; (b) position of the reflective glass plate underneath the BAM laser and analyser housing.	72
Fig 3.1	π -A isotherms of clean subphases of HPLC-grade water, PBS and ATE without the presence of contamination.	75
Fig 3.2	Determination of π_c of SA (1.0×10^{-3} moldm $^{-3}$; 25 μ l aliquot)	76
Fig 3.3	π -A isotherms (a) of SA on different subphases (1.0×10^{-3} moldm $^{-3}$; 25 μ l aliquot; 25°C). (b) surface pressure versus volume aliquot	76
Fig 3.4	Collapse pressure (π_c) and post collapse minimum surface pressure (π_{min}) of SA on different subphases (1.0×10^{-3} moldm $^{-3}$; 25 μ l aliquot; 25°C).	77
Fig 3.5	π -A isotherms (a) of SA at different subphase temperatures (1.0×10^{-3} moldm $^{-3}$; 25 μ l). (b) surface pressure versus volume aliquot	78
Fig 3.6	π -A isotherms of increasing concentrations of SA at different aliquot volumes	80
Fig 3.7	Relationship between the number of SA molecules applied to the subphase surface against maximum surface pressure	80
Fig 3.8	π -A isotherms of saturated fatty acids (1.0×10^{-3} moldm $^{-3}$; 25 μ l aliquot; 25°C).	83
Fig 3.9	π -A isotherms (a) of saturated fatty acids (1.0×10^{-3} moldm $^{-3}$; 25 μ l aliquot) compressed to π_c . (b) π_c against number of carbon atoms in acyl chain	84
Fig 3.10	π -A isotherms of unsaturated fatty acids (1.0×10^{-3} moldm $^{-3}$; 25 μ l aliquot).	86
Fig 3.11	π -A isotherms (a) of C18-unsaturated fatty acids (1.0×10^{-3} moldm $^{-3}$; 25 μ l aliquot); (b) π_{max} against degree of unsaturation.	86
Fig 3.12	π -A isotherms of fatty alcohols (1.0×10^{-3} moldm $^{-3}$; 25 μ l aliquot)	87
Fig 3.13	Comparison of π -A isotherms of FAlc and FA molecules (1.0×10^{-3} moldm $^{-3}$; 25 μ l aliquot): (a) C18 (1-octadecanol vs. SA); (b) C20 (1-eicosanol vs. AA)	87
Fig 3.14	π -A isotherms of cholesterol and cholesterol-based esters	89
Fig 3.15	π -A isotherms of wax esters (1.0×10^{-3} moldm $^{-3}$; 25 μ l aliquot).	91
Fig 3.16	π -A isotherms of choline-based phospholipids (1.0×10^{-3} moldm $^{-3}$; 25 μ l aliquot).	93
Fig 3.17	π -A isotherms of phospholipids (1.0×10^{-3} moldm $^{-3}$; 25 μ l aliquot) compressed past the limited π_{max} .	93

Figure	Title	Page
Fig 3.18	π -A isotherms of glyceride mixtures ($1.0 \times 10^{-3} \text{ moldm}^{-3}$; 25 μl aliquot).	95
Fig 3.19	π -A isotherms of a 100 μl aliquot of tear protein and mucin analogues.	98
Fig 3.20	π -t adsorption isotherm of β -2 microglobulin (lipocalin analogue; Lc), lysozyme (Lz) and bovine serum mucin (BSM) to an ATLF monolayer.	100
Fig 3.21	π -A isotherms of an ATLF monolayer before and after adsorption of tear protein and mucin analogues	101
Fig 4.1	π -A isotherms of glass capillary extracted samples on Trough A for Px1, Px2 and Px3 tear samples and control sample (900 μl aliquot).	111
Fig 4.2	π -A isotherms of glass capillary extracted samples on Trough B for Px4 tear sample and control sample (950 μl aliquot).	111
Fig 4.3	π -A isotherms of extracted left eye (LE; Column A) and right eye (RE; Column B) tear samples from subject Px1	114
Fig 4.4	π -A isotherms of extracted left eye (LE; Column A) and right eye (RE; Column B) tear samples from subject Px2.	115
Fig 4.5	π -A isotherms of extracted left eye (LE; Column A) and right eye (RE; Column B) tear samples from subject Px3.	116
Fig 4.6	π -A isotherms of a Schirmer strip adsorbed with saline (wetted length = 30mm) extracted in 0.5ml chloroform.	117
Fig 4.7	π_{max} as a function of volume of extracted samples from Px1, Px2 and Px3 based on the percentage (%) of extracting solution.	118
Fig 4.8	π -A isotherms of chloroform and hexane extracted tear samples from subject Px4.	120
Fig 4.9	π -A isotherms of hexane extracted control samples.	121
Fig 4.10	π_{max} as a function of volume of extracted samples from Px4. Left eye (LE; WL = 18mm) sample extracted in chloroform. Right eye (RE; WL = 18mm) sample extracted in hexane (percentage (%) of extracting solution).	122
Fig 4.11	π -A isotherms of tear sample from subject Px5 on Trough B	123
Fig 4.12	π -A isotherms of control samples obtained from collection and extraction of a Visispear™ ophthalmic sponge soaked in saline on Trough A.	124
Fig 4.13	π -A isotherms of tear samples obtained from collection and extraction of a Visispear™ ophthalmic sponge on Trough A: Row 1 - Px1; Row 2 - Px2; Row 3 - Px3.	125
Fig 4.14	Comparative π -A isotherms of three separate studies of the Px1 tear sample obtained from collection and extraction of Visispear™ ophthalmic sponges on Trough A.	126
Fig 4.15	Volume aliquot vs. maximum surface pressure	127
Fig 4.16	π -A isotherms of tear sample Px4 obtained from a Visispear™ ophthalmic sponge extracted in hexane	129
Fig 4.17	π -A isotherms of control sample obtained from a Visispear™ ophthalmic sponge soaked in saline and extracted in hexane.	129
Fig 4.18	Comparison between chloroform and hexane extracted control and subject samples collected using Visispear™ ophthalmic sponges	130

Figure	Title	Page
Fig 4.19	π -A isotherms of tear sample obtained from a Visispear™ ophthalmic sponge: Row 1 - Px5; Row 2 - Px6; Row 3 - Px7.	132
Fig 4.20	π -A isotherms of control samples obtained from collection a Visispear™ ophthalmic sponge soaked in saline.	133
Fig 4.21	BAM images taken during the π -A compression isotherm of the 500 μ l aliquot of tear sample: Px5 (column A), Px6 (column B) and Px7 (column C).	134-135
Fig 4.22	Intra-subject reproducibility of π -A isotherms from a single CL sample.	137
Fig 4.23	Inter-subject reproducibility of π -A isotherms from three CL samples.	137
Fig 4.24	Comparison of π -A isotherms (Trough A) of tear samples obtained from worn FN+D contact lenses extracted using different solvents: CHCl ₃ :CH ₃ OH (1:1 w/w; row 1); C ₆ H ₁₄ (row 2); C ₆ H ₁₄ :CH ₃ OH (9:1 w/w; row 3).	139
Fig 4.25	Comparison of π -A isotherms (Trough A) of samples obtained from unworn FN+D contact lenses extracted using different solvents: CHCl ₃ :CH ₃ OH (1:1 w/w; row 1); C ₆ H ₁₄ (row 2); C ₆ H ₁₄ :CH ₃ OH (9:1 w/w; row 3).	140
Fig 4.26	Comparison between the three solvents used to extract sample from worn and unworn FN+D contact lenses.	141
Fig 4.27	Comparison of π -A isotherms (Trough B) of tear samples obtained from worn FN+D contact lenses extracted using different solvents: CHCl ₃ :CH ₃ OH (1:1 w/w; row 1); C ₆ H ₁₄ (row 2); C ₆ H ₁₄ :CH ₃ OH (9:1 w/w; row 3).	143
Fig 4.28	Comparison of π -A isotherms (Trough B) of samples obtained from unworn FN+D contact lenses extracted using different solvents: CHCl ₃ :CH ₃ OH (1:1 w/w; row 1); C ₆ H ₁₄ (row 2); C ₆ H ₁₄ :CH ₃ OH (9:1 w/w; row 3).	144
Fig 4.29	Comparison of π_{\max} as a function of the volume of sample from worn and unworn FN+D Contact lenses by three different solvents.	145
Fig 4.30	BAM images taken during the π -A compression isotherm of the sample obtained from extraction of a worn FN+D contact lens (CHCl ₃ :CH ₃ OH (1:1 w/w) extraction; 1000 μ l aliquot).	146
Fig 5.1	Subject sample size based on lens type, wear modality and extraction protocol	154
Fig 5.2	π -A isotherms of control FN+D contact lens extracted in CHCl ₃ :CH ₃ OH (1:1 w/w)	155
Fig 5.3	π -A isotherms of FN+D contact lens worn under a CW modality extracted in CHCl ₃ :CH ₃ OH (1:1 w/w): Row 1 - Px02; Row 2 - Px11; Row 3 - Px16	156
Fig 5.4	π -A isotherms of FN+D contact lens worn under a DW modality extracted in CHCl ₃ :CH ₃ OH (1:1 w/w): Row 1 - Px05; Row 2 - Px13; Row 3 - Px25	157
Fig 5.5	Comparison of π_{\max} as a function of wear modality of samples obtained from worn and unworn FN+D contact lenses extracted in CHCl ₃ :CH ₃ OH (1:1 w/w).	158
Fig 5.6	π -A isotherms of control FN+D contact lens extracted in C ₆ H ₁₄	159
Fig 5.7	π -A isotherms of FN+D contact lens worn under a CW modality extracted in C ₆ H ₁₄ : Row 1 - Px16; Row 2 - Px38; Row 3 - Px71.	160

Figure	Title	Page
Fig 5.8	π -A isotherms of FN+D contact lens worn under a DW modality extracted in C_6H_{14} : Row 1 - Px13; Row 2 - Px25; Row 3 - Px62.	161
Fig 5.9	Comparison of π_{max} as a function of wear modality of samples obtained from worn and unworn FN+D Contact lenses extracted in C_6H_{14} .	162
Fig 5.10	π -A isotherms of control FN+D contact lens extracted in $C_6H_{14}:CH_3OH$ (9:1 w/w). π -A isotherms for 100-400 μ l aliquots not shown.	163
Fig 5.11	π -A isotherms of FN+D contact lens worn under a CW modality extracted in $C_6H_{14}:CH_3OH$ (9:1 w/w): Row 1 - Px11; Row 2 - Px12; Row 3 - Px26.	164
Fig 5.12	π -A isotherms of FN+D contact lens worn under a DW modality extracted in $C_6H_{14}:CH_3OH$ (9:1 w/w): Row 1 - Px5; Row 2 - Px22; Row 3 - Px25.	165
Fig 5.13	Comparison of π_{max} as a function of wear modality of samples obtained from worn and unworn FN+D Contact lenses extracted in $C_6H_{14}:CH_3OH$ (9:1 w/w).	166
Fig 5.14	π -A isotherms of control PV contact lenses extracted in $CHCl_3:CH_3OH$ (1:1 w/w).	167
Fig 5.15	π -A isotherms of PV contact lens worn under a CW modality extracted in $CHCl_3:CH_3OH$ (1:1 w/w): Row 1 - Px29; Row 2 - Px41; Row 3 - Px56.	168
Fig 5.16	π -A isotherms of PV contact lens worn under a DW modality extracted in $CHCl_3:CH_3OH$ (1:1 w/w): Row 1 - Px17; Row 2 - Px53; Row 3 - Px61.	169
Fig 5.17	Comparison of π_{max} as a function of wear modality of samples obtained from worn and unworn PV Contact lenses extracted in $CHCl_3:CH_3OH$ (1:1 w/w).	170
Fig 5.18	π -A isotherms of control PV contact lenses extracted in C_6H_{14} .	171
Fig 5.19	π -A isotherms of PV contact lens worn under a CW modality extracted in C_6H_{14} : Row 1 - Px30; Row 2 - Px31; Row 3 - Px56	172
Fig 5.20	π -A isotherms of PV contact lens worn under a DW modality extracted in C_6H_{14} : Row 1 - Px24; Row 2 - Px51; Row 3 - Px53	173
Fig 5.21	Comparison of π_{max} as a function of wear modality of samples obtained from worn and unworn PV Contact lenses extracted in C_6H_{14} .	174
Fig 5.22	π -A isotherms of control PV contact lenses extracted in $C_6H_{14}:CH_3OH$ (9:1 w/w)	175
Fig 5.23	π -A isotherms of PV contact lens worn under a CW modality extracted in $C_6H_{14}:CH_3OH$ (9:1 w/w) solvent: Row 1 - Px41; Row 2 - Px46; Row 3 - Px49.	176
Fig 5.24	π -A isotherms of PV contact lens worn under a DW modality extracted in $C_6H_{14}:CH_3OH$ (9:1 w/w) solvent: Row 1 - Px24; Row 2 - Px50; Row 3 - Px61.	177
Fig 5.25	Comparison of π_{max} as a function of wear modality of samples obtained from worn and unworn PV Contact lenses extracted in $C_6H_{14}:CH_3OH$ (9:1 w/w)	178
Fig 5.26	Comparison of the average maximum surface pressure at each 100 μ l aliquot: (a) $CHCl_3:CH_3OH$ (1:1 w/w); (b) C_6H_{14} ; (c) $C_6H_{14}:CH_3OH$ (9:1 w/w)	182
Fig 5.27	Comparison of the average initial surface pressure at each 100 μ l aliquot: (a) $CHCl_3:CH_3OH$ (1:1 w/w); (b) C_6H_{14} ; (c) $C_6H_{14}:CH_3OH$ (9:1 w/w)	183

Figure	Title	Page
Fig 6.1	Subject sample size based on lens type and extraction protocol	186
Fig 6.2	π -A isotherms of control Clariti 1day contact lens. Row 1 - C_6H_{14} ; Row 2 - $C_6H_{14}:CH_3OH$ (9:1 w/w); Row 3 - $CHCl_3:CH_3OH$ (1:1 w/w)	188
Fig 6.3	π -A isotherms of worn Clariti 1day contact lens extracted in C_6H_{14} .	190-191
Fig 6.4	π -A isotherms of worn Clariti 1day contact lens extracted in $C_6H_{14}:CH_3OH$ (9:1 w/w)	193-194
Fig 6.5	π -A isotherms of worn Clariti 1day contact lens extracted in $CHCl_3:CH_3OH$ (9:1 w/w)	196-197
Fig 6.6	Comparison of π_{max} of samples obtained from worn and unworn Clariti 1day contact lenses at the 1000 μ l aliquot: (a) C_6H_{14} ; (b) $C_3H_{14}:CH_3OH$ (9:1 w/w); (c) $CHCl_3:CH_3OH$ (1:1 w/w).	200
Fig 6.7	π -A isotherms of control TE contact lens samples Row 1 - C_6H_{14} ; Row 2 - $C_6H_{14}:CH_3OH$ (9:1 w/w); Row 3 - $CHCl_3:CH_3OH$ (1:1 w/w)	202
Fig 6.8	π -A isotherms of worn TE contact lens extracted in C_6H_{14}	204-205
Fig 6.9	π -A isotherms of worn TE contact lens extracted in $C_6H_{14}:CH_3OH$ (9:1 w/w)	207-208
Fig 6.10	π -A isotherms of worn TE contact lens extracted in $CHCl_3:CH_3OH$ (9:1 w/w)	210-211
Fig 6.11	Comparison of π_{max} of samples obtained from worn and unworn TE contact lenses at the 500 μ l aliquot: (a) C_6H_{14} ; (b) $C_3H_{14}:CH_3OH$ (9:1 w/w); (c) $CHCl_3:CH_3OH$ (1:1 w/w).	214
Fig 6.12	π -A isotherms of a 1.0×10^{-3} moldm $^{-3}$ solution of decanoic acid (DA; 10:0)	215
Fig 6.13	Comparison of π_{max} of worn and unworn narafilecon A and narafilecon B samples	216
Fig 6.14	π -A isotherms of a control (Row 1) and a worn (Row 2) narafilecon B contact lens extracted in $CHCl_3:CH_3OH$ (1:1 w/w)	216
Fig 6.15	π -A isotherms for a 250 μ l aliquot of an extracted Batch 1 pre-production contact lenses and a 25 μ l aliquot of a 1.0×10^{-3} moldm $^{-3}$ DMPC solution	219
Fig 6.16	π -A isotherm for a 200 μ l aliquot of the extracted Batch 2 pre-production contact lenses and a 25 μ l aliquot of a 1.0×10^{-3} moldm $^{-3}$ DMPC solution	220
Fig 6.17	π -A isotherms for a 200 μ l aliquot of the extracted Batch 3 pre-production contact lenses and a 25 μ l aliquot of a 1.0×10^{-3} moldm $^{-3}$ DMPC solution	221
Fig 6.18	π -A isotherms for extracted Trial 1 worn and unworn DT1 contact lenses extracted in $CHCl_3:CH_3OH$ (1:1 w/w).	223
Fig 6.19	π -A isotherms of four sets of samples collected from the lens wearing eye and from a lens wipe after removal from eye.	224
Fig 6.20	π -A isotherms for 200 μ l aliquots of extracted Trial 2 worn and unworn DT1 and TE contact lenses extracted in $CHCl_3:CH_3OH$ (1:1 w/w).	226
Fig 6.21	Relationship between π_{max} and Hildebrand solubility parameter of the extracted sample data for Clariti 1day (1000 μ l aliquot) and 1-Day Acuvue TruEye (500 μ l aliquot).	230

List of Tables

Table	Title	Page
Table 1.1	The functions of tear lipids within the marginal lid reservoirs and the tear film lipid layer.	24
Table 1.2	Lipid composition within the TFLL	26
Table 1.3	Composition of phospholipids and sphingolipids	30
Table 1.4	Tear protein concentrations	35
Table 1.5	Electrolyte composition of the aqueous phase	38
Table 1.6	Tear film mucin genes	38
Table 1.7	Rates of oxidation of fatty acids	51
Table 1.8	Spreading coefficients on water and vapour pressures of solvents	59
Table 2.1	Electrolyte concentrations within the artificial tear electrolyte solution	64
Table 2.2	Formulae required to calculate the area underneath the compression isotherm	67
Table 2.3	Calculation of area under the lines between two adjacent points from the compression isotherm sample data found in Fig 2.2	67
Table 2.4	Formulae required to calculate the hysteresis between compression and expansion isotherms	68
Table 2.5	Calculation of hysteresis between compression and expansion from the isocycle sample data found in Fig 2.3	68
Table 3.1	pH values for the subphase solutions	74
Table 3.2	Key characteristic data for the π -A isotherm of SA ($1.0 \times 10^{-3} \text{ mol dm}^{-3}$; 25 μl aliquot; 25°C) in Fig 3.3	77
Table 3.3	Key characteristic data for the 20 μl and 25 μl aliquot π -A isotherms of SA ($1.0 \times 10^{-3} \text{ mol dm}^{-3}$; PBS subphase) in Fig 3.5	79
Table 3.4	List of the lipids studied for their surface behaviour	82
Table 3.5	Characteristic data for the 25 μl aliquot π -A isotherms of the saturated fatty acids ($1.0 \times 10^{-3} \text{ mol dm}^{-3}$; PBS subphase; 25°C) in Fig 3.8-3.9: myristic acid (MA); palmitic acid (PA); stearic acid (SA); arachidic acid (AA).	84
Table 3.6	Characteristic data for the 25 μl aliquot π -A isotherms of the unsaturated fatty acids ($1.0 \times 10^{-3} \text{ mol dm}^{-3}$; PBS subphase; 25°C) in Fig 3.10-3.11: oleic acid (OA); linoleic acid (LoA); α -linolenic acid (α -LnA); γ -linolenic acid (γ -LnA).	85
Table 3.7	Characteristic data for the 25 μl aliquot π -A isotherms of the C18 and C20 based fatty acids and fatty alcohols ($1.0 \times 10^{-3} \text{ mol dm}^{-3}$; PBS subphase; 25°C) in Fig 3.12-3.13: 1-octadecanol (C18-OH); stearic acid (SA); 1-eicosanol (C20-OH); arachidic acid (AA).	88
Table 3.8	Characteristic data for the 25 μl aliquot π -A isotherms of cholesterol (Ch) and cholesterol esters ($1.0 \times 10^{-3} \text{ mol dm}^{-3}$; PBS subphase; 25°C) in Fig 3.14: cholesterol palmitate (Ch-16:0); cholesterol stearate (Ch-18:0); cholesterol oleate (Ch-18:1).	90

Table	Title	Page
Table 3.9	Characteristic data for the 25 μ l aliquot π -A isotherms of wax esters (1.0×10^{-3} moldm $^{-3}$; PBS subphase; 25°C) in Fig 3.15: palmityl palmitate (16:0-16:0); oleoyl oleate (18:1-18:1); behenyl oleate (22:0-18:1).	91
Table 3.10	Characteristic data for the 25 μ l aliquot π -A isotherms of phosphatidylcholines (1.0×10^{-3} moldm $^{-3}$; PBS subphase; 25°C) in Fig 3.16-3.17 (* data for DOPC was recorded at π_{eq})	92
Table 3.11	Characteristic data for the 25 μ l aliquot π -A isotherms of glyceride molecules (1.0×10^{-3} moldm $^{-3}$; PBS subphase; 25°C) in Fig 3.16-3.17: monoolein (MO); diolein (DO); triolein (TO).	94
Table 3.12	Key characteristic data for the π -A isotherm of β -2-microglobulin (Lc), lysozyme (Lz) and bovine serum mucin (BSM) (100 μ l aliquot; 35°C).	97
Table 3.13	π -t isotherm data for adsorption of β -2 microglobulin (lipocalin analogue; Lc), lysozyme (Lz) and bovine serum mucin (BSM) to a ATLF monolayer	99
Table 3.14	π -A isotherm data for an ATLF monolayer before instillation of the protein/mucin components and after complete adsorption of the studied components.	101
Table 4.1	Calibrated extracting volumes of CHCl $_3$ based upon volume collected for sample and control microcapillary tubes.	108
Table 4.2	Usable volume (UV) of extracting volumes (EV) of solvent based upon wetted length (WL) of sample and control Schirmer strips.	108
Table 4.3	Calibrated extracting volumes of CHCl $_3$ based upon absorbed length of sample and control Visispear™ ophthalmic sponges (* was extracted in hexane).	109
Table 4.4	Applied volume of sample solution represented as a percentage of the total usable extracted volume of sample for Px1, Px2, Px3 and Control 1.	119
Table 4.5	Applied volume of sample solution represented as a percentage of the total usable extracted volume of sample for Px4 and Control 2.	122
Table 6.1	Comparison of π_{max} (mN/m) between LE and RE worn Clariti 1day samples obtained using different solvent extraction methodology at the 1000 μ l aliquot.	199
Table 6.2	Comparison of π_{max} (mN/m) between LE and RE worn 1-Day Acuvue TruEye samples obtained using different solvent extraction methodology at the 1000 μ l aliquot.	213
Table 6.3	Hildebrand solubility parameters (δ_t ; MPa $^{1/2}$) of the three solvent mixtures.	228
Table 6.4	π_{max} data for Clariti 1day (1000 μ l aliquot) and 1-Day Acuvue TruEye (500 μ l aliquot) and Hildebrand solubility parameter of the three extraction solvents.	229

List of Symbols and Abbreviations

Symbol / Abbreviation	
TF / TFLL	tear film / tear film lipid layer
ATLF / ATE	artificial tear lipid film / artificial tear electrolyte
CL	contact lens
PV	PureVision
FN+D	Focus Night+Day
TE	Acuvue TruEye 1day
DT1	Focus Dailies Total-1
SiHy / CoHy	silicone hydrogel / conventional hydrogel
CW / DW / DD	continuous wear / daily wear / daily disposable
FDA	Food & Drug Administration
PCTF / PLTF / PoLTF	pre-corneal tear film / pre-lens tear film / post-lens tear film
TBUT / NI-TBUT	tear break-up time / non-invasive tear break-up time
PL / NPL	polar lipid / non-polar lipid
FA / FFA / HFA / OAHFA	fatty acid / free fatty acid / hydroxy fatty acid / (O-acyl)-omega hydroxy fatty acid
FAlc	fatty alcohol
Ch	cholesterol
CE	cholesterol ester
WE	wax ester
AG / MAG / DAG / TAG	acylglyceride / monoacylglyceride / diacylglyceride / triacylglyceride
LA / MA / PA / SA / AA	lauric acid / myristic acid / palmitic acid / stearic acid / arachidic acid
OA / LoA / LnA / α -LnA / γ -LnA / PoA	oleic acid / linoleic acid / linolenic acid / alpha linolenic acid / gamma linolenic acid / palmitoleic acid
DMPC / DPPC / DSPC / DOPC	dimyristoylphosphatidylcholine / dipalmitoylphosphatidylcholine / distearoylphosphatidylcholine / dioleoylphosphatidylcholine
PC / PE	phosphocholine / phosphoethanolamine
Lc / TLC / apo-Lc / holo-Lc	lipocalin / tear lipocalin / apo-lipocalin / holo-lipocalin
Lz	lysozyme
BSM	bovine submaxillary gland mucin
BSA / HSA	bovine / human serum albumin
Lf	lactoferrin
β -Lg	β -lactoglobulin
IgA	immunoglobulin A
SP-A,B,C,D	surfactant protein A, B, C, D
PBS	phosphate buffered saline
LT	Langmuir trough
BAM	Brewster angle microscope

Symbol / Abbreviation	
PEO / PPO / PVP / PHEMA / PEG / PSMA	poly(ethylene oxide) / poly(propylene oxide) / poly (vinyl pyrrolidone) / poly(2-hydroxymethyl methacrylate) / poly(ethylene glycol) / poly(styrene- <i>alt</i> -maleic anhydride)
CH ₃ Cl	chloroform
CH ₃ OH	methanol
C ₆ H ₁₄	hexane
GC-MS	gas chromatography-mass spectroscopy
HPLC	high pressure liquid chromatography
t	time
T	temperature
F	force
V / UV / EV	volume / usable volume / extraction volume
P / VP	pressure / vapour pressure
l / w / d	length / width / depth
π	surface pressure
π -A / π -t	surface pressure-area / surface pressure-time isotherm
G / LE / LC (LC ₁ /LC ₂)	gaseous / liquid expanded / liquid condensed (tilted LC/aligned LC)
π_{\max} / π_{\min}	maximum / minimum surface pressure
π_{eq}	equilibrium surface pressure
π_t	phase transition surface pressure
π_{init}	initial surface pressure
π_c	collapse surface pressure
$\Delta\pi$	change in surface pressure ($\pi_{\max} - \pi_{\min}$)
γ	surface tension
γ_{\min}	minimum surface tension
γ_{LG}	surface tension of liquid and gas
$\gamma_{\text{aq}} / \gamma_{\text{lipid}}$	surface tension of tear aqueous / tear lipid
γ_i	interfacial tension
$\gamma_{\text{LS}} / \gamma_{\text{L1-L2}}$	interfacial tension between liquid and solid / liquid 1 and liquid 2
$\gamma_{\text{aq-lipid}}$	interfacial tension between tear lipid and tear aqueous
γ^d / γ^p	dispersive / polar component of surface tension
A / A _{mol}	surface area / molecular area
A _t	area of phase transition
A _{π}	area at surface pressure, π
$\frac{dA}{d\pi}$	slope of isotherm at a certain surface pressure
b _{Δ} / \square / h _{Δ} / \square	base of triangle / rectangle and height of triangle / rectangle
A _{Δ} / A _{\square}	area of triangle / rectangle
A _{tot}	total area between two adjacent data points
ΣA_{tot} (com / exp)	sum of total areas for compression / expansion isotherm
Rev	reversibility of isocycle (%)
t _{π_{eq}}	time for equilibrium surface pressure
S	Harkins spreading coefficient

Symbol / Abbreviation	
ΔG	Gibbs free energy
N_A	Avogadro's number (6.022×10^{23})
STP	standard temperature and pressure (298K, 1atm)
ρ	density
g	acceleration due to gravity
θ	contact angle
α°	Brewster angle
δ_t	Hildebrand solubility parameter
L / mL / μ L	litre / millilitre / microlitre
g / mg / μ g	gram / milligram / microgram
Da / kDa	dalton / kilodalton
Mwt	molecular weight
%wt / %w/v	percent by weight / percent weight by volume
Pa / kPa / MPa	Pascals / kiloPascals / megaPascals
mN/m / dyn/cm	milliNewton per metre / dynes per centimetre
mol	moles
mol/mol	mole per mole ratio
M / mM	molar / millimolar concentration
s / min / hr	second / minute / hour
atm	atmosphere
$^\circ\text{C}$ / K	degree Celsius / Kelvin
m / cm / mm / μ m / nm	metre / centimetre / millimetre / micrometre / nanometre
\AA / $\text{\AA}^2\text{molecule}^{-1}$	angstrom / square angstrom per molecule

Chapter 1

Introduction

The focus of this thesis is to evaluate and develop the Langmuir trough method for routine use in surface chemistry studies of the tear film. Understanding the physical, chemical and biological aspects of why the tear film is stable and how it can be destabilised can potentially form the basis for a greater understanding of clinical factors relating to tear film stability.

Over millions of years the eye has evolved from the earliest ability to distinguish between light and dark, to the first complex eye that provided an advantage for prehistoric predators, to our absolute reliance on our vision in everyday life. As the visual aspect of the eye has evolved so to have the biological, chemical and physical ways in which the eye is protected. One such evolution is the tear film. This complex, micrometre-thin fluid layer forms the barrier between the cornea and conjunctival surfaces, and the air. Its primary functions are protecting and maintaining the integrity of the ocular system through various biochemical and physicochemical activities.

Much of our understanding of tear film stability is based on observations and measurements of the tear film when it is detrimentally affected by biological and artificially-created adverse conditions. These factors affect the balance of forces that exist within the tear film which can lead to disruption and potential loss of tear film integrity. It is with the physicochemical aspect of tear film stability - the surface and interfacial forces between tear film components - that this thesis will be primarily concerned.

1.1 The Tear Film

The tear film is a highly specialised fluid film that plays an essential role in maintaining the health of the eye and the visual system [1] [2]. It covers the corneal and conjunctival surfaces to form a $\sim 7\mu\text{m}$ thick protective barrier that lies across the entire exposed area of the ocular surface [3] [4] [5] [6]. The properties of the unique and specialised structure of the film provides thermodynamic stability [7] [8]. In order for it to function properly the composition of aqueous, lipid, protein and mucous components must be contained within narrow limits for optimum functionality.

1.1.1 Structure of the Tear Film

The classical representation of the pre-corneal tear film (PCTF) proposed by Wolff [9] is of a trilaminar (three layered) structure (Fig 1.1a). This consists of a mucus layer spread across the corneal surface, an aqueous layer that covers this and comprises the majority of the films composition, and a lipid layer that forms the anterior section of the tear film between the aqueous phase and the air. As understanding of the tear film and its components has increased, and measurement and analytical techniques have evolved, the traditional three-layer representation of the tear film structure has been expanded to a more complex six-layer model (Fig 1.1b) [10] [11] [12] [13]. This six-layer representation indicates the presence of more interfaces and more complex intra-molecular interactions than could be observed and understood with the original model.

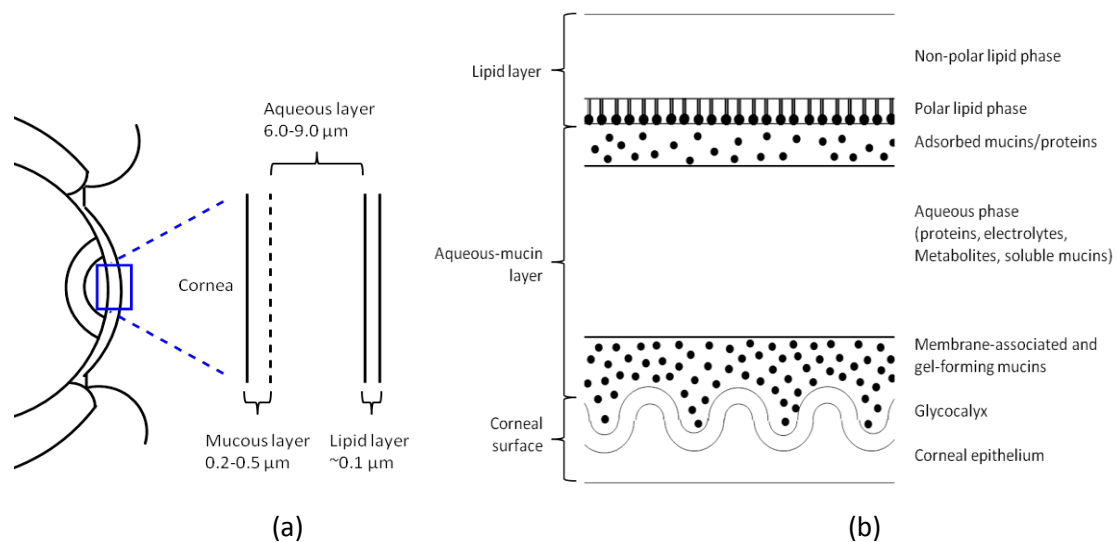


Fig 1.1. Structure of the tear film: (a) Traditional three-layer representation; (b) six-layer representation of the tear film [9] [10] [11] [12] [13] [14] [15]

A high-concentration region exists at the corneal surface consisting of membrane-associated and gel-forming mucin genes. The aqueous phase forms the majority of the tear film and consists predominantly water (98%) with a mixture of proteins, electrolytes and metabolites. Soluble mucin is found within the bulk of the aqueous and as an adsorbed layer at the lipid-aqueous interface. The lipid layer forms the anterior layer of the tear film, covering the aqueous phase in a two-step formation that involves separate, favourable hydrophilic and hydrophobic interactions between polar and non-polar lipid components [10] [15] [16].

1.1.2 Role of the Tear Film

The tear film is a highly specialised, multifunctional fluid film that maintains a stable and healthy ocular system through four main functions [1] [7] [8] [17]:

- The maintenance of a smooth optical surface that allows light refraction. The tear film must remain transparent to allow light to refract and travel through to the cornea;
- The fluid film system provides lubrication for the eyelids, the conjunctiva and the cornea in order to avoid mechanical damage of the ocular surface;
- The tear film provides nutrition to the avascular cornea through the transport of oxygen (dissolved from the air) and nutrients (e.g. glucose from a vascular source such as the palpebral conjunctiva);
- Prevents damage to the corneal and conjunctival surfaces through dynamic responses to environmental, microbial and bacterial conditions.

1.2 The Lipid-Aqueous Interface

The tear film is a dynamic system, the stability of which is significantly characterised by the interactions that occur between the different lipid types within the tear film lipid layer (TFLL) and the components within the tear aqueous. It is important to understand how each component interacts in inter- and intra-layer considerations.

1.2.1 The Lipid Layer

The TFLL forms the anterior section of the tear film and forms the intermediate layer between the aqueous tears and the air. The thickness of the TFLL is ~100 nm and roughly 20 molecules thick based on the end-to-end alignment of acyl chains of lipids [2] [13] [18] [19]. The lipids that form the TFLL are secreted primarily from the Meibomian glands located within the upper and lower eyelids [20] [21] [22]. A small amount of lipid comes from other sources such as the glands of Moll and Zeiss, adsorbed molecules within the aqueous tears, the corneal and conjunctival epithelium and other cellular debris [2]. Delivery of lipids from the Meibomian glands to the lid margin reservoirs is by a steady secretory process during a blink action. As the eyelids open, the upper lid draws Meibomian lipids from the marginal reservoirs and the lipid film spreads rapidly over the aqueous surface of the tear film.

The thickness of the TFLL has been correlated to the expression of lipids from the Meibomian glands, with forced secretion producing a thicker TFLL [23] [24] [25] [26]. Roughly half of the Meibomian glands are functional at any one time [27] [28]. A decrease in the amount of functioning Meibomian glands leads to decreased lipid production and increased rates of tear thinning, TFLL instability, TFLL rupture and aqueous evaporation [21] [25] [28] [29] [30] [31].

1.2.1.1 The Role of Lipid Layer

The TFLL plays an essential role in the stability and function of the tear film despite the relatively small volume and thickness compared to the aqueous layer [2] [17] [21]. The roles of the lipid molecules can be split in to those at the marginal reservoirs of the eyelids and those within the PCTF (Table 1.1).

Lid Margin Reservoirs
Prevention of tear overspill; Prevention of mechanical damage caused by eyelids during a blink; Resist contamination of lipids from other sources.
Tear Film Lipid Layer
Impart tear film stability; Thicken the aqueous subphase; Retard evaporation of the aqueous subphase; Provide a smooth optical corneal surface; Prevent contamination by foreign particles and microbes; Seal lid margins during prolonged closure.

Table 1.1. The functions of tear lipids within the marginal lid reservoirs and the tear film lipid layer.

At the marginal lid reservoirs, the lipid molecules prevent the overspill of tears by maintaining a hydrophobic lid surface, resistance against contamination by preventing sebaceous lipids from entering the TFLL and prevent mechanical damage through lubrication between the eyelid and corneal surfaces.

Upon delivery from the marginal lid reservoirs to the PCTF, the tear lipids spontaneously spread across the aqueous layer. In doing so they impart stability to the tear film through decreasing the free energy and surface tension of the system [10] [32] [33]. Surface tension is the tendency of the surface or interface of a liquid to contract caused by the cohesion of

molecules within the liquid [34] [35]. It has been shown that lipid deficient tears have an increased surface tension when compared to the normal tear film [36] [37] [38]. The role of surface tension on lipid-aqueous interfacial stability will be discussed in more detail in section 1.5.

The lipid layer acts as a barrier to prevent evaporation of the aqueous layer [39] [40] [41] [42]. Evaporation has been shown to increase by two- to four-fold in the absence or dysfunction of the lipid layer [41] [42] [43] [44] [45] [46]. Meibomian gland dysfunction (MGD) - where the amount of Meibomian glands that work to secrete lipids is decreased - has been linked to the onset of evaporative dry eye, one of the two major classifications for dry eye disease [47]. The smaller amount of lipid released from the Meibomian glands of dry eye disease sufferers produce a poorer quality lipid layer that is not as stable as a normal secretion.

The viscoelastic properties of the tear film is also an important factor in tear film stability. Tears are non-Newtonian fluids and the usual shear rate-shear stress relationship is different to the linear relationship observed in Newtonian fluids [48] [49] [50]. As high rates of shear are observed during a blink, the tear film adopts a low viscosity in order to avoid damage to the corneal and conjunctival surfaces. When the eye is open, the tear film has a higher viscosity so that drainage and break-up is resisted [48] [49]. It has been observed that with the removal of Meibomian lipids that the tear film becomes more Newtonian in character [51]. As no free lipids have been found within the aqueous layer, it has been suggested that tear lipocalin - a lacrimal protein with non-specific lipid binding - could be a potential aid in tear viscosity by binding to lipids within the aqueous layer [38] [49] [52] [53]. Maragoni flow can be observed when the tear lipids spread due to the presence of surface tension gradients between the water (high surface tension) and the lipids (relatively low surface tension) [2] [48] [49] [54].

As well as a barrier to evaporation, the lipid layer acts as a barrier to prevent contamination by foreign particles and microbes that might disrupt the stability of the tear film and health of the ocular surface. The structure of the PCTF provides a smooth and clear optical surface, that does not impede visual acuity and provide $\sim 1/3$ of the refractive index of the tear film [2] [10] [55].

1.2.1.2 Tear Film Lipid Layer Composition

The tear film lipid layer consists of a range of lipid types that contribute to the stability and function of the tear film. Table 1.2 shows estimated concentrations levels of each lipid component type. The major lipid types are the non-polar lipid (NPL) wax esters (WE) and cholesterol esters (CE), which make up ~60-90% of the total lipid composition. ~10% of the total lipid composition is thought to comprise of polar lipid (PL) molecules. The amount of diversity within each lipid type coupled with vast differences in inter-patient TFLL compositions are obstacles to studying and measuring the exact lipid composition.

Lipid Types	Concentration	
	Average (%)	Range (%)
Wax ester (WE)	43.0	13.0 - 68.0
Cholesterol ester (CE)	25.0	8.0 - 39.0
Hydrocarbons (HC)	10.0	1.0 - 38.0
Diesters	2.0	1.0 - 7.5
Acylglycerides (TAGs)	5.0	4.0 - 6.0
Cholesterol (Ch)	2.0	0.5 - 3.0
Fatty alcohols (FAlc)	4.0	3.0 - 5.0
Free fatty acids (FFA)	2.0	1.0 - 24.0
Polar lipids (PL)	6.0	0.5 - 16.0
Phospholipids	~4.0	
Sphingolipids	~2.0	
(O-acyl-omega)hydroxy fatty acids (OAHFA)	4.0	3.5 - 5.0

Table 1.2. Lipid composition within the TFLL [12] [41] [56] [57] [58] [59] [60] [61]

All tear lipid molecules are based upon aliphatic or cyclic hydrocarbon structures and are often split in to two types: **polar** and **non-polar**. The non-polar lipids are primarily composed of a hydrocarbon chain or ring structures that are insoluble in water due to the hydrophobic characteristics of the chain. These molecules are lipophilic due to their favourable interactions with other non-polar components and solvents, especially other lipoidal molecules. Polar lipids differ slightly in structure, often based on similar hydrocarbon structures to the non-polar lipids but also contain one or more functional groups that interact favourably with water and other polar molecules. These molecules are amphiphilic due to the presence of a hydrophilic group and hydrophobic/lipophilic chain within the same structure. This balance between hydrophilicity and hydrophobicity dictates the solubility of a lipid molecule in water and the behaviour at a surface.

1.2.1.2.1 Fatty Acids, Alcohols and Cholesterol

The major tear lipid types are predominantly formed from three main component molecules: cholesterol (Ch), fatty acids (FA) and fatty alcohols (FAlc). These also exist as a free molecule products of degradation reactions caused by the breakdown of the main tear lipid types into component molecules [56] [57] [60] [62] [63] [64]. Fatty acids (FA) are structural components of all major tear film lipid types. They comprise a hydrocarbon chain of an even number of carbon atoms with a carboxylic acid functional group attached at a terminal carbon (Fig 1.2). FA are termed saturated (if no double bonds are present) or unsaturated (if one or more double bonds are present) and can also exist with branched alkyl groups bonded to the main hydrocarbon chain.

Conventional nomenclature for FA indicates the number of carbon atoms in the chain, the number and position of any double bonds, and any branched groups present. The positions of double bonds are counted either from the carboxylic acid terminal group (Δ -numbering scheme) or from the methyl group at the other terminal end of the chain (ω -numbering scheme). The chain length, degree of unsaturation and branched groups affect the melting point of fatty acids. Longer hydrocarbon chains increase the melting point whereas the presence of mono- and polyunsaturation decreases the melting point and adds a more fluid behaviour to the molecule [65]. Branched fatty acids can have a varied effect on the melting point.

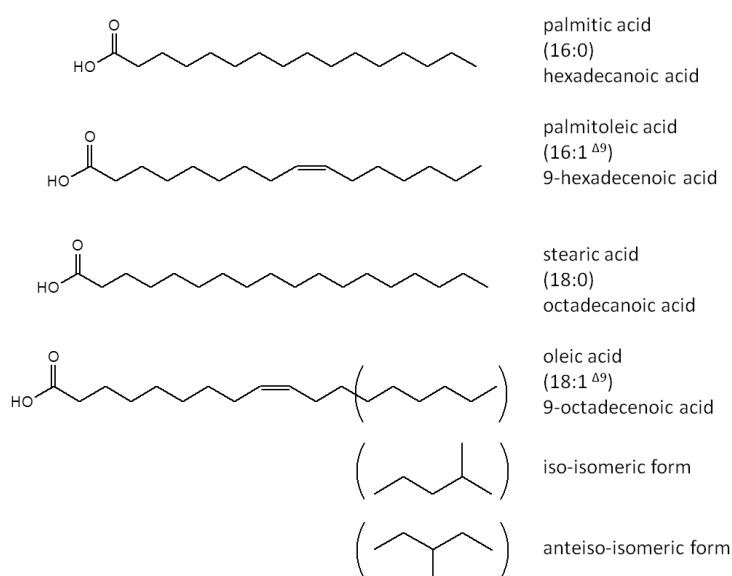


Fig 1.2. General structures of saturated, unsaturated and branched fatty acids.

Fatty alcohols (FAlc) are aliphatic alcohols that are found primarily within WE molecules (Fig 1.3). They consist of a hydrocarbon chain with a hydroxyl group at a terminal carbon. In biological systems such as the TFL, it is common to find fatty alcohols with longer chain of anything from 24 to 36 or more carbons. A significant amount of FAlc also has iso- or anteisomeric structures in addition to the straight chain forms more commonly found.

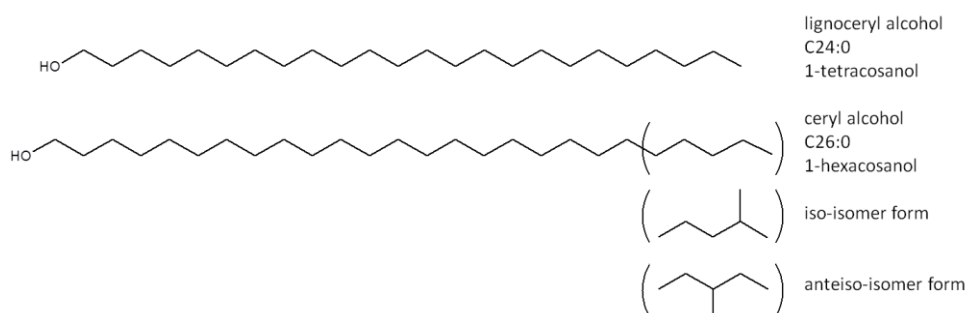


Fig 1.3. General structures of fatty alcohols showing straight chain, iso- and anteiso-isomeric forms.

Cholesterol (Ch) contains four planar cycloalkane rings and a hydroxyl group. The planar ring structure provides a great deal of non-polar, hydrophobic behaviour that dominates any polarity from the hydroxyl functional group (Fig 1.4).

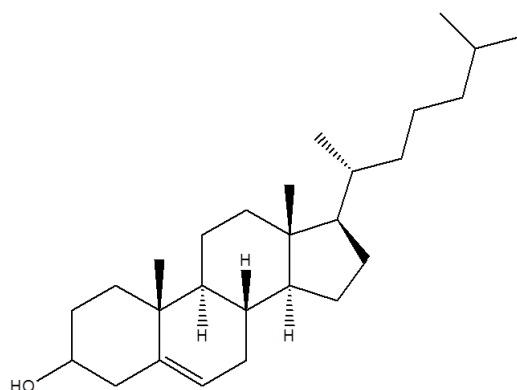


Fig 1.4. Structure of a cholesterol molecule

1.2.1.2.2 Wax Esters

Wax esters (WE) are one of the major non-polar lipid types that account for roughly a third of the total lipid composition of tear film lipids. These molecules are formed by an esterification reaction between a fatty alcohol and a fatty acid (Fig 1.5). The most common wax esters detected were based on oleic acid (18:1^{ω9}) with a significant, yet smaller, amount of palmitoleic acid (16:1^{ω7}) also found.

The ratio of saturated to unsaturated fatty acids detected was 1:4 [56] [66] [67]. The most commonly detected fatty alcohols had hydrocarbon chain lengths of C24 to C27 with a ratio of 4:1 for saturated to unsaturated alcohols [56] [66] [67] [68].

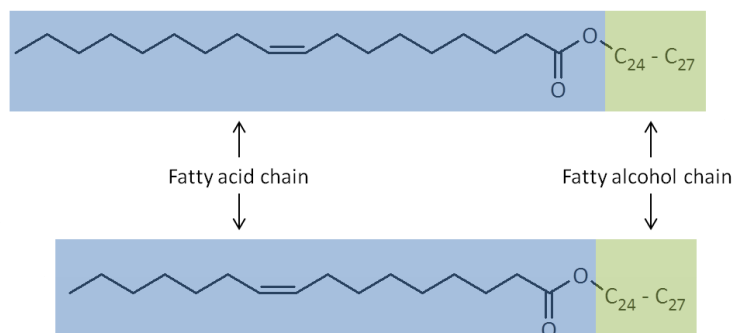


Fig 1.5. General structure of a wax ester and examples of TFL WE species.

1.2.1.2.3 Cholesterol Esters

Cholesterol esters (CE) are formed by esterification reactions between cholesterol and a fatty acid (Fig 1.6). These molecules are non-polar in nature due to the loss of the polar regions hydroxyl groups of both molecules. CE are consistently detected as a major lipid class present in Meibomian lipid samples (~30%). Analytical studies of the FA composition of CE has shown that the majority of fatty acids found in cholesterol esters contained very long chain fatty acids (C24 or more). C24-32 saturated hydrocarbon chains were the most abundant with small amounts of monounsaturated FA also being detected. Saturated and unsaturated FA with chains of C18 or smaller were found in minute amounts. Despite its abundant presence within the TFL, oleic acid was only found as a minor constituent of the total CE [60] [67] [69] [70].

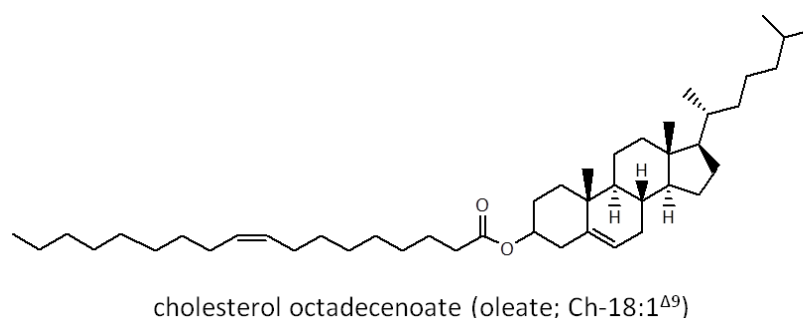


Fig 1.6. General structure of a cholesterol ester (cholesterol 9-octadecenoate (Ch-18:1^{Δ9}))

1.2.1.2.4 Phospholipids and Sphingolipids

The polar lipids account for a small percentage (0-15%) of the overall composition of tears of which, arguably, phospholipids contribute the greater proportion (Table 1.3). The polar lipid fraction was found to comprise ~70% phospholipid components and ~30% of sphingolipids (e.g. cerebroside and ceramides) [71]. Of the phospholipid components, phosphocholine (PC), phosphoethanolamine (PE) and sphingomyelin containing compounds were found to be the most predominant species detected [12] [61] [71] [72].

PL Type	Composition (%)	Typical lipids
Phospholipids	70	PC (38%); PE (16%); sphingomyelin (7%); unknowns (39%)
Sphingolipids	30	ceramides (30%); cerebroside (70%)

Table 1.3. Composition of phospholipids and sphingolipids [71]

The structure of a phospholipid molecule is similar to that of an acylglyceride. A phosphate group with an attached alcohol is bonded to an end carbon of the glycerol backbone molecule. The remaining two carbons of the glycerol backbone are esterified to acyl chains that are predominantly short chain (C12-18) saturated fatty acids with minimal degrees of branching and saturation (Fig 1.7). The presence of the phosphatidyl-alcohol head group produces a much more polar molecule with a larger HLB when compared to a diacylglyceride molecule.

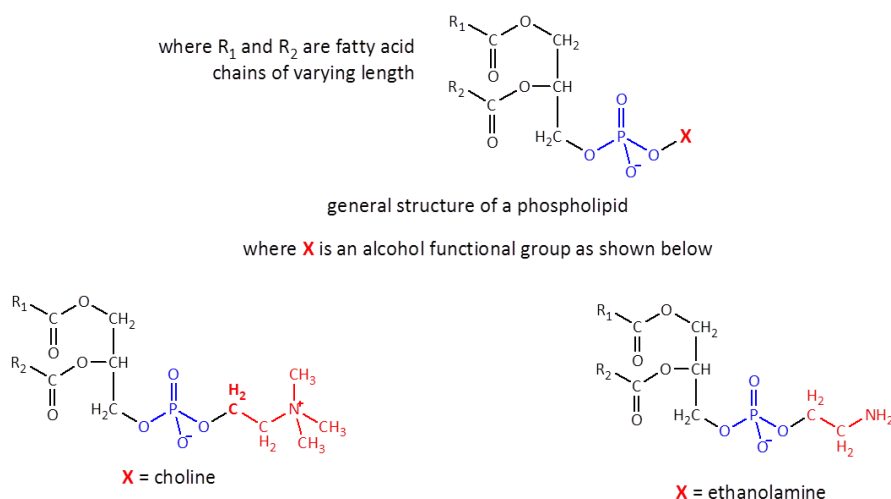


Fig 1.7. General structure of a phospholipid molecule with examples of common alcohol functional groups.

Sphingolipids are a class of lipids that contain a backbone of the aliphatic amino alcohol sphingosine (Fig 1.8). A fatty acid molecule forms an amide linkage between the amino group of sphingosine and the carboxyl group of the FA. Ceramides are N-acylated sphingosine based molecules that lack an additional head group. A head group can be attached to the ceramide molecule through the formation of an ester linkage at the 1-hydroxy group of the sphingosine component. Sphingomyelins have a phosphocholine or phosphoethanolamine attached to the 1-hydroxy group of a ceramide molecule, whereas glycosphingolipids have one or more sugar residues attached at that position instead. Similar chain length fatty acids found in phospholipids are also present in the sphingolipids, but FA within sphingolipids in human meibum show a significant presence of hydroxylation [19] [73].

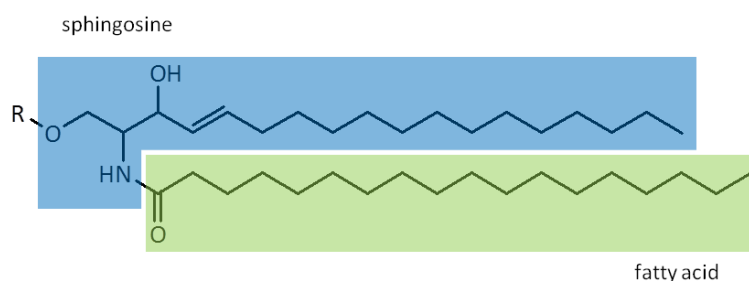


Fig 1.8. General structure of sphingolipids
(R = H - ceramide; PC/PE - sphingomyelin; sugar - glycosphingolipids).

There is still debate as to the source and amount of phospholipids and other polar lipids present within the TFLL. Whilst some studies have detected a significant presence [19], others have found very little to no phospholipids [74] [75] [76] [77]. The primary source of these lipids being the Meibomian glands is not yet agreed upon, leading to the theory that whilst phospholipids are generally present they may in fact be obtained from different sources such as from the conjunctival and corneal surfaces, through the lacrimal glands and from skin lipids and other cellular debris [74] [75]. As phospholipids are generally believed to form a substantial part of the polar lipid sublayer, the discrepancies in concentration will have an effect on the ability to lower the surface free energy and therefore the overall stability of the tear film.

1.2.1.2.5 (O-acyl)-omega-hydroxy Fatty Acid Esters

The presence of (O-acyl)-omega-hydroxy fatty acid (OAHFA) esters has only been theorised and not fully confirmed by study. As such, the amount of OAHFA found within human meibum is unknown [75] [78] [79], with estimates that combine it with other components being less

than 10% [80] [81]. These molecules are formed by an esterification reaction between the hydroxyl group of a long chain (C30+) unsaturated hydroxy fatty acid (HFA) and the carboxyl group of a fatty acid (Fig 1.9). This combines structural and characteristic aspects of a wax ester and a fatty acid within the same molecule [68] [75] [78] [82]. They are thought to be precursors to the di- and triesters detected in small amounts within the TFL by esterification reactions between OAHFA and a variety of FA, FALC and Ch molecules [78]. The carboxyl groups ionise at physiological pH and the HFA double bond produce multiple points of contact with water molecules at the lipid-aqueous interface (Fig 1.10) [75]. It is thought that this may aid in the stabilisation of the TFL through forming the PL sublayer that has been commonly thought to be attributed to phospholipids [12] [68] [82].

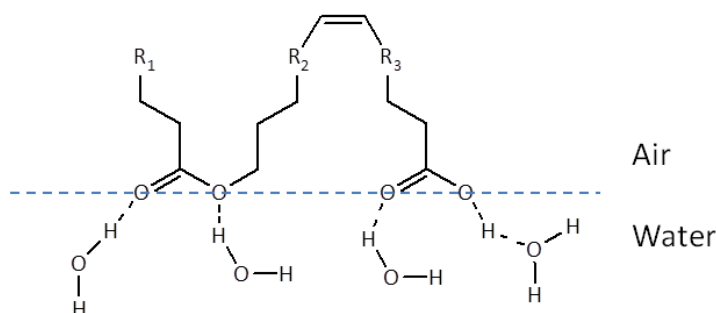


Fig 1.9. General structure of OAHFA (R1, R2 and R3 represent saturated hydrocarbon chains of varying lengths) [68] [75].

1.2.1.2.6 Acylglycerides

Acylglycerides (AGs) are a minor group of lipids (~3-6%) found within the tear film lipid layer [12] [41] [56] [57] [63] of which the presence of triacylglycerides (TAGs) have been consistently detected [22] [56] [60] [67] [83] [84] [85] [86] [87]. AGs are based on a glycerol molecule with up to three esterified acyl chains attached (Fig 1.10). TAGs have all three carbons of the glycerol backbone esterified to fatty acid chains and are non-polar due to the presence of the three hydrophobic acyl chains. Elucidation of the structures of TAGs show that they are dominated by the presence of short chained FA (C18 and less). The most abundant of these FAs was OA (18:1^{Δ9}) with amounts of ~40% detected. PoA (16:1^{Δ9}) and PA (16:0) were also most commonly detected in large amounts (~10-20%) [13] [56] [57] [84]. The majority of FAs from TAGs were straight chain (~70-80%) with small concentrations of iso- and anteisomeric forms composing the remainder of FAs present. Only trace amounts of C12-14 and C20-26 saturated and unsaturated FA detected [56] [84].

Monoacylglycerides (MAGs) have a single fatty acid chain at the sn-1 or sn-2 position and are the most polar of the acylglycerides due to the presence of two hydroxyl groups as part of the glycerol backbone. Diacylglycerides (DAGs) have two acyl chains and exist as either in 1,2- or 1,3-diacylglyceride conformational isomers. DAG molecules, with a single hydroxyl group remaining, are polar molecules to a lesser extent than MAGs. Although reported in publications, DAGs and MAGs have not been reliably detected within TFL samples [73] [83] [75] [86] [88]. As such there is no detail on the structural characteristics of the molecules in terms of the FA attached to them. Confirmation of the presence of these molecules in meibum requires further analytical study. It is a possibility that DAG and MAG molecule constitute part of polar lipid extractions that are currently poorly characterised in to individual lipid types.

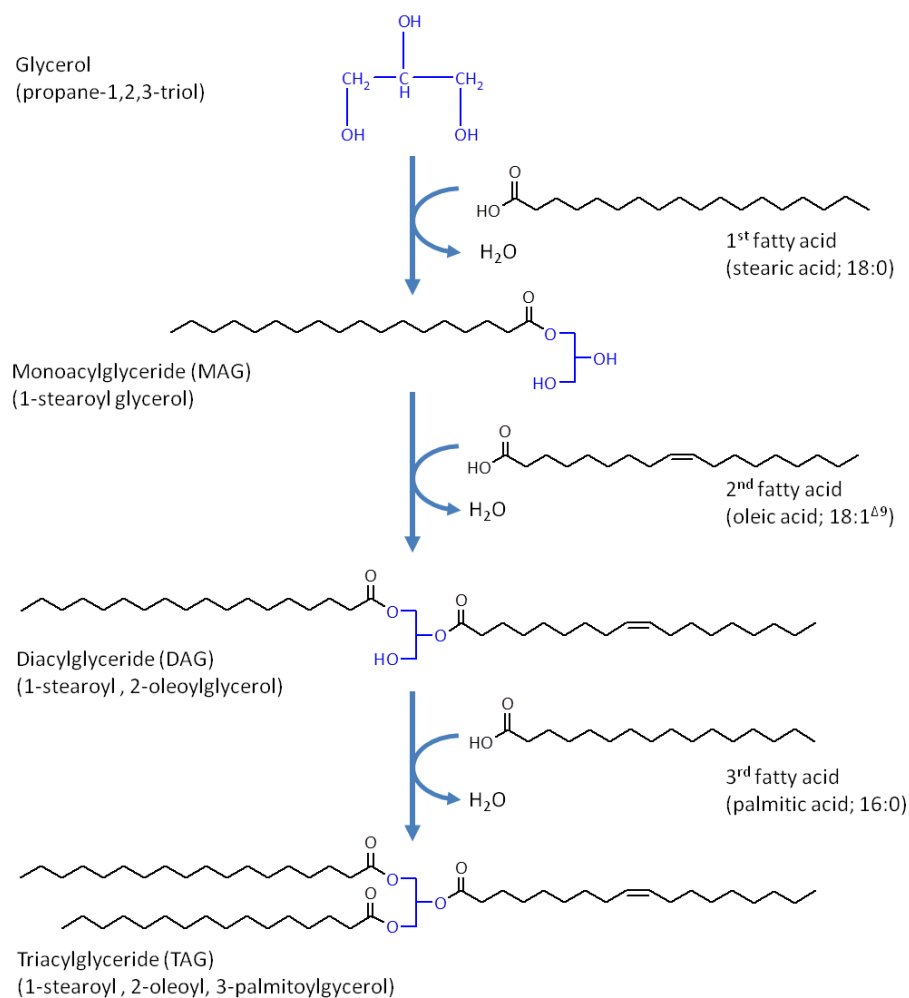


Fig 1.10. Formation of monoacylglyceride (MAG), diacylglyceride (DAG) and triacylglyceride (TAG) from glycerol and fatty acids.

1.2.1.3 Structure of the Lipid Layer

The structure of the lipid layer was first proposed as a two-phase (biphasic) structure by Holly [15] where the PL phase spreads initially with subsequent formation of a NPL phase. This has since been adapted by McCulley and Shine who theorise a superlattice model structure that involves understanding the behaviour of individual lipid types and the role that acyl chain structure has on promoting stability [10] [12]. Biphasic formation occurs with the rapid spreading of the amphiphilic PL to form a sub-layer "raft" between the aqueous layer and NPL (Fig 1.11). Phospholipids, sphingolipids, FFA and OAHFAs are the main components of this polar phase. FALc, MAGs and DAGs are also thought to be present within the PL sublayer. This first stage of bilayer formation involves favourable interactions between the hydrophilic regions of the polar lipids and the water within the aqueous phase due to surfactant behaviour. As the hydrophobic regions of the polar lipids orientate themselves away from the aqueous phase, a stable platform for the non-polar lipids to spread across is formed. WE, CE, TAGs and HC interact with the hydrocarbon chains of the polar lipids through van der Waals interactions.

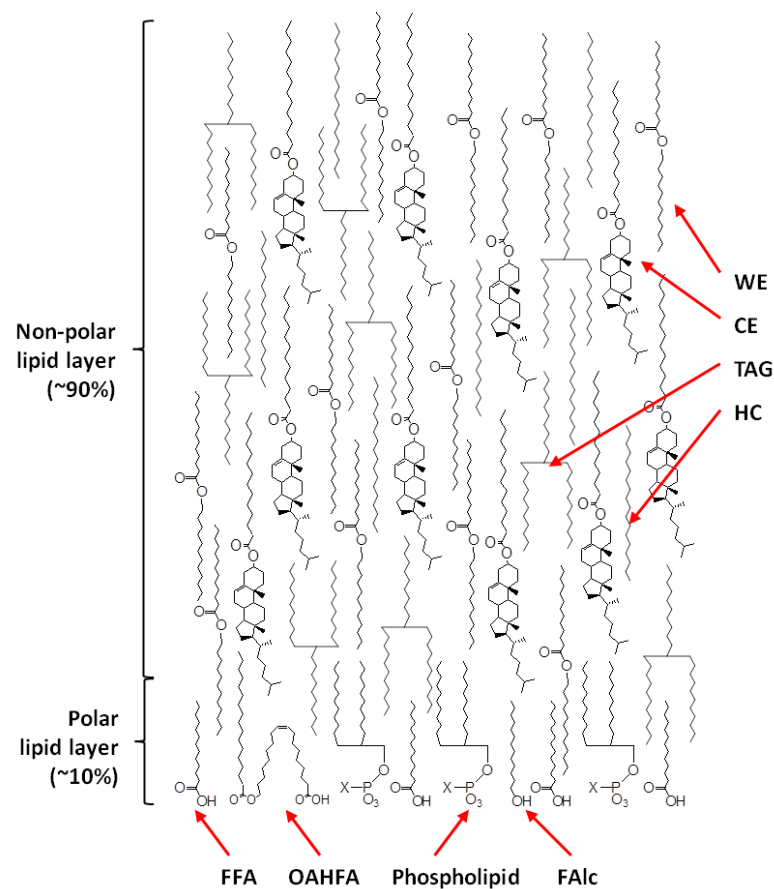


Fig 1.11. Biphasic representation of the lipid layer [10] [12] [82]

1.2.2 The Aqueous Layer

The aqueous-mucin layer forms the bulk of the PCTF and the thickness of this phase (~7 µm) [3] [11] [89]. It is composed mainly of water (~98%) with the remainder comprised of proteins, enzymes, mucins, electrolytes and metabolites [39] [90].

1.2.2.1 Tear Proteins

More than 100 different proteins have been detected and identified within human tears [91] [92] [93]. The concentrations of the most abundant are found in Table 1.4. Tear proteins are mainly sourced from the main lacrimal gland and the accessory glands of Krause and Wolving [94]. Similar to tear lipids, the concentrations of protein varies depending on the characteristics of the patient (e.g. age, gender, ocular health and contact lens wear).

Protein	Source	Concentration (mg/ml)
Lipocalin	Lacrimal	1.23 - 1.67
Lysozyme	Lacrimal	1.85 - 3.30
Lactoferrin	Lacrimal	1.65 - 2.10
Albumin	Serum	0.042 - 1.30
IgA	Lacrimal/Serum	0.012 - 0.790
IgE	Serum	0.017
IgG	Serum	0.003 - 0.13
IgM	Serum	0.0029 - 0.014
Total Protein		7.30 - 7.86

Table 1.4. Tear protein concentrations [95] [96] [97] [98] [99] [100] [101] [102] [103]

1.2.2.1.1 Tear Lipocalin

Tear lipocalin is a low-molecular weight sourced from the lacrimal glands and is thought to influence tear film stability [52] [104] [105]. It is abundant in tears constituting a concentration of approximately 1.23-1.67 mg/ml (15-33% of the total tear protein) [52] [102] [106] [107]. The lipid binding and release capability may benefit the stabilisation of the tear film [104] [108] [109]. It maintains the non-Newtonian characteristics of tears by increasing the viscosity of tears [49] and removes harmful products produced by oxidation of lipid molecules that can harm the ocular surfaces [110]. A deficiency could lead to migration of lipid components by precipitation, formation of mucous strands and disruption of the tear film [108].

1.2.2.1.2 Other Tear Proteins

Lysozyme is a long chain, low molecular weight enzyme molecule that contributes 20-40% of the total protein content in tears. It has an antibacterial activity by enzymatic cleaving of the glycosidic bonds between residues within the peptidoglycan structure of gram-positive bacteria [94] [111] [112] [113] [114]. Lactoferrin is a glycoprotein produced in the lacrimal gland and has antibacterial properties through binding to the iron needed to facilitate replication, direct attack of common strains of bacteria and through breakdown of the membranes of gram-negative bacteria [1] [17] [115] [116] [117]. Transferrin has a similar mode of action to lactoferrin, but is present in much lower concentrations in tears [17] [92] [118]. Albumin forms only a minor component of human tears that has been observed to rise with conjunctival stimulation by inflammatory reaction or irritation [17] [92].

The immunoglobulins found in tears - immunoglobulin A (IgA), immunoglobulin E (IgE), immunoglobulin G (IgG) and immunoglobulin M (IgM) - play a role in the neutralisation of bacteria and viruses. They are synthesised by plasma cells and comprise approximately 20% of the total protein levels of tears [1] [17] [94] [103]. IgA is the most abundant immunoglobulin within tears, often existing in the dimeric form known as secretory IgA (sIgA). IgA has been proposed as the first line of immunologic defence by coating the conjunctiva [119]. Greater amounts of IgE, IgM and IgG are measured in the tear film in the presence of ocular inflammation or conjunctival stimulation during tear sample collection.

1.2.2.2 Surfactant Proteins

Recently, the presence of the surfactant proteins A, B, C and D - key components within lung surfactant - have been identified within the tear film as potential significant components [120] [121] [122] [123]. The surfactant proteins A (SP-A) and D (SP-D) are water-soluble molecules and are thought to exist within the aqueous phase of the tear film where they have been shown to have antimicrobial properties [120] [122] [124]. Surfactant proteins B (SP-B) and C (SP-C) fulfil a role in aiding the formation and stability of the lipid-aqueous interface. They are understood to exist within the tear film lipid layer, embedded within the lipid component of the tear film and orientated accordingly due to the amphiphilic characteristics of the protein molecules [122].

SP-C and SP-B are thought to improve the adsorption and spreading velocity of phospholipids within the polar lipid sublayer to ensure that the lipid-aqueous interface is richer in phospholipids through selective attraction and subsequent prevention of expulsion from the interface [125] [126] [127]. This decreases the interfacial tension between the lipid and aqueous layers, similar to the behaviour observed with lung surfactant at the air-water interface of the alveoli [121] [122]. Currently the roles of these proteins are based upon generalisations gleaned from the roles within lung surfactant. The implications for dysfunctions in surfactant protein production within the tear film should certainly be considered significantly. The decreased presence or absence of SP-B and SP-C could result in alterations of tear film stability. Similarly, decreased production or a lack of SP-A and SP-D might impair the host immune defence of the tear film and lead to bacterial and/or viral infections [122].

1.2.2.3 Metabolites

Metabolites are mainly transported to the tear film from serum. These metabolites predominantly include glucose, squalene, ascorbic acid, lactate and urea [1] [22] [128] [129]. Amino-based metabolites - including amino acids (essential, non-essential and derivatives), amino alcohols and amino ketones - have been identified [128] [130]. Other metabolites include aromatic acids (cinnamic and coumaric acids), carnitines, nucleosides and nucleotides such as cytidine, guanosine, adenosine, inosine and uridine-based phosphates, peptides, cyclic and quaternary amines, pyruvate, and purines (uric acid, xanthine and theobromine) [128] [129].

1.2.2.4 Electrolytes

Electrolyte ions affect the osmolarity of tears (amount of ions that contribute to the osmotic pressure of the tear film). The osmolarity of tears has been measured to be between 282-323 mOsm/kg [131] [132] [133] [134]. A list of the major ions found within the aqueous phase is shown in Table 1.6 [135] [136] [137]. The predominant cations found in the aqueous phase are sodium (Na^+) and potassium (K^+) (131-133 mmol/L and 23-24 mmol/L respectively). Smaller concentrations of magnesium (Mg^{2+}) and calcium (Ca^{2+}) are also found (0.5-1.0 mmol/L). Bicarbonate (HCO_3^-) and chloride (Cl^-) ions are the main anions detected (~33 mmol/L and 96-130 mmol/L respectively) [134] [135] [138]. The concentration of ions within the tear film is similar to that within serum with the exception of potassium (~3-6 times higher).

Ion	Conc. (mmol/L)	Ion	Conc. (mmol/L)
Na ⁺	131.0 - 133.2	Mg ²⁺	0.6
K ⁺	23.0 - 24.0	HCO ₃ ⁻	32.8
Ca ²⁺	0.8 - 1.0	Cl ⁻	96 - 130

Table 1.5. Electrolyte composition of the aqueous phase

1.2.2.5 Mucin

Mucins are high molecular weight glycoproteins with large degrees of glycosylation (50-80% of their mass comprised of carbohydrates) that are secreted onto the corneal surface by the goblet cells located in the conjunctiva [139] [140] [141] [142]. Within the tear film mucin is present in three main forms: membrane-bound, gel-forming and solubilised (Table 1.6). The membrane-bound mucins (MUC1, MUC4 and MUC16) form the glycocalyx [15] [143] [144] [145] and interact with gel-forming mucins (MUC2 and MUC5AC) to form the high-concentrate mucin region at the tear film-corneal interface [146]. The main role of the membrane-associated and gel-forming mucins is to maintain hydration and prevent desiccation by forming a hydrophilic layer over the hydrophobic corneal epithelium. This facilitates the spread of the aqueous layer evenly over the ocular surface [15] [143] [144] [145] [147] through decreasing surface tension. Soluble mucins are present in the aqueous layer [15] [143] and as an absorbed layer at the lipid-aqueous interface [3] [32] [89]. At the air-liquid interface, mucin interacts with Meibomian lipids that would also aid spreading and promote condensation of the lipids that increased the tear film thickness through Marangoni flow.

Gene	Characteristic	Gene	Characteristic
MUC1	Membrane-associated	MUC9	Secreted
MUC2	Gel-forming/secretory	MUC11	-
MUC3A	Membrane-associated	MUC12	Membrane-associated
MUC3B	Membrane-associated	MUC13	Membrane-associated
MUC4	Membrane-associated	MUC15	Membrane-associated
MUC5AC	Gel-forming/secretory	MUC16	Membrane-associated
MUC5B	Gel-forming/secretory	MUC17	Membrane-associated
MUC6	Gel-forming/secretory	MUC19	Secreted
MUC7	Soluble/secretory	MUC20	Membrane-associated
MUC8	-		

Table 1.6. Tear film mucin genes.

1.3 Surface Chemistry

In order to understand why the lipid-aqueous layer is stable, it is important to study the fundamentals of interfacial science in terms of molecular behaviour as a way to understand the stable and unstable lipid-aqueous interface. An interface is defined as the region where two dissimilar phases meet: either two different states (e.g. liquid-gas, liquid-solid, solid-gas) or two phases of the same state with different characteristics (e.g. two liquids with different densities). It is thought the interface has a negligible thickness when compared to the bulk phases of both components, but at the molecular level the thickness is significant and the properties of the interfacial region are an important factor to consider [34] [35]. Throughout this thesis, the term 'surface' will be used when discussing gas-liquid interfaces and 'interface' will be used primarily when discussing liquid-liquid interfaces.

1.3.1 Defining The Interfacial Region

At a fluid interface between two continuous phases (where one or both phases is a liquid) there is a region where the properties change from that of either continuous phase. The properties of the interface are important at the molecular level, especially if there are small concentrations of one continuous phase dispersed within another. The interfacial region is characterised by heterogeneity and non-uniformity where components from both phases interact with each other.

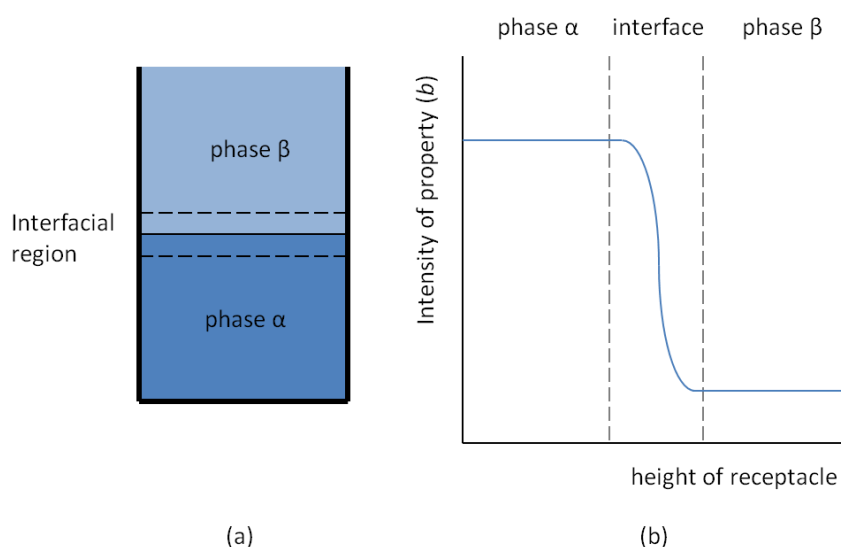


Fig 1.12. Example interfacial system: (a) interfacial region σ between two homogeneous phases (phase α and phase β); (b) Profile of the intensity of an extensive property (e.g. density, concentration, free energy) across the interface.

The system shown in Fig 1.12 is divided into three regions: a continuous phase α (liquid subphase), a continuous phase β (either air or a second liquid) and the interfacial region σ . Properties such as concentration and density do not smoothly transition from one continuous phase to the other. The behaviour and structure of the interface depends entirely upon the chemical characteristics of the components that comprise that region.

1.3.2 Surface and Interfacial Tension

Surface tension (γ) - and by extension, interfacial tension (γ_i) - represents extra energy within a system. This is an unfavourable state to be in and systems will attempt to minimise the surface free energy by contraction of the surface area. It is helpful to picture the system in molecular and energy terms. The forces that act upon on a molecule at the surface and within the bulk of the liquid are different (Fig 1.13). A molecule in contact with a neighbour is in a lower state of energy than if it were not in contact with another molecule. Molecules within the bulk phase experience attractive forces from all directions, with no net force pulling the molecule in any one direction. A molecule within the bulk phase has the maximum number of neighbours and therefore has the lowest energy. Molecules situated at the surface experience an unbalanced force due to the relative scarcity of other molecules in the direction of the gas phase. These molecules are in a higher energy state than those in the bulk.

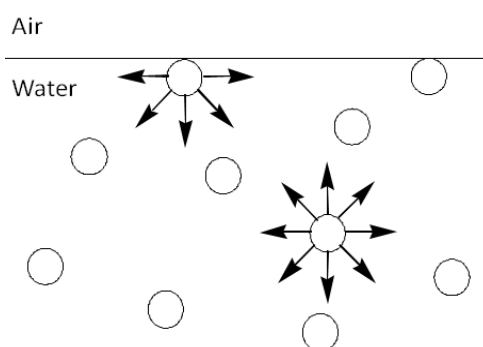


Fig 1.13. Attractive forces between water molecules within the bulk and at the surface [35].

In order to minimise the Gibbs free energy (ΔG) and maintain stability at equilibrium, the surface area of the interface will tend to a minimum by decreasing the number of higher energy boundary molecules. Gibbs free energy is a thermodynamic potential that measures the amount of work exchanged by the system with its surroundings when it changes from a well-defined initial state to a well-defined final state. All spontaneous changes to the system are accompanied by a decrease in Gibbs free energy. Decreasing the surface area is always

favoured over an increase of the surface area. Surface tension is defined as the Gibbs free energy (ΔG) required to expand the surface area by unit amount (ΔA).

$$\gamma = \Delta G / \Delta A \quad \text{Eq 1.1}$$

The SI units of surface tension are milliNewtons per metre (mN/m) although dynes per centimetre is often used in the literature (1 mN/m = 1 dynes/cm).

The example shown in Fig 1.13 is the situation observed in pure water. The large degree of hydrogen bonding that occur between water molecules produce the strongest attractive forces of any liquid except for the metallic bonding within mercury. The surface tension of pure water produces a value of 72.8mN/m at STP. The short range intermolecular forces which are responsible for surface or interfacial tensions include van der Waals forces (dispersion forces) and hydrogen bonding (polar forces). Because these forces are independent of each other, it is assumed that they are additive and that the surface tension of water can be considered a sum of the polar ($\gamma_{\text{water}}^{\text{p}}$) and dispersive ($\gamma_{\text{water}}^{\text{d}}$) force contributions (Eq 1.2).

$$\gamma_{\text{water}} = \gamma_{\text{water}}^{\text{d}} + \gamma_{\text{water}}^{\text{p}} \quad \text{Eq 1.2}$$

The principals of surface tension within a single component liquid are expanded when dealing with two immiscible liquids such as the floating of oil upon water. In hydrocarbon liquids there is no polarity in the structure of the hydrocarbon molecule and the surface tension is entirely due to the dispersive forces. When spread upon the surface of water, the two phases are immiscible and the oil spreads upon the surface rather than become dissolved. The interface is a product of interactions between components within and between each phase (Fig 1.14).

At an interface between two liquids there is an imbalance of forces, but these are of a lesser magnitude when compared to a liquid-air interface. As shown in Fig 1.14, water molecules at the interface are surrounded by both water and oil molecules. The same is seen for oil molecules. Water molecules in the interfacial region will interact with other water molecules in water-water interactions - a result of both dispersion and polar forces - and with the oil molecules in close proximity by the dispersive forces of oil-water interactions.

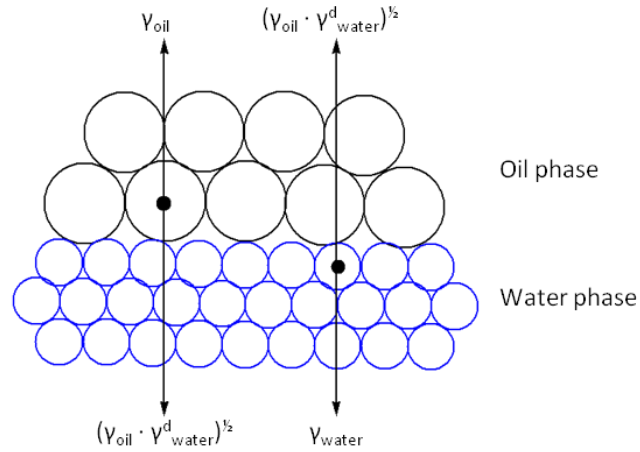


Fig 1.14. Attractive forces between molecules at the interface between two immiscible liquids [35].

Oil molecules within the interfacial region are attracted to the bulk oil phase by oil-oil interactions and to water by oil-water interactions, both of which are as a result of dispersion forces. Fowkes [148] outlined the relationship of polar and dispersive forces at the interface between water and oil molecules (Eq 1.3 and 1.4). This value usually lies between the surface tension of the two individual liquids. These relationships can be applied to any two liquids that form an immiscible system where one spreads upon the surface of the other.

$$\gamma_{\text{Oil-Water}} = \gamma_{\text{Oil}}^d + (\gamma_{\text{Water}}^d + \gamma_{\text{Water}}^p) - 2 \cdot (\gamma_{\text{Water}}^d \times \gamma_{\text{Oil}}^d)^{1/2} \quad \text{Eq 1.3}$$

$$\gamma_{\text{Oil-Water}} = \gamma_{\text{Oil}} + \gamma_{\text{Water}} - 2 \cdot (\gamma_{\text{Water}}^d \times \gamma_{\text{Oil}})^{1/2} \quad \text{Eq 1.4}$$

1.3.3 Adsorption

Adsorption is the energetically-favourable tendency for one component of a system to be found in higher concentrations at an interface between two continuous phases. Surface active agents (surfactants) are an example of polar molecules that accumulate at an interface as a result of the balance between hydrophobic and hydrophilic regions. Such materials adsorb at the interface and are crucial to the process of detergency (the dispersal of oils into water that would otherwise be insoluble). The forces affecting the polar head groups submerged in the aqueous subphase are due to hydrogen bonding whilst the forces between the hydrocarbon chains are due to the longer range van der Waal's interactions.

1.3.4 Wetting and Spreading

The wettability of a solid or liquid surface is determined by the forces acting at the three relative interfaces between the surface (solid or liquid), gas and liquid (Fig 1.15). When a droplet of liquid is placed on a surface, a three phase boundary is formed. The relationship between the surface and interfacial tensions between the three phases and the contact angle can be defined by Eq 1.5.

$$\gamma_{GS} = \gamma_{LS} + \gamma_{GL} \cos \theta \quad \text{Eq 1.5}$$

The forces that arise from interactions between the liquid droplet and the surface (γ_{LS} for a solid surface; γ_{L1-L2} for a liquid subphase surface), the surface tension of the liquid droplet (γ_{LG}) and surface tension of the solid or liquid subphase (γ_{GS}) will spontaneously change until the system reaches a point of equilibrium where the forces are balanced. These forces determine the wetting behaviour of a liquid component.

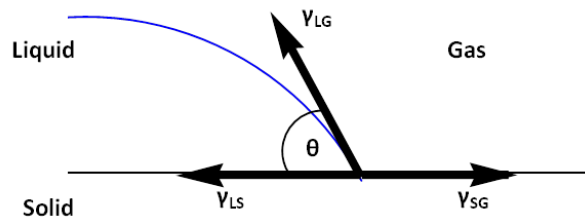


Fig 1.15. The triple interface between gas, liquid and solid phases [34] [35].

The spreading coefficient (S) of surfactant molecules on a liquid surface (Fig 1.16) can be calculated by the equation to account for one liquid spreading upon another (Eq 1.6). In order to calculate the spreading coefficient, it is necessary to know the surface tension of the surfactant component and the liquid, and the interfacial tension between the two layers. The lowest energy configuration is thermodynamically favoured and determines the spontaneity of spreading. Positive values of the spreading coefficient means that the surfactant molecule will spread spontaneously as a monolayer or duplex film. A negative value - often observed with non-polar molecules - causes the formation of droplets on the surface that form to minimise the amount of unfavourable, higher energy sites of oil-water interactions.

$$S = \gamma_{WA} - (\gamma_{OA} + \gamma_{WO}) \quad \text{Eq 1.6}$$

γ_{WA} is the surface tension of the liquid, γ_{OA} is the surface tension of the surfactant oil molecule and γ_{WO} is the interfacial tension between the two components.

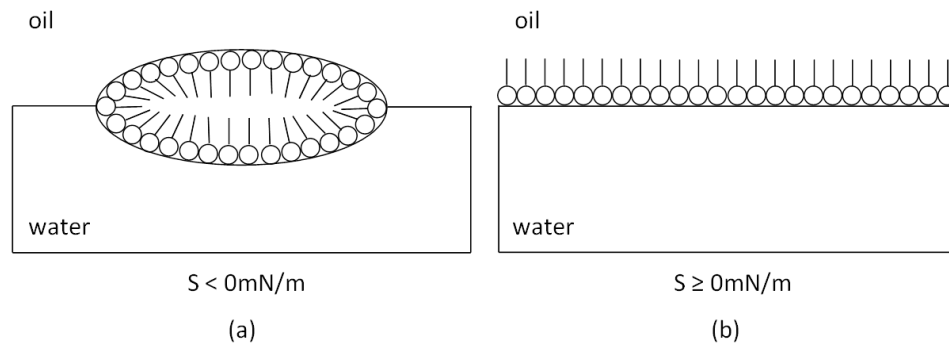


Fig 1.16. Behaviour of oil molecules on the surface of water: (a) lens formation; (b) surface spreading.

1.4 Interfaces in Biological Systems

Biological interfaces form some of the most fundamental and important aspects of life and many of these system are dominated by interfacial science. The fluid mosaic model of cell membranes highlights the bilayer structure with specific membrane proteins accounting for the selective and controlled permeability of solutes through the membrane, and passive and active transport mechanisms. The bilayer forms by the spontaneous arrangement of phospholipid molecules so that the hydrophobic regions are isolated from the surrounding polar fluid. The hydrophilic regions associate with the intracellular (cytosolic) and extracellular faces of the resulting bilayer.

An important example of a biological interface-driven system concerns the inner lining of the lung. A layer of fluid lines the alveoli within lungs to form a barrier between those and the air breathed in. At the surface of this fluid - in direct contact with the air - is a monolayer mixture called lung (or pulmonary) surfactant. It is a surfactant mixture that contains phospholipids (predominantly DPPC) and four surfactant proteins designated SP-A, SP-B, SP-C and SP-D. Lung surfactant maintains the active process of gaseous exchange by the alveolar tissue by ensuring the functionality of the large exchange area and allowing expansion of the lungs by the reduction of surface tension [125] [127].

The components and layers within the tear film - specifically those at the lipid-aqueous interface - are dominated by interfacial chemistry. The biphasic formation of the lipid layer shown in Fig 1.13 theorises that polar lipids within act as surfactant molecules that favourably interact with water within the aqueous phase [12] [13]. The interfacial tension between the polar and non-polar phases of the lipid layer, as well as that between the polar lipid layer and the aqueous phase, are important physical properties of tears that enables spreading and formation of the stable tear film across the ocular surface.

1.5 Stability of the Lipid-Aqueous Interface

The lipid-aqueous interface is understood to play a significant role in the overall stability and function of the tear film [9] [40] [42] [149] [150] [151]. Components from both the lipid layer and the aqueous layer are thought to contribute to the formation of a stable interfacial region [32] [38].

1.5.1 Tear Film Stability as a Function of Surface Tension

The nature and behaviour of surface active lipid molecules within tears has long been associated with stabilisation of the tear film [152]. Low values of surface tension have been observed in highly stable tear films that show high break-up times [32] [33] [153]. Holly stated that the tear film is stable if the total free energy of the film - the sum of the surface and interfacial tensions of the tear film layers - is less than the corneal epithelium surface free energy [15] [36] [54]. It is important to understand the impact of the free energy of the tear film based on the components.

Surface tension measurements of tear samples by Tiffany indicate a difference in values from healthy and unhealthy tear films [32]. A stable tear film was shown to have a lower surface tension when compared to that of a tear sample from a patient that suffered from a common ocular dysfunction that is affected by changes in the composition of the tear film leading to an inadequate tear film. Minimum surface tension (γ_{\min}) values of 42-46 mN/m was reported on measurements of healthy, normal tear films whereas γ_{\min} values in the range of 50-53 mN/m were obtained from tear films that suffered from dry eye disease [32]. If assuming that the differences in interfacial areas between patients are negligible, the Gibbs free energy of the healthy tear film would be lower and therefore more stable.

These values correlate with measurements of lipid-extracted healthy tear films [32] [38] [33] [154]. Changes in the quantity or composition of meibum as a result of ocular dysfunction result in a change in the interactive forces that occur at the lipid-aqueous interface that may compromise the health of the ocular surface and lead to pathological conditions such as dry eye disease [21] [54] [155].

1.5.2 Physicochemical Structure of the Lipid Layer

The stability of the lipid-aqueous interface has also been attributed to the viscoelastic and thixotropic properties of the lipid layer [10] [12] [13] [15] [42] [151]. Thixotropy is a shear thinning property which is essential for the proper fluidisation and restructuring of the lipid layer during a blink. A thixotropic fluid show non-Newtonian pseudoplastic properties that are viscous under normal conditions and become less viscous over time when agitated or stress is applied. These fluids take time to reach an equilibrium viscosity when a step change in shear rate is introduced and will return to a more viscous state upon removal of the shear stress.

The lattice model structure of the lipid layer proposed by McCulley and Shine [12] [13] produces viscoelastic properties essential for fluidisation and compressibility during a blink and restructuring through the replenishment of lipid molecules [12] [80] [156]. Studies have shown that large regions of the lipid layer show a constant, stable structure that is maintained over a series of blinks. During a blink, the lipid layer is folded during the down-phase as it approaches the lower lid margin and unfolds as the eye lids open in the up-phase. The folds remain separated by the repulsive forces between lipid molecules at the anterior face of the sheet and by lipid-protein complexes near the lipid-aqueous interface. Spreading of the lipid layer as the eyelids open is promoted by the repulsive forces between lipid molecules aided by the unsaturated fatty acid content of tear lipids.

1.5.3 Lipid Layer Spreading

A triple interface can be used to represent the lipid layer spreading and breaking across the aqueous layer. The interactive forces that occur at the interface between the lipid and aqueous layers dictate the spontaneous spreading ability of the lipid layer. It has been observed to spread rapidly and uniformly upon transference from the marginal lid reservoir to the tear film. This promotes rapid resurfacing of the tear lipid layer during prolonged exposure

to air that causes breakup of the tear film lipid layer. Kinetic studies of the spreading lipid layer show that the lipid layer spreads to form a stable film ~1 second after the eyelids open. The velocity of spreading decreases significantly continuing long after upper lid movement has completed (~300msec) [150] [157] [158]. The visible spreading of the lipid layer has been a suggested observation for the more numerous non-polar lipids that represents the dispensation between full layer stabilisation and the completion of a blink. The polar lipids still form the surfactant layer between aqueous and non-polar sublayer but are not visible using conventional microscopic techniques [13] [15].

1.5.4 The Role of Protein and Aqueous Layer Components

Whilst the lipid layer has been shown to be the principal factor in the lowering of surface tension and the increase in stability, the concept that the interface between lipid and aqueous layers is comprised of just the lipid has been challenged. The interactions between lipids and protein components within the aqueous layer must also be considered [32] [38]. The lipid binding characteristics of tear lipocalin may prove beneficial for stabilisation through interaction with the polar lipid sublayer and may also play a role in the removal of unwanted lipid molecules [52] [104] [105] [106]. The stabilising association of lipocalin has been demonstrated to have a significant effect at the interface to a similar extent that the Meibomian lipids have [36] [38] [51]. Other tear film components such as soluble mucins, lysozyme and lactoferrin are also surface active. In most cases, a synergistic environment is believed to exist whereby the various proteins, mucins and lipids all interact with each other to some extent that provides an increase in stability [32] [37] [38] [154] [159]. The presence of the surfactant proteins B (SP-B) and C (SP-C) aid in the formation and stability of the lipid-aqueous interface [120] [121] [122] [123]. SP-B and SP-C are thought to be embedded within the lipid layer and improve the adsorption and spreading velocity of phospholipids within the polar lipid sublayer. This ensures that the lipid-aqueous interface is richer in phospholipids through selective attraction and subsequent prevention of expulsion from the interface [125] [126] [127].

1.6 Degradation of Tear Film Stability

The tear film is under constant stresses and strains by the environment within and without the ocular system. Biochemical changes to the delivery and/or structure of tear film components, changes within the environment outside the body (such as temperature, wind, humidity) and the use of artificial materials in improving sight can have a dramatic effect on the stability and function of the tear film, often to a detrimental effect.

1.6.1 Ocular Diseases

Stability of the tear film can be affected by common ocular dysfunction and diseases. The common problems exist due to some alteration to the composition and/or production of the tear film components, most commonly in the lipid layer. Meibomian gland dysfunction (MGD) is an abnormality of the Meibomian glands that is commonly characterised by obstruction of the glands and/or changes in quality of the lipid secretion [160] [161]. As lipid production is decreased, the lipid layer of the tear film is thinner and far less stable, leading to an increase in tear break up time (TBUT) and evaporation. MGD is often associated predominantly with evaporative dry eye disease (EDE) where the patient suffers from desiccation of the cornea caused by the lipid-deficient tear film evaporating more rapidly [162] [163] [164]. Aqueous deficient dry eye (ADE) has also been suggested as being affected by the abnormal lipid production due to Maragani flow of lipid molecules throughout the tear film [161]. Pre-corneal non-invasive tear break-up time (NI-TBUT) has been used to assess the stability of the tear film in dry eye patients, finding that NI-TBUT for the EDE patients are lower (3-10 seconds) when compared to healthy tear films (20-30 seconds) [42] [165] [166].

1.6.2 Degradation of Tear Lipids - Oxidation and Hydrolysis

Tear lipids can undergo degradation by two main pathways - hydrolysis of ester bonds and autoxidation of unsaturated fatty acids [167] [168] - and can occur through enzymatic or non-enzymatic pathways.

1.6.2.1 Hydrolysis

Complex lipids such as wax esters, sterol esters and acylglycerides can undergo non-enzymatic hydrolysis that separates the molecule at the ester bond to produce a larger amount of 'simpler' molecules such as free FA, free FALc, cholesterol and glycerol (Fig 1.17) [167]. Phospholipids are hydrolysed by enzymatic hydrolysis through the action of phospholipases (Fig 1.18). Acyl chains are cleaved through the action of phospholipase A1 (PLA₁) and A2 (PLA₂) which cleaves the fatty acid at position 1 and position 2 respectively or through the hydrolysis by phospholipase B (PLB) which cleaves both fatty acids. Phospholipases C and D (PLC and PLD) hydrolyse bonds within the phosphate group. PLC cleaves before the phosphate group to produce a DAG and the phosphatidyl alcohol head group. PLD cleaves after the phosphate group to produce a phosphatidic acid and an alcohol [169] [170].

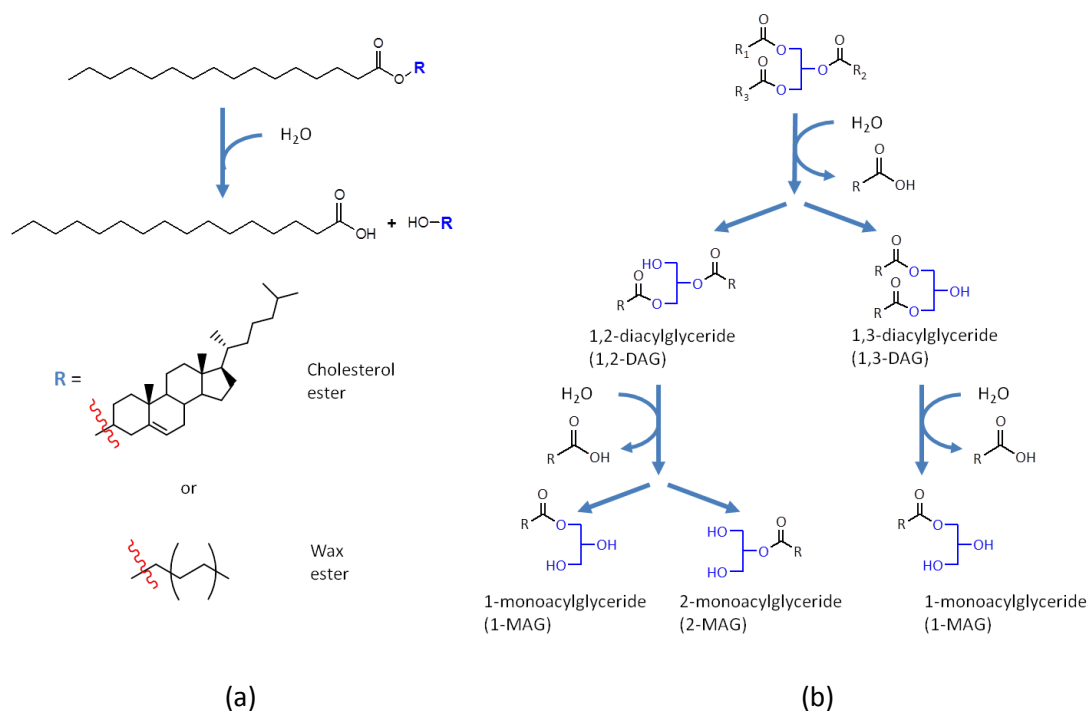


Fig 1.17. Hydrolysis of non-polar lipids: (a) wax esters and cholesterol esters (R = FALc / Ch); (b) triacylglycerides (R = FA).

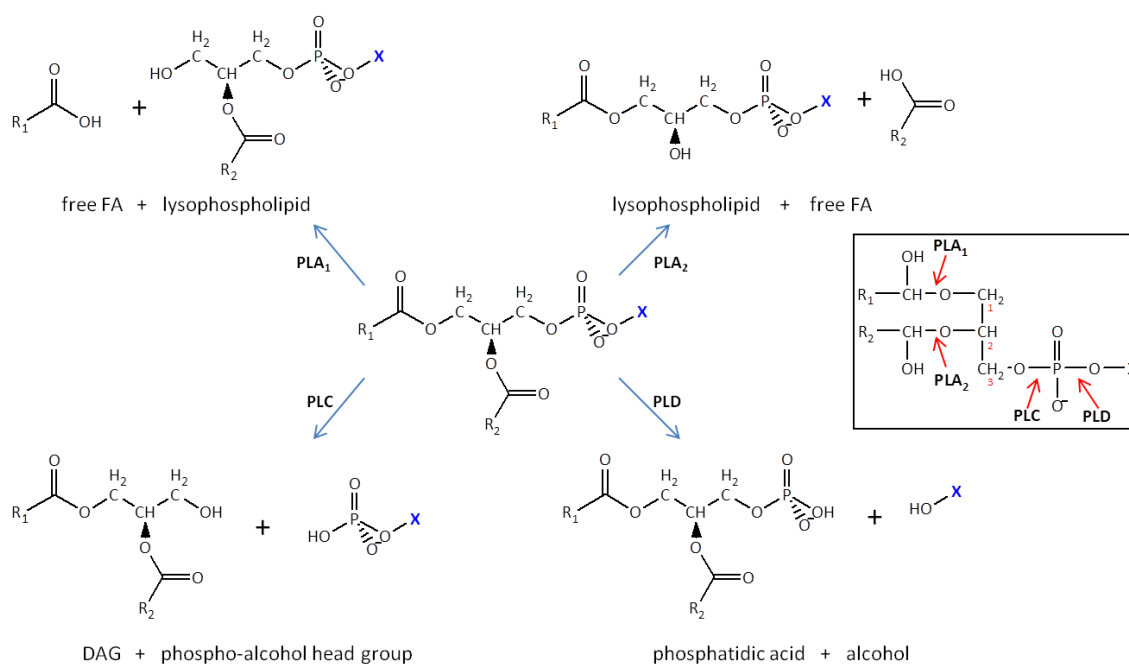


Fig 1.18. Enzymatic hydrolysis by phospholipases on phospholipid molecules.
Inset - position on the phospholipid molecule where each phospholipase cleavage occurs.

Despite the degradation of these key lipid types, it may be somewhat beneficial. The major hydrolysis products of wax esters, cholesterol esters, glycerides and phospholipids - fatty acids, fatty alcohols, DAGs and MAGs - are predominantly polar molecules. Despite the need for the non-polar lipids to produce the stable thick tear film, the proposed biphasic formation of the lipid layer would be enhanced by an increase in the polar lipid composition caused by hydrolysis of a small amount of these molecules [77].

1.6.2.2 Oxidation

Whilst hydrolysis could be potentially beneficial in generating polar lipids, lipid degradation through autoxidation produces harmful products that may inhibit stability within the tear film. Due to the exposed nature of the corneal surface, the tear film is at particular risk of oxidative damage by photo-induced and environmental reactive oxygen species (ROS) [75] [171] [172] [173] [174] [175]. Autoxidation is much more complex because a number of factors can cause the breakdown of lipids via this route. The key factors that influence autoxidation are higher oxygen concentrations, unsaturation and levels of antioxidant concentration. There are many routes that oxidation of acyl chains can undergo - with many intermediate products formed - that vary dependent on conditions. One of the major prerequisites for lipid oxidation is the presence of one or more double bonds in the lipid structure.

The double bonds can undergo enzymatic or non-enzymatic oxidation. Lipids that contain fatty acid chains with higher degrees of polyunsaturation ($n > 2$) are more susceptible to autoxidation due to the ease of extracting an allylic hydrogen from the unconjugated double bond system [123] [167] [168] [175]. Table 1.7 shows the rates of oxidation for 18-carbon fatty acids with varying degrees of unsaturation ($n = 0 - 3$).

Fatty Acid	Unsaturation	Relative Rate of Oxidation
stearic acid	0	1
oleic acid	1	100
linoleic acid	2	1200
linolenic acid	3	2500

Table 1.7. Rates of oxidation of fatty acids [175]

Figs 1.19 and 1.20 show how unsaturated fatty acids can undergo autoxidation and the formation pathways of intermediate oxidative products that can be formed. These intermediates are unstable and will therefore oxidise further to produce various hydroperoxy-oleic acid end products. Malondialdehyde (MDA) is a common oxidation product formed from polyunsaturated fatty acids. MDA has been shown to cause tissue damage through disruption of the normal function of proteins and DNA by reaction with thiol and amino groups within the molecule structure [168] [176]. If a high level of MDA is present due to PUFA oxidation, this may lead to a loss in function of the key proteins within tears affecting both biochemical and physical stability.

The tear film contains antioxidants that act to prevent oxidative damage by neutralising and removing reactive oxygen species (ROS) [177] [178] [179] [180] [181] [182]. The most abundant antioxidants in tears are ascorbic acid and uric acid, which constitute ~50% of the total antioxidant activity in tears, and cysteine, glutathione and tyrosine [177] [178] [179] [180] [181] [183]. The tear proteins lysozyme and lactoferrin have also been shown to have antioxidative roles in tears [135] [174] [182].

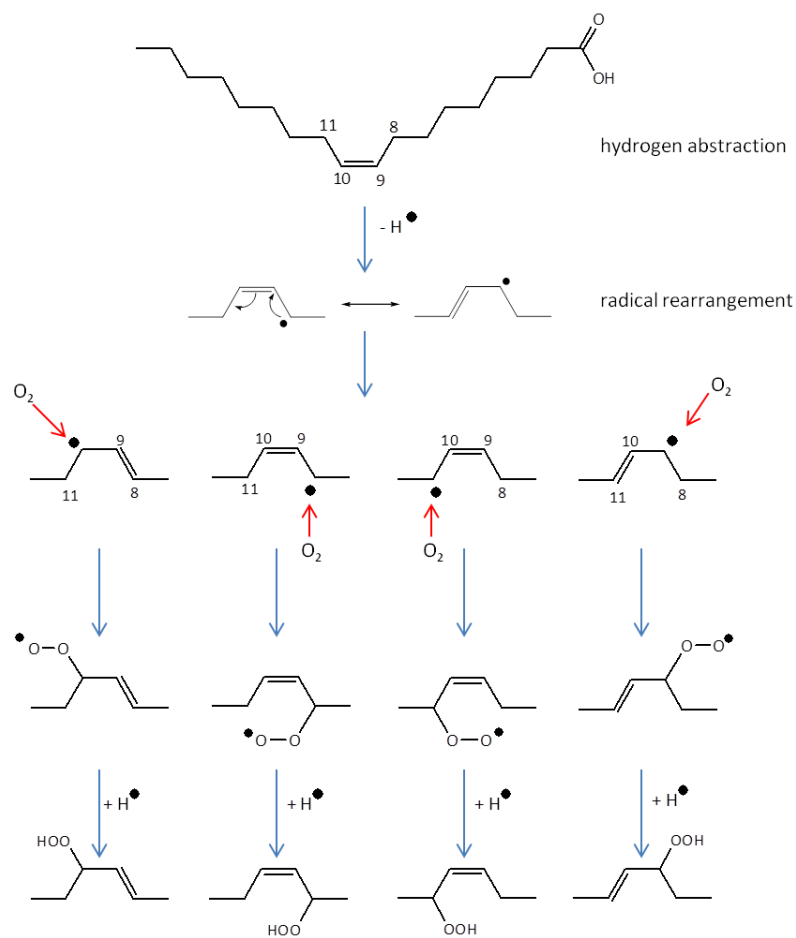


Fig 1.19. Oxidation of unsaturated fatty acids.

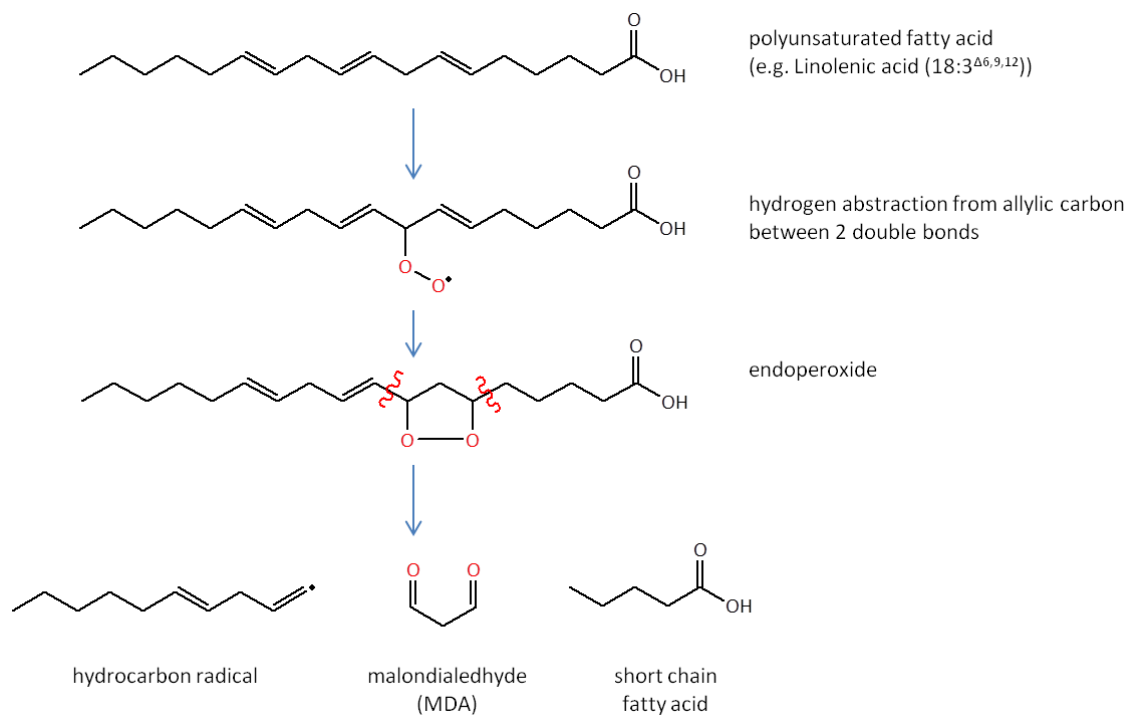


Fig 1.20. Formation of malondialdehyde (MDA) from oxidation of a polyunsaturated fatty acid (PUFA).

1.6.3 Contact Lens Wear

In the last few decades, the use of contact lenses as an alternative to spectacles in improving eyesight has grown significantly in popularity and has become a huge global business. There are approximately 130 million wearers of contact lenses worldwide with around 3.7 million wearers in the UK (~7.5% of the population) and 38 million in the USA (~12% of the population) [184] [185]. However, the numbers belie the percentage that discontinue lens wear as a result of a loss in visual acuity, severe discomfort and the onset of ocular diseases [186] [187] [188].

1.6.3.1 Development of Contact Lenses

The original contact lenses were constructed of polymethylmethacrylate (PMMA) which interfered with the functions of the tear film (such as oxygen permeability and stability) and had issues of high modulus effects on the comfort of the eyelid and corneal surfaces. Oxygen permeability was improved with the advent of rigid gas permeable contact lenses but these still suffered with issues of ocular comfort. The advent of hydrogel-based contact lens materials based on the hydrophilic polymer polyhydroxyethylmethacrylate (polyHEMA) vastly improved the market due to increased comfort and ease of manufacture. In terms of comfort, these conventional hydrogels had decreased modulus, improved wettability and good permeability that provided oxygen to the avascular cornea during the normal course of wear. Additional monomers and crosslinking agents have been used to modify the lens in order to improve water content and wettability.

With the increased popularity of contact lenses came the demand for increased wear times including 24-hour wear. Contact lenses interfere with the natural supply of oxygen (oxygen permeability; Dk) from tears especially during closed eye. In the open eye, this interference is minimal and the supply of oxygen is sufficient. Within the closed eye environment, oxygen permeability is decreased to severe hypoxic levels. Hence, contact lens materials needed to be developed in order to improve overnight oxygen transmission. Holden and Mertz [189] determined that to prevent hypoxia in the closer eye, a contact lens of 0.1mm centre thickness should have an oxygen permeability of 87 barrers. This led to the third generation of lenses that introduced silicone into the hydrogel polymer: silicone hydrogels (SiHy).

As the Si-C bond (1.87-1.90 Å) is longer than the C-C bond (1.2-1.5 Å) steric hindrance of the polymer chain is reduced and oxygen diffusion through the material is greatly improved. In addition to the mechanical and surface properties of hydrogel materials, the silicon-based monomers were utilised to form a polymer that produced a soft material with high oxygen permeability. With the solution to the oxygen permeability issue resolved, new problems arose in the inherent water-repellent properties of SiHy lenses and the potential issues of biocompatibility within the tear film. In order to improve wettability of the SiHy contact lens, surface modification or internal wetting agents have been introduced to produce a wettable lens surface. Whilst surface modification has gone some way to address the issues of wettability within the tear film, the tendency of polymer chains to rotate exposes more hydrophobic regions making SiHy contact lenses still highly susceptible to lipid deposition.

1.6.3.2 Biocompatibility

Any artificial material being placed within a biological system experiences issues of biocompatibility. For a contact lens to be considered biocompatible, it must behave like the natural corneal surface as best as possible. If it performs its intended function of correcting vision during wear, fits well within the geometry of the ocular environment with the desired incorporation in to the tear film without any undesirable effects, then the likelihood of tolerant contact lens wear will increase. The ocular environment is a dynamic system and the introduction of a contact lens produces three main interactions that affect lens biocompatibility: the corneal/conjunctival surfaces, the eyelids and the tear film [190]. When placed in to the tear film, the factors that induce biocompatibility include the wetting of the contact lens, the pre- and post-lens tear film environments, the conditions of the front and back surfaces of the lens and the adsorption of lipid and protein components onto and into the lens.

As the thickness of a contact lens is ten times that of the tear film the structure of the tear film is altered, creating a pre- and post-lens tear film (PLTF and PoLTF respectively) environment (Fig 1.21) [131] [191] [192]. The changes to the structure of the tear film, specifically the PLTF between lens and the air, affect the stability and function of the tear film and can ultimately lead to severe problems to the health of the ocular system. To maintain a stable, functional PLTF, the contact lens must remain wetted in order to act as an effective anchor for the tear film [131] [193].

The corneal surface comprises membrane-bound mucins that act as a hydrophilic base for the aqueous layer. The relatively hydrophobic surface of the contact lens, whether through material- or lipoprotein deposition-based behaviour, means that the aqueous layer forms an altered supportive base for the lipid layer to spread naturally, decreasing the stability imparted to the tear film by lipid molecules [191].

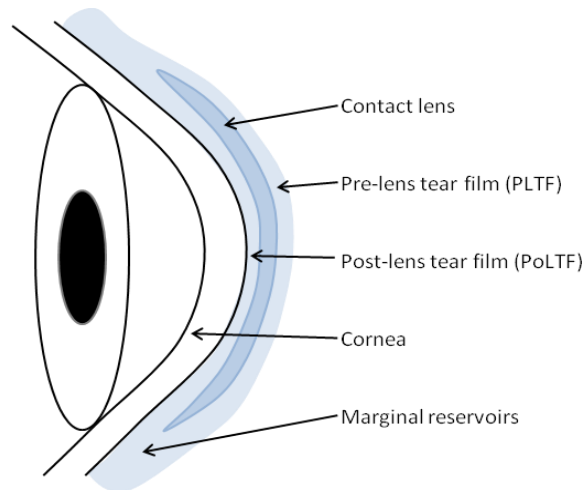


Fig 1.21. Position of contact lens in the tear film.

Like most biomaterials, components from the natural system interact with the artificial material. In the case of contact lenses, deposition of lipid and protein components of the tear film can occur predominantly on the front surface of the lens. This deposition occurs at the lens surface and can even penetrate in to the lens matrix and occurs almost instantaneously upon lens insertion and continues throughout the wear time [194] [195]. A small degree of deposition is often beneficial to aid in initial biocompatibility of the lens, especially of hydrophobic lens surfaces, but often deposition continues with more non-polar lipids interacting with the lens surface that reduces wettability.

1.6.3.3 Lipid Degradation during Contact Lens Wear

Lipid adsorption combined with increased lens wear time and progressively larger deposition from the tear film is detrimental to the long-term biocompatibility of SiHy lenses [168] [190] [191]. Whilst initial deposition upon lens insertion proves beneficial in forming a base layer for the aqueous phase, the breakup of the tear film due to the altered state of the PLTF exposes the lens surface to the lipid/air interface and deposition is increased. The deposited lipid components at the lens surface become dominated by hydrophobic lipids such as cholesterol

and wax esters. Once immobilised, lipids are more susceptible to various degradation reactions such as autoxidation, enzymatic hydrolysis and oligomerisation. This increases dewetting of the lens and ultimately the biocompatibility of the lens [190]. The autoxidation of unsaturated fatty acids can lead to the production of harmful oxidative end products such as malondialdehyde (MDA) and hydroperoxide fatty acids [168]. Significantly higher levels of MDA have been detected in the tears of intolerant contact lens wearers [176].

1.6.3.4 Tear Breakup and Contact Lens-related Dry Eye Disease

Contact lens-related dry eye is a commonly observed condition amongst lens wearers. Approximately 25-50% of contact lens wearers report experiencing dry eye symptoms [196] [197] [198] [199] [200]. An increased rate of tear layer thinning and faster tear break up times (TBUT) is observed in contact lens wearing patients [41] [46] [193] [201] [202]. Measurement of TBUT is taken from a completed upwards movement of the eyelid during a blink to the first onset of a dry spot or streak within the tear film: the longer the TBUT, the more stable the tear film generally is [131] [165] [202] [203]. TBUT is usually measured under non-invasive methods (NI-TBUT) due to the reported destabilising effect that fluorescein (or any fluorescent molecule) has on the tear film [204] [205]. The PLTF has a thinner aqueous phase that alters the spreading behaviour of tear lipids, forming a lipid layer that is much thinner and not as stable as that of the PCTF [46] [159] [206] [207].

Tolerant contact lens wearers show TBUT similar to those of healthy, non-contact lens wearing tears whilst intolerant contact lens wearers show an immediate decrease in TBUT similar to those seen in cases of dry eye disease. Patients that have been observed to show an initial tolerance to contact lens wear show a significant decrease in TBUT towards similar levels of initially intolerant wearers over the course of a day's wear. Intolerant wearers show only a slight decrease in NI-TBUT from the initial [202] [208] [209] [210]. Patients that show the onset of dry eye symptoms during contact lens wear have pre-lens TBUT in the region of 6-8 seconds, well within the range of 3-10 seconds observed in non-contact lens-wearing dry eye sufferers and in symptomatic lens wearers [42] [165] [166] [202] [208] [211] [212] [213]. The mechanisms for contact lens-related dry eye are similar to those that cause a general intolerance to lens wear but are of a much more severe circumstance. It is thought that thicker, stable lipid layers observed before fitting have the best chance of successful contact lens wear [20] [211].

1.7 Langmuir Trough Method

The Langmuir surface pressure balance technique takes the principles of interfacial chemistry and applies them to the dynamic relationship between component molecules at the air-water interface as they are compressed and decompressed. Materials within the bulk and adsorbed at the interface will change the chemistry of the subphase. The Langmuir trough technique involves the use of a shallow trough made of a hydrophobic material (usually PTFE) filled with a liquid subphase (Fig 1.22). Two barriers made of the same hydrophobic material pass across the surface of the subphase and reduce the working area. A balance is used to measure the surface pressure by way of an attached probe situated between the two barriers. This measures the vertical pull of surface tension which is counteracted by the pressure balance and registers the data as surface pressure. Sample material is then spread between the two barriers and the surface pressure measured over the course of surface area compression and expansion.

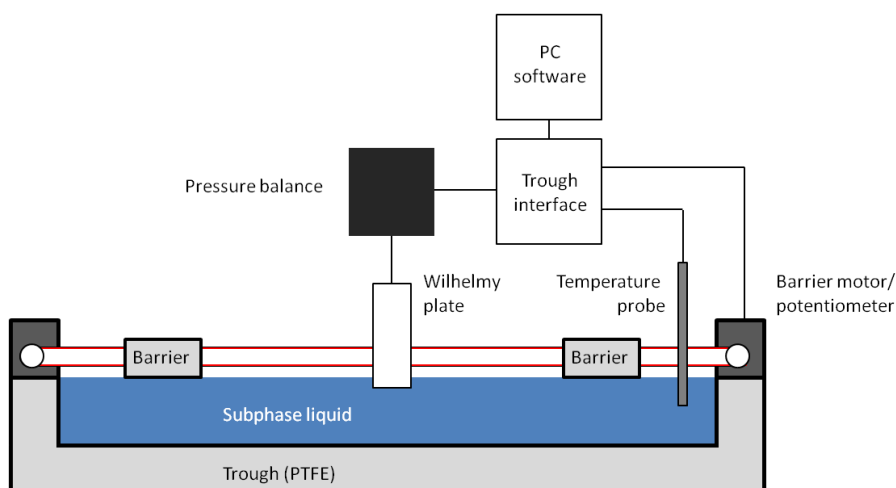


Fig 1.22. Schematic of the Langmuir trough apparatus.

The presence of a monolayer on the surface of water alters the pure-hydrogen bonding based surface pressure measurement (π) for pure water ($\pi_{\text{water}} = 0\text{mN/m}$). Weaker, longer range forces between surfactant molecules and the liquid become an increasing part of the characteristics at the interface and the surface tension is reduced as a result. As such, the surface tension of that monolayer at a certain area can be calculated (Eq 1.7).

$$\gamma_{\text{monolayer}} = \gamma_{\text{water}} - \pi \quad \text{Eq 1.7}$$

1.7.1 Measurement of Surface Pressure

A Wilhelmy plate is used as the probe to measure surface pressure. It is hung from the surface pressure balance and immersed through the gas-liquid interface (Fig 1.23). It is essential that the contact angle for the Wilhelmy plate be zero by using chromatography paper as the probe. These become saturated with water and ensure a contact angle of 0° . This enables surface pressures to be reliably measured during compression (receding contact angle) and expansion (advancing contact angle) whilst giving a greater level of positional control during constant measurement [214]. Whilst roughened plates of mica, platinum or glass are suitable for surface pressure measurements, they can only be used with a receding contact angle.

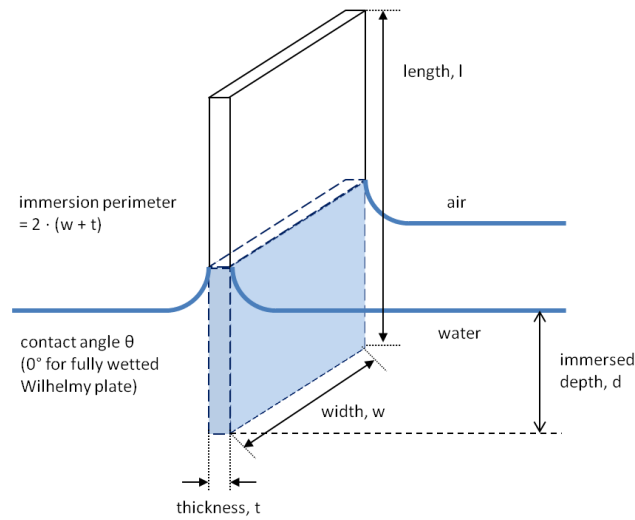


Fig 1.23. Wilhelmy plate diagram [34]

A Wilhelmy plate experiences downward pulling forces due to the weight of the plate and the surface tension of the liquid, whilst buoyancy due to displaced water acts with forces in an upwards direction. A plate with dimensions $l \cdot w \cdot t$ immersed in water to a depth (d) will experience a net force (F) that acts in a downwards direction (Eq 1.8).

$$F = [g \cdot (\rho_{\text{plate}} \cdot l \cdot w \cdot t)] - [g \cdot (\rho_{\text{liquid}} \cdot d \cdot w \cdot t)] + [2 \cdot (w + d) \cdot \gamma \cdot \cos\theta] \quad \text{Eq 1.8}$$

ρ_{plate} is the density of the plate, ρ_{liquid} the density of the liquid, γ the surface tension of the liquid, θ the contact angle of liquid to plate and g the acceleration due to gravity (9.8 m/s^2).

This relationship can be simplified by elimination of the weight term (by taring the pressure balance) and buoyancy term (by maintaining the Wilhelmy plate at a constant immersed depth) to a purely surface tension-based contribution (Fig 1.9).

$$F = [2 \cdot (w + d) \cdot \gamma \cdot \cos\theta] \quad \text{Eq 1.9}$$

The use of a perfectly wetted Wilhelmy plate (by using a chromatography paper plate [214]) ensures a contact angle of 0° . Surface tension can be expressed as a function of the force experienced over the immersed perimeter at the liquid surface (Eq 1.10-1.11).

$$F = [2 \cdot (w + d) \cdot \gamma] \quad \text{Eq 1.10}$$

$$\gamma = F / [2 \cdot (w + d)] \quad \text{Eq 1.11}$$

1.7.2 Surface Pressure-Area Isotherms

Surface pressure studies using a Langmuir trough often involve the preparation of a Langmuir monolayer of the studied material. A Langmuir monolayer is a one-molecule thick layer formed from the amphiphilic surfactant molecules. The balance between the hydrophilic and hydrophobic regions of the molecules defines the solubility of a molecule. The hydrophilic region pulls the molecule into the bulk of the water in order to solubilise it whilst the hydrophobic regions work to prevent this. Insoluble molecules have hydrophobic regions large enough to counteract the polar forces and will adsorb at the gas-liquid interface. The relationship between surface/molecular area and surface pressure is recorded in a surface pressure-area (π -A) isotherm (Fig 1.24). Test material is dissolved in a non-aqueous volatile solvent with a positive spreading coefficient (Table 1.8) and introduced to the subphase surface (commonly pure water). Instantaneous spreading of the solution occurs and the solvent evaporates to leave a spread monolayer of surfactant molecules.

Solvent	S (mN/m)	VP (kPa at 25°C)
Hexane	3.4	20.2
Benzene	8.9	12.7
Toluene	6.8	3.79
Chloroform	13.9	26.2
Water	-	3.17

Table 1.8. Spreading coefficients on water and vapour pressures of solvents [34] [215].

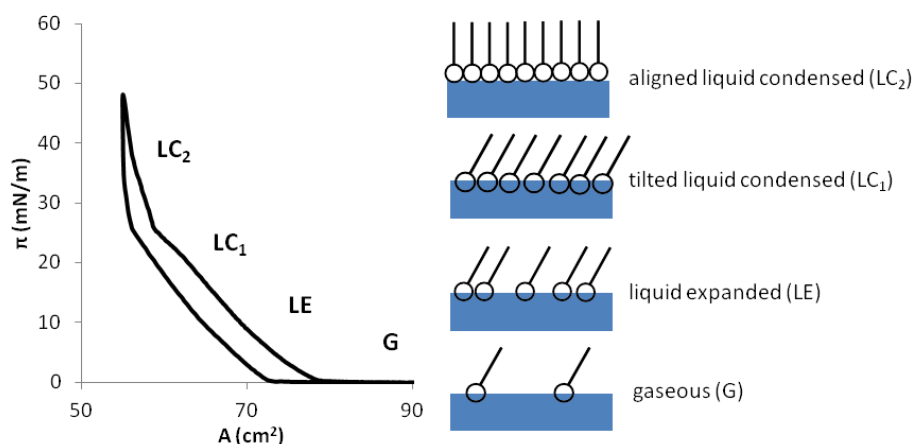


Fig 1.24. Example π -A isotherm for a fatty acid with diagrammatic representation of the behaviour of lipid molecules during compression.

The shape of the π -A isotherm is characteristic of the surface behaviour of the monolayer, with distinct regions observed regarding the interactions between the molecules at a certain film pressure over the course of compression (Fig 1.24). The stages of monolayer compression consist of the following phase descriptions:

- **Gaseous Phase (G)**

The gaseous phase is marked by a constant surface pressure of 0 mN/m. After initial spreading onto the subphase there is no external pressure applied to the monolayer and no internal pressure due to a negligible amount of interactions between molecules.

- **Liquid Expanded (LE)**

On compression of the monolayer, some ordering of the film takes place and it behaves as an expanded two-dimensional liquid. The transition from gaseous to liquid-expanded phase is marked by the onset of an increase in surface pressure. The molecules at this point have been brought close enough together to begin to have an effect on each other, however weak the intermolecular forces at this range may be.

- **Liquid Condensed (LC) Phases**

Further compression of the barriers induces a more compressed liquid phase that shows large regions of rigidity with a slight degree of fluidity remaining. This is known as the tilted liquid condensed (LC_1) phase. The molecules within the condensed phase have undergone movement into their preferred orientation but a small degree of movement is possible. With a continued compression, the monolayer attains an aligned liquid condensed phase (LC_2) where the film acts like a rigid two-dimensional solid. The molecules within the monolayer are in optimal orientation and are at the

smallest available surface area. The LC phase of the π -A isotherm is characterized by a steep linear relationship that provides quantitative information on the molecular dimensions and packing interactions of the monolayer. The area occupied by a molecule (A_0) can be obtained by extrapolating the slope of the solid phase to zero pressure - the point at which this line crosses the x-axis is the hypothetical area occupied by one molecule in the condensed phase.

- **Monolayer Collapse**

As compression continues, the monolayer reaches a collapse point where the surface film will irretrievably lose its monomolecular form (Fig 1.25). The π -A isotherm is marked by a collapse pressure (π_c) where the forces exerted upon the monolayer become too strong for confinement in the two dimensions of the surface. The monolayer fractures and molecules are forced out, the π -A characterised by a sharp decrease in surface pressure. Collapse is not uniform across the monolayer and is initiated at discontinuities in the trough (leading edge of barrier, edge of the trough or at the Wilhelmy plate). Post collapse, the surface consists of large areas of uncollapsed monolayer, small regions of polylayers and clean surface.

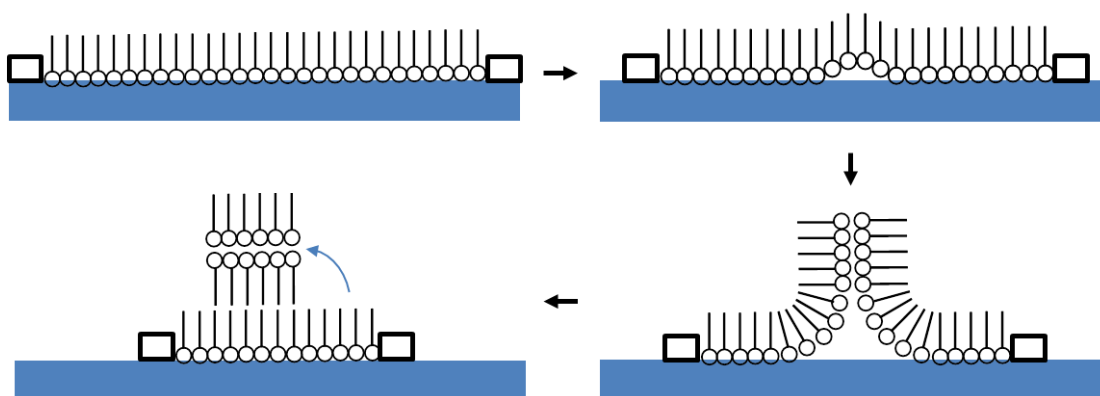


Fig 1.25. Collapse of a surfactant monolayer as surface area is decreased. [216].

1.8 Scope of Research

Studying the interfacial behaviour between the lipid and aqueous layers of the tear film is difficult. Non-invasive methods such as the measurement of tear break up time and observations of the appearance of the lipid layer allow for qualitative studies of *in-vivo* tear film stability. Trying to obtain quantitative data on tear film stability in an *in-vivo* environment is not possible without direct interference with its natural structure and function. However, the study of *ex-vivo* tears in an *in-vitro* environment is possible with a suitable method of

measurement. The Langmuir trough method of studying the interfacial behaviour of monolayers can be - and has been - demonstrated as a valuable technique in studying the viscoelastic and surface monolayer properties of samples of lipids taken from the Meibomian glands [58] [80] [156] [217].

1.9 Aims of Research

The work presented in this thesis is designed to evaluate the benefits of surface pressure measurements using the Langmuir trough technique as an effective way of modelling, observing and measuring the behaviour at the lipid-aqueous interfacial region. The objectives of the present work are:

- Investigation of the individual contributions to surface activity by tear film components, predominantly the tear film lipids;
- Comparison of four methods for the collection of tear film samples and optimisation of extraction procedure;
- Optimisation of surface pressure-area (π -A) measurements and Brewster Angle Microscopic observations for tear samples;
- Investigation of the fate of lipids bound to silicone hydrogel contact lenses in terms of the surface activity of extracted lipoidal material. This will deal with the effect of lens material and wear modality (continuous wear, daily wear, daily disposable wear);
- Investigation of the efficacy of two novel developmental methods for the supplementation of the tear film lipid layer.

Chapter 2

Methodology

2.1 Langmuir Trough

2.1.1 Instrumentation

Surface pressure relationships with surface area were conducted on two Langmuir troughs sourced from KSV NIMA (Coventry, UK).

- **Trough A (model 102M)**

The surface area range of Trough A was 98-14cm² which was manipulated by two mechanically coupled barriers that can be moved independently or together.

- **Trough B (model 312D)**

The surface area range of Trough B is 450-52cm² which was manipulated by two mechanically coupled barriers that are moved together.

The troughs are constructed of polytetrafluoroethylene (PTFE) with moving barriers made of the same material. To ensure a level working area, the heights of four adjustable legs were manipulated until balanced by spirit level. Both troughs were contained within environment boxes to maintain suitable conditions and to ensure no wind or vibration affected experimentation. The temperature of the trough and subphase was controlled by heating elements contained within the Langmuir trough instrument, situated below the working area. This was used in conjunction with a temperature sensor that measured temperature values when placed within the liquid subphase. Each trough was calibrated once every month to ensure perfect instrument performance using the Langmuir trough software. The calibrations included barrier positioning for correct area, testing the barrier speeds and testing the pressure sensor correctly measures force by calibrating with a 100mg weight.

A surface pressure balance, present on both troughs, is positioned to minimise the working area without the barriers interacting with the Wilhelmy probe used to measure surface pressure. Wilhelmy probes are constructed of Whatman Number 1 chromatography paper and cut to dimensions 23mm x 10mm x 0.5mm. These were attached to S-shaped hooks from the pressure balance to ensure the Wilhelmy plate was positioned at least 2mm below the edge of the trough to ensure that it would cross the subphase surface.

2.1.2 Materials

To ensure no contamination of the working area during cleaning, powder-free nitrile gloves (Fisherbrand, Fisher Scientific, UK) and Kimtech precision wipes (Code 75512, Kimberley Clark Professional, UK) were used.

2.1.2.1 Solvents

All of the solvents used were of HPLC-gradient grade and sourced from Fisher Scientific (Fisher Scientific, UK). Chloroform (CHCl_3) was used to clean the trough to remove any contamination, for preparations of lipid component and as part of extraction solvents for tear samples. Methanol (CH_3OH) and hexane (C_6H_{14}) were also used as a part of solvent mixtures for extracting tear samples. Water (H_2O) was used in the preparation of subphases and component solutions.

2.1.2.2 Subphase Solutions

In addition to HPLC-grade water subphases being used, two further subphases were utilised in order to mimic tear-like behaviour. A phosphate buffered saline (PBS) was used to replicate the pH of tears. The solutions were prepared using PBS tablets (Life Technologies) dissolved in the recommended 500ml of HPLC grade water per tablet within a volumetric flask. An artificial tear electrolyte (ATE) solution was prepared to mimic the electrolyte composition of aqueous tears (Section 1.2.2.3) [8] [136] [152] [134]. The ATE solution was formulated by dissolving various salts within a prepared PBS solution to concentrations detected within the tear aqueous (Table 2.1). In order to maintain tear pH (~ 7.4) sodium hydroxide (NaOH) was added to the tear-like electrolyte solution.

Electrolyte	Concentration	
	mg/ml	mol dm^{-3}
Sodium chloride (NaCl)	6.62	0.1133
Potassium chloride (KCl)	1.71	0.0230
Sodium hydrogen carbonate (NaHCO_3)	1.37	0.0164
Calcium chloride (CaCl_2)	0.15	0.0013

Table 2.1. Electrolyte concentrations within the artificial tear electrolyte solution [134] [136].

2.1.3 Surface Pressure-Area (π -A) Isotherm

The details of the materials and methodology for the Langmuir trough experiments designed to achieve the aims found in Section 1.9 will be found in the Experimental Design sections for each respective chapter. This will include the preparation of samples, the setup for the Langmuir trough, the application of sample solutions to the trough surface and the Langmuir trough surface pressure measurements.

The working temperatures of the subphase were ambient, 25°C, 30°C and 37°C with ambient humidity maintained within the environment boxes. Once a clean subphase was attained, shown by a π -A isotherm that remained at 0.0 ± 0.1 mN/m from maximum to minimum working area, sample solutions were introduced to the surface of the subphase using a 50 μ l Hamilton syringe (Hamilton Co., Switzerland). The sample layer was allowed to equilibrate and any spreading solvent to evaporate for ten minutes before the first isotherm was commenced. Table 2.1 details the data taken on each surface pressure-area isotherms.

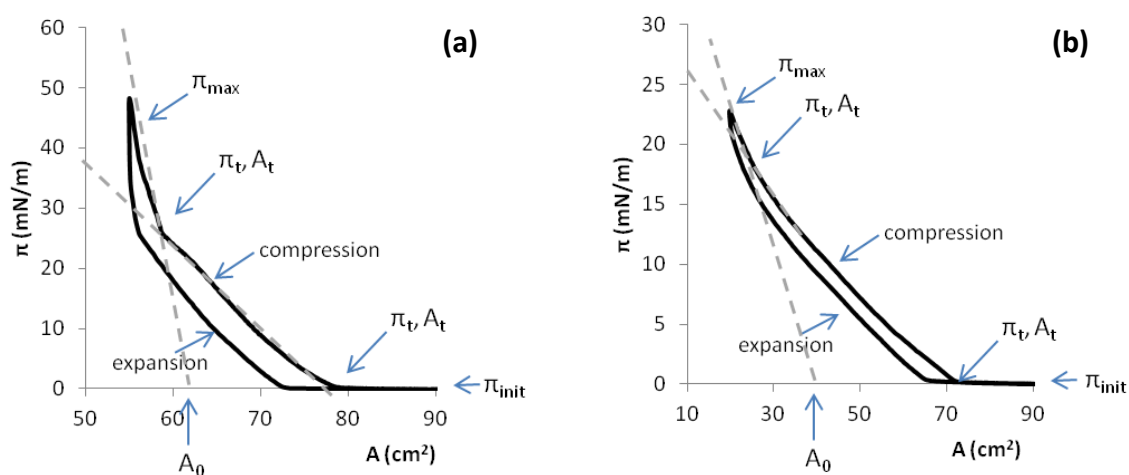


Fig 2.1. Example π -A isotherms for stearic acid (a) and a tear sample (b) showing the key characteristics recorded for the isocycle.

2.1.3.1 Reversibility

Reversibility measures the difference in monolayer behaviour between the compression and expansion isotherms. For ideal surface behaviour, a film must be both resistant to compression and spread uniformly upon expansion of the working area. The hysteresis of the π -A isocycle must be at a minimum, that is, there is only a small difference between the compression and expansion isotherms. Reversibility is the percentage discrepancy between the compression and expansion cycles. To obtain this value, integration of the compression and expansion cycles of the π -A isotherm is necessary, calculated using the *trapezoidal rule* to obtain the area under the compression and expansion isotherms (Fig 2.2).

To calculate the total area (A_{tot}) underneath the line between two adjacent data points, a straight line is assumed between the two points. A_{tot} can be seen to be formed from the area of a triangle (A_{Δ}) and a rectangle (A_{\square}) (Fig 2.2). The calculations needed to work out A_{tot} between two adjacent points using the data from the π -A isotherm (Fig 2.2). This allows formulae to be established that can calculate A_{tot} from the raw π -A isotherm data (Table 2.2). A complete total area for the compression isotherm ($\Sigma A_{\text{tot (com)}}$) can be calculated as the sum of each individual A_{tot} value.

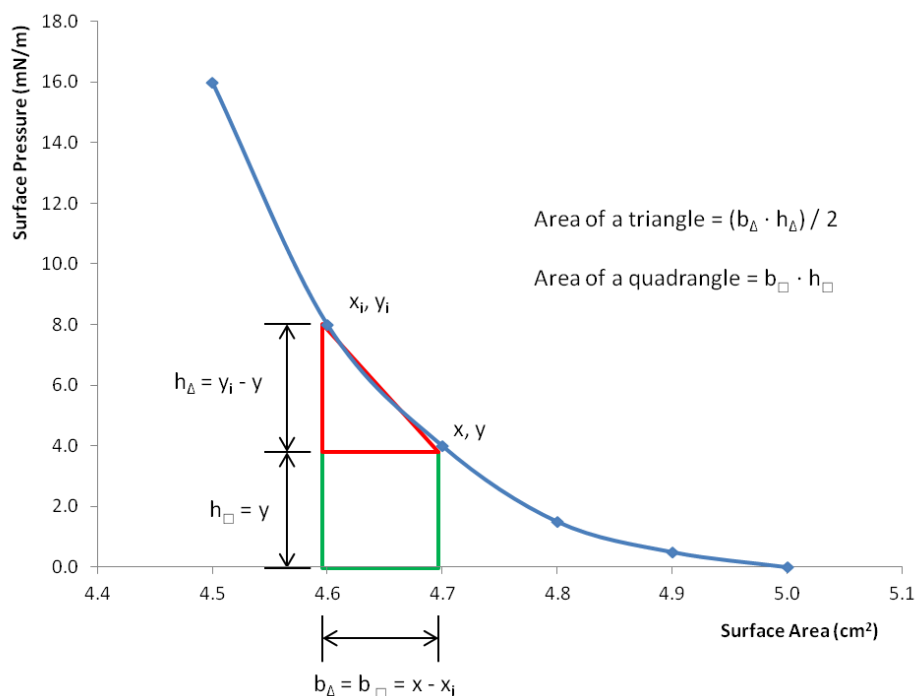


Fig 2.2. Calculating the area between two adjacent data points.

Calculated Value	Calculation	Excel Formulae
A_{Δ}	$[(x - x_i) \cdot (y_i - y)] / 2$	<code>=sum((A2-A3)*(B3-B2)/2)</code>
A_{\square}	$(x - x_i) \cdot y$	<code>=sum((A2-A3)*B2)</code>
A_{tot}	$A_{\Delta} + A_{\square}$	<code>=sum(C3+D3)</code>
+ve $A_{\text{tot (com)}}$	$\sqrt{[(A_{\text{tot (com)}})^2]}$	<code>=sqrt(E3^2)</code>
$\Sigma A_{\text{tot (com)}}$	$A_{\text{tot (1)}} + A_{\text{tot (2)}} + \dots A_{\text{tot (n)}}$ (where n is the final data cell)	<code>=sum(F3:F_n)</code>

Table 2.2. Formulae required to calculate the area underneath the compression isotherm.

	A	B	C	D	E	F	G
1	A	π		A_{Δ}	A_{\square}	A_{tot}	
2	5.0	0.0					
3	4.9	0.5		0.025	0.000	0.025	0.025
4	4.8	1.5		0.050	0.050	0.100	0.1
5	4.7	4.0		0.125	0.150	0.275	0.275
6	4.6	8.0		0.200	0.400	0.600	0.6
7	4.5	16.0		0.400	0.800	1.200	1.2
8							
9						$\Sigma A_{\text{tot (com)}}$	2.200
10							
11							

Table 2.3. Calculation of area under the lines between two adjacent points from the compression isotherm sample data found in Fig 2.2.

The same formulae in Table 2.2 are used to calculate the area total of the expansion cycle ($\Sigma A_{\text{tot (exp)}}$) from the data obtained in a full isocycle that contains both compression and expansion isotherms (Fig 2.3). When worked out from the raw data using the formulae, the value of $\Sigma A_{\text{tot (exp)}}$ will produce a negative value. This undergoes the square-square root treatment to obtain a positive value for the area under the expansion isotherm. Table 2.4 shows the calculations needed to work out values of $\Sigma A_{\text{tot (com)}}$ and $\Sigma A_{\text{tot (exp)}}$, the square-square root treatment of the negative $\Sigma A_{\text{tot (exp)}}$ value and the reversibility value (Rev). Also contained is an example of the Excel formula that needs to be entered based upon the cell codes in Table 2.5. These codes would change dependant on how the data is entered in to the spreadsheets.

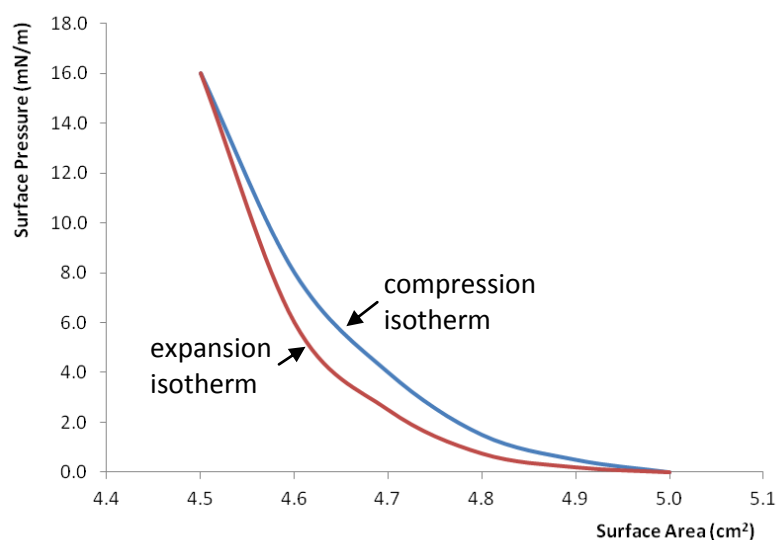


Fig 2.3. Sample π -A isocycle showing the compression and expansion isotherm.

Value	Calculation	Excel Formulae
$\Sigma A_{\text{tot (com)}}$	$A_{\text{tot}} (1) + A_{\text{tot}} (2) + \dots A_{\text{tot}} (n)$ (n = final data point of the compression cycle)	=sum(F3:F n)
$\Sigma A_{\text{tot (exp)}}$	$A_{\text{tot}} (Fn) + \dots + A_{\text{tot}} (Fn+n)$ (n / n+n = first / final data point of the expansion cycle)	=sum(F n :F $n+n$)
Rev (%)	$\Sigma A_{\text{tot (exp)}} / \Sigma A_{\text{tot (com)}}] * 100$	=sum((F16/F14)*100)

Table 2.4. Formulae required to calculate the hysteresis between compression and expansion isotherms

	A	B	C	D	E	F	G
1	A	π		A_{Δ}	A_{\square}	A_{tot}	
2	5.0	0.0					
3	4.9	0.5		0.025	0.000	0.025	0.025
4	4.8	1.5		0.050	0.050	0.100	0.1
5	4.7	4.0		0.125	0.150	0.275	0.275
6	4.6	8.0		0.200	0.400	0.600	0.6
7	4.5	16.0		0.400	0.800	1.200	1.2
8	4.6	6.0		0.500	-1.600	-1.100	1.1
9	4.7	2.5		0.175	-0.600	-0.425	0.425
10	4.8	0.8		0.087	-0.250	-0.162	0.1625
11	4.9	0.2		0.028	-0.075	-0.048	0.0475
12	5.0	0.0		0.010	-0.020	-0.010	0.01
13							
14						$\Sigma A_{\text{tot (com)}}$	2.200
15						$\Sigma A_{\text{tot (exp)}}$	1.745
16						Hys (%)	79.318
17							

Table 2.5. Calculation of hysteresis between compression and expansion from the isocycle sample data found in Fig 2.3.

2.1.4 Surface Pressure-Time (π -t) Isotherms

It is also possible to measure the effect on film stability and surface pressure by observing the adsorption of molecules to an interface over time, observed in a surface pressure-time (π -t) isotherm. Adsorption of test materials were performed under a surface with and without the presence of tear film or lipoprotein material. This involves the partitioning of components into the subphase by applying the test solutions outside of the working surface area (behind the barriers) when the maximum area was limited to 80cm². In order to study the adsorption to a pre-prepared monolayer of tear film/lipoprotein material, the protocols described in section 2.1.3 were followed until a π -A isotherm for the monolayer at equilibrium is achieved. The surface area of the monolayer was then compressed to a set initial surface pressure (π_{init}). Once achieved, the test substance was introduced to the subphase **behind** the barriers via a Hamilton syringe (Fig 2.4). An 'Area Control' predefined programme within the Langmuir trough software [218] was used to maintain the surface area at the point where π_{init} was attained. The change in surface pressure over time was measured until $\pi_{eq (adsorb)}$ was obtained.

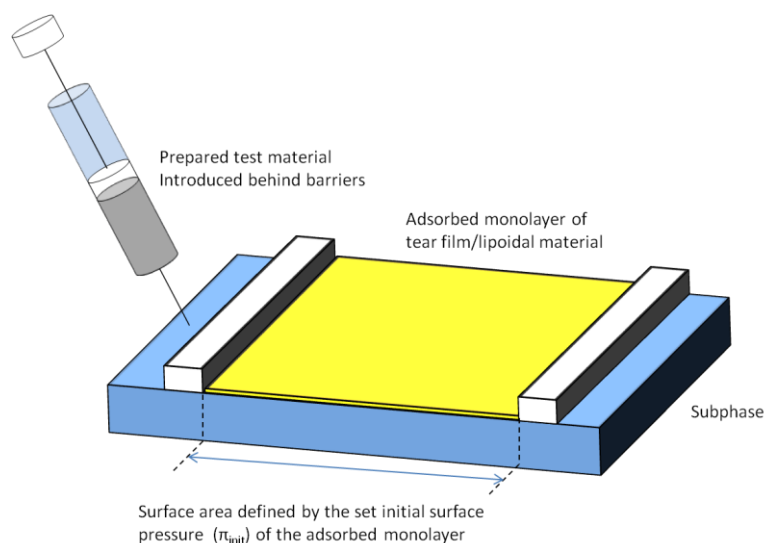


Fig 2.4. Experimental procedure for obtaining surface pressure-time adsorption isotherms

The surface pressure-time (π -t) isotherm obtained shows the change in surface pressure over time (Fig 2.5). Relaxation of the film takes place after compression of the monolayer to a certain surface pressure (π_{init}) as the molecules spontaneously orientate themselves to a desired packing scheme. As film relaxation occurs, a minimum surface pressure (π_{min}) is observed that is lower than π_{init} . Surface pressure is recorded over time until an equilibrium surface pressure is attained after full adsorption of molecules injected into the subphase ($\pi_{eq (adsorb)}$).

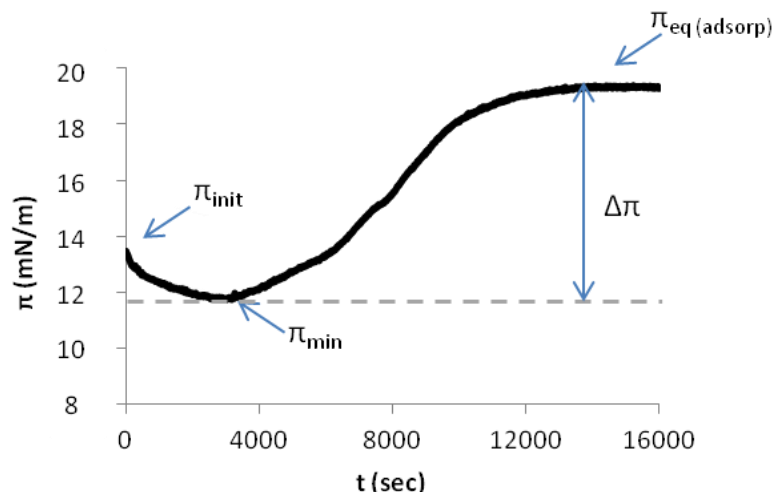


Fig 2.5. Example surface pressure-time (π -t) isotherm

2.2 Brewster Angle Microscopy

The Brewster angle microscope (BAM) is a novel technique that allows the real time observation of monolayer behaviour over the course of compression and expansion. BAM eliminates the need for molecular markers such as heavy atoms, fluorophores or other contrast agents that could potentially disrupt and alter the natural interfacial behaviour of the monolayer components [219] [220].

2.2.1 Principles

The interface between the air and the liquid subphase forms a boundary between two phases that differ in refractive index. When an plane-polarized (p-polarised) light source is shone upon a pure, clean subphase surface at the Brewster angle (α°) - the angle of incidence at which light with a particular polarization is perfectly transmitted through a medium - a minimum intensity value of the reflected p-polarised light is observed. For pure water the Brewster angle is 53.1° . The presence of salts and other contaminants can change α° for a particular solution by as much as 2° . The refractive index of a monolayer adsorbed at the air-aqueous interface differs from those of the air or the subphase. As the p-polarised light beam hits the surface, the incident p-polarized light is reflected when a monolayer is present. At areas where there is no monolayer present, the beam will refract into the aqueous subphase (Fig 2.6). The BAM image results from a change in the refractive index of the system and an increase in molecular density at the air-aqueous interface. As the monolayer becomes denser, brighter images appear. Bright regions of a BAM image represent an area of high

intermolecular organization in the monolayer and are typically referred to as 'domains'. Darker regions of the image represent a less ordered, more expanded phase of the monolayer.

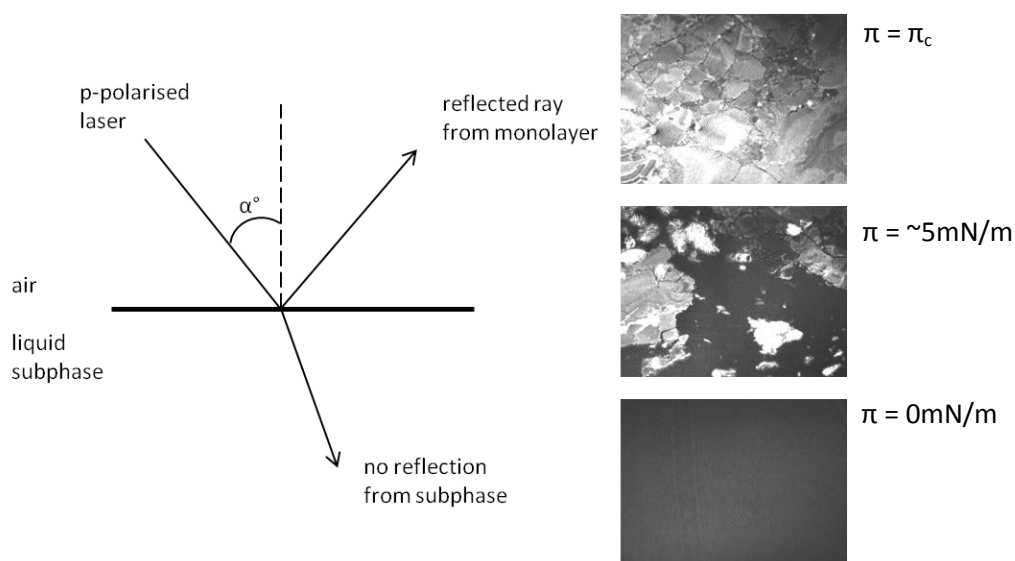


Fig 2.6. The Brewster angle and the changes in reflection from a clean surface to one with an adsorbed monolayer at various stages of compression.

2.2.2 Instrumentation

The Brewster angle microscope used was a MicroBAM2 supplied by NIMA KSV (Coventry, UK) used in conjunction with the Langmuir trough B (section 2.2.1). Due to the bulk of the Brewster Angle Microscope (BAM) laser housing, which obstructs the barrier during compression, the minimum working area is limited to 100 cm^2 when the BAM was in operation. The general set up for the Brewster angle microscope is shown in Fig 2.7. The BAM is attached to a tripod where the height and tilt can be adjusted. The incident light source is a 659nm helium-neon (He-Ne) laser beam. This is attached to a motor that allows manipulation of the angle of incidence through the computer software. A black glass plate is positioned at the bottom of the Langmuir trough, underneath the laser beam, in order to absorb any incident light that penetrates the aqueous subphase. Any light reflected by monolayer present at the surface passes through a detector. The detector consists of a lens, an analyser and a charge coupled device (CCD). This is attached to a computer via USB connection to allow BAM images and video to be saved.

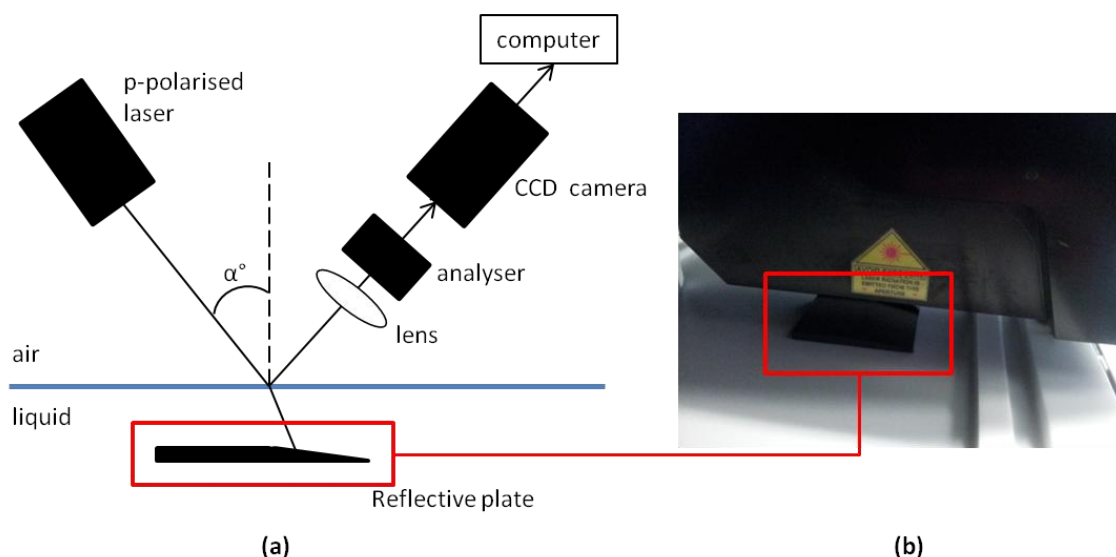


Fig 2.7. MicroBAM2 Instrument: (a) MicroBAM2 instrument schematic; (b) position of the reflective glass plate underneath the BAM laser and analyser housing.

The environment box that contained the Langmuir trough coupled with the BAM was constructed of shaded perspex to ensure no errant laser beams escaped the working environment. This included an interlock that would cut power to the laser if the door to the box was opened.

2.2.3 Imaging Procedure

Prior to setting up for a normal surface pressure measurement, the black glass plate was polished using a KimTech wipe and HPLC-grade chloroform. This was then placed underneath the BAM laser housing, with the wedge placed at the position where the polarised laser beam would hit the surface (Fig 2.8). The subphase was then introduced to the trough. In most cases, the level of the subphase was well above the trough edges in order to completely immerse the glass plate. Once covered, the surface was aspirated under normal cleaning procedures until the subphase surface was level with the trough edges. The glass plate remained fully immersed after cleaning. BAM imaging was initially observed for a clean subphase to further ensure no contamination by surface active materials. BAM images were then observed for monolayers that had reached equilibrium, taken at 50cm^2 intervals over the course of compression and expansion. Once the π -A isotherm showed an equilibrated monolayer, the images were retaken at the same intervals with additional images taken at defined transition points and then smaller intervals (25cm^2) within the $100\text{-}200\text{ cm}^2$ range.

Chapter 3

Preliminary Study: Understanding the Surface Chemistry of Individual Tear Film Components

Artificial models of biological systems studied in an in-vitro environment have the inherent problem that it is impossible to replicate the natural system exactly. Any study of the tear film is hindered in efficacy by the difficulty of studying it. Conditions within the tear film can greatly affect the way in which the components behave and it is important to understand this during application of ex-vivo studies. The careful balance of forces at the lipid-aqueous interface can be affected by small changes in the biochemistry of the tear components and in the physical and environmental conditions to which it is subject. It is important to understand the individual surface chemistry of the major tear film components that have been thought to have an effect on the interfacial behaviour of the tear film.

3.1 Condition Testing

3.1.1 Objective

It is important to understand how each individual lipid component is affected by changes in conditions when studied on the Langmuir trough in order to understand the physical conditions to which these components become subject within the ocular system. The key objective is to distinguish any differences in surface behaviour as a cause of a change in temperature, pH, electrolyte and surface concentration.

3.1.2 Experimental design

The effect of changes in conditions on the surface activity of a standard fatty acid (stearic acid; SA) was studied using Langmuir trough A with a working surface area of 90-20 cm² and barrier speed of 20cm²/min set for all condition tests. The variable conditions studied were:

- Subphase solutions (see section 2.1.2.2): HPLC-grade water, phosphate buffered saline (PBS) solution, artificial tear electrolyte (ATE) solution;
- Subphase temperature: 25°C, 30°C and 37°C.
- Monolayer surface concentration: solutions of SA were formulated to concentrations 0.5×10^{-3} , 1.0×10^{-3} , 1.5×10^{-3} and 2.0×10^{-3} mol dm⁻³ when dissolved in CHCl₃.

The pH values of the subphase solutions at STP were measured using an Accumet Basic AB10 pH benchtop meter. Subphases were cleaned using a vacuum-aspiration pump to ensure no significant increase in surface pressure of 0mN/m. SA solutions were applied to the subphase surface from a 50µl Hamilton syringe onto the subphase surface. Ten minutes were allowed to ensure full evaporation of the spreading solvent. π -A compression-expansion isotherms were run at a barrier speed of 20cm²/min until the equilibrium surface pressure (π_{eq}) was reached. Initially the maximum surface pressure (π_{max}) was set at 50mN/m in order to prevent collapse of the monolayer. The number of moles of stearic acid within the aliquot volume and at maximum (90cm²) and minimum (20cm²) surface areas are found in Appendix 2.

3.1.3 Results

To ascertain any direct effect on the surface pressure of π -A isotherm by phosphate buffering and electrolyte components, the subphases were prepared following the prescribed method without the presence of any extraneous contaminant or adsorbed monolayer (Fig 3.1). For a clean subphase to be suitable for use in Langmuir monolayer studies, no deviation from 0mN/m should be detected from maximum to minimum working area. All three solutions showed no significant effect on surface pressure, with no increase above the desired 0mN/m detected (Table 3.1). HPLC-grade water subphases that were determined to be clean produced π_{max} of 0.022 ± 0.006 mN/m. The PBS and ATE subphases that produced low π_{max} values of 0.114 ± 0.041 mN/m and 0.209 ± 0.052 mN/m respectively. During cleaning, it is necessary to aspirate the surface of the subphase to remove any contamination. To ensure that the components added to the subphase to produce the desired tear-like characteristics are not removed during surface aspiration, the pH values of the three solutions used were tested before and after aspiration of the subphase surface (Table 3.1). No significant changes were observed in pH before and after surface cleaning.

Solution	pH before cleaning	pH after cleaning
HPLC-grade Water	5.94 ± 0.10	5.88 ± 0.06
PBS	7.33 ± 0.08	7.37 ± 0.09
ATE	7.41 ± 0.08	7.38 ± 0.07

Table 3.1. pH values for the subphase solutions

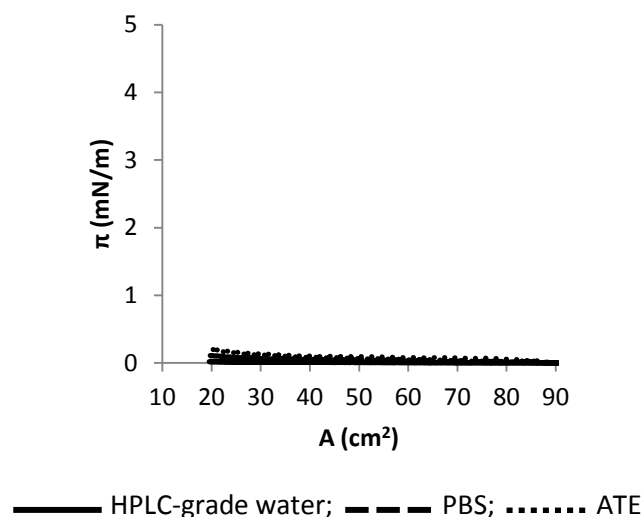


Fig 3.1. π -A isotherms of clean subphases of HPLC-grade water, PBS and ATE without the presence of contamination.

3.1.3.1 Subphase Composition

Whilst a direct subphase-related effect on the surface pressure was not detected, components within the liquid can have an effect on the surfactant properties of lipid molecules and affect the behaviour of adsorbed surface monolayer. The pH of the subphase and the presence of dissolved monovalent and divalent ions can alter the surfactant properties of a lipid molecule [221] [222] [223] [224] [225]. In order to obtain an equilibrium π -A isotherm, an adsorbed monolayer must be compressed several times without noticeable collapse of the film. By setting a maximum surface pressure (π_{\max}) limit, the stability of the monolayer can be maintained through annealing the film through successive compression and expansion cycles. A preliminary π -A isotherm for SA was measured in order to determine the collapse pressure (π_c) and a suitable maximum surface pressure (π_{\max}) limit (Fig 3.2). SA has a π_c value of $\sim 54 \text{ mN/m}$ at a surface area of $\sim 30 \text{ cm}^2$ ($A_{\text{mol}} = \sim 19.9 \text{ \AA}^2 \text{ molecule}^{-1}$) [224]. Based on this result, the limited π_{\max} value for SA would be set at 50 mN/m . Compression would continue until this surface pressure is achieved, at which point the expansion cycle would begin despite not being compressed to the minimum working area (A_{\min}).

The surface behaviour of SA changes significantly as a result of subphase pH and the presence or absence of ionic components. Figure 3.3 and Table 3.2 highlights the difference in the π -A isotherms of SA. Equilibrium π -A isotherms were obtained on the third isocycle upon all subphases. The general trend for equilibrium surface pressures (π_{eq}) at lower loading

concentrations (5-15 μ l) was: HPLC-grade water < PBS < ATE. Maximum surface pressures (π_{\max} = ~50mN/m) were obtained at different surface concentrations for each subphase. On the ATE subphase, SA reached a maximum surface pressure at an initial surface concentration of 1.66×10^{-10} mol/cm² (15 μ l aliquot). Stearic acid on PBS and HPLC-grade water subphases reached π_{\max} at initial surface concentrations of 2.22×10^{-10} mol/cm² (20 μ l aliquot) and 2.77×10^{-10} mol/cm² (25 μ l aliquot) respectively. At the highest load (25 μ l; Fig 3.3a), where the stearic acid monolayer reached a π_{\max} of 50mN/m on all three subphases, there is a shift in the surface area and molecular area (A_{mol}) where this value was obtained. Higher A_{mol} values were recorded for the two subphases at a pH of ~7.4. The π_{\max} was attained at a molecular area of 22.6 Å² molecule⁻¹ on the ATE subphase and 20.2 Å² molecule⁻¹ for the PBS subphase. HPLC-grade water produced an A_{mol} value of 18.2 Å² molecule⁻¹.

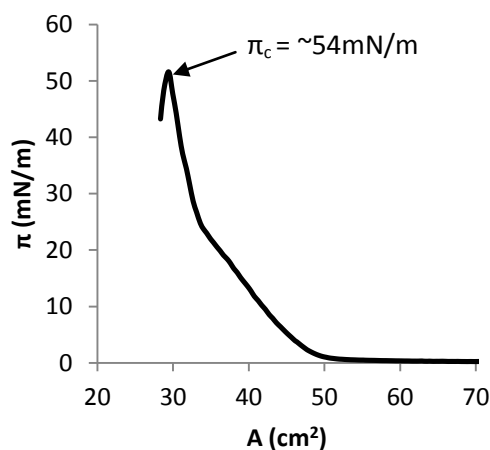


Fig 3.2. Determination of π_c of SA (1.0×10^{-3} moldm⁻³; 25 μ l aliquot)

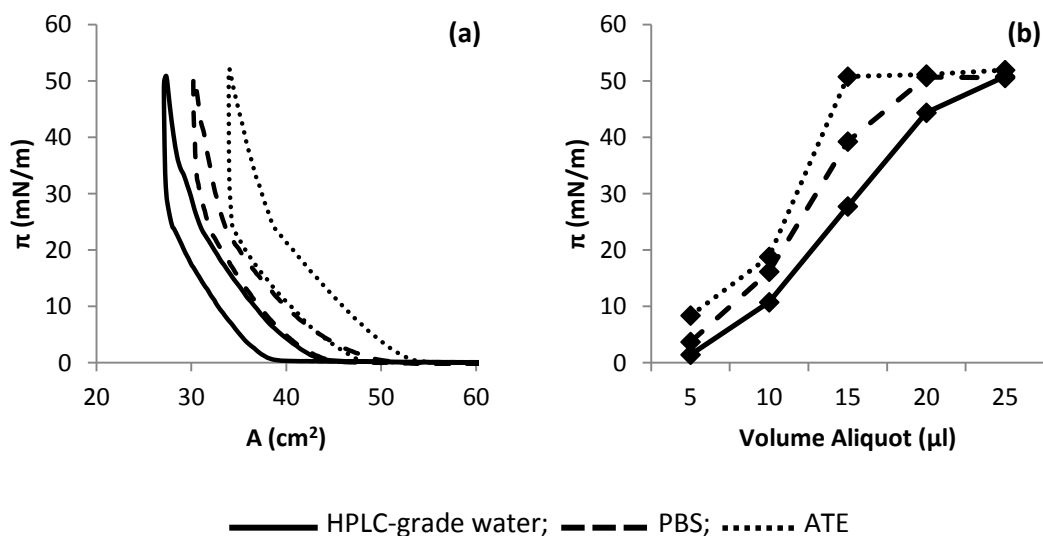


Fig 3.3. π -A isotherms (a) of SA on different subphases (1.0×10^{-3} moldm⁻³; 25 μ l aliquot; 25°C). (b) surface pressure versus volume aliquot.

	Subphase		
	Water	PBS	ATE
pH	5.98	7.34	7.38
π_{eq} (mN/m)	50.78	50.53	51.91
$A_{\pi_{eq}}$ (cm ²)	27.36	30.35	33.96
A_{mol} (Å ² molecule ⁻¹)	18.17	20.16	22.56
π_t (mN/m)	0, ~23	0, ~21	0, ~23
A_t (cm ²)	~38, ~26	~50, ~34	~53, ~38
Rev (%)	59.82	70.25	52.74

Table 3.2. Key characteristic data for the π -A isotherm of SA (1.0×10^{-3} moldm⁻³; 25 μ l aliquot; 25°C) in Fig 3.3.

Differences in the collapse pressures of SA were recorded depending on the subphase (Fig 3.4). Upon the two subphases at pH ~7.4, the collapse pressure recorded was slightly increased compared to the HPLC-grade water subphase. The SA monolayer on ATE and PBS subphases produced π_c of 55.0mN/m and 54.0mN/m respectively, whereas upon the water subphase the π_c was recorded at 51.8mN/m. A difference in the post-collapse behaviour of the remnant monolayer was also observed when the monolayer was compressed to the A_{min} . ATE and PBS subphases showed a more stable post-collapse film, with surface pressure decreasing to a minimum surface pressure (π_{min}) of 36.0mN/m ($\Delta\pi = 19.0$ mN/m) and 34.5mN/m ($\Delta\pi = 19.5$ mN/m) respectively, compared to the water subphase which recorded a larger decrease in surface pressure to π_{min} of 22.1mN/m ($\Delta\pi = 29.7$ mN/m).

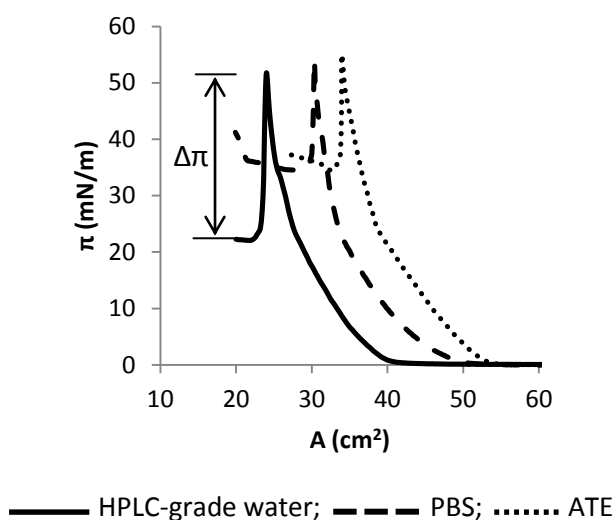


Fig 3.4. Collapse pressure (π_c) and post collapse minimum surface pressure (π_{min}) of SA on different subphases (1.0×10^{-3} moldm⁻³; 25 μ l aliquot; 25°C).

3.1.3.2 Temperature

Differences in π -A isotherm characteristics of a SA solution of concentration $1.0 \times 10^{-3} \text{ mol dm}^{-3}$ were observed as the temperature is increased (Fig 3.5 and Table 3.3). At low loading concentrations (5-15 μl), the 37°C subphase produced higher π_{eq} than the subphases at 25°C and 30°C. π_{max} values of 50.7 mN/m and 50.9 mN/m were obtained on the 30°C and 37°C subphases respectively at an initial surface concentration of $1.66 \times 10^{-10} \text{ mol/cm}^2$ (15 μl aliquot), whilst a π_{max} value of 49.3 mN/m was obtained for the 25°C isotherm at a higher initial surface concentration ($2.22 \times 10^{-10} \text{ mol/cm}^2$ (20 μl aliquot)).

The limited maximum surface pressure of $\sim 50 \text{ mN/m}$ was recorded for all three temperatures at surface concentrations of $2.22 \times 10^{-10} \text{ mol/cm}^2$ (20 μl aliquot) and $2.77 \times 10^{-10} \text{ mol/cm}^2$ (25 μl aliquot). A slight increase in π_{max} ($\sim 1 \text{ mN/m}$) was noticed at the higher loading concentration. At 25°C, the monolayer produced an average π_{max} value of 49.8 mN/m (range 49.3-50.2 mN/m) with an average A_{mol} of $21.2 \text{ \AA}^2 \text{ molecule}^{-1}$. An increase in π_{max} to 50.9 mN/m (range 50.2-51.6 mN/m) and A_{mol} to $23.3 \text{ \AA}^2 \text{ molecule}^{-1}$ (range 23.2 - $23.4 \text{ \AA}^2 \text{ molecule}^{-1}$) was recorded when the temperature was increased to 30°C. A further increase in the average π_{max} and A_{mol} values was recorded when the temperature was further increased to 37°C. π_{max} increased to 51.5 mN/m (range 50.9-52.0 mN/m) and A_{mol} increased to $25.9 \text{ \AA}^2 \text{ molecule}^{-1}$.

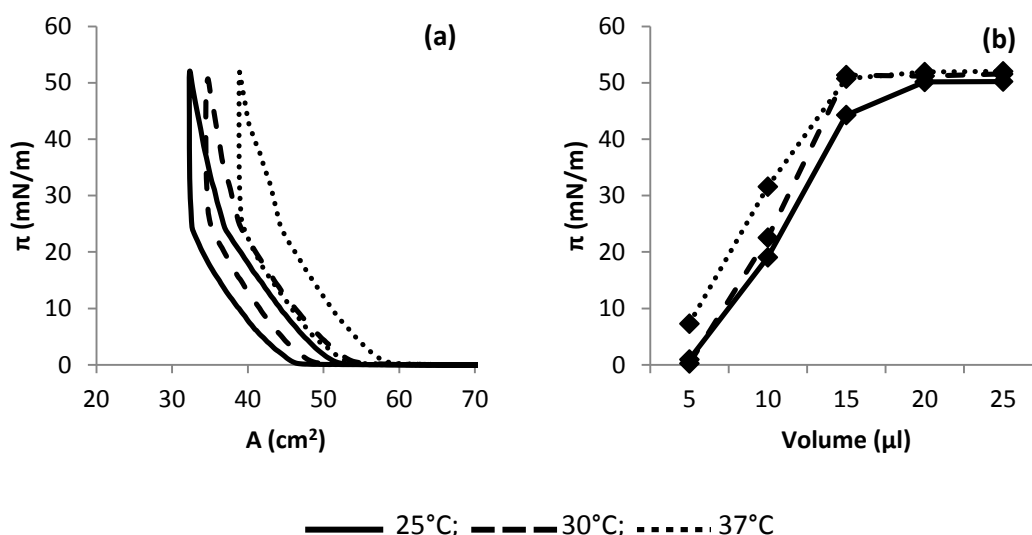


Fig 3.5. π -A isotherms (a) of SA at different subphase temperatures ($1.0 \times 10^{-3} \text{ mol dm}^{-3}$; 25 μl). (b) surface pressure versus volume aliquot.

	Temperature					
	25°C		30°C		37°C	
	20µl	25µl	20µl	25µl	20µl	25µl
pH	7.37	7.40	7.35	7.37	7.36	7.30
π_{\max} (mN/m)	49.30	50.22	50.24	51.55	50.88	52.02
$A_{\pi\text{eq}}$	25.56	32.29	28.17	34.74	31.25	38.90
A_{mol} (Å ² molecule ⁻¹)	21.22	21.26	23.39	23.26	25.95	25.85
Rev (%)	57.64	52.75	54.44	55.44	70.03	51.58

Table 3.3. Key characteristic data for the 20µl and 25µl aliquot π -A isotherms of SA (1.0×10^{-3} moldm⁻³; PBS subphase) in Fig 3.5.

3.1.3.3 Surface Concentration

The characteristics of the π -A isotherm are often dictated by the surface concentration of the studied material. Surface pressure values will change with increasing surface concentration until a maximum is reached. The relationship between compression and expansion isotherms, the presence of clear transitions in monolayer phase state and reversibility of the monolayer also changes at lower surface concentrations before the π_{\max} is reached.

Surface pressure increases with each aliquot interval until the maximum surface pressure (π_{\max}) of SA was obtained (Fig 3.6). The maximum surface pressure obtained for the stearic acid is 52.2mN/m (range 51.3-52.7mN/m) is obtained at a critical number of molecules at the surface of 12.044×10^{15} molecules (Fig 3.7). Before the π_{\max} is reached, surface pressure increases $\sim 10\text{mN/m}$ per 1.5055×10^{15} molecule interval from an initial number of 3.011×10^{15} molecules to 12.044×10^{15} molecules. The average molecular area after the critical number of molecules had been applied to the surface was $20.9 \text{ Å}^2 \text{ molecule}^{-1}$ (range $16.3\text{-}25.9 \text{ Å}^2 \text{ molecule}^{-1}$). Reversibility between compression and expansion cycles of the π -A isotherms recorded for concentrations above the critical number of molecules was 62.2% (range 57.4-66.1%).

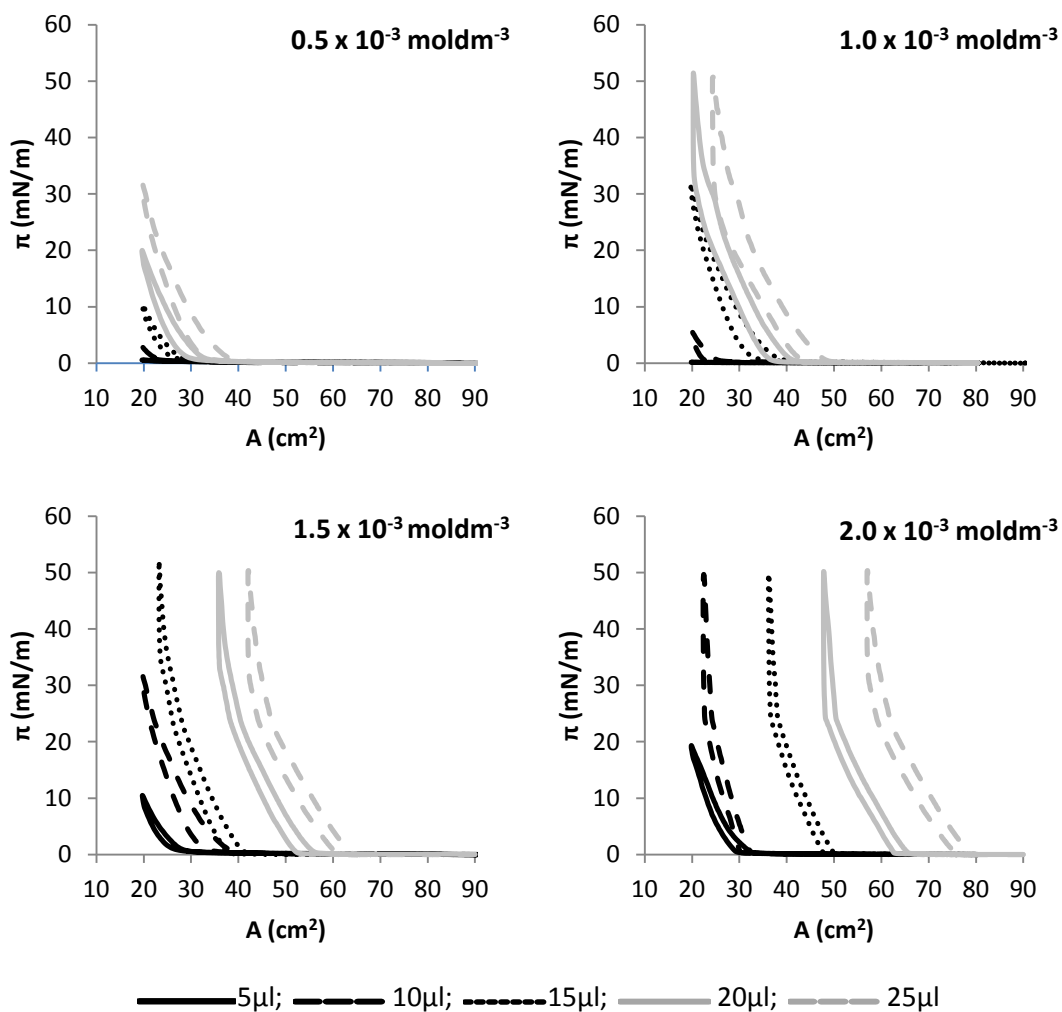


Fig 3.6. π -A isotherms of increasing concentrations of SA at different aliquot volumes.

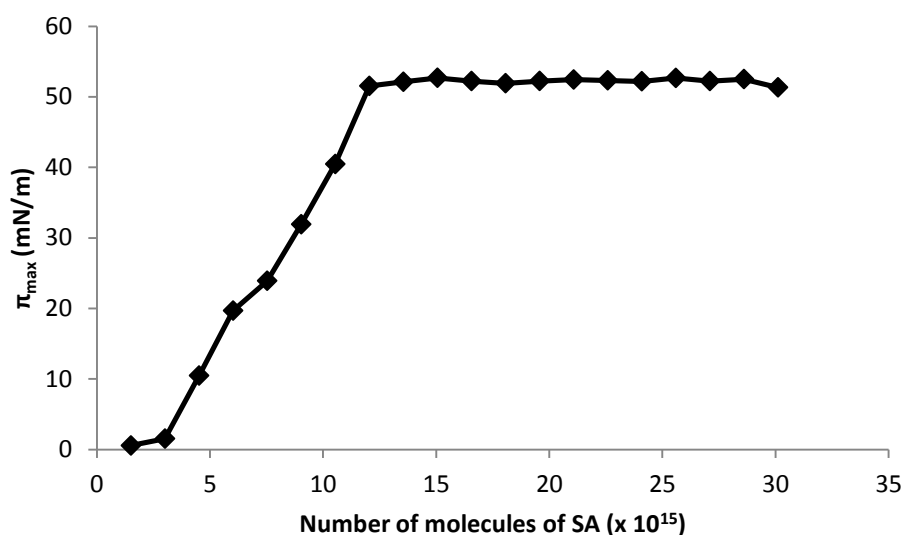


Fig 3.7. Relationship between the number of SA molecules applied to the subphase surface against maximum surface pressure. Additional data was obtained for each 1.505×10^{15} molecule aliquot (5 μ l) between 1.505×10^{15} and 30.110×10^{16} molecules (5-50 μ l).

3.2 Lipid Components

To understand the behaviour of the tear film lipid layer as a whole, it is important to understand the individual surface behaviour of the common types of tear lipids. The composition of different lipid types must be kept within fairly narrow limits in order to optimise lipid layer formation and function. Because of the varied structures found within the tear film lipid composition, some species show surface activity through favourable interactions with the aqueous phase whilst others provide other key aspects of the lipid layer's behaviour.

3.2.1 Objective

The main objective is to understand how the structure of the various lipid types found within the tear film differ in surface behaviour. It also aims to understand the effect that changes to the fatty acid molecule of a lipid can affect spreading, compressibility and stability of a monolayer film in relation to the tear film.

3.2.2 Experimental Design

The various lipid types were sourced from Sigma-Aldrich (Table 3.4). These were stored in their unopened packaging at -20°C until used. Solutions of these lipids were made by dissolving the lipid material in HPLC grade chloroform to a concentration of $1.0 \times 10^{-3} \text{ mol/dm}^3$. These solutions were prepared on the day of the experiment in pre-weighed glass vials. If necessary, the lipid solutions were stored at -20°C to prevent evaporation of the spreading solvent and manipulation of the concentration. Lipid solutions were applied to the subphase surface from a 50 μl Hamilton syringe onto the subphase surface. A period of ten minutes before compression was taken to ensure full evaporation of the spreading solvent. A working surface area of 90 to 20 cm^2 was used with a barrier speed of 20 cm^2/min . The number of moles of each lipid molecule within the aliquot volume and at maximum (90 cm^2) and minimum (20 cm^2) surface areas are found in Appendix 2. A phosphate buffered saline (PBS) was used as a subphase ($\text{pH} = 7.31 \pm 0.16$). All π -A isotherms were recorded at temperature of 25°C . The maximum surface pressure (π_{max}) was set below the collapse pressure (π_{c} - obtained from an initial test) in order to prevent collapse of the monolayer and obtain an equilibrium surface pressure (π_{eq}). Once π_{eq} was reached, the subsequent isotherm had the π_{max} limit removed and allowed to continue past the collapse pressure.

Lipid Type	Lipids Used
Free Fatty Acids	myristic acid (MA; 14:0); palmitic acid (PA; 16:0); stearic acid (SA; 18:0); oleic acid (OA; 18:1 ^{Δ9}); linoleic acid (LoA; 18:2 ^{Δ9,12}); α-linolenic acid (α-LnA; 18:3 ^{Δ9,12,15}); γ-linolenic acid (γ-LnA; 18:3 ^{Δ6,9,12}); arachidic acid (AA; 20:0)
Fatty Alcohols	1-octadecanol; 1-eicosanol
Wax Esters	palmitoyl palmitate (16:0-16:0); oleoyl oleate (18:1 ^{Δ9} -18:1 ^{Δ9}); behenyl oleate (22:0-18:1 ^{Δ9})
Cholesterol Esters	cholesterol (Ch); cholesterol palmitate (Ch-16:0); cholesterol stearate (Ch-18:0); cholesterol oleate (Ch-18:1 ^{Δ9})
Acylglycerides	1-oleoylglyceride (monoolein; MO); 1,2-dioleoylglyceride (diolein; DO); 1,2,3-trioleoylglyceride (triolein; TO)
Phospholipids	dimyristoylphosphatidylcholine (DMPC); dipalmitoylphosphatidylcholine (DPPC); distearoylphosphatidylcholine (DSPC); dioleoylphosphatidylcholine (DOPC)

Table 3.4. List of the lipids studied for their surface behaviour

3.2.3 Results

3.2.3.1 Fatty Acids

3.2.3.1.1 Saturated Fatty Acids

The length of the hydrophobic chain affects the surface behaviour of saturated fatty acids. There is no amphiphilic behaviour of fatty acids with short chains (C4-10), as the hydrophilic groups overcome the hydrophobic effect that the hydrocarbon chain has and the molecules are solubilised. With at least 12 carbons in the chain produce insoluble monolayers with surfactant behaviour and a phenomenon known as Traube's rule becomes apparent. To achieve a certain surface pressure, the concentration of a member of a homologous series decreases by nine for each additional ethylene group ($-\text{CH}_2\text{CH}_2-$) that the chain contains. Whilst Traube's rule is not directly apparent in the data obtained in this study, there is evidence for an effect of chain length on π_{max} and π_{c} values (Fig 3.9 and Table 3.5). The collapse pressure (π_{c}) values increased for each additional ethylene group added to the fatty acid chain: 38.6mN/m for myristic acid; 47.3mN/m for palmitic acid; 54.8mN/m for stearic acid; 58.0mN/m for arachidic acid. To obtain the reversible isocycle, π_{max} values were limited to: MA = 38mN/m, PA = 45mN/m, SA = 50mN/m, AA = 54mN/m. Molecular area also is shown to increase for each additional ethylene group in the fatty acid chain: 14.7 Å² molecule⁻¹ for MA; 16.9 Å² molecule⁻¹ for PA; 20.3 Å² molecule⁻¹ for SA; 24.1 Å² molecule⁻¹ for AA.

PA, SA and AA show two transitions in phase: the first from gaseous phase to a liquid expanded phase (G-LE) $\pi_t = 0\text{mN/m}$ and a second from a liquid expanded to a liquid condensed phase (LE-LC) at $\pi_t = \sim 23\text{mN/m}$. MA shows the presence of two further transitions in the π -A in addition to the G-LE and LE-LC transitions. The normal G-LE transition is present, but a transition is reached at $\sim 5.5\text{mN/m}$ where the rate of change of surface pressure decreases from $\sim 1\text{mN/m per cm}^2$ to $\sim 0.25\text{mN/m per cm}^2$. At $\sim 7.0\text{mN/m}$, another transition occurs where the rate increases to $\sim 1\text{mN/m per cm}^2$ again until the normal transition from the LE to LC phase occurs at $\sim 24\text{mN/m}$. These further transitions were also apparent on the expansion isotherm. Due to the straight chain nature of the saturated fatty acids, the time to reach an equilibrium π -A isotherm was short. Palmitic acid, myristic acid and stearic acid reached equilibrium after the third isotherm, whilst arachidic acid reached equilibrium after the fourth isotherm. Reversibility after the critical number of molecules was applied did not significantly differ between subsequent isotherm or as the acyl chain length increased ($\sim 72\%$).

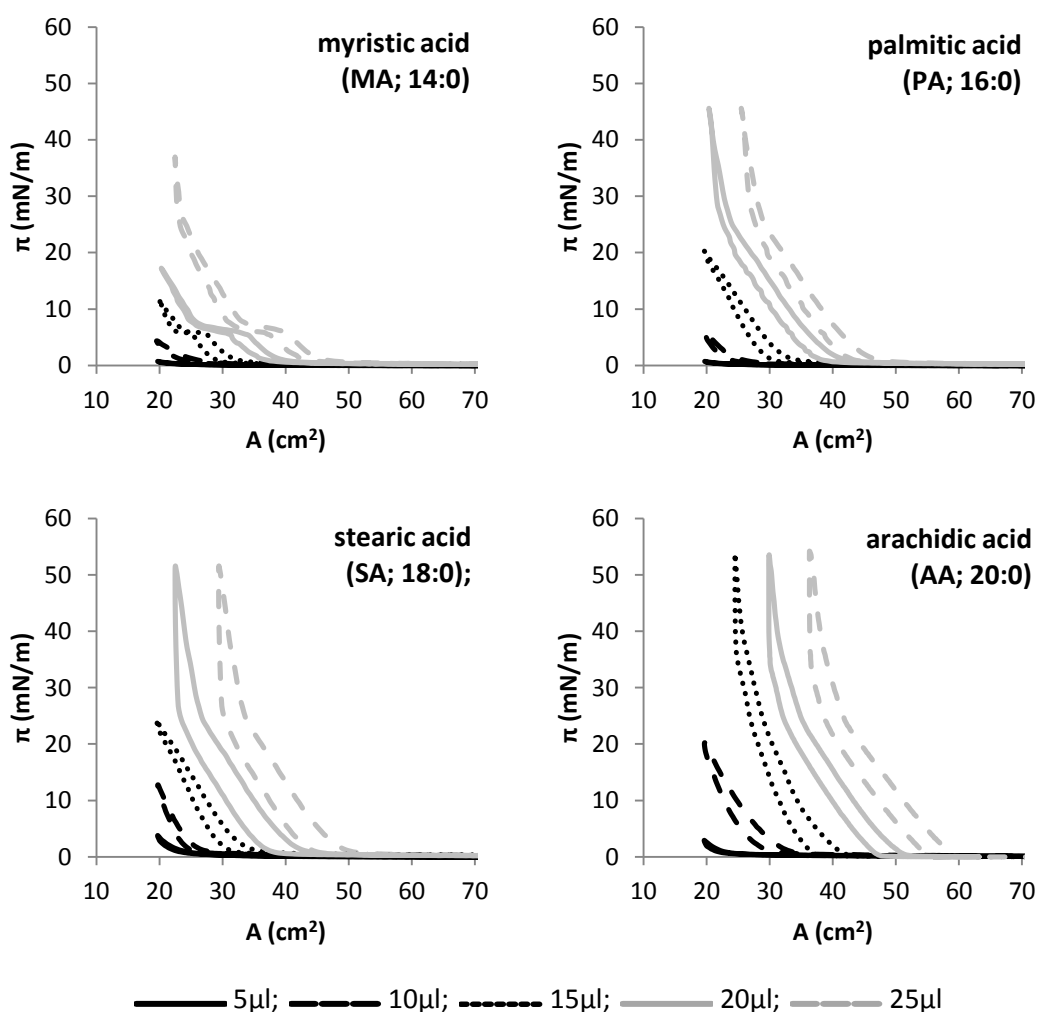


Figure 3.8. π -A isotherms of saturated fatty acids ($1.0 \times 10^{-3} \text{ mol dm}^{-3}$; $25\mu\text{l}$ aliquot; 25°C).

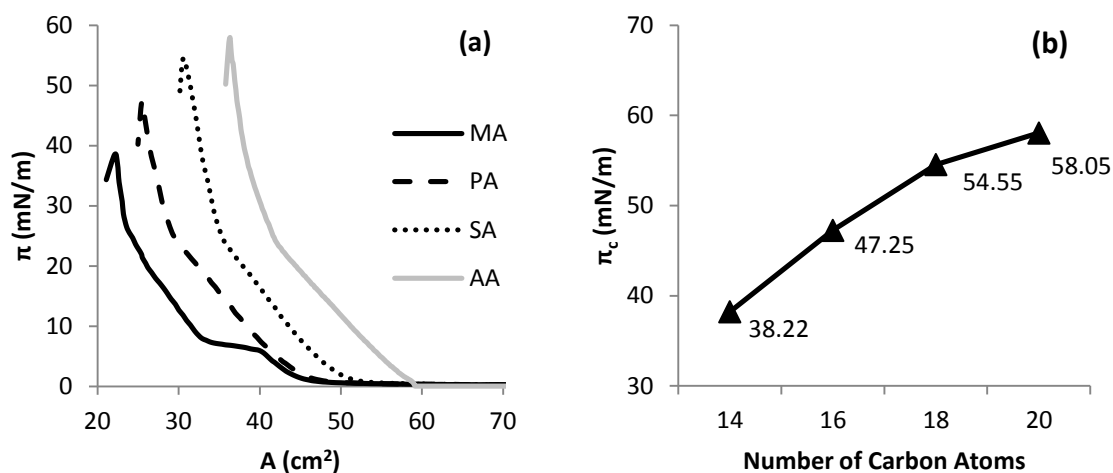


Figure 3.9. π -A isotherms (a) of saturated fatty acids ($1.0 \times 10^{-3} \text{ mol dm}^{-3}$; 25 μl aliquot) compressed to π_c . (b) π_c against number of carbon atoms in acyl chain.

	Saturated FA			
	MA	PA	SA	AA
$\pi_{eq} \text{ (mN/m)}$	38.02	45.11	51.89	54.78
$\pi_c \text{ (mN/m)}$	38.55	47.34	54.55	58.00
$A_{\pi c} \text{ (cm}^2\text{)}$	22.10	25.45	30.55	36.33
$A_{mol} \text{ (Å}^2 \text{ molecule}^{-1}\text{)}$	14.68	16.91	20.30	24.14
$\pi_t \text{ (mN/m)}$	0.00, 5.35, 6.92, 27.27	0.00, 23.45	0.00, 22.89	0.00, 21.45
$A_t \text{ (cm}^2\text{)}$	48, 40, 32, 24	48, 29	53, 36	60, 43
Rev (%)	76.14	73.25	69.73	71.04

Table 3.5. Characteristic data for the 25 μl aliquot π -A isotherms of the saturated fatty acids ($1.0 \times 10^{-3} \text{ mol dm}^{-3}$; PBS subphase; 25°C) in Fig 3.8-3.9: myristic acid (MA); palmitic acid (PA); stearic acid (SA); arachidic acid (AA).

3.2.3.1.2 Effect of Unsaturation in 18-carbon Fatty Acids

All unsaturated fatty acids in this study are based upon a C18 acyl chain with varying numbers of double bonds. The way in which the molecules interact and pack at a minimum area is dictated by the molecular orientation with respect to kink caused by the *cis*-configuration double bonds. Unsaturated fatty acids show no definable point of transition between phases from G through to an LC phase. As compression of monolayer continues, the molecules orientate themselves an increasingly aligned film structure as it approaches an equilibrium surface pressure (π_{eq}). Instead of an LE-LC transition, a plateau in surface pressure is attained that would indicate that the molecules have attained an optimum molecular orientation at π_{eq} that further monolayer compression brings the molecules closer. Molecular orientation caused

by degree of unsaturation affects the π_{eq} and A_{mol} of the unsaturated fatty acids. The molecular area of each unsaturated C18 fatty acid is larger as the degree of unsaturation increases. This is a response to the extra area needed to accommodate the increasing three-dimensional area that the molecule exists within.

The single chain kink caused by the monounsaturated chain of oleic acid (OA; 18:1^{Δ9}; Fig 3.10a) causes the molecule to attain an ideal equilibrium orientation at a higher π_{eq} (31.51mN/m) and a smaller A_{mol} (27.27 Å² molecule⁻¹) where the LC phase occurs. The addition of a second double bond to the 18-carbon acyl chain as in the diunsaturated linoleic acid (LoA; 18:2^{Δ9,12}; Fig 3.10b) decreases the π_{eq} to 27.99mN/m and increases the A_{mol} to 36.74 Å² molecule⁻¹. The effect of a third double bond added to the acyl chain decreases the π_{eq} and increases A_{mol} , but the effect of increased work of orientation is not as strong as the addition of the second bond to the chain produces. The triunsaturated fatty acids α-linolenic acid (α-LnA; 18:3^{Δ9,12,15}; Fig 3.10c) and γ-linolenic acid (γ-LnA; 18:3^{Δ6,9,12}; Fig 3.10d) shows a slight decrease in π_{eq} to 26.63mN/m and 26.16mN/m respectively. A molecular area also increased to 40.70 Å² molecule⁻¹ and 39.93 Å² molecule⁻¹ respectively. There was no significant difference recorded in π_{eq} and A_{mol} between the two triunsaturated fatty acids dependent upon the position of the third double bond (Δ15 in α-LnA and Δ6 in γ-LnA)

The time to reach equilibrium increased due to the orientation of unsaturated fatty acids during compression and repulsion of molecules during expansion. Equilibrium was reached on the 7th isotherm for OA, the 9th for LoA and the 10th for both α-LnA and γ-LnA. There was no difference in reversibility for the unsaturated fatty acids between compression and expansion isotherms at equilibrium. Significant increase in reversibility was notable from the 1st through to equilibrium isotherm in all cases.

	Unsaturated FA			
	OA	LoA	α-LnA	γ-LnA
π_{eq} (mN/m)	31.51	27.99	26.63	26.16
$A_{\pi_{eq}}$ (cm ²)	41.04	55.30	61.25	60.09
A_{mol} (Å ² molecule ⁻¹)	27.27	36.74	40.70	39.93
Rev (%)	75.87	70.19	71.36	65.34

Table 3.6. Characteristic data for the 25μl aliquot π-A isotherms of the unsaturated fatty acids (1.0 x 10⁻³ moldm⁻³; PBS subphase; 25°C) in Fig 3.10-3.11: oleic acid (OA); linoleic acid (LoA); α-linolenic acid (α-LnA); γ-linolenic acid (γ-LnA).

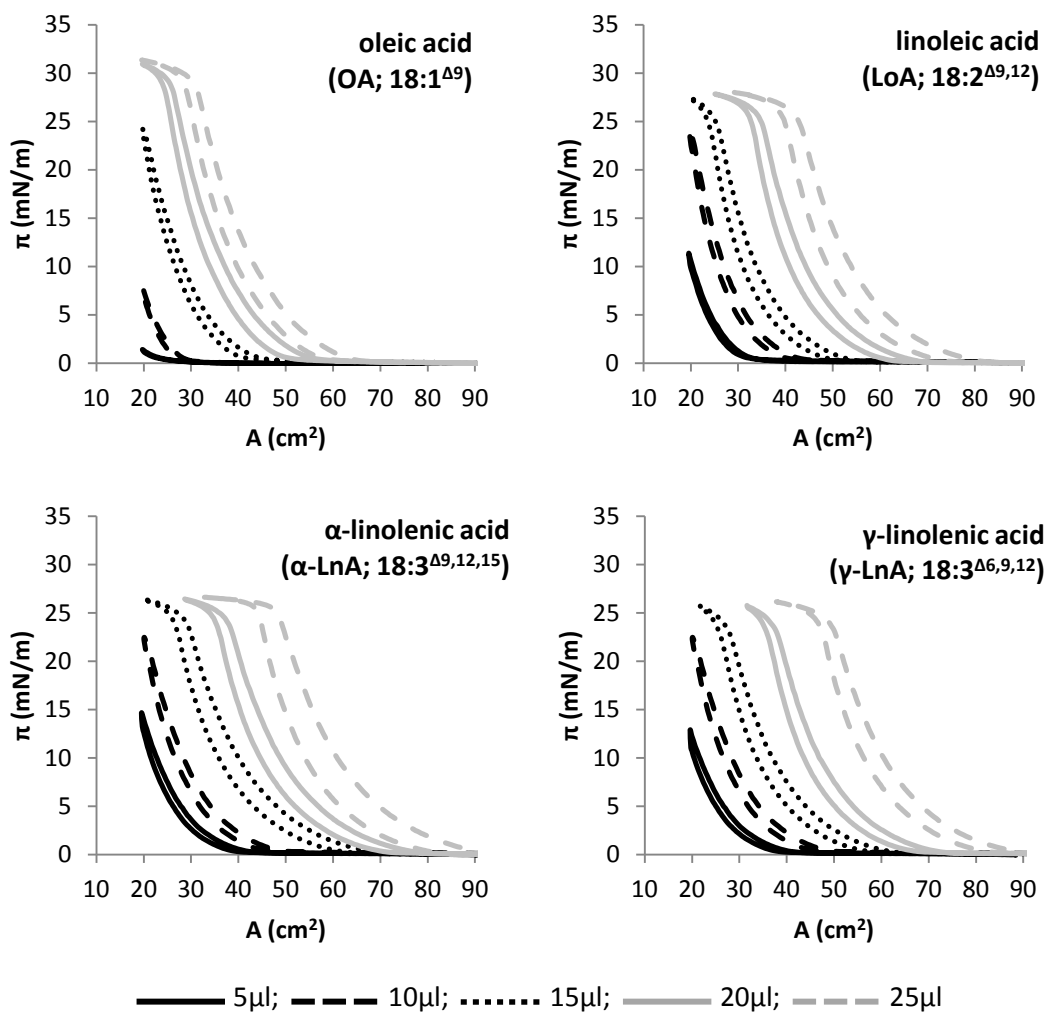


Figure 3.10. π -A isotherms of unsaturated fatty acids ($1.0 \times 10^{-3} \text{ mol dm}^{-3}$; 25μl aliquot).

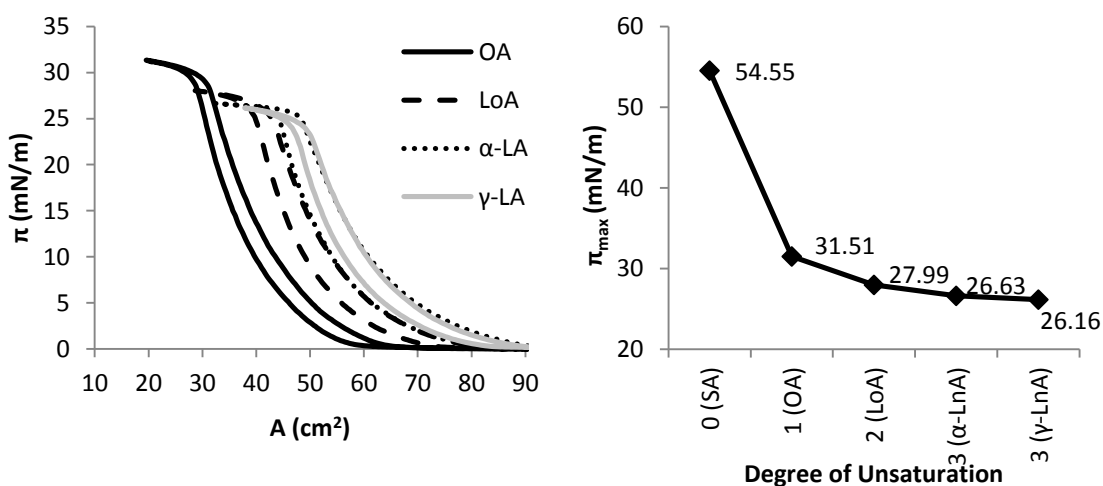


Figure 3.11. π -A isotherms (a) of C18-unsaturated fatty acids ($1.0 \times 10^{-3} \text{ mol dm}^{-3}$; 25μl aliquot); (b) π_{max} against degree of unsaturation.

3.2.3.2 Fatty Alcohols

Fatty alcohols are long chain hydrocarbons with a hydroxyl group at a terminal carbon atom that gives the molecule polar behaviour similar to their carboxylic analogues. High surface pressure values are obtained for 1-octadecanol (C18-OH; Fig 3.12a) and 1-eicosanol (C20-OH; Fig 3.12b). A comparison of the isotherms for the FAlc to the FA chain length analogues can be found in Fig 3.13 and Table 3.7. The general trend for the fatty alcohols is comparable to the differences in characteristics recorded for the fatty acids of the same chain length from section 3.2.3.1.1. Both show similar π_c values (~ 54 mN/m for the C18 molecules; ~ 58 mN/m for the C20 molecules) and π_t values at the LE-LC transition (~ 22.5 mN/m for the C18 molecules; ~ 21.4 mN/m for the C20 molecules).

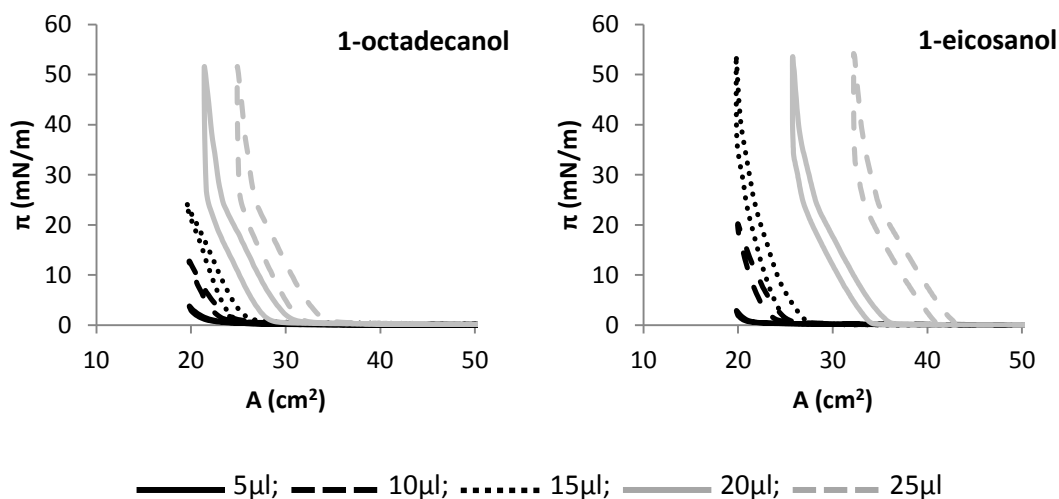


Figure 3.12. π -A isotherms of fatty alcohols (1.0×10^{-3} mol dm $^{-3}$; 25 μ l aliquot)

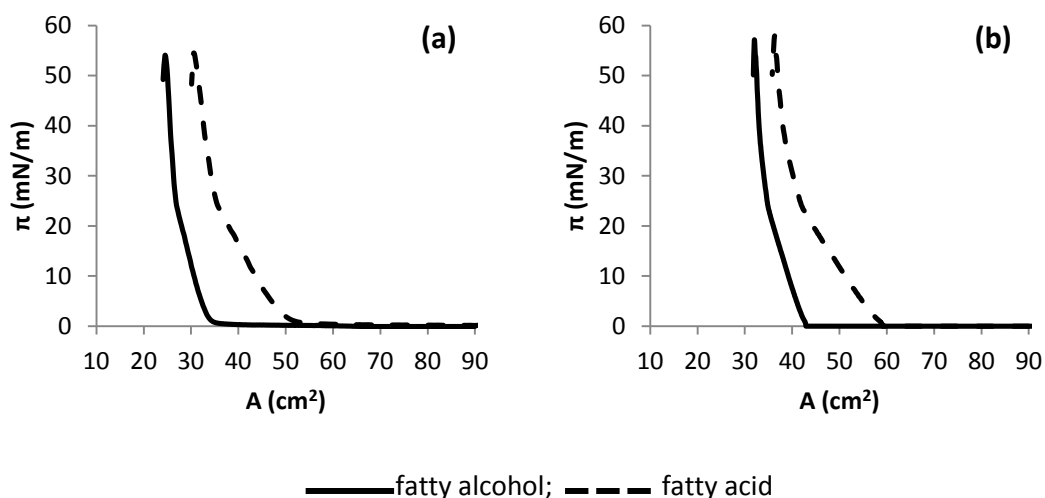


Figure 3.13. Comparison of π -A isotherms of FAlc and FA molecules (1.0×10^{-3} mol dm $^{-3}$; 25 μ l aliquot): (a) C18 (1-octadecanol vs. SA); (b) C20 (1-eicosanol vs. AA)

	C18		C20	
	C18-OH	SA	C20-OH	AA
π_c (mN/m)	53.89	54.55	57.22	58.00
$A_{\pi_{eq}}$ (cm ²)	29.78	30.55	35.17	36.33
A_{mol} (Å ² molecule ⁻¹)	19.79	20.30	23.39	24.14
π_t (mN/m)	0.00, 22.36	0.00, 22.89	0.00, 21.36	0.00, 21.45
A_t (cm ²)	35, 28	53, 36	43, 36	60, 43
Rev (%)	-	69.73	-	71.04

Table 3.7. Characteristic data for the 25 μ l aliquot π -A isotherms of the C18 and C20 based fatty acids and fatty alcohols (1.0×10^{-3} moldm⁻³; PBS subphase; 25°C) in Fig 3.12-3.13: 1-octadecanol (C18-OH); stearic acid (SA); 1-eicosanol (C20-OH); arachidic acid (AA).

3.2.3.3 Cholesterol Esters

Despite the highly non-polar characteristic of the four-ring structure of cholesterol (Ch), the lone hydroxyl group produces amphiphilic behaviour that results in a high π_c of ~ 45 mN/m (Fig 3.14a). A smaller overall transition from the onset of surface pressure increase through to collapse when compared to the saturated fatty acids - a ~ 6 cm² area decrease for Ch compared to a ~ 20 cm² decrease for a saturated FA - suggests a highly ordered monolayer with a quick G-LC phase transition. The planar nature of four-ring structure lies perpendicular to the surface (hydroxyl group at the surface; planar ring pointing up in to the superphase) that compresses to a point where the planar cholesterol molecules are orientated vertically in to a parallel sheet. With a bulkier molecules that has a higher degree of repulsion caused by more neighbouring hydrocarbon structures, the average molecular area of cholesterol is larger than that of a saturated fatty acid (~ 30 Å² molecule⁻¹). Also of note with cholesterol is the film stability after collapse. The change in surface pressure ($\Delta\pi$) is ~ 3 mN/m after collapse and is indicative of a highly stable film where small degrees of film rupture are present.

The surface active properties of the Ch molecule are lost when a fatty acid is esterified to the molecule to form a cholesterol ester (CE). The initial π -A isotherm of the three CE recorded after application of a 25 μ l aliquot of a 1.0×10^{-3} moldm⁻³ showed extremely little surface activity ($\pi_{max} < 2$ mN/m). This changed over time as the equilibrium isotherm was attained. The saturated fatty acid-based cholesterol esters is characterised by π_{eq} of ~ 40 mN/m for cholesterol palmitate (Ch-16:0; Fig 3.14b) and ~ 42 mN/m for cholesterol stearate (Ch-18:0; Fig 3.14c). In both cases, there were no discernible transition in the LE region and the isotherms appear to go from G through to a very condensed LC phase at a rate of 4.02 mN/m per cm² and 2.80 mN/m per cm² for Ch-16:0 and Ch-18:0 respectively.

The unsaturated oleate-based cholesterol ester (Ch-18:1; Fig 3.14d) produced a different π -A isotherm, reaching a π_{eq} of ~ 15 mN/m. There was no presence of a LC phase at equilibrium for Ch-18:1, producing a LE monolayer film with a rate of change of surface pressure increase of 0.5mN/m per cm^2 . Whilst the differences in the π -A isotherms of the cholesterol ester versus cholesterol may be a result of the changes caused by the structure of the ester and the loss of amphiphilic behaviour, one source of contention in the result is the role played by hydrolysis reactions. Small amounts of these reaction may break apart the cholesterol ester to produce a mixed monolayer of the cholesterol ester, cholesterol and fatty acid molecules.

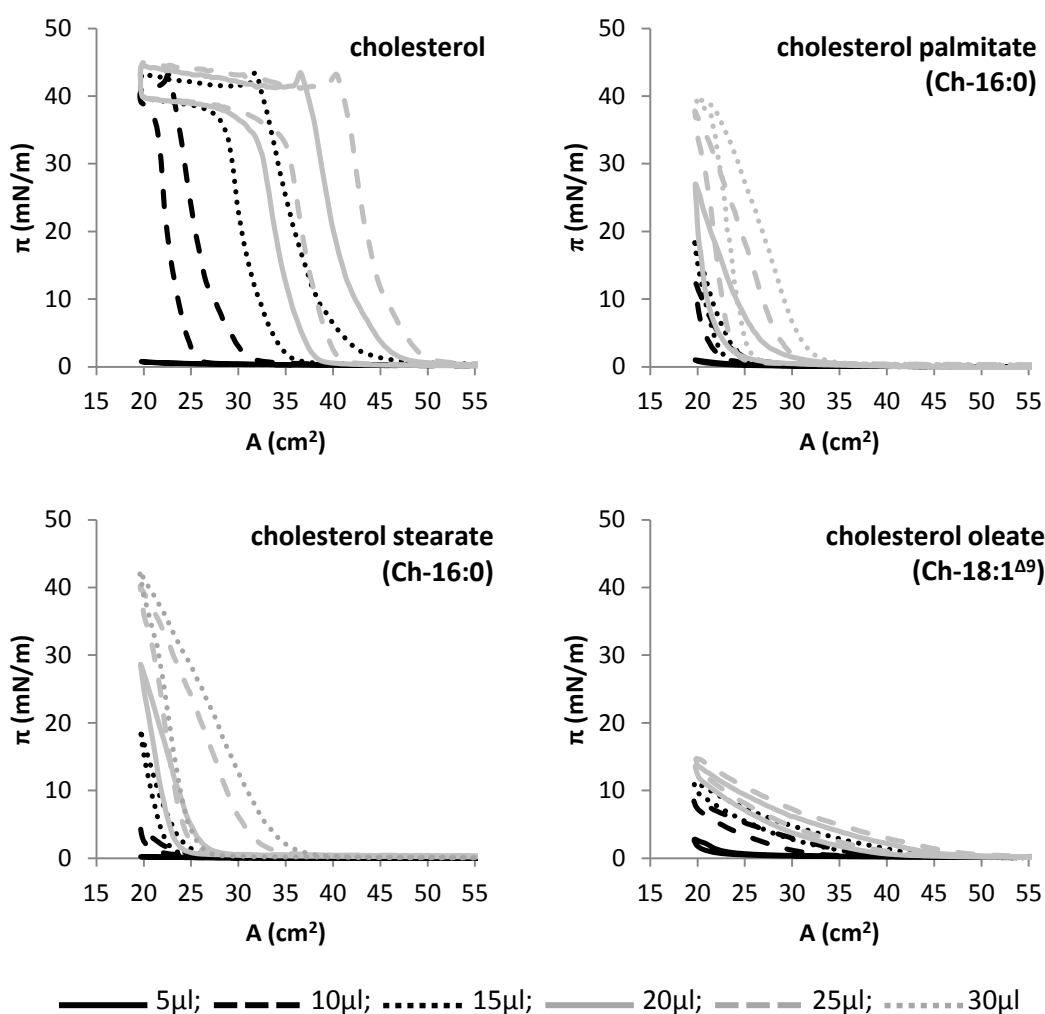


Figure 3.14. π -A isotherms of cholesterol and cholesterol-based esters.

	Cholesterol Ester		
	Ch-16:0	Ch-18:0	Ch-18:1
π_{eq} (mN/m)	40.15	41.98	15.79
$A_{\pi eq}$ (cm ²)	22.03	19.98	-
A_{mol} (Å ² molecule ⁻¹)	14.63	13.28	-
Rev (%)	75.87	57.23	86.36

Table 3.8. Characteristic data for the 25μl aliquot π -A isotherms of cholesterol (Ch) and cholesterol esters (1.0×10^{-3} moldm⁻³; PBS subphase; 25°C) in Fig 3.14: cholesterol palmitate (Ch-16:0); cholesterol stearate (Ch-18:0); cholesterol oleate (Ch-18:1).

3.2.3.4 Wax Esters

The initial π -A isotherm of the three wax esters (WE) recorded after application of a 25μl aliquot of a 1.0×10^{-3} moldm⁻³ showed extremely little surface activity ($\pi_{max} < 3$ mN/m). This changed over time as the equilibrium isotherm was attained. The full saturated chain containing ester palmityl palmitate (16:0-16:0; Fig 3.15a) shows definable points of phase transition almost akin to those observed in the π -A isotherms of fatty acids and fatty alcohols: a transition from G to LE phase at 0.0mN/m followed by a sharp transition from the LE phase through to a LC phase at a surface pressure of ~2.5mN/m. The presence of an oleate fatty acid substituent instead of a saturated fatty acid gives the resultant π -A isotherm a distinctly more unsaturated fatty acid-like quality.

As opposed to the potential further increase to an π_{max} of >30mN/m seen in the fully saturated 16:0-16:0 wax ester, behenyl oleate (22:0-18:1; Fig 3.15b) and oleoyl oleate (18:1-18:1; Fig 3.15c) begin to plateau to a π_{eq} of ~23mN/m and ~18mN/m respectively. This suggests a similar orientation and packing behaviour noticed with unsaturated fatty acids occurring within the two unsaturated fatty-containing molecules. With oleoyl oleate, a molecular where both substituent chains contain a double bond at C9 further need for ideal orientation during compression results in a lower π_{eq} and a slightly higher A_{mol} . As with the cholesterol esters discussed in the previous section, some consideration must be made as to the possibility of hydrolysis forming a mixed monolayer of polar fatty acids and fatty alcohols mixed with the wax ester.

	Wax Ester		
	16:0-16:0	18:1-18:1	22:0-18:1
π_{eq} (mN/m)	26.46	19.08	23.17
$A_{\pi eq}$ (cm ²)	35.81	43.41	42.19
A_{mol} (Å ² molecule ⁻¹)	23.79	28.84	28.03
Rev (%)	39.37	77.12	73.03

Table 3.9. Characteristic data for the 25 μ l aliquot π -A isotherms of wax esters (1.0×10^{-3} moldm⁻³; PBS subphase; 25°C) in Fig 3.15: palmitoyl palmitate (16:0-16:0); oleoyl oleate (18:1-18:1); behenyl oleate (22:0-18:1).

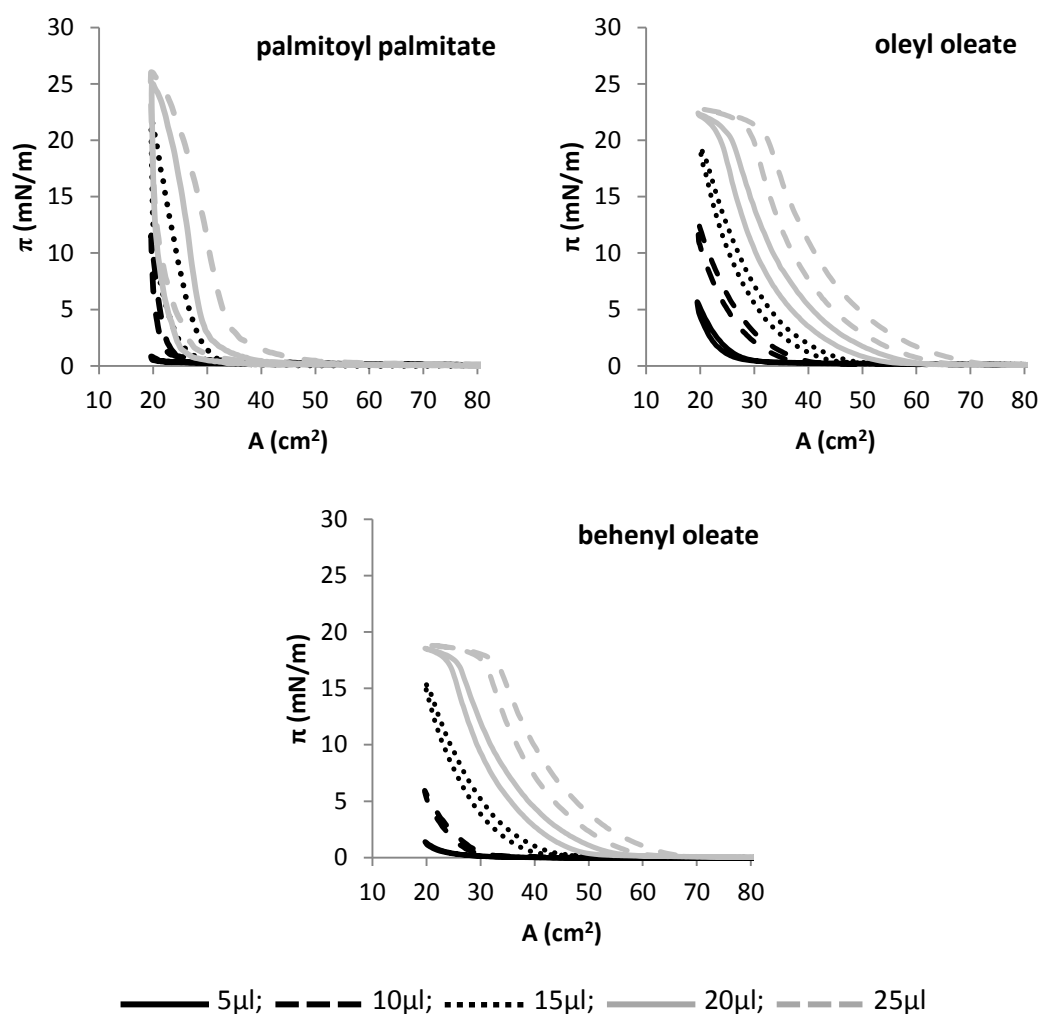


Figure 3.15. π -A isotherms of wax esters (1.0×10^{-3} moldm⁻³; 25 μ l aliquot).

3.2.3.5 Phospholipids

The surface activity of phospholipids (PL) are dictated by two key structural features: the two acyl chains esterified at positions 2 and 3 on the glycerol constituent or the alcohol head group attached to the phosphate group at position 1. Acyl chains will affect the balance between hydrophilicity and hydrophobicity of the molecule, as well as the way in which molecules will

interact during compression. The alcoholic head groups attached will also affect the amphiphilic balance dependent on the interacts with water molecules and ions within the subphase. In this study, the effect of acyl chain length and degree of unsaturation on choline-based phospholipids will be discussed.

Dimyristoylphosphatidylcholine (DMPC; Fig 3.16a) reaches a high π_c of 55.0mN/m synonymous with polar lipids but there is no evidence of this occurring at the end of an LC phase. There is no apparent transition to a LC phase from the LE phase. This might suggest slight solubility caused by the polar phosphatidyl group overpowering the hydrophobicity of the shorter chained myristoyl substituents. Dipalmitoylphosphatidylcholine (DPPC; Fig 3.16b) transitions from G to LE phase between from 0.0mN/m up to the LE-LC transition at ~11mN/m. Distearoylphosphatidylcholine (DSPC; Fig 3.16c) shows an almost direct transition from G to LC phase with a small LE phase notable between 0 - 4mN/m. Both DPPC and DSPC show π_c of 54.0mN/m and 54.9mN/m at A_{mol} of 18.7 Å² molecule⁻¹ and 46.6 Å² molecule⁻¹ respectively (Fig 3.17).

The presence of unsaturated acyl chain within dioleoylphosphatidylcholine (DOPC; Fig 3.16d) produces a highly stable film where an equilibrium surface pressure ($\pi_{eq} = 45.9$) is reached with no collapse of the monolayer. The equilibrium state of the film is indicative of a balance between the contribution of the unsaturated oleoyl chains to molecular orientation and the increased polarity from the phosphatidyl group. The presence of the two unsaturated fatty acids within DOPC induced a much larger decrease in reversibility compared to the saturated analogues. This could be indicative of an increased need to orientate the molecule at the surface in order to obtain a preferred alignment. The added structural hindrance may lead to the increasing reversibility as the surface concentration of DOPC is increased.

	Phosphatidylcholine			
	DMPC	DPPC	DSPC	DOPC
π_c (mN/m)	55.05	53.96	54.89	45.89*
$A_{\pi_{eq}}$ (cm ²)	31.75	28.19	70.15	52.27*
A_{mol} (Å ² molecule ⁻¹)	21.10	18.73	46.61	34.73*
π_t (mN/m)	0.00, ~11-18	0.00, ~12	0.00, ~26	0.00
A_t (cm ²)	86, ~50-60	60, 29	83, ~74	>90
Rev (%)	78.12	84.33	87.25	18.24

Table 3.10. Characteristic data for the 25µl aliquot π -A isotherms of phosphatidylcholines (1.0 x 10⁻³ mol dm⁻³; PBS subphase; 25°C) in Fig 3.16-3.17 (* data for DOPC was recorded at π_{eq}).

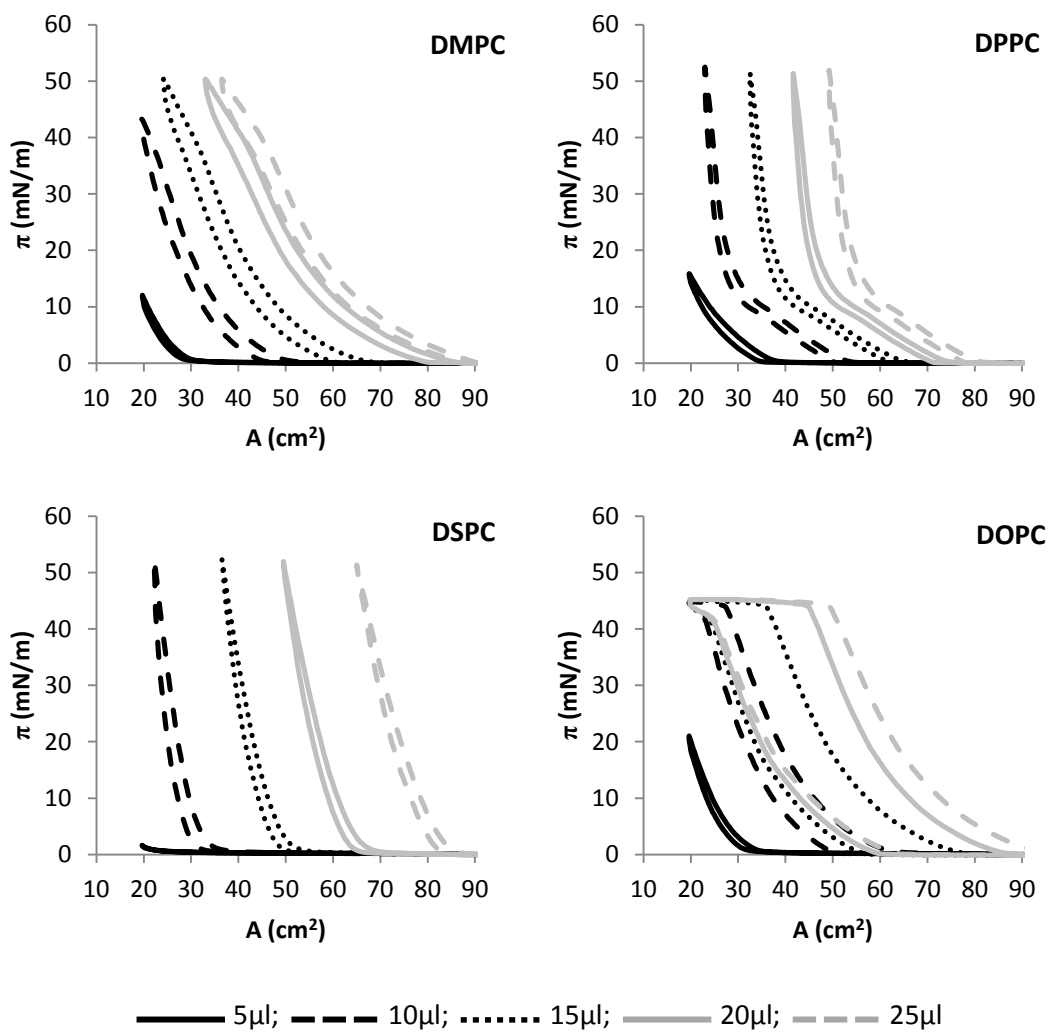


Figure 3.16. π -A isotherms of choline-based phospholipids ($1.0 \times 10^{-3} \text{ mol dm}^{-3}$; 25 μ l aliquot).

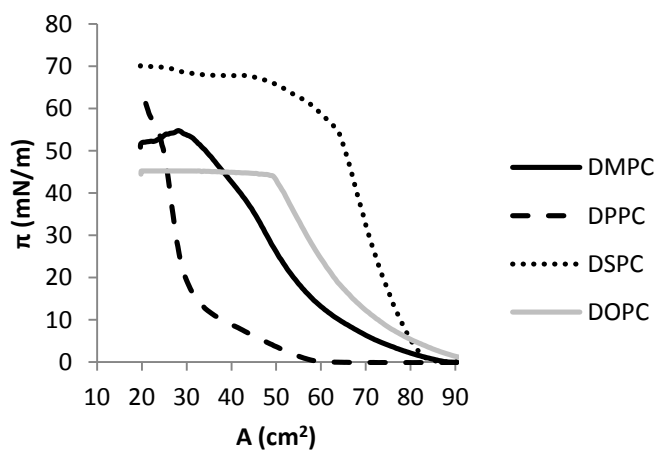


Figure 3.17. π -A isotherms of phospholipids ($1.0 \times 10^{-3} \text{ mol dm}^{-3}$; 25 μ l aliquot) compressed past the limited π_{max} .

3.2.3.6 Acylglycerides

Monoacylglycerides (MAG) and diacylglycerides (DAG) are based upon a glycerol molecule but only contain have one and two acyl chains esterified to the backbone structure respectively. Hydroxyl groups upon the glycerol structure are unesterified to a fatty acid chain and the polarity of the molecule begins to resemble that of a phospholipid. Monoolein (MO; Fig 3.18a) and diolein (DO; Fig 3.18b) both show polar lipid-like surface activity with high π_{eq} values $>45\text{mN/m}$. The presence of oleoyl based orientation and packing is evident in the distinct plateau between LE and LC phases. The main difference between the two polar glyceride molecules is the π where this plateau occurs. DO plateaus between an LE-LC₁ and LC₂ phases at $\sim 30\text{mN/m}$ before increasing to a $\pi_{eq} >50\text{mN/m}$. MO has a higher polarity due to two hydroxyl groups forming a hydrophilic head group and hence reaches an LC₁ phase π of $\sim 45\text{mN/m}$ at the end of the LE-LC₁ phase. Further experimentation would be necessary to determine if an LC₂ phase is present upon increased loading of the test material and compression to smaller working areas.

Triacylglycerides (TAG; Fig 3.18c) are non-polar molecules. Any polarity from the carboxyl group of the fatty acids or the three hydroxyl groups of the glycerol molecule are lost when they undergo an esterification to produce the TAG molecule. Triolein (TO; Fig 3.18c) shows a small degree of surface activity, in that a surface pressure increases is recorded, but the large presence of an LE phase from maximum to minimum working area would indicate a stable film that interacts only slightly with the subphase.

	Glyceride		
	MO	DO	TO
π_{eq} (mN/m)	45.63	51.92	27.59
A_{mol} ($\text{\AA}^2 \text{ molecule}^{-1}$)	26.57	26.61	-
π_t (mN/m)	0, 15-20, ~ 45	0, ~ 30 , ~ 32	0, ~ 14
A_t (cm^2)	>90 , 40-50, ~ 38	>90 , ~ 75 , 40-50	>90 , >90
Rev (%)	81.24	78.12	88.12

Table 3.11. Characteristic data for the 25 μl aliquot π -A isotherms of glyceride molecules ($1.0 \times 10^{-3} \text{ mol dm}^{-3}$; PBS subphase; 25°C) in Fig 3.16-3.17: monoolein (MO); diolein (DO); triolein (TO).

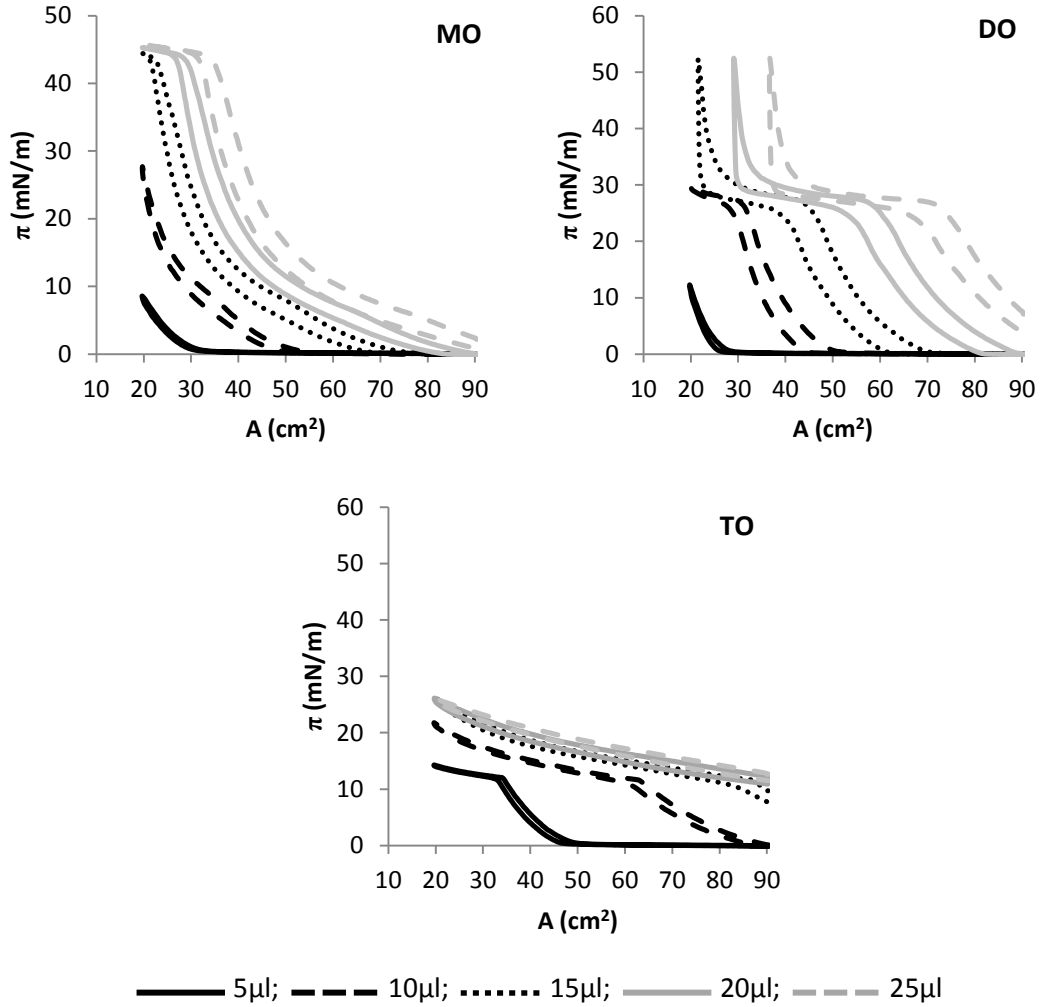


Figure 3.18. π -A isotherms of glyceride mixtures ($1.0 \times 10^{-3} \text{ moldm}^{-3}$; 25 μ l aliquot).

3.3 Protein and Mucin Components

Recent studies have shown that in addition to the surface active behaviour of the tear film lipid layer and its components, some of the major tear proteins and mucin also exhibit surface activity [38] [51]. It is thought that this characteristic may have some degree of relevancy at the lipid-aqueous interface.

3.3.1 Objective

To determine any related surface activity of lipocalin, lysozyme and mucin that might directly affect the surface pressure isotherm. To determine protein/mucin adsorption and subsequent effect on a prepared monolayer film of a tear sample.

3.3.2 Experimental design

3.3.2.1 π -A Isotherms

The surface activity of the protein and mucin components were tested upon Langmuir trough A. π -A isotherms were recorded with a working surface area of 90 to 20 cm² and a barrier speed of 20cm²/min. A phosphate buffered saline (PBS) subphase was used (pH 7.32; 35°C). Subphases were cleaned using a vacuum-aspiration pump to ensure no significant increase in surface pressure of 0mN/m. Solutions of lysozyme (Lz), β -2-microglobulin (a tear lipocalin analogue (Lc)) and bovine serum mucin (BSM) using PBS (pH 7.33 \pm 0.03) were prepared by weighing out 3.2mg/ml, 1.0 mg/ml and 1.0 mg/ml respectively [32]. Protein and mucin solutions were applied to the subphase surface from a 50 μ l Hamilton syringe onto the subphase surface. Ten minutes were allowed to ensure full spreading of the film. Compression and expansion isocycles were replicated until an equilibrium surface pressure (π_{eq}) was reached.

3.3.2.2 Adsorption of Tear Protein and Mucin Analogues to Interface

The change in surface pressure ($\Delta\pi$) caused by the adsorption of protein/mucin analogues to an ATLF monolayer was measured using a surface pressure-time (π -t) isotherm. 25 μ l of the ATLF was applied to the subphase surface from a 50 μ l Hamilton syringe onto the subphase surface and ten minutes was allowed to ensure full spreading of the film. π -A isotherms were recorded for the ATLF before instillation of protein or mucin components and replicated until reaching equilibrium. After the equilibrium π -A isotherm was obtained, the ATLF monolayer was compressed to an initial surface pressure (π_{init}) of 10mN/m. A 50 μ l volume of Lz, Lc and BSM solutions (from section 3.3.2.1) were delivered into the subphase in two aliquots at either end of the trough according to the procedure outlined in section 2.1.4. Measurements of the change in surface pressure ($\Delta\pi$) continued until an equilibrium surface pressure ($\pi_{eq (adsorb)}$) was obtained, after which a π -A isotherm was recorded.

3.3.3 Results

3.3.3.1 π -A Isotherms

Surface activity was notable in the three protein/mucin components studied. β -2 microglobulin, utilised in this study as an analogue of lipocalin (Lc), produced a π_{eq} of 25.8mN/m (Fig 3.19a). Compared to extracted and purified tear lipocalin (TLc) this value is similar to those recorded in other studies [226] [227] [217]. Lysozyme (Lz; Fig 3.19b) and bovine serum mucin (BSM; Fig 3.19c) attained π_{eq} of 28.3mN/m and 35.0 mN/m respectively which correlate well with others studies [217] [228] [229]. Equilibrium π -A isotherms were recorded after a lengthy period of time relatively high number of cycles. Lc and Lz attained equilibrium after \sim 6.5hr and \sim 5.5hr respectively, whilst BSM reached an equilibrium after \sim 8.0hr An increase in the π_{max} was observed from the first isotherm, throughout the consecutive isocycles, until the monolayer had achieved it equilibrium π -A isotherm. The π_{max} values recorded on the first isotherm run with a fresh monolayer of molecules were 17.2mN/m for Lc, 24.4mN/m for Lz and 19.9mN/m for BSM. Hysteresis between compression and expansion was observed in all three π -A isotherms with values of 84.0% for Lc, 79.4% for Lz and 89.3% for BSM. The reversibility of the monolayer is uniform in that macromolecules within the film compress together in the same way that they are repulsed and disaggregate during expansion.

	Component		
	Lc	Lz	BSM
π_{eq} (mN/m)	25.77	28.29	35.03
$T\pi_{eq}$ (hr)	\sim 6.5	\sim 5.5	\sim 8.0
Rev (%)	83.97	79.35	89.32

Table 3.12. Key characteristic data for the π -A isotherm of β -2-microglobulin (Lc), lysozyme (Lz) and bovine serum mucin (BSM) (100 μ l aliquot; 35°C).

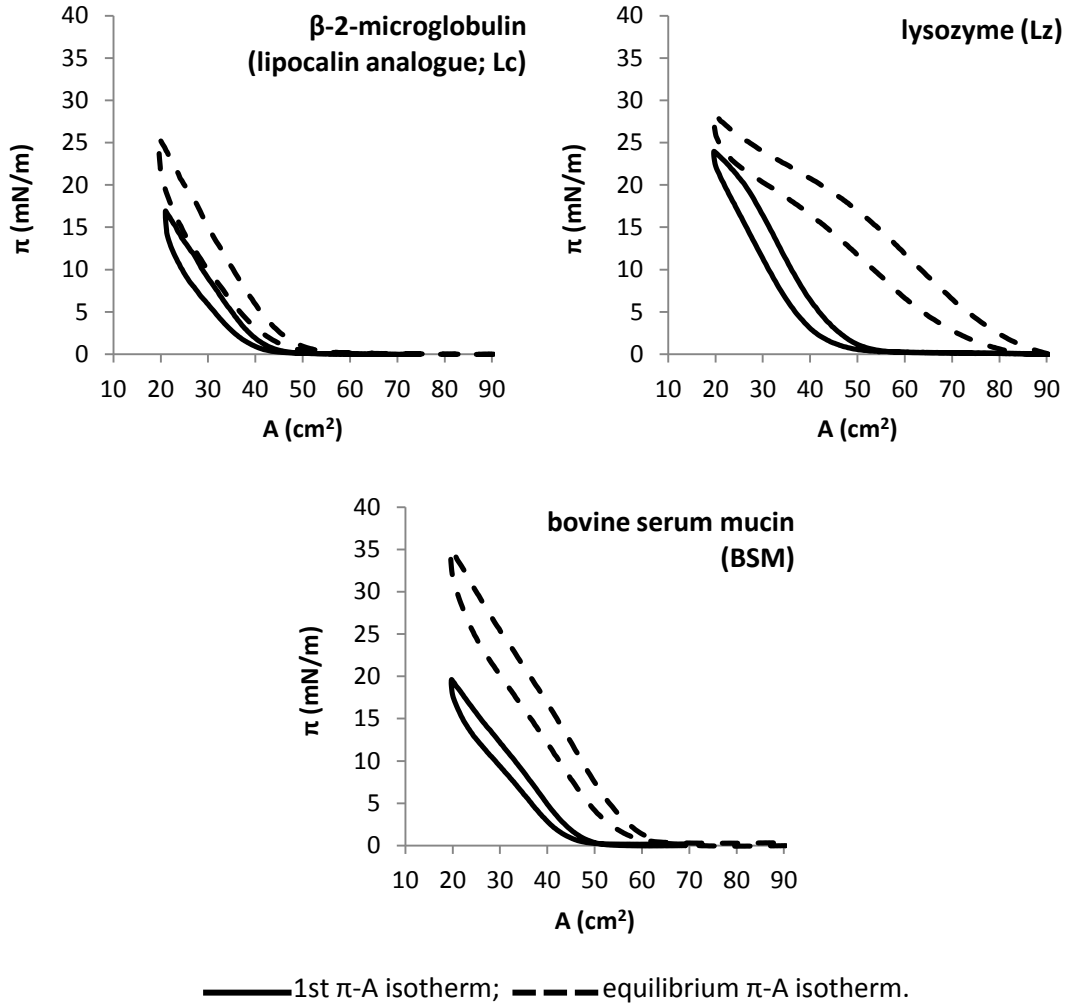


Fig 3.19. π -A isotherms of a 100 μ l aliquot of tear protein and mucin analogues.

3.3.3.2 π -t Adsorption Isotherms

The π -t isotherms of protein and mucin analogue adsorption are found in Fig 3.20. In all π -t isotherms, π_{init} was consistent at an average of 10.1mN/m (range 9.8-10.2mN/m). The ATLF showed a decrease in surface pressure to a π_{min} ($\pi_{min} = \pi_{eq}$) of 4.6mN/m ($\Delta\pi = -5.6$ mN/m). The time to reach this equilibrium surface pressure ($T\pi_{eq}$) was ~ 4000 s, indicative of normal film relaxation. The three test substances all showed varying degrees of affect to the ATLF monolayer. BSM stabilised the ATLF monolayer by increasing the π_{min}/π_{eq} to 8.4mN/m ($\Delta\pi = -1.7$ mN/m; $T\pi_{eq} = \sim 1500$ s) but showed no surface pressure increase indicative of complete monolayer penetration. The time taken to reach π_{eq} As observed in Fig 3.19c, BSM has surface activity that would become apparent by a positive $\Delta\pi$ if adsorbed into the monolayer. We can assume that some interactive role does take place between BSM and the components of the ATLF that maintains the surface pressure close to π_{init} during film relaxation.

Lysozyme (Lz) and β -2 microglobulin (lipocalin analogue; Lc) show a positive effect on $\Delta\pi$ that would indicate a fully interactive role for both molecules at an interface, with or without the presence of lipid material such as the ATLF monolayer [113] [217] [230]. It has been suggested that lysozyme (Lz) has some association with polar lipid molecules as a result of its antibacterial activity, where it interacts and disrupts the phospholipid bilayer of bacterial cell walls [99]. The surface activity of the hydrophilic lysozyme molecule has been previously established but full unfolding of the protein chains may prevent its penetration of lipid monolayer, limiting its activity to interactions beneath the surface [113] [231]. The π -t profile for Lz showed a very small decrease in surface pressure as a result of film relaxation and Lz-ATLF interactions ($\pi_{\text{init}} = 10.2\text{mN/m}$ to $\pi_{\text{min}} = 9.9\text{mN/m}$). $\Delta\pi$ was $+3.8\text{mN/m}$ with a π_{eq} of 13.7mN/m reached after $T\pi_{\text{eq}} = \sim 12000\text{s}$.

Lc shows the greatest change in surface pressure. Film relaxation causes π_{init} to fall by 3.7mN/m to π_{min} of 6.1mN/m which then increases to a π_{eq} value of 22.3mN/m ($\Delta\pi = +16.2\text{mN/m}$). The time to reach equilibrium ($T\pi_{\text{eq}}$) for Lc was much slower than that for Lz ($\sim 12000\text{s}$ for Lz as opposed to $>25000\text{s}$ for Lc). The large change in surface pressure between π_{init} to π_{min} and π_{min} to π_{eq} might be an indicator to the complex lipid binding characteristics of lipocalin. It is possible that the initial film relaxation is acting concurrently with potential lipid binding actions of the lipocalin drawing lipid molecules out of the monolayer. Evidence suggests that lipid release from lipocalin does not induce a great stability in a monolayer and that any increase in surface pressure observed is due to penetration of both conjugated and unconjugated molecules [52] [105] [226] [227].

	π_{init} (mN/m)	π_{min} (mN/m)	π_{eq} (mN/m)	$\Delta\pi$	$T_{\pi_{\text{eq}}}$ (s)
ATLF	10.14	4.58	4.58	- 5.56	4000
Lz	10.21	9.86	13.65	+ 3.81	12000
Lc	9.83	6.13	22.34	+ 16.21	>25000
BSM	10.09	8.37	8.39	- 1.70	1500

Table 3.13. π -t isotherm data for adsorption of β -2 microglobulin (lipocalin analogue; Lc), lysozyme (Lz) and bovine serum mucin (BSM) to a ATLF monolayer.

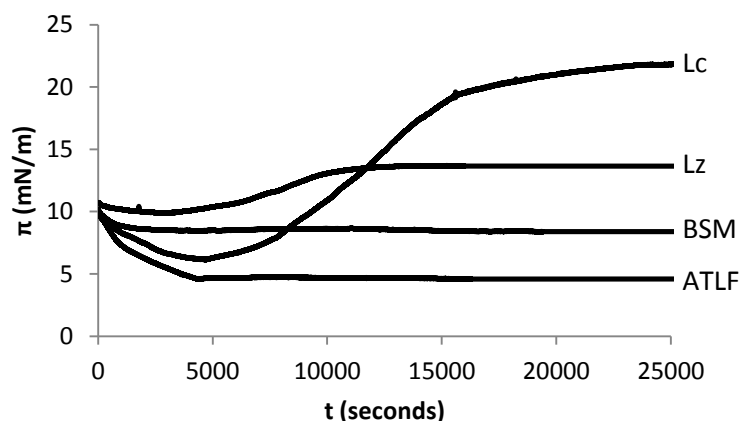


Fig 3.20. π -t adsorption isotherm of β -2 microglobulin (lipocalin analogue; Lc), lysozyme (Lz) and bovine serum mucin (BSM) to an ATLF monolayer.

After complete adsorption of the protein/mucin components π -A isotherms were recorded for the mixed ATLF/component monolayer (Fig 3.21). This was compared against the equilibrium isotherm of the ATLF monolayer prior to instillation of the protein/mucin solutions. Higher π_{eq} and reversibility is noticed in the ATLF/protein-mucin monolayers after complete adsorption, indicating an increased surface activity of the mixed monolayer either through direct component penetration or a stable interaction at the liquid-gas interface. π -A isotherms taken after adsorption of the test materials were recorded at the first isocycle. This was in order to obtain the compression and expansion behaviour of the monolayer exactly where the protein/mucin components locate themselves during penetration/interaction.

Lc shows an increase in π_{eq} from 25.1mN/m to 36.7mN/m and a decrease in the reversibility from 89.5% to 71.3%. The equilibrium surface pressure reached after adsorption exists within the LE phase, but there is no indication whether it maintains this phase as compression would increase or transition from the LE phase to either an LC phase or a plateau. Lz similarly showed an increase in surface pressure from 21.68mN/m to 32.08mN/m and a decrease in reversibility to 76.02%. It is understood that lysozyme is selective to only phospholipids - as opposed to the lipocalin that can bind to a larger variety of lipid types - and shows a lesser ability of ATLF monolayer penetration compared to lipocalin [99]. Despite only having a limited effect on the ATLF monolayer over time, BSM (Fig.21c) does have some stabilising effect at the surface observed in the π -A isotherm after. Much like Lc and Lz, some interaction or penetration of mucin has occurred to produce a mixed monolayer where π_{eq} increased from 22.5mN/m to 26.0mN/m. Reversibility of the monolayer during compression and expansion was also observed to decrease from 92.7% to 72.4%.

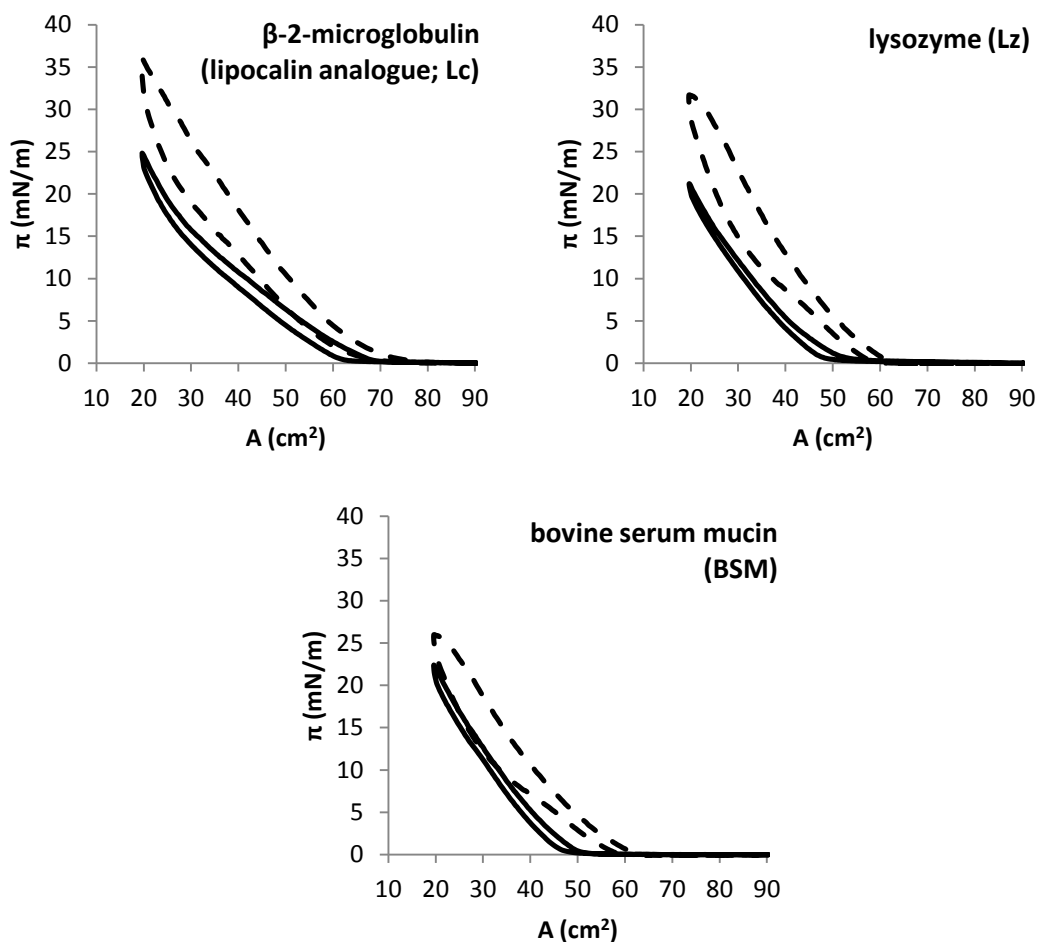


Fig 3.21. π -A isotherms of an ATLF monolayer before (—) and after (---) adsorption of tear protein and mucin analogues

	Before Instillation		After Adsorption	
	π_{\max} (mN/m)	Rev (%)	π_{\max} (mN/m)	Rev (%)
Lc	25.13	89.46	36.41	71.33
Lz	21.68	88.63	32.08	76.02
BSM	22.51	92.67	25.97	72.39

Table 3.14. π -A isotherm data for an ATLF monolayer before instillation of the protein/ mucin components and after complete adsorption of the studied components.

3.4 Discussion

The research presented in this section has provided information regarding the complex nature of the surface chemistry of lipid molecules based upon predominately on the structure and characteristics of the molecule. There are also major experimental considerations that have to be taken when designing Langmuir trough-based experiments of lipid molecules.

3.4.1 Lipid Structure and Interaction

As observed, lipid structure plays a main role in forming a stable layer, especially when stability at the lipid-aqueous interface of the tear film is discussed. Despite contention on the exact composition of the tear film lipid layer, it is generally accepted that the amount of each lipid type must be maintained within small ranges to produce a stable film system [2] [75]. Disease and dysfunctional states that affect the composition of the lipid layer can lead to increased instability and rate of aqueous evaporation [42] [232]. The study of the individual lipid types indicate their behaviour at the gas-liquid interface and highlight the difference between surfactant polar lipid molecules and the non-polar lipid. Langmuir trough and surface pressure measurements corroborate the idea that the tear film lipid layer forms in two phases. Polar lipids produce a much higher surface pressure when compared to non-polar lipid layers, resulting in the decrease in surface tension of the layer.

Whilst the differences in surface activity between polar and non-polar lipids are quite distinct, there are other factors that must also be accounted. The fatty acid content of the main lipid types will affect surface behaviour, specifically the way in which the molecules interact with the nearest molecular neighbours [18] [233] [234]. Saturated fatty acid-containing lipids are straight chained and are observed to have a smaller average molecular area than unsaturated and branched fatty acids. The bulky side groups and kinks in the chain caused by the presence of double bonds increase molecular area. When compressed, these molecules attempt to optimise the orientation in order to pack together. These bulkier molecules also produce an extra amount of repulsion cause by structural hindrance between molecules that aids in rapid spreading during expansion of the monolayer [235] [236]. A balance between saturated and unsaturated lipids is necessary to observe dense packing, prevention of collapse as the eyelids close and the spreading as they open again, and remaining a fluid film at the exposed ocular surface [14] [18] [237] [238].

In order to relate the data in this study to the perceived interactions at the aqueous-lipid interface, the interaction between different lipid types has to be considered. Individual surface pressure measurements can only in part explain the potential surface behaviour in relation to other molecules. By looking at how mixed monolayers of different concentrations of lipids, the relationship between lipid types provides an extra dimension of understanding as to how lipid molecules compress. According to the lipid layer schematic proposed by McCulley and Shine [12] [13] the various polar molecules within the thin polar lipid subphase will interact through hydrogen bonding of hydroxyl, carboxyl and phosphatidyl groups to an increasing extent as compression brings them in to closer proximity [12] [13] [235]. In much the same way, the interaction between hydrophobic regions should be considered. With ~90% of the tear film lipid layer consisting of non-polar molecules, the interactions between different types of hydrophobic structure and the dimensions that they exist within are important in relating surface pressure measurements to co-operative surface activity in mixtures.

The abundant amount of literature that has studied the surface interaction between two or more lipid components provides a great deal of information on the consequent effect that these mixed monolayers on surface activity. Apart from the well-established tear film lipid layer, these mixed interactions form the characteristics of many other biological systems including cell membranes and pulmonary surfactant. All of these systems have in common an interfacial region - whether gas-liquid or liquid-liquid - that is a product of various lipid molecules interacting between two adjacent phases and within the same phase.

3.4.2 Interactions with Proteins and Mucins

The concept that the lipid-aqueous interface of the tear film consists purely of contributions from the tear lipids has been challenged. Recent studies have highlighted that some non-lipid components of the tear film play an important role in the surface activity at the aqueous-lipid interface [38] [51] [217]. There is increasing evidence of tear lipocalin [38] [51] [226] [227], lysozyme [113] [239], lactoferrin [240] and soluble mucins [36] [37] [38] [154] molecules having a role by increasing stability of the interface through decreasing surface tension [15] [241] [242] [243]. Low surface tensions indicate that a high surface pressure in Langmuir trough experiments is desirable for stable lipid-protein film.

3.4.3 Experimental Considerations

The Langmuir trough method provides a great deal of information to be gathered on the surface activity of monolayer of individual and mixed components, but considerations on the experimental design are necessary. The considerations taken within this chapter will form the basis of the experimental design for the extraction and study of tear samples. As observed in temperature based studies of surface pressure, temperature plays a key role in the surface activity of individual molecules and the fluidity of the monolayer. Small changes to the temperature, especially for mixed lipid layer with a small melting range, can significantly change their surfactant behaviour and inhibit or promote fluidity of the monolayer film. The melting range of Meibomian lipids is $\sim 20-40^{\circ}\text{C}$ [244] [245] [246] and is a product of the complex composition of lipid types and structures. Whilst saturated fatty acid-based molecules have high melting points, it is the presence of branched and unsaturated fatty acids and fatty alcohols that lowers the melting range [10] [21] [247]. It is assumed that the lipids within the tear film lipid layer are at the exposed corneal temperatures ($\sim 32^{\circ}\text{C}$ [237]).

Consequently, a change in environmental conditions such as temperature, humidity and wind can affect the exposed ocular environment to the point of a deleterious influence on lipid layer fluidity and stability. The troughs that were used in this thesis both had built-in heating elements that increased the temperature to a desired ocular temperature. Any effect from a breeze that would affect the monolayer and the Wilhelmy plate is virtually non-existent in these measurements due to the use of environment boxes to enclose the trough during use.

The effect of pH and electrolyte ion concentrations within subphase is another key experimental consideration [222] [248] [249]. Much like the composition of the tear lipid types, pH and electrolyte concentration within the aqueous phase must also be maintained in small ranges for the natural system to be stable [1] [94] [250]. The spreading behaviour and interactions between Meibomian lipids and the aqueous phase can be affected by the pH of the subphase and electrolyte concentration [152] [224]. Ions within the subphase lead to the formation of complexes with polar molecules that alters the surfactant properties of the molecule [218] [222] [249]. The relationship between ion concentration and tear film stability becomes clear in the observed hyperosmolarity in disease state tear films, where increased levels of electrolytes have been detected [1] [134]. In cases such as dry eye disease, this

increase in the concentration of electrolytes comes from the higher rate of evaporation caused by an insufficient lipid layer.

Other Langmuir trough experimental conditions such as compression speed (in terms of area), the compressible area ratio have not been studied as part of this research. The speed of barrier compression and expansion was not taken into account due to the observed limited effect on the π -A isotherm of mono- and bimolecular monolayers [251] [252]. Another consequence of the method is the inability to match the speed of a blink using the barriers. Whilst the speed of the barriers can be set to quite high levels (in excess 100cm²/min), they are not near the closing speed of 0.1-0.3 ms⁻¹ that the eyelids close at during a blink [158]. This has ramifications for ex-vivo measurements of spreading and compressing characteristics of prepared tear sample monolayers.

3.5 Summary

The following conclusions can be observed from the experimental data within this chapter.

- The surface behaviour of tear lipids is varied depending on the structure of the lipid molecule;
 - Polar lipids show significantly different surface chemistry to non-polar lipids;
 - Cholesterol - despite containing a large hydrophobic, four-planar ring structure - is observed to have surface activity akin to polar lipids
 - The fatty acid content (length of the hydrocarbon chain, the degree of unsaturation) affects the packing behaviour of the monolayer at small surface area;
- The surface chemistry of the tear film lipid layer will thus be dictated by the composition of the various lipid types and fatty acid contents. An excess or deficiency in any of the major tear lipid types can significantly alter the surface behaviour of the tear film lipid layer;
- The conditions used in Langmuir trough experiments (subphase pH and composition, temperature, amount of loaded sample material) have a significant effect on the π -A isotherm data;
- The behaviour of proteins and soluble mucins found within the tear film aqueous layer is potentially significant in aiding the stability of the lipid-aqueous interface.

Chapter 4

In-vitro Study of Tear Film Samples: Preliminary Evaluation of Collection Methodology

The need for a suitable method of the study of the interfacial characteristics of the lipid-aqueous interface is paramount: non-invasive techniques of observing tear film stability provides limited quantitative information. The Langmuir trough provides the means to study the surface characteristics of tear film samples. However, the benefits of using surface pressure measurements to understand the surface behaviour of tear film lipids is counterbalanced by the ability to obtain *ex-vivo* tear samples. Particular concern is the efficient collection of samples and the need to obtain an adequate quantity for subsequent analysis [253] [254]. In order for *in-vitro* Langmuir trough based studies of *ex-vivo* tear lipids to be valid two main considerations have to be made: the sampling technique and the extraction methodology.

4.1 Objectives

The main objectives are to optimise and evaluate the methodology of collection and extraction of tear samples to obtain representative π -A isotherms. This will include the use of various sampling probes for tear film component collection. The suitability of each sampling probe will be based upon the method of collection, the storage and the extraction solvents used to obtain sample material in order to optimise the way in which the small volumes of sample would be studied. Further considerations will be taken as to the repeatability of experiments for a single tear sample.

4.2 Experimental Design

The following probes were used to collect samples from subjects:

- Glass microcapillary tubes - Sigma Microcapillary pipettes (volume 1-10 μ L);
- Schirmer strips - Mid Optic Schirmer Tear Test Strips;
- Visispear™ ophthalmic sponges - Visispear Eye Sponge™, Visitec, Becton Dickinson and Company, USA;
- Contact lenses - Focus Night+Day (FN+D; lotrafilcon A; CIBA Vision, USA);

All tear samples were obtained from clinical trials conducted within the Biomaterials Research Unit or from external trials conducted by the Vision Sciences department at Aston University. Sampling probes were stored within glass vials and stored in at $\sim 4^{\circ}\text{C}$. Extraction protocols for each sampling probe will be detailed in sections 4.2.1 - 4.2.4.

The surface behaviour study of tear samples was conducted on both Langmuir troughs. These were set up according to the procedure described in section 2.1. Langmuir trough A has a working surface area of $90\text{-}20\text{ cm}^2$ and a barrier speed of $20\text{cm}^2/\text{min}$. Langmuir trough B had a working surface area of $400\text{-}100\text{ cm}^2$ and a barrier speed of $50\text{cm}^2/\text{min}$. HPLC-grade water was used as a subphase and kept at a constant temperature of $35.0^{\circ}\text{C} \pm 0.2^{\circ}\text{C}$. All sample solutions were applied to the subphase surface by a $50\mu\text{l}$ Hamilton syringe. At least ten minutes was allowed to ensure full spreading of the solution, solvent evaporation and spontaneous movement and arrangement of components. Tear sample films were repeatedly compressed and expanded until the equilibrium surface pressure (π_{eq}) was reached.

A minimum area of 100cm^2 was set for Trough B experiments in order to accommodate the Brewster Angle Microscope (BAM) prior to the first aliquot of samples being introduced to the subphase surface (Section 2.2). Images of the subject sample monolayer was taken at a loading volume where a maximum surface pressure and after an equilibrium π -A isotherm had been recorded.

4.2.1 Microcapillary Tube Collection

Narrow-bore glass capillary tubes (Sigma Microcapillary pipettes, volume range $1\text{-}10\text{ }\mu\text{L}$ (P6804)) were used to sample tears taken from the marginal regions of the exposed ocular surface according to the methodology detailed by Mann & Tighe [255] (Table 4.1). The capillary tubes were carefully broken in order to be covered in the solvent when placed within glass vials and extracted for 1hr in CHCl_3 . After extraction, the solvent was transferred to a clean vial by pipette. This was then stored at -20°C to prevent solvent evaporation. Control samples were produced by drawing up $5\mu\text{l}$ of saline solution (Saline, Sauflon Pharmaceuticals Ltd, UK) into a fresh microcapillary tube and extracted by the same protocol.

	Volume collected (μl)	Volume of solvent (cm^3)
Control 1	5.1	1.02
Control 2	5.0	1.00
Px1	4.0	0.80
Px2	3.9	0.78
Px3	4.0	0.80
Px4	4.2	0.84

Table 4.1. Calibrated extracting volumes of CHCl_3 based upon volume collected for sample and control microcapillary tubes.

4.2.2 Schirmer Strip Collection

Schirmer strips (Mid Optic Schirmer Tear Test Strips) were placed in the lower temporal cul-de-sac of the eye and gently closed. The samples are collected for 5 minutes or until the strip is filled and the wetted length of the strip measured. The strip is then placed within a 1.5ml amber vial for storage and extraction. Two strips per subject (one per eye) were collected and extracted using hexane and chloroform for 1hr. The necessary volume of extracting solvent was determined dependent upon the wetted length of the strip (Table 4.2). Control Schirmer strips wetted with saline solution (Saline, Sauflon Pharmaceuticals Ltd, UK) to a wetted length of 30mm were also extracted. Roughly 5% of the extracting volume of solvent was lost during removal of the strip from the extraction vessel.

	Left Eye			Right Eye		
	WL (mm)	EV (cm^3)	UV (cm^3)	WL (mm)	EV (cm^3)	UV (cm^3)
Control 1	30	0.50	0.46	-	-	-
Px1	18	0.30	0.28	30	0.50	0.47
Px2	22	0.36	0.32	19	0.32	0.30
Px3	25	0.42	0.39	20	0.33	0.31
Px5	20	0.34	0.31	24	0.40	0.37

	Chloroform			Hexane		
	WL (mm)	EV (cm^3)	UV (cm^3)	WL (mm)	EV (cm^3)	UV (cm^3)
Px4	18	0.30	0.29	18	0.30	0.30
Control 2	30	0.50	0.46	30	0.50	0.48

Table 4.2. Usable volume (UV) of extracting volumes (EV) of solvent based upon wetted length (WL) of sample and control Schirmer strips.

4.2.3 Sponge Collection

Samples were collected by placing Visispear™ ophthalmic sponges (Visispear Eye Sponge, Visitec, Becton Dickinson and Company, USA) within the marginal regions of the exposed ocular surface. A suitable amount of sample was collected as determined by the swelling of the sponge. The sponge was cut from the stalk and placed in to a clean glass vial for storage and extraction. The sponges were then extracted for 1hr using a suitable amount of chloroform or hexane. The volume of extracting solvent utilised was dependent upon the dimensions of the swelled region of the sponge according to the calibration parameters set by Maissa [256] (Table 4.3). A control sponge sample that had been adsorbed with saline (Saline, Sauflon Pharmaceuticals Ltd, UK) was also extracted by the same protocol.

	Absorbed length (mm)	Volume of solvent (cm ³)
Control 1	10.1	1.01
Control 2*	10.0	1.00
Px1	7.8	0.78
Px2	6.7	0.67
Px3	9.2	0.92
Px4*	8.8	0.88
Px5	7.9	0.79
Px6	8.4	0.84
Px7	8.9	0.89

Table 4.3. Calibrated extracting volumes of CHCl₃ based upon absorbed length of sample and control Visispear™ ophthalmic sponges (* was extracted in hexane).

4.2.4 Contact Lenses

Worn and unworn Focus Night+Day (FN+D) contact lenses (lotrafilcon A; CIBA Vision, USA) were used as probes for obtaining tear samples. FN+D lenses were worn by the same subject for one month under a daily wear modality (DW). Once removed from the eye, the contact lens was placed into a vial containing saline (Sauflon Pharmaceuticals Ltd, UK) to keep the lens hydrated and stored at ~4°C. Three worn lenses were collected and extracted in 1.5ml CHCl₃:CH₃OH solution (1:1 w/w) and then studied on Trough A to determine the reproducibility between samples taken from the same subject. Comparative extraction of worn FN+D lenses using different solvents was also studied. Two worn contact lenses were collected and extracted in 1.5ml of each of CHCl₃:CH₃OH (1:1 w/w); two extracted in C₆H₁₄; two extracted in C₆H₁₄:CH₃OH (9:1 w/w).

Unworn FN+D lenses were taken from their packaging, rinsed with saline to wash any remaining packaging solution from the lens and blotted on filter paper to remove excess saline. These were extracted using the same protocols and solvents detailed above. Due to potential breakdown of the contact lens during extraction, the extracting solutions were transferred to a clean glass vial by pipette. This was to prevent any further extraction of unwanted surfactant components from broken lens material remaining in the extracting solution. All samples were studied within 24hr of extraction.

4.3 Results

4.3.1 Microcapillary Tubes

The overall observations of the extraction of tear samples from microcapillary tubes were that surface pressure values at high aliquot volumes applied to the subphase surface. With a maximum aliquot volume of 750 μ l that could be applied to the subphase surface none of the three samples achieved a maximum surface pressure (π_{max}). At maximum loading (750 μ l), the tear samples Px1, Px2 and Px3 produced π_{max} values of 13.4mN/m, 8.8mN/m and 12.5mN/m respectively. Evidence suggests that a larger concentration of tear sample would produce a higher maximum surface pressure. The first detectable increase in surface pressure from the 0mN/m observed for a clean subphase was at 450 μ l, 550 μ l and 550 μ l for Px1, Px2 and Px3 respectively. Reversibility between compression and expansion cycle was high at all loaded volumes for the three samples (~90-95%).

The control sample produced no discernible increase in surface pressure from the baseline recorded for the clean subphase surface (~0.0mN/m) for the full loading of 950 μ l of the extracted control sample (Fig 4.1d). Studies of tear samples collected using microcapillary tubes on the larger working surface area of Trough B is not feasible. The π -A isotherms obtained for the sample collected from subject Px4 on trough B (Fig 4.2) showed minimal increase in maximum surface pressure at maximum loading volume. An increase in surface pressure was detected at a loaded volume of 650 μ l and π_{max} of 2.9mN/m was recorded for a 750 μ l aliquot of the tear sample and an increase was only collected from subject Px4. A control sample collected from a microcapillary tube adsorbed with saline produced no increase in surface pressure at the highest loading (950 μ l aliquot).

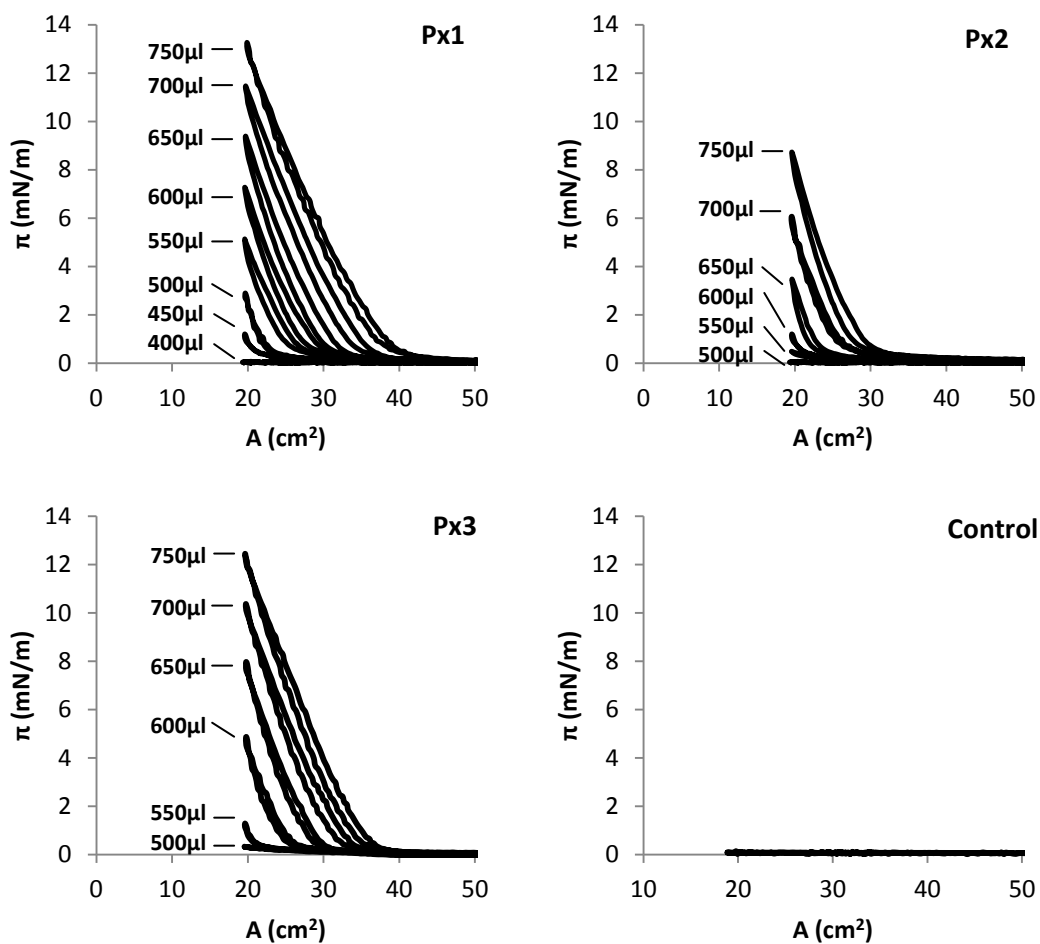


Fig 4.1. π -A isotherms of glass capillary extracted samples on Trough A for Px1, Px2 and Px3 tear samples and control sample (900 μl aliquot).

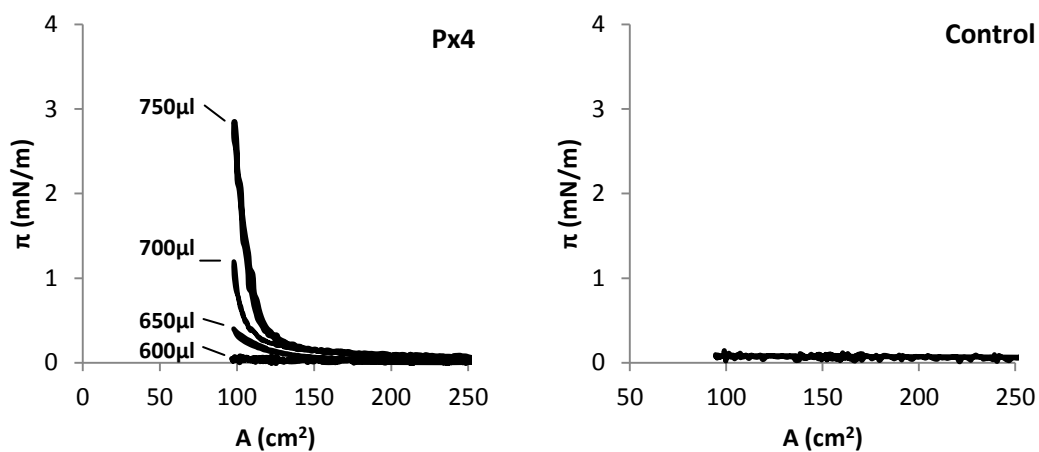


Fig 4.2. π -A isotherms of glass capillary extracted samples on Trough B for Px4 tear sample and control sample (950 μl aliquot).

A suggestion for the development of the microcapillary tube as a sampling probe in Langmuir trough based experiments will be the necessity for sample pooling. Collection of several days' worth of tear samples followed by extraction within the same volume of solvent may solve the issue of the high surface concentration/low surface pressure values. This would of course eliminate the uniqueness of surface behaviour for a single tear sample collected. Decreasing the volume of solvent used to extract may have the desired effect of increasing the concentration of extractable components, but would limit the amount of sample that can be worked with. For example, if the extracted volume used to extract the sample from Px1 was halved from 0.8ml to 0.4ml, the maximum surface pressure of 13.4mN/m would instead be obtained at a general aliquot volume of 375 μ l (~94% of the sample). Certainly, repeat π -A isotherms from the same sample would be impossible.

4.3.2 Schirmer Strip Collection

4.3.2.1 Inter- and Intra-subject Variability

It is possible to compare subjects to determine any potential differences in the surface behaviour of tear samples, as well as any differences that may occur between samples taken from left and right eyes of the same subject. Fig 4.3-4.5 shows the left eye (LE) and right eye (RE) data for subjects Px1, Px2 and Px3. 25 μ l aliquot intervals of each sample were applied to the subphase surface and π -A isotherms recorded until a maximum surface pressure (π_{\max}) was attained. As these aliquot volume intervals may not represent the same concentration of component, the volume of sample is represented as the percentage of the total usable volume (UV) of the extraction solution (Table 4.2).

The left eye tear sample of Px1 (Fig 4.3; Column A) produced a π_{\max} of ~27.0mN/m obtained at the 225 μ l aliquot (UV = 80.35%) and initial surface pressure (π_{init}) was 3.5mN/m. Increase in surface pressure was observed at a loaded volume of 25 μ l (UV = 8.93%) where a π_{\max} of 7.6mN/m was recorded (π_{init} = 0.0mN/m; A_t = ~32cm²). The right eye tear sample (Fig 4.3; Column B) produced a π_{\max} of 26.3mN/m obtained at the 350 μ l aliquot (UV = 74.46%) and π_{init} was 3.7mN/m. Increase in surface pressure was observed at a loaded volume of 50 μ l (UV = 10.64%) where a π_{\max} of 4.9mN/m was recorded (π_{init} = 0.0mN/m; A_t = ~26cm²).

The left eye tear sample of Px2 (Fig 4.4; Column A) produced a π_{\max} of 30.3mN/m obtained at the 250 μ l aliquot (UV = 78.13%) and π_{init} of 13.8mN/m. Increase in surface pressure was observed at a loaded volume of 25 μ l (UV = 7.81%) where a π_{\max} of 9.7mN/m was recorded (π_{init} = 0.0mN/m; A_t = $\sim 31\text{cm}^2$). The right eye tear sample (Fig 4.4; Column B) produced a π_{\max} of 30.2mN/m obtained at the 225 μ l aliquot (UV = 75.00%) and an π_{init} of 13.8mN/m. Increase in surface pressure was observed at a loaded volume of 25 μ l (UV = 8.33%) where a π_{\max} of 16.4mN/m was recorded (π_{init} = 0.0mN/m; A_t = $\sim 57\text{cm}^2$).

The left eye tear sample of Px3 (Fig 4.5; Column A) produced a maximum surface pressure (π_{\max}) of 29.4mN/m obtained at the 325 μ l aliquot (UV = 83.33%) and an π_{init} of 3.1mN/m. Increase in surface pressure was observed at a loaded volume of 50 μ l (UV = 12.82%) where a π_{\max} of 9.5mN/m was recorded (π_{init} = 0.0mN/m; A_t = $\sim 32\text{cm}^2$). Right eye tear sample (Fig 4.5; Column B) produced a π_{\max} of 28.3mN/m obtained at the 250 μ l aliquot (UV = 80.64%) and an π_{init} of 3.8mN/m. Increase in surface pressure was observed at a loaded volume of 25 μ l (UV = 8.06%) where a π_{\max} of 2.4mN/m was recorded (π_{init} = 0.0mN/m; A_t = $\sim 22\text{cm}^2$).

The π -A isotherm obtained for the extraction of a Schirmer strip that had been adsorbed up to a wetted length of 30mm in saline obtained results that are similar to those observed in the subject samples. The control Schirmer strip extracted in chloroform (Fig 4.6) produced a maximum surface pressure (π_{\max}) of 26.3mN/m obtained at the 375 μ l aliquot (78.12% of extraction solution). The initial surface pressure (π_{init}) for the π -A isotherm recorded for the 375 μ l aliquot was 0.0mN/m with a gradual transition from gaseous to liquid expanded phase between π_t of 0.0-7.5mN/m at an area region (A_t) of 88-55 cm^2 .

The extraction of the control sample strip leads to a single conclusion: that chloroform is too harsh as an extracting solvent when using Schirmer strips as a sampling probe. Whilst Fig 4.3 - 4.5 indicate that using chloroform as a solvent for extracting samples from subject from a Schirmer strip might prove beneficial, any significant surface behaviour observed in the data obtained is negated due to the π -A isotherm data obtained for the control strip (Fig 4.6). The fact that successive loading (increasing surface concentration) produces a maximum surface pressure that is similar to that seen with tear samples - π_{\max} values of ~ 25 -30mN/m and LE phase behaviour of the monolayer - only further proves that chloroform is not suitable for obtaining tear samples without any contamination

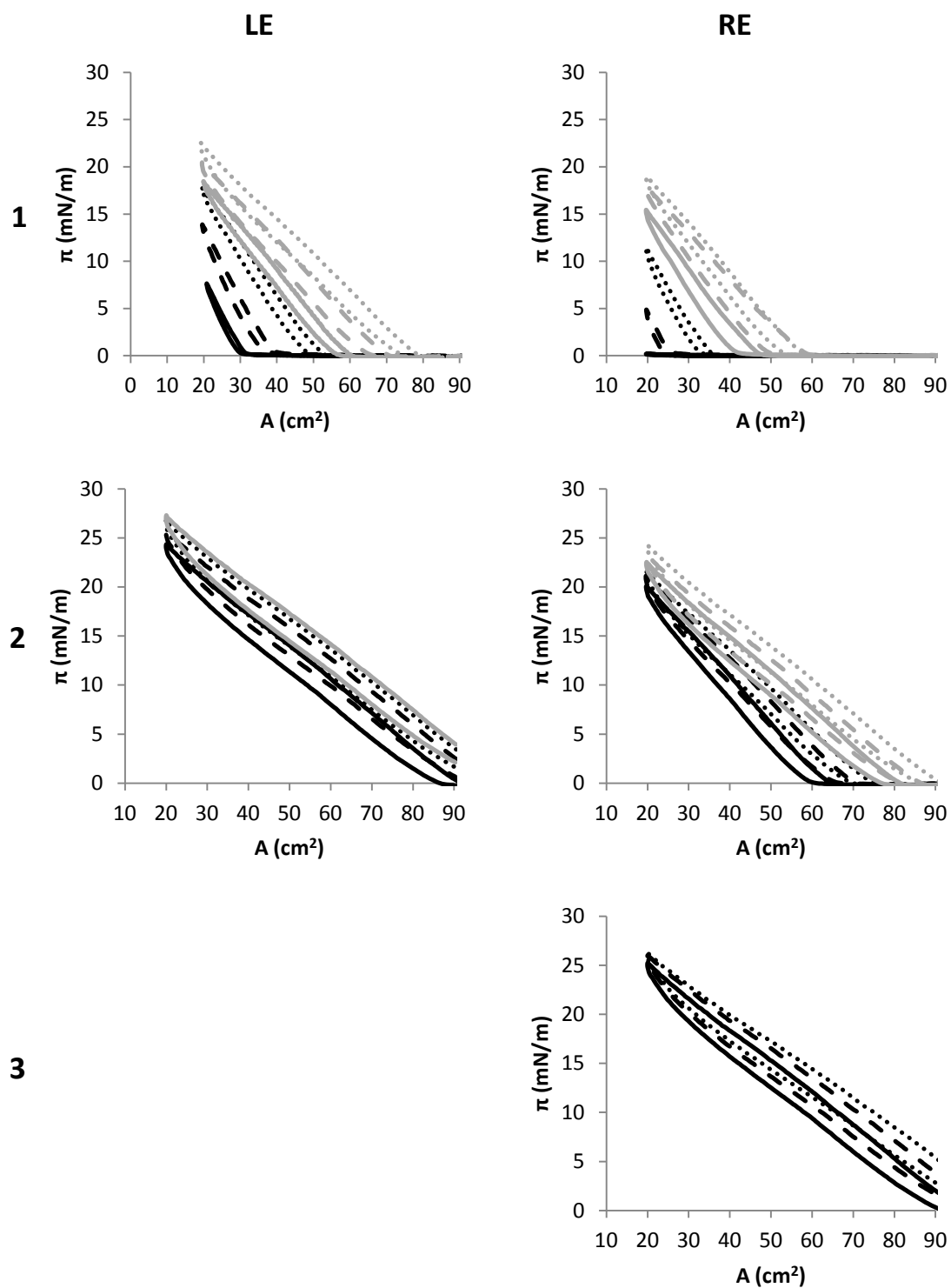


Fig 4.3. π -A isotherms of extracted left eye (LE; Column A) and right eye (RE; Column B) tear samples from subject Px1.

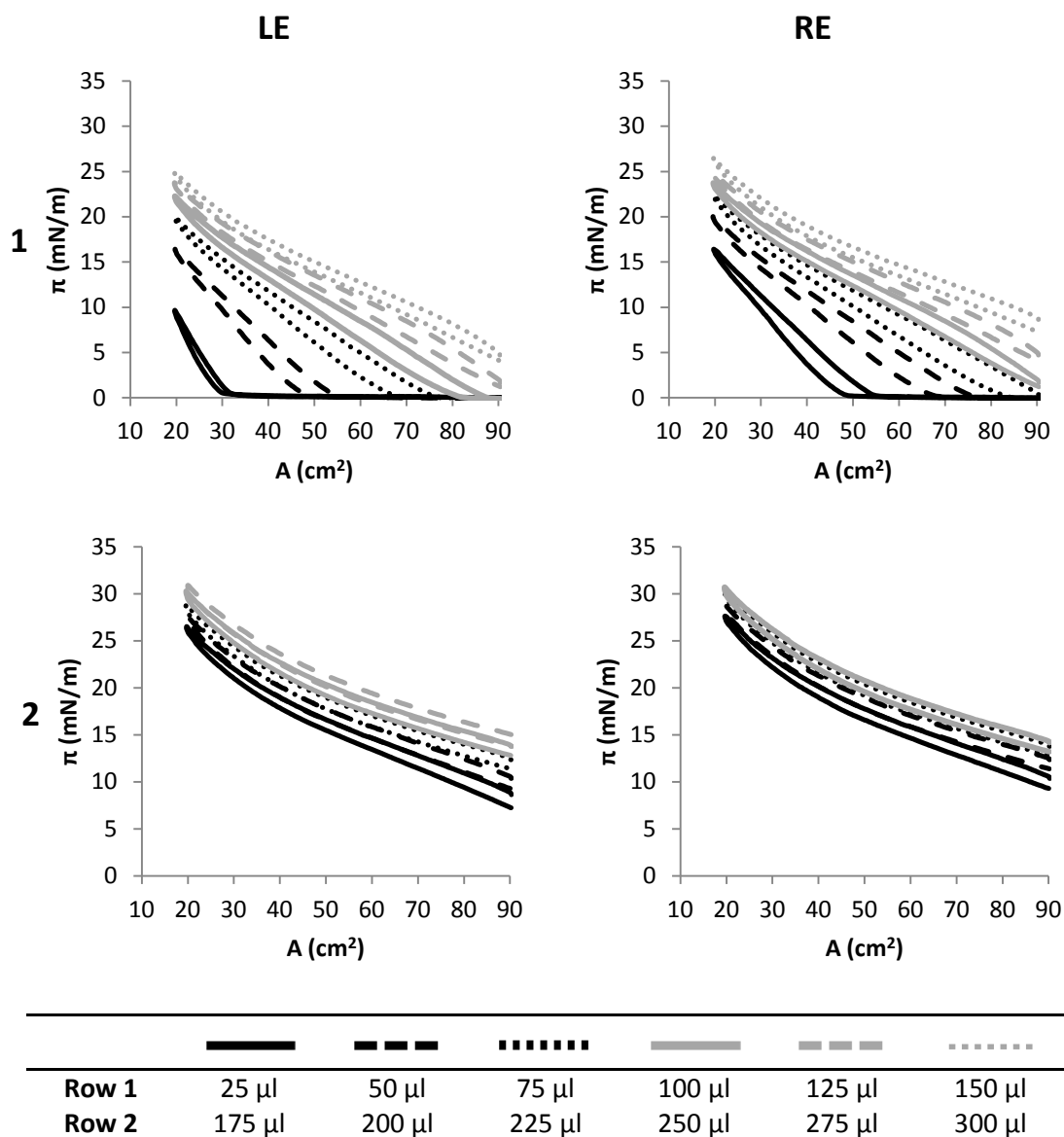
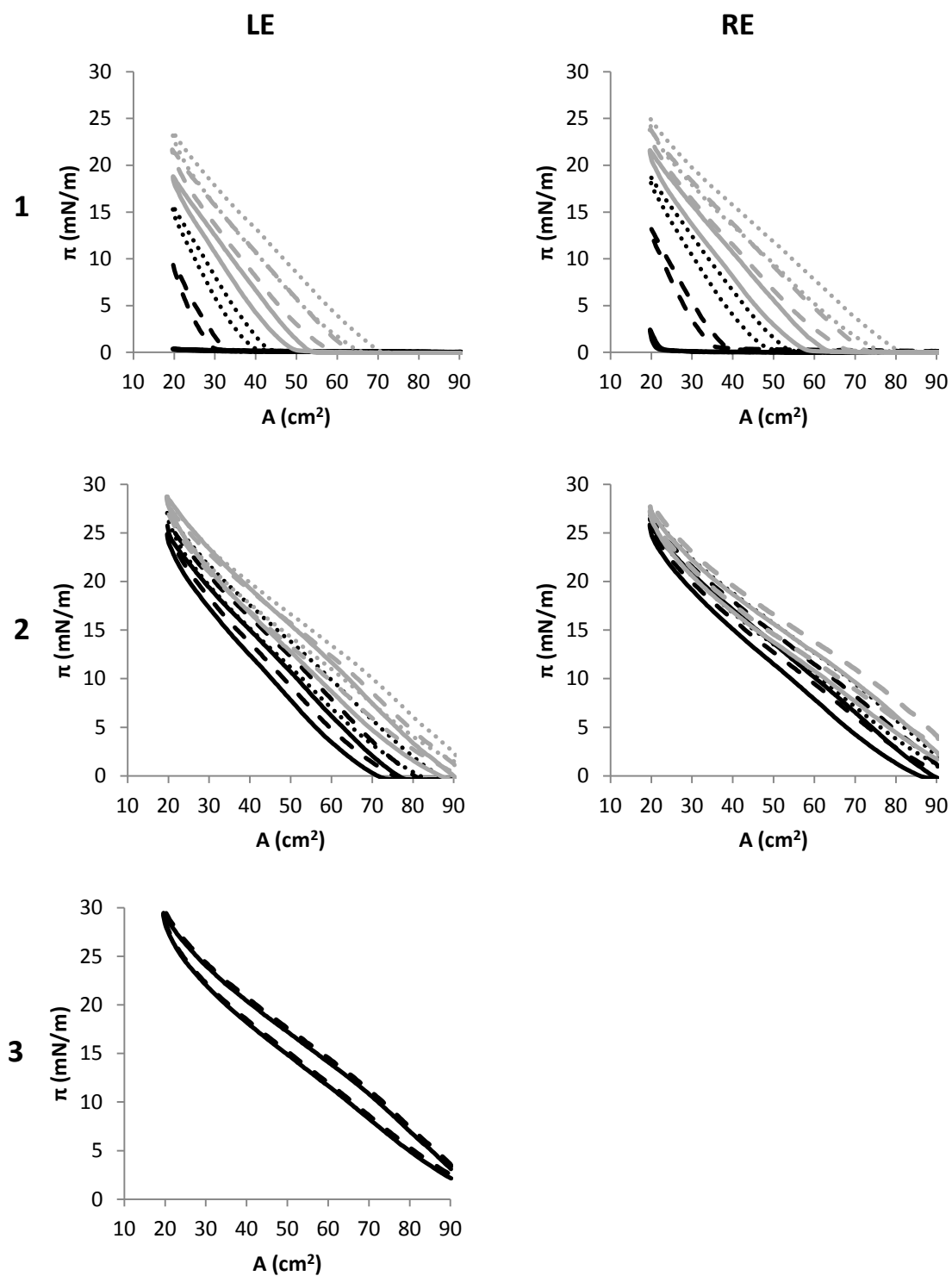


Fig 4.4. π -A isotherms of extracted left eye (LE; Column A) and right eye (RE; Column B) tear samples from subject Px2.









						
Row 1	25 μ l	50 μ l	75 μ l	100 μ l	125 μ l	150 μ l
Row 2	175 μ l	200 μ l	225 μ l	250 μ l	275 μ l	300 μ l
Row 3	325 μ l	350 μ l	-	-	-	-

Fig 4.5. π -A isotherms of extracted left eye (LE; Column A) and right eye (RE; Column B) tear samples from subject Px3.

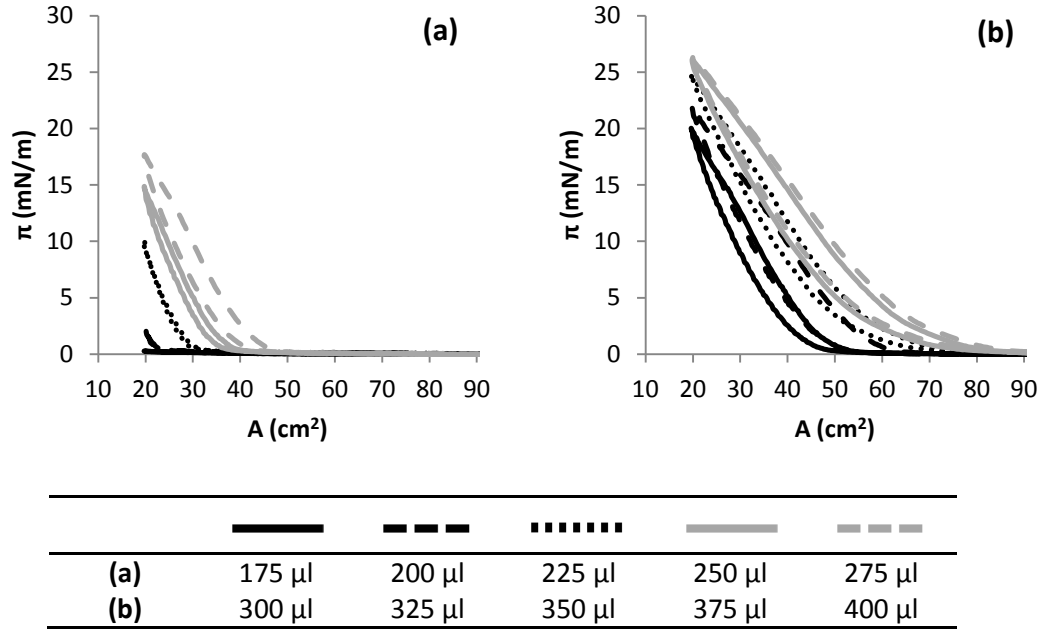


Fig 4.6. π -A isotherms of a Schirmer strip adsorbed with saline (wetted length = 30mm) extracted in 0.5ml chloroform (π -A isotherms for 25-150 μ l aliquots not shown).

An increase in maximum surface pressure (π_{\max}) as the surface concentration of the control Schirmer strip sample is increased in 25 μ l intervals is significantly different to those seen in the three sets of subject-collected samples. This is observed at lower loading concentrations (25 μ l to ~300 μ l). Once above a critical percentage concentration of ~70% of the total extraction volume - where π_{\max} is attained in the subject and control samples - there is a significant difference between the π_{\max} values of the control sample and the three sample obtained subjects Px1, Px2 and Px3. Whilst the π_{\max} values for the RE from subject Px1 were not significantly higher than that observed in the control strip ($\pi_{\max} = 26.3\text{mN/m}$ for both Px1 and control samples), the left eye sample from Px1 ($\pi_{\max} = 27.0\text{mN/m}$) as well as both LE and RE samples from subjects Px2 ($\pi_{\max}(\text{LE}) = 30.3\text{mN/m}$; $\pi_{\max}(\text{RE}) = 30.2\text{mN/m}$) and Px3 ($\pi_{\max}(\text{LE}) = 29.9\text{mN/m}$; $\pi_{\max}(\text{RE}) = 28.3\text{mN/m}$) was significantly higher.

Whilst π_{\max} does not give a succinct indicator as to whether any tear components have an additive effect with the extracted Schirmer strip material on surface behaviour, there are other pieces of data that might give insight. The six tear sample monolayers at this loading is initially in a liquid expanded phase (LE) noted by an initial surface pressure $>0\text{mN/m}$ and the immediate increase in surface pressure upon commencement of the compression cycle. Compare this with the π -A isotherm of the control sample at the critical percentage concentration where π_{\max} is achieved, and it is apparent that there is a presence of a G-LE phase transition at large surface areas.

Inter-subject and intra-subject variability cannot be easily compared due to the differences in the concentration of extractable components. As the same applied volume aliquots (up to 400 μ l in 25 μ l intervals) are used for each sample, the concentrations of extracted material will differ upon application to the surface of the subphase. Calculating the percentage of the sample used for each 25 μ l aliquot interval (Table 4.4) allows an accurate correlation between maximum surface pressure and percentage concentration of extractable components applied to the surface to be observed (Fig 4.7). The loading of sample material (discussed in Chapter 3) is an important factor in determining key characteristics of the sample monolayer. A suitable volume of the solution extracted from a sampling probe must be applied to the surface to produce a maximum surface pressure with an ample volume remaining to at least allow subsequent π -A isotherms to be recorded using the sample solution.

In this case, a percentage concentration of the extracted tear samples above $\sim 7.5\%$ was enough to produce the first onset of increase in surface pressure above the baseline 0mN/m that is observed for a clean subphase. However in order to reach a maximum surface pressure it would take a percentage concentration of $>75\%$ to attain a maximum surface pressure for the tear samples. This is not suitable for repeatability of π -A isotherms to be observed from a single tear sample. Effectively all of the sample has to be used up to produce one set of data at the maximum surface pressure the monolayer will achieve.

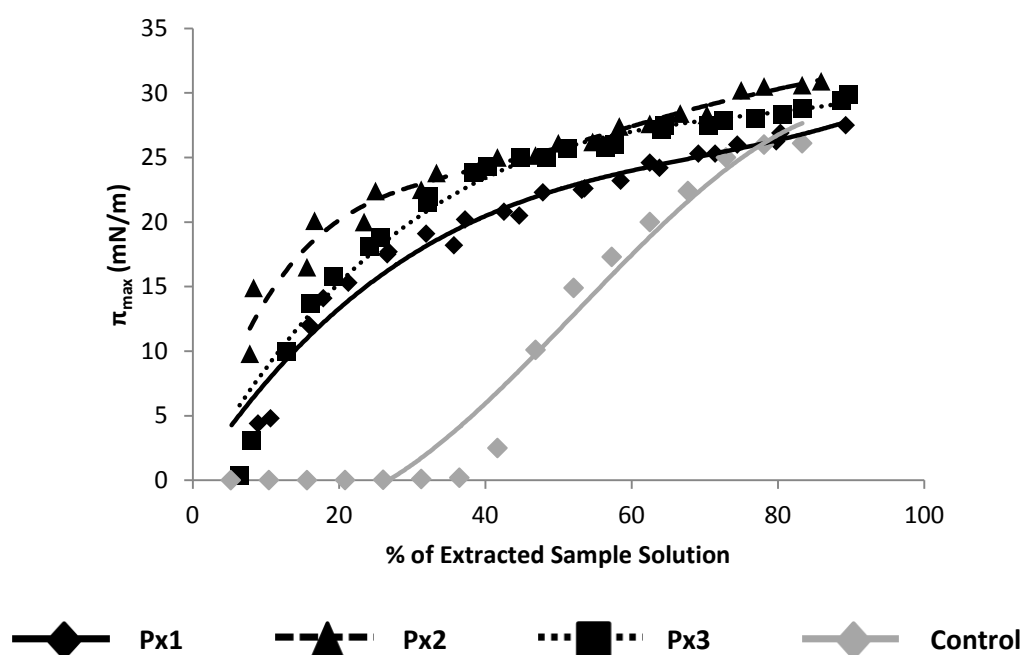


Fig 4.7. π_{max} as a function of volume of extracted samples from Px1, Px2 and Px3 based on the percentage (%) of extracting solution.

Volume (μ l)	Px1		Px2		Px3		Control 1
	LE	RE	LE	RE	LE	RE	
25	8.93	5.32	7.81	8.33	6.41	8.06	5.21
50	17.86	10.64	15.63	16.66	12.82	16.12	10.42
75	26.79	15.96	23.44	25.00	19.23	24.19	15.63
100	35.71	21.28	31.25	33.33	25.64	32.26	20.83
125	44.64	26.60	39.06	41.66	32.05	40.32	26.04
150	53.57	31.92	46.88	50.00	38.46	48.38	31.25
175	62.50	37.24	54.69	58.33	44.87	56.45	36.46
200	71.43	42.56	62.50	66.66	51.28	64.52	41.66
225	80.35	47.88	70.31	75.00	57.69	72.58	46.88
250	89.29	53.20	78.12	83.33	64.10	80.64	52.08
275	98.21	58.51	85.93	91.66	70.51	88.71	57.29
300	-	63.82	93.75	-	76.92	96.77	62.50
325	-	69.14	-	-	83.33	-	67.71
350	-	74.46	-	-	89.74	-	72.91
375	-	79.79	-	-	96.15	-	78.13
400	-	85.10	-	-	-	-	83.33

Table 4.4. Applied volume of sample solution represented as a percentage of the total usable extracted volume of sample for Px1, Px2, Px3 and Control 1.

4.3.2.2 Extraction Solvent: Hexane vs. Chloroform

The π -A isotherm data obtained for the Schirmer strip adsorbed with saline (Fig 4.6) indicate that chloroform is too harsh a solvent. The amount of surface active material extracted from the strip material masks any potential surface behaviour of tear components that may have been collected. Hence the need to test of other solvents for their efficacy in extracting the required material. Fig 4.8 shows the comparative extraction of the left eye (LE) and right eye (RE) tear samples collected from subject Px4. Both LE and RE Schirmer strip samples produced wetted lengths of 18mm and as such extracted using the same volume of solvent. The left eye was extracted in 0.30ml chloroform whilst the right eye was extracted in 0.30ml hexane. There would be slight differences in tear behaviour between left and right eyes but this was deemed negligible when compared to the differences observed from the solvent variable.

The left eye tear sample extracted in CHCl_3 (Fig 4.8; Column A) produced a π_{max} of 29.6mN/m obtained at the 250 μ l aliquot (UV = 86.21%) and π_{init} of 8.8mN/m. Increase in surface pressure was observed at a loaded volume of 25 μ l (UV = 8.6%) where a π_{max} of 3.3mN/m was recorded (π_{init} = 0.0mN/m; A_t = $\sim 27\text{cm}^2$). The right eye tear sample extracted in C_6H_{14} (Fig 4.8; Column B) produced a π_{max} of 17.4mN/m obtained at the maximum available 275 μ l aliquot (UV = 91.66%)

and an π_{init} of 0.0mN/m with a G-LE transition at an A_t of 76cm². Increase in surface pressure was observed at a loaded volume of 75 μ l (UV = 15.60%) where a π_{max} of 1.4mN/m was recorded (π_{init} = 0.0mN/m; A_t = ~28cm²). At the critical surface concentration where π_{max} was attained, the sample monolayer remains in an LE phase through full area compression and expansion, noted by the immediate increase in surface pressure at maximum area. The control Schirmer strip extracted in CHCl₃ (Fig 4.6) produced a π_{max} of 26.3mN/m obtained at the 375 μ l aliquot (UV = 78.12%) and an π_{init} of 0.0mN/m with a gradual G-LE transition between π_t of 0.0-7.5mN/m at an A_t of 88-55cm². The control Schirmer strip extracted in C₆H₁₄ (Fig 4.9) produced a π_{max} of 16.3mN/m obtained at the 375 μ l aliquot (UV = 81.52%). π_{init} was 0.0mN/m with a G-LE transition at an A_t of ~72cm².

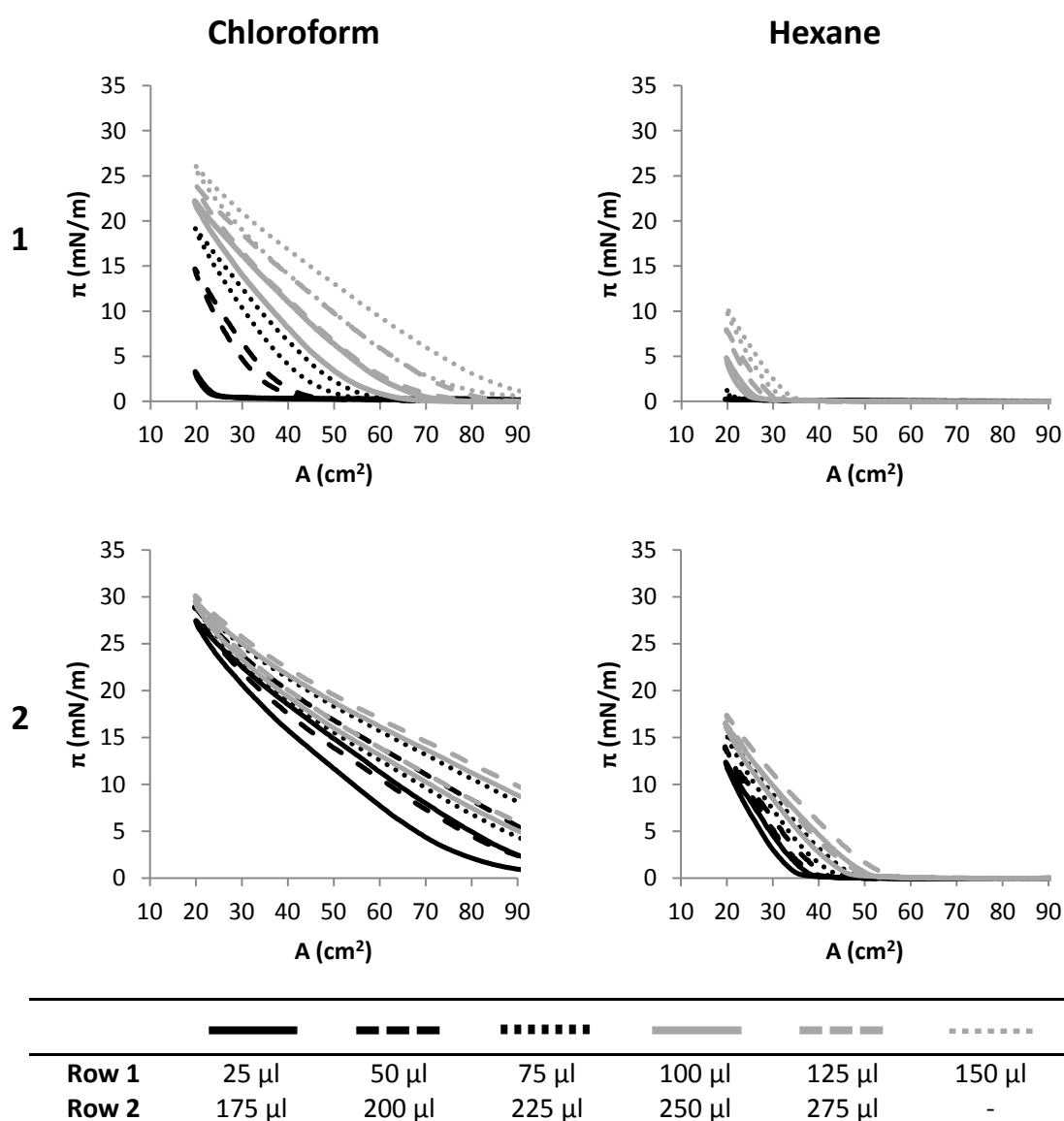


Fig 4.8. π -A isotherms of chloroform and hexane extracted tear samples from subject Px4.

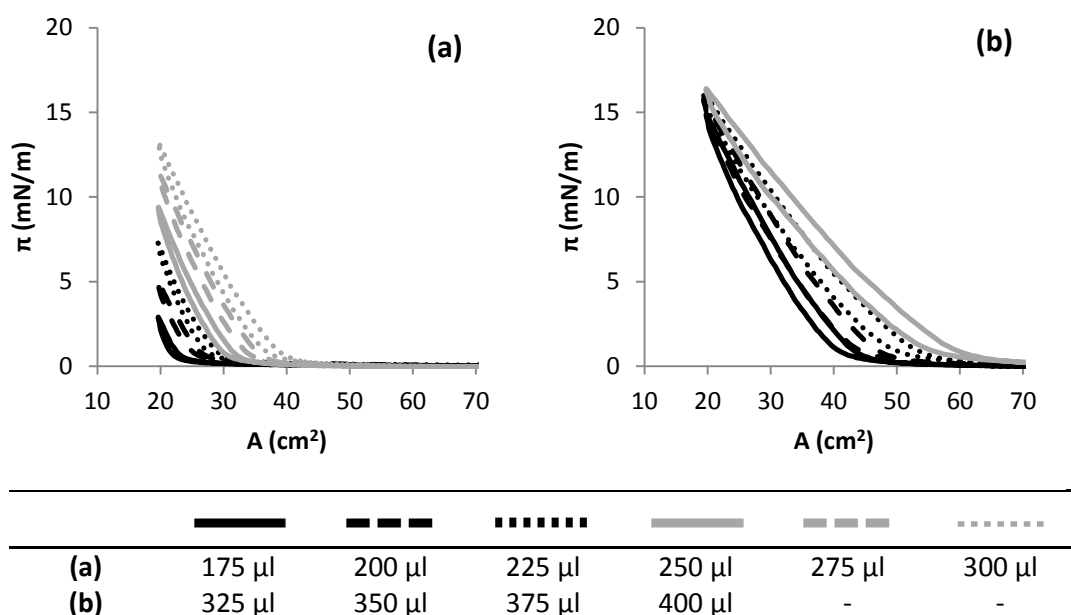


Fig 4.9. π -A isotherms of hexane-extracted control samples: (a) 175-300 μ l; (b) 325-400 μ l.
(Data for the 25-150 μ l aliquots not shown)

From the data obtained in Fig 4.6 and Fig 4.8-4.10 it is possible to conclude that the use of hexane as an extracting solvent for tear sample collected using Schirmer strips is as unfeasible as the chloroform-based extractions. A significant amount of extraneous matter is extracted from the control strips when exposed to hexane. At the critical percentage concentration where a maximum surface pressure for the sample is achieved, it is difficult to ascertain whether the surface pressure is a product of tear film components or Schirmer strip material. A significant difference in maximum surface pressure between the subject Px4 sample and the control when extracted in chloroform is similar to those observed in Fig 4.7. When compared to the difference between the subject and control samples extracted in hexane, the preference in this case would be to use chloroform as an extracting solvent.

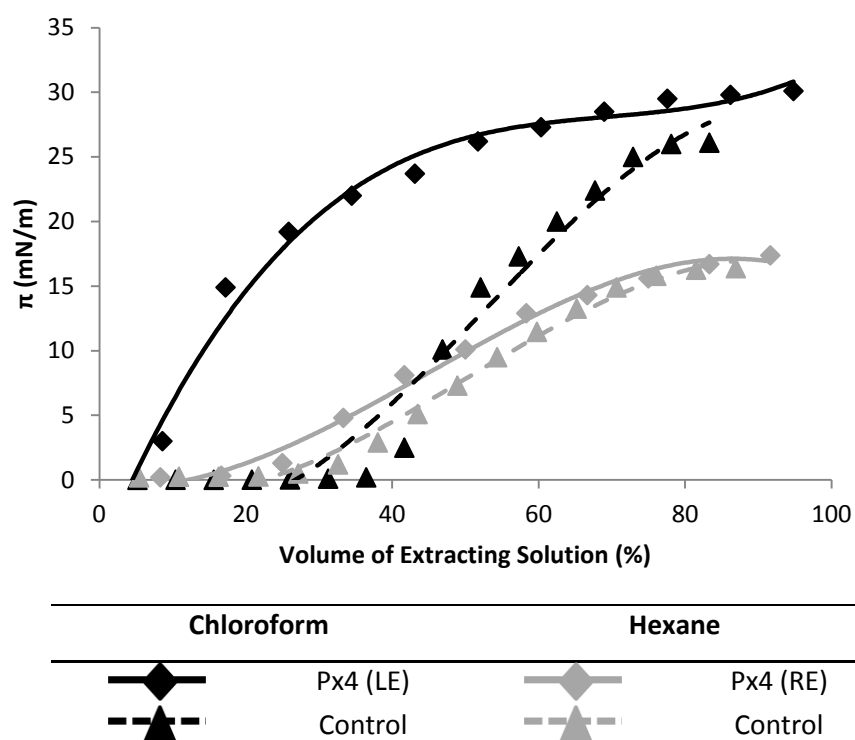


Fig 4.10. π_{\max} as a function of volume of extracted samples from Px4. Left eye (LE; WL = 18mm) sample extracted in chloroform. Right eye (RE; WL = 18mm) sample extracted in hexane (percentage (%) of extracting solution).

Volume (μ l)	Px4 Tear Sample		Control 2	
	LE; CHCl_3	RE; Hex	CHCl_3	Hex
25	5.43	5.21	5.21	5.43
50	10.86	10.42	10.42	10.86
75	16.30	15.63	15.63	16.30
100	21.74	20.83	20.83	21.74
125	27.17	26.04	26.04	27.17
150	32.61	31.25	31.25	32.61
175	38.04	36.46	36.46	38.04
200	43.48	41.66	41.66	43.48
225	48.91	46.88	46.88	48.91
250	54.34	52.08	52.08	54.34
275	59.78	57.29	57.29	59.78
300	65.21	62.50	62.50	65.21
325	70.65	67.70	67.71	70.65
350	76.08	72.91	72.91	76.08
375	81.52	78.12	78.13	81.52
400	86.95	83.33	83.33	86.95

Table 4.5. Applied volume of sample solution represented as a percentage of the total usable extracted volume of sample for Px4 and Control 2.

4.3.2.3 Trough B π -A Isotherm Study

Tear samples applied to Trough B (working area = 400-100cm²) is not a feasible experimental option: the concentration of extracted components per unit area is far too large initially to produce a maximum surface pressure. The UV was 310 μ l and 370 μ l for Schirmer strips collected from the left eye (WL = 21mm) and right eye (WL = 24mm) respectively. The left eye sample of Px4 (Fig 4.11a) showed a π_{\max} of 5.2mN/m, a π_{init} was 0.0mN/m and G-LE transition at an A_t of \sim 148cm² at the 300 μ l aliquot volume (UV = 96.77%). Similarly, the right eye data (Fig 4.11b) showed a low π_{\max} of 9.7mN/m at the 350 μ l aliquot (UV = 94.95%). π_{init} was 0.0mN/m with a G-LE transition at an A_t of \sim 170cm².

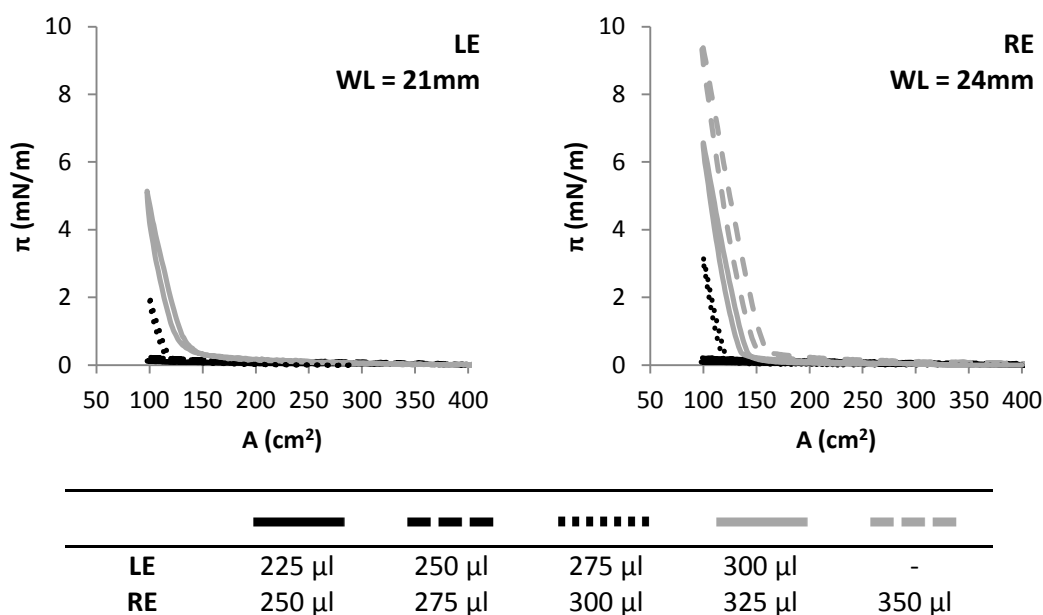


Fig 4.11. π -A isotherms of tear sample from subject Px5 on Trough B.

4.3.3 Visispear™ Ophthalmic Sponges

4.3.3.1 Trough A π -A Isotherms

The π_{\max} for the subject Px1 sample (Fig 4.13, Row 1) is \sim 27.9mN/m (π_{\max} = 27.6-28.2mN/m between 40-50 μ l). π_{init} for all loading aliquots up to 50 μ l was 0.0mN/m. G-LE transition areas (A_t) of 81 cm², 85 cm² and 88cm² were observed for the 40 μ l, 45 μ l and 50 μ l respectively. Reversibility remains constant over these three loading concentrations at a value of \sim 92.0% (range = 90.8-93.2%). The π_{\max} for the subject Px2 sample (Fig 4.13, Row 2) is \sim 29.1mN/m (π_{\max} = 28.4-29.6mN/m between 30-50 μ l). π_{init} for all loading aliquots up to 50 μ l was 0.0mN/m. The

only significant change observed in the π -A isotherm is the surface area where a gaseous to liquid expanded phase is observed. G-LE transition areas (A_t) between 68cm^2 (for the $30\mu\text{l}$) and 88cm^2 (for the $50\mu\text{l}$). Reversibility also remains constant over these loading concentrations at a value of $\sim 88.9\%$ (range = 86.2 - 92.4%). The π_{max} for the subject Px3 sample (Fig 4.13, Row 3) is $\sim 27\text{mN/m}$ ($\pi_{\text{max}} = 26.8$ - 27.9mN/m between 30 - $50\mu\text{l}$). π_{init} for all loading aliquots up to $30\mu\text{l}$ was 0.0mN/m which increased to $>0.0\text{mN/m}$ from the $35\mu\text{l}$ aliquot ($35\mu\text{l}$, $\pi_{\text{init}} = 0.2\text{mN/m}$; $40\mu\text{l}$, $\pi_{\text{init}} = 0.3\text{mN/m}$; $45\mu\text{l}$, $\pi_{\text{init}} = 0.8\text{mN/m}$; $50\mu\text{l}$, $\pi_{\text{init}} = 1.0\text{mN/m}$). G-LE transition occurs over a gradual increase in surface pressure between 0 - 10mN/m over a large transition area (A_t). The hysteresis between compression and expansion also remains constant over these loading concentrations at a value of $\sim 90.4\%$ (range = 87.9 - 94.0%).

The π_{max} for the control sample (Fig 4.12) is $\sim 19.4\text{mN/m}$ ($\pi_{\text{max}} = 19.0$ - 19.7mN/m between 40 - $50\mu\text{l}$). π_{init} for all loading aliquots up to $50\mu\text{l}$ was 0.0mN/m and the transition from G to LE phase occurs over a gradual increase in surface pressure between 0 - 5mN/m over a large transition area (A_t) of 70 - 40cm^2 . The hysteresis between compression and expansion also remains constant over these loading concentrations, at a value of $\sim 94.7\%$ (range = 93.5 - 96.0%).

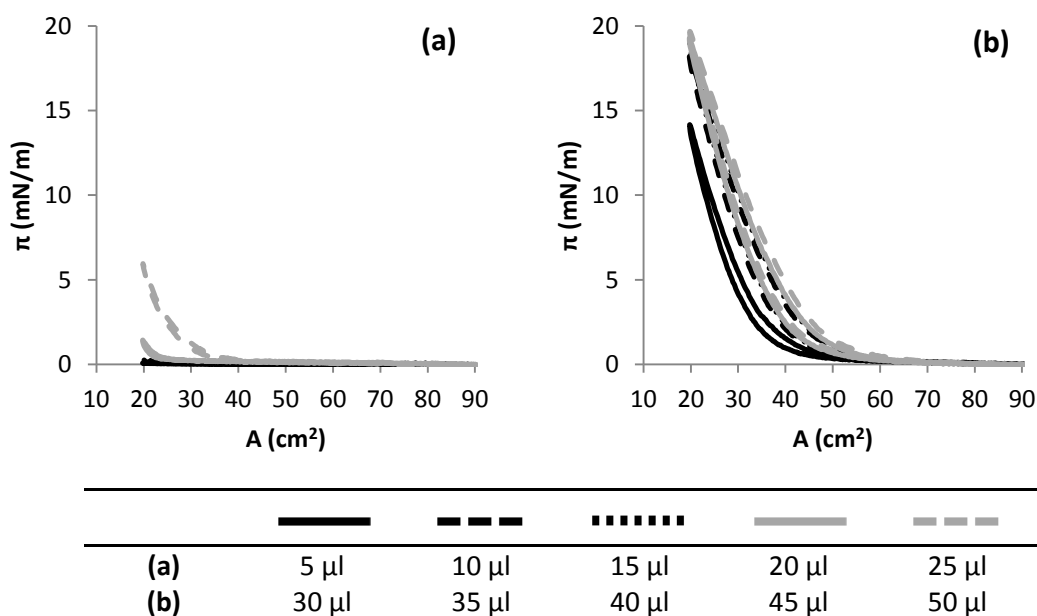


Fig 4.12. π -A isotherms of control samples obtained from collection and extraction of a Visispear™ ophthalmic sponge soaked in saline on Trough A.

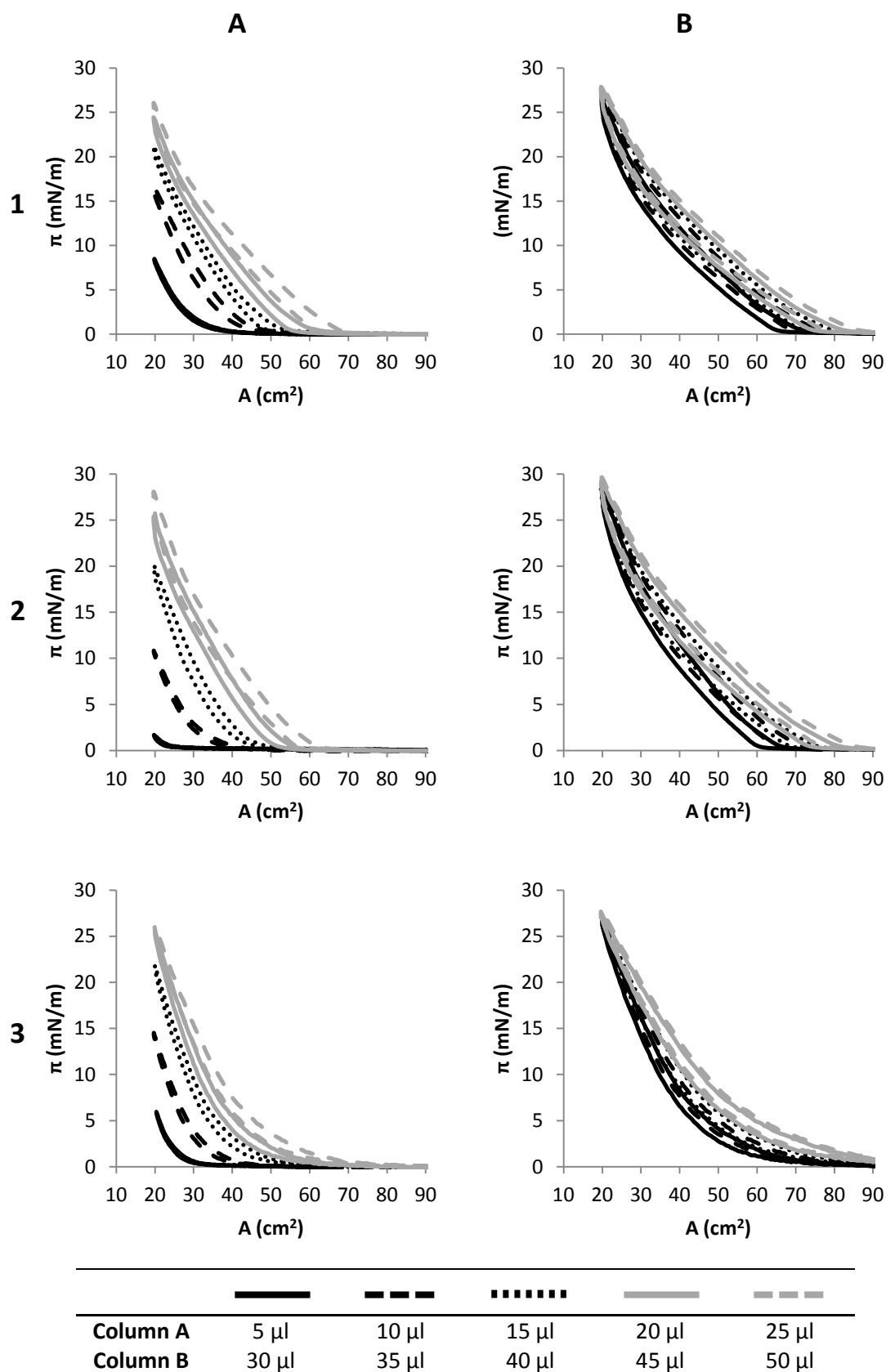


Fig 4.13. π -A isotherms of tear samples obtained from collection and extraction of a Visispear™ ophthalmic sponge on Trough A: Row 1 - Px1; Row 2 - Px2; Row 3 - Px3.

The main observation of using Visispear™ sponges as a sampling probe - as opposed to glass capillary tubes or Schirmer strips - is the much smaller volume (UV = ~10%) needed to achieve a maximum surface pressure for the tear sample upon application of the sample solution to the subphase surface. This is important as it provides the opportunity for multiple π -A isotherms to be recorded using the same stock of solution obtained and extraction from a single sponge. This allows further experimentation that would eliminate any differences that might occur in a subject's tear film from one day to the next.

Three separate π -A isotherm studies of the tear sample from Px1 were recorded in order to obtain information on the reproducibility of data from a single extracted sample (Fig 4.14). For a 25 μ l aliquot (Fig 4.16a), the maximum surface pressure (π_{\max}) for the three isotherms were 21.2mN/m for run 1, 18.4mN/m for run 2 and 16.2mN/m for run 3. In all three runs, the initial surface pressure (π_{init}) was 0.0mN/m. The transition from gaseous (G) to liquid expanded (LE) phase occurred at a clear point in run 1 at an area of 51cm². The G-LE transition in the isotherms for run 2 and 3 showed a gradual change in surface pressure of 0-5mN/m between a surface area of 50-38cm². For a 50 μ l aliquot (Fig 4.14b), the maximum surface pressure (π_{\max}) for the three isotherms were 25.1mN/m for run 1, 23.5mN/m for run 2 and 24.4mN/m for run 3. In all three runs, the initial surface pressure (π_{init}) was 0.0mN/m. The transition from gaseous (G) to liquid expanded (LE) phase occurred at a clear point in run 1 and run 2 at an area of 66cm² and 71cm² respectively. The G-LE transition in the isotherm for run 3 showed a gradual change in surface pressure of 0-5mN/m between a surface area of 65-55cm².

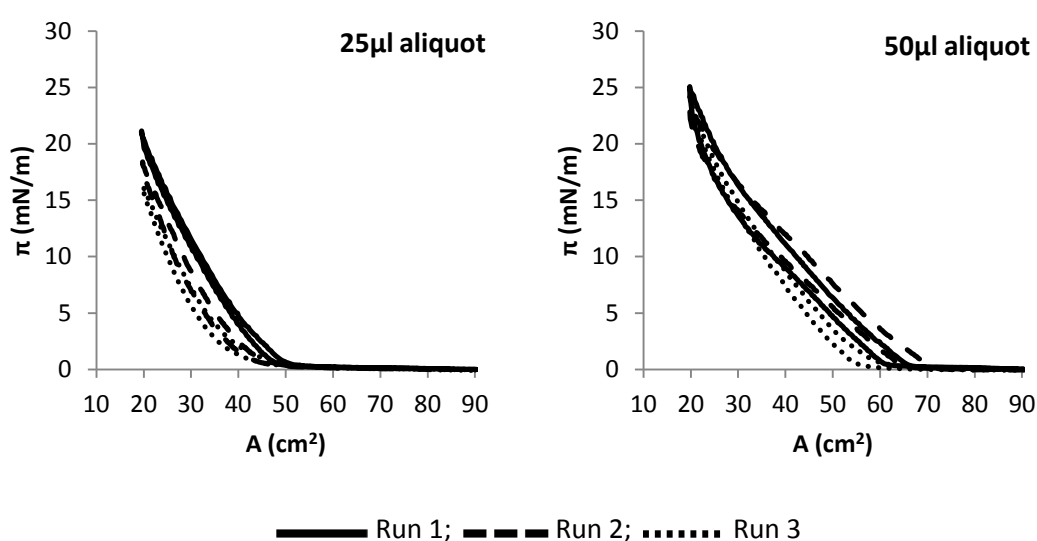


Fig 4.14. Comparative π -A isotherms of three separate studies of the Px1 tear sample obtained from collection and extraction of Visispear™ ophthalmic sponges on Trough A.

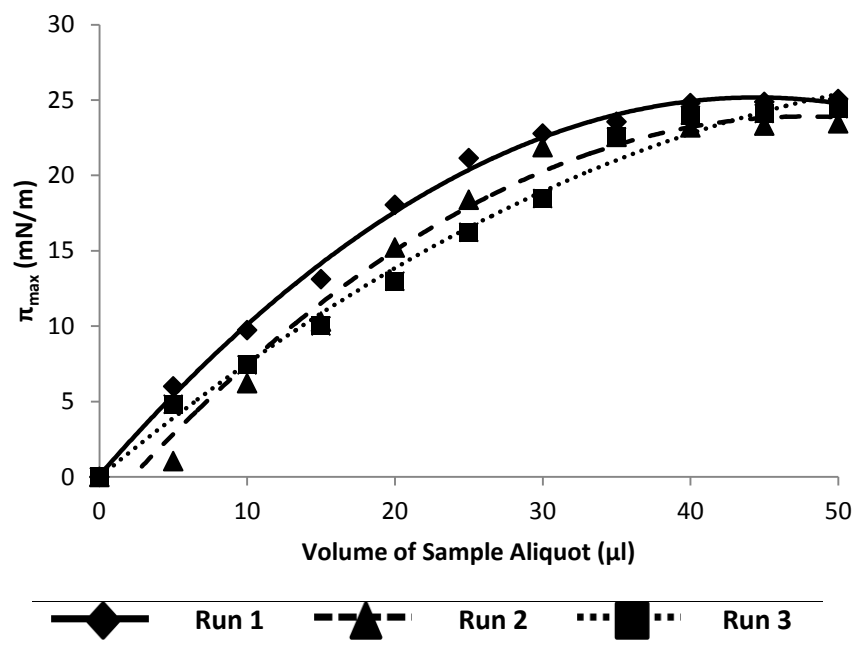


Fig 4.15. Volume aliquot vs. maximum surface pressure

There are significant differences apparent in the π -A isotherm at lower loading concentrations (Fig 4.15). π_{max} , π_{init} and A_t can differ significantly as can the relationship between compression and expansion cycles denoted by reversibility (hysteresis). At higher concentrations where a maximum surface pressure for the tear sample is reached (~ 40 - $50\mu\text{l}$ volume aliquot of sample), the only differences that are observed in the π -A isotherm is in reversibility (hysteresis), initial surface pressure and the area where transition from G to LE occurs.

4.3.3.2 Extraction Solvent: Hexane vs. Chloroform

Whilst the use of the Visispear sponges could be beneficial as a tear sampling probe to some extent, consideration has to be made on the amount of sponge material that has also been extracted as observed in the extraction of a blank sponge. A large part of the maximum surface pressure values obtained within the tear samples ($\pi_{max} = \sim 27$ - 29mN/m) could potentially be due to components extracted from the sponge material, where the π_{max} for the control sample was recorded at $\sim 19\text{mN/m}$. Other aspects of the π -A isotherms such as the initial surface pressure and the reversibility between compression and expansion should be taken into consideration.

The π -A isotherm data for hexane-extracted subject Px4 sample (Fig 4.16) produced a π_{\max} of 26.1mN/m, comparable to the tear sample extractions using chloroform as a solvent. Evidence suggests that an increase in sample concentration may produce a further increase in π_{\max} . π_{init} for the 50 μ l loading aliquot was 0.0mN/m and the G-LE transition occurs over a gradual increase in surface pressure between 0-10mN/m and A_t of 90-45cm². The hysteresis between compression and expansion is 89.3%. The π -A isotherm data for the hexane-extracted control sponge adsorbed with saline (Fig 4.17) produced a π_{\max} of 16.0mN/m with a further increase in surface pressure as the volume of tear sample is increased possible. π_{init} for all loading aliquots up to 50 μ l was 0.0mN/m. Transition from G to LE phase occurs through a gradual increase in surface pressure between 0-5mN/m over a large transition area (A_t) of 70-40cm². Hysteresis is higher (94.9%) indicating a more ordered relationship between compression and expansion.

As observed in Fig 4.18, hexane potentially produces a better prospect for an extracting solvent for sponges than chloroform. The extraction of a subject sample produces a maximum surface pressure for the subject's sample comparable to that observed in chloroform extractions (~28mN/m for the chloroform extraction compared to ~26mN/m at a 50 μ l aliquot). Extraction using hexane also shows a marked difference in the surface pressure data observed for similar experiments using the Schirmer strip as a sampling probe. The difference between the maximum surface pressure of the tear sample compared to the control sample is larger than that observed in similar experiments with the Schirmer strips (section 4.3.2). With the Schirmer strip data, the difference was insignificant with subject and control samples observed to have similar π_{\max} of ~17mN/m. Extraction of the subject sample obtained from the Visispear sponge produced a π_{\max} of ~26mN/m compared to the control sample which produced a π_{\max} of ~16mN/m. Evidence however suggests that surface pressure will continue to increase above an applied volume of 50 μ l.

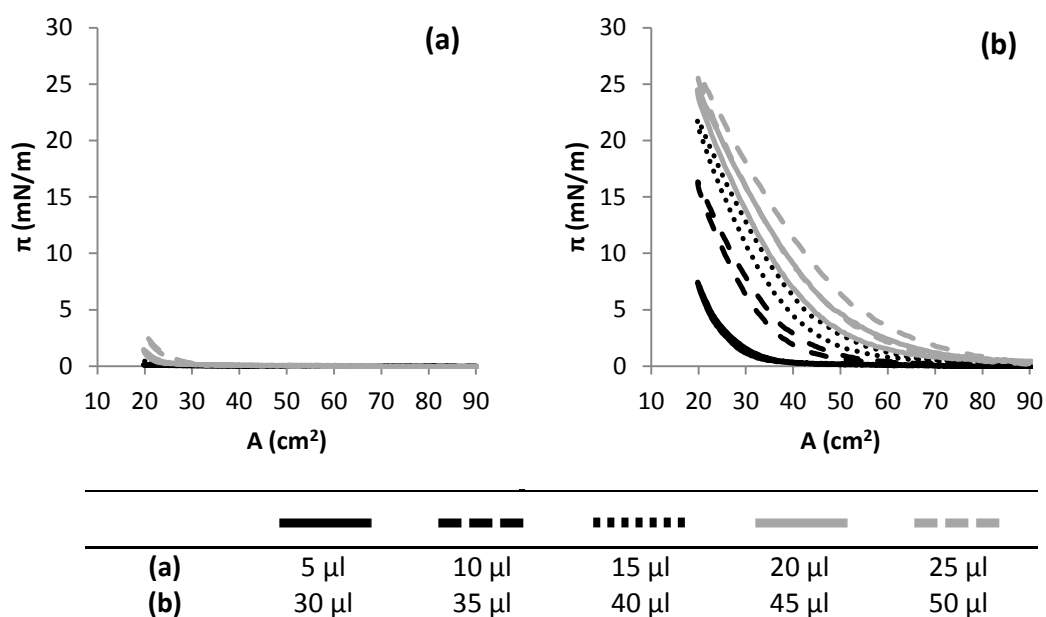


Fig 4.16. π -A isotherms of tear sample Px4 obtained from a Visispear™ ophthalmic sponge extracted in hexane: (a) 5-25 μl ; (b) 30-50 μl .

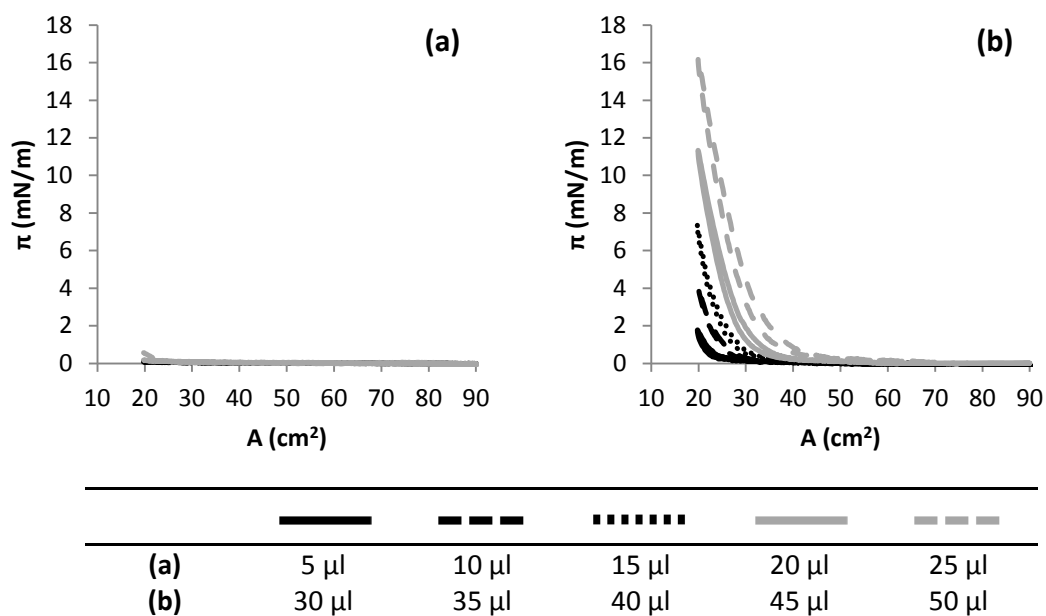


Fig 4.17. π -A isotherms of control sample obtained from a Visispear™ ophthalmic sponge soaked in saline and extracted in hexane: (a) 5-25 μl ; (b) 30-50 μl .

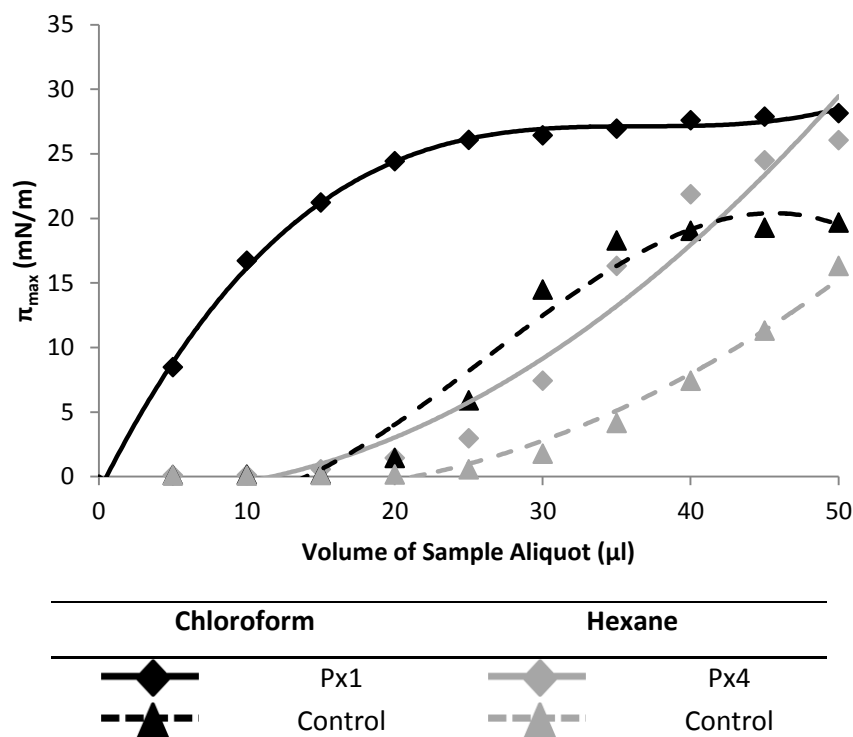


Fig 4.18. Comparison between chloroform and hexane extracted control and subject samples collected using Visispear™ ophthalmic sponges.

4.3.3.3 Trough B π -A Isotherms

The π_{\max} for the subject Px5 sample (Fig 4.19, Row 1) is ~ 26.7 mN/m ($\pi_{\max} = 26.3$ -27.1 mN/m between 400-500 μ l. π_{init} for all loading aliquots up to 350 μ l was 0.0 mN/m. Transition from G to LE phase occurs over a gradual increase in surface pressure between 0-10 mN/m over a large transition area (A_t). As loading concentration was increased past this volume, π_{init} recorded values > 0.0 mN/m (400 μ l, $\pi_{\text{init}} = 0.2$ mN/m; 450 μ l, $\pi_{\text{init}} = 1.0$ mN/m; 500 μ l, $\pi_{\text{init}} = 1.7$ mN/m). The reversibility between compression and expansion cycles was $\sim 96.1\%$ (range = 95.0-97.1%). The π_{\max} for the subject Px6 sample (Fig 4.19, Row 2) is ~ 24.8 mN/m ($\pi_{\max} = 24.4$ -24.9 mN/m between 450-500 μ l. π_{init} for all loading aliquots up to 500 μ l was 0.0 mN/m. Transition from G to LE phase occurs over a gradual increase in surface pressure between 0-10 mN/m over a large transition area (A_t). As loading concentration is increased up to the maximum 500 μ l utilised, this transition occurs over an increasingly gradual change in surface pressure between 0 - 5 mN/m over a large transition area (300 μ l, $A_t = 210$ -200 cm^2 ; 350 μ l, $A_t = 250$ -230 cm^2 ; 400 μ l, $A_t = 260$ -240 cm^2 ; 450 μ l, $A_t = 280$ -260 cm^2 ; 500 μ l, $A_t = 330$ -290 cm^2). The reversibility between compression and expansion cycles was $\sim 95.1\%$ (range = 93.3-97.7%).

The π_{\max} for the subject Px7 sample (Fig 4.19, Row 3) is $\sim 23.5 \text{ mN/m}$ ($\pi_{\max} = 23.1\text{-}23.9 \text{ mN/m}$ between $400\text{-}500 \mu\text{l}$). π_{init} for all loading aliquots up to $500 \mu\text{l}$ was 0.0 mN/m . Transition from G to LE phase occurs over a gradual increase in surface pressure between $0\text{-}10 \text{ mN/m}$ over a large transition area (A_t). Initial surface pressure (π_{init}) for all loading aliquots up to $500 \mu\text{l}$ was 0.00 mN/m and the G-LE transition occurs at a more definable transition area (A_t) for all loading volumes ($300 \mu\text{l}$, $A_t = \sim 255 \text{ cm}^2$; $350 \mu\text{l}$, $A_t = \sim 280 \text{ cm}^2$; $400 \mu\text{l}$, $A_t = \sim 320 \text{ cm}^2$; $450 \mu\text{l}$, $A_t = \sim 355 \text{ cm}^2$; $500 \mu\text{l}$, $A_t = \sim 400 \text{ cm}^2$). The reversibility between compression and expansion cycles was $\sim 95.5\%$ (range = $94.0\text{-}96.8\%$). π_{\max} for the control sample (Fig 4.20) was $\sim 19.6 \text{ mN/m}$ ($\pi_{\max} = 19.4\text{-}19.7 \text{ mN/m}$ between $450\text{-}500 \mu\text{l}$) with π_{init} of 0.0 mN/m for all loading aliquots up to $500 \mu\text{l}$. The transition from G to LE phase occurs between $0\text{-}5 \text{ mN/m}$ at indefinable A_t ($300 \mu\text{l}$, $210\text{-}150 \text{ cm}^2$; $350 \mu\text{l}$, $A_t = \sim 290\text{-}220 \text{ cm}^2$; $400 \mu\text{l}$, $A_t = 320\text{-}255 \text{ cm}^2$; $450 \mu\text{l}$, $A_t = 350\text{-}260 \text{ cm}^2$; $500 \mu\text{l}$, $A_t = 350\text{-}265 \text{ cm}^2$).

A large part of the maximum surface pressure values obtained within the tear samples ($\pi_{\max} = 23.5\text{-}26.7 \text{ mN/m}$) could potentially be due to components extracted from the sponge material, where the π_{\max} for the control sample was recorded at $\sim 19.6 \text{ mN/m}$. Other aspects of the π -A isotherms such as the initial surface pressure and the reversibility between compression and expansion should be taken into consideration. Hysteresis from the reversibility between compression and expansion cycles was high, with only a small decrease from $\sim 98\%$ for the control sample to $\sim 95\text{-}96\%$ for the tear samples. The transition from G to LE phase commences at a surface area (A_t) of 300 cm^2 . The only noticeable difference is the surface area range during transition where a more definable change in transition area of $\sim 25 \text{ cm}^2$ is observed within the samples collected from tears compared to the larger area range for the control sample $\sim 60\text{-}70 \text{ cm}^2$.

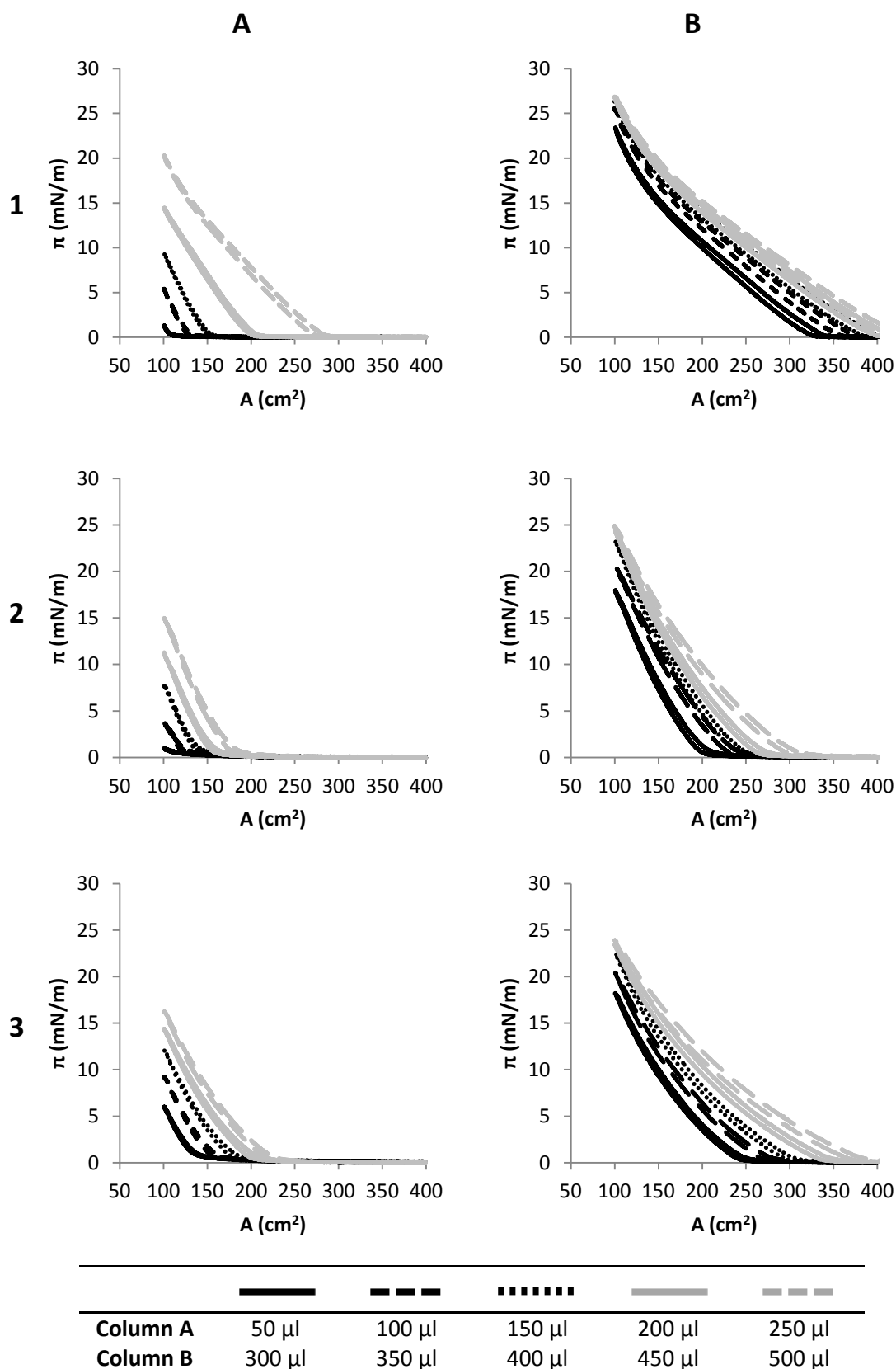


Fig 4.19. π -A isotherms of tear sample obtained from a Visispear™ ophthalmic sponge:
Row 1 - Px5; Row 2 - Px6; Row 3 - Px7.

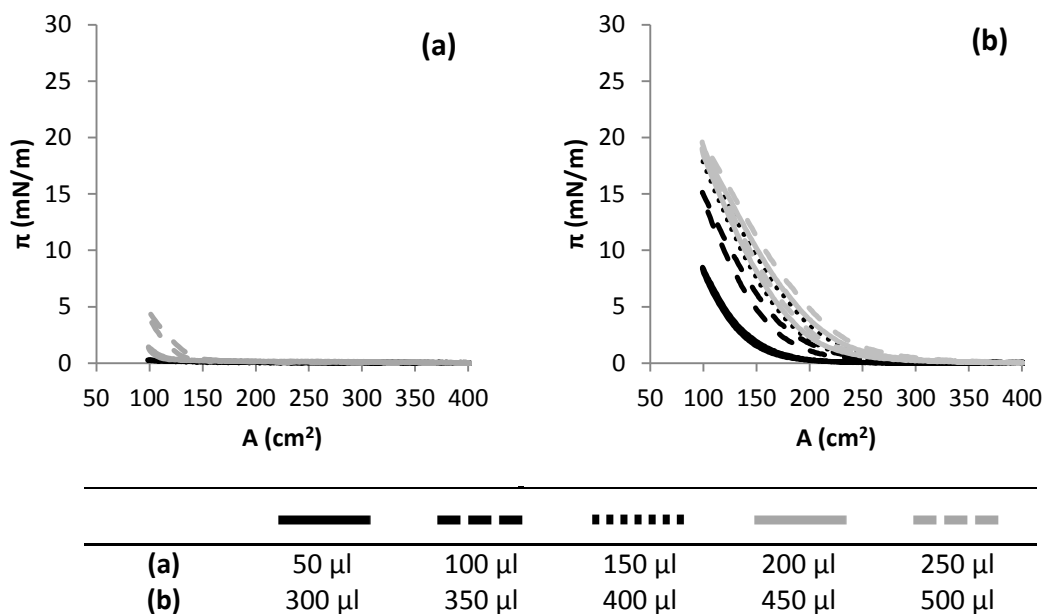


Fig 4.20. π -A isotherms of control samples obtained from collection a Visispear™ ophthalmic sponge soaked in saline.

4.3.3.4 Brewster Angle Microscopy

The BAM imagery taken simultaneously alongside the 500 μ l aliquot π -A isotherms of subject samples Px5, Px6 and Px7 is shown in Fig 4.21. The images taken over the course of compression serve to provide visual observation of the way the monolayer is compressed by an almost uniform rate of surface pressure increase. As observed in the three sets of images, the monolayer films formed from the three subject samples compress in slightly different ways that might be indistinguishable from comparisons of the π -A isotherms, although similarities can be seen at each surface area interval. All monolayers remain within the liquid expanded (LE) phase described by the π -A isotherms and the existence of regions of minimal or absence of components. Px5 (Fig 4.21, Column A) shows that as surface pressure increases, islands of material agglomerate in a uniform manner across the monolayer, increasing in size as the surface area decreases. As the initial surface pressure of the π -A isotherm was $>0.0\text{mN/m}$, there is evidence already of material at the surface within a close enough proximity to affect surface pressure. Opposed to this, we see the cases observed for Px6 (Fig 4.21, Column B) and Px7 (Fig 4.21, Column C) where islands of component form in different sizes, adsorbing close neighbouring molecules yet leaving large areas of 'clear' subphase.

Although surface pressure remains at 0.0mN/m at larger surface areas, such as that seen for sample Px2 and Px3 between 350-400cm², the BAM images show that monolayer materials exist at the subphase surface. These materials are present at the surface, but the actual surface concentration as a function of the surface area is so large that the molecules have minute interactions in small islands of components with no significant effect on the surface tension of the subphase surface.

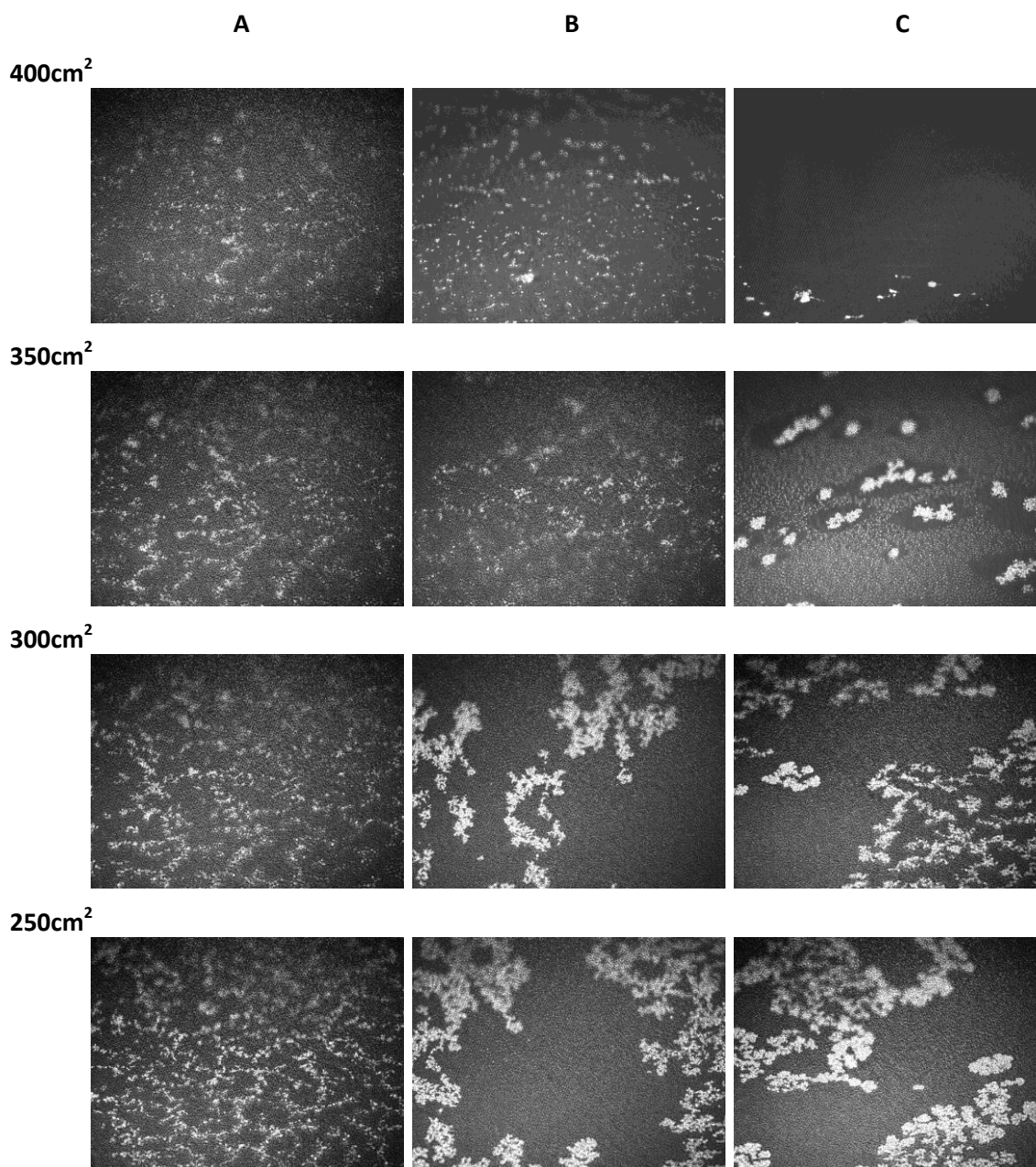


Fig 4.21. BAM images taken during the π -A compression isotherm of the 500 μ l aliquot of tear sample: Px5 (column A), Px6 (column B) and Px7 (column C).

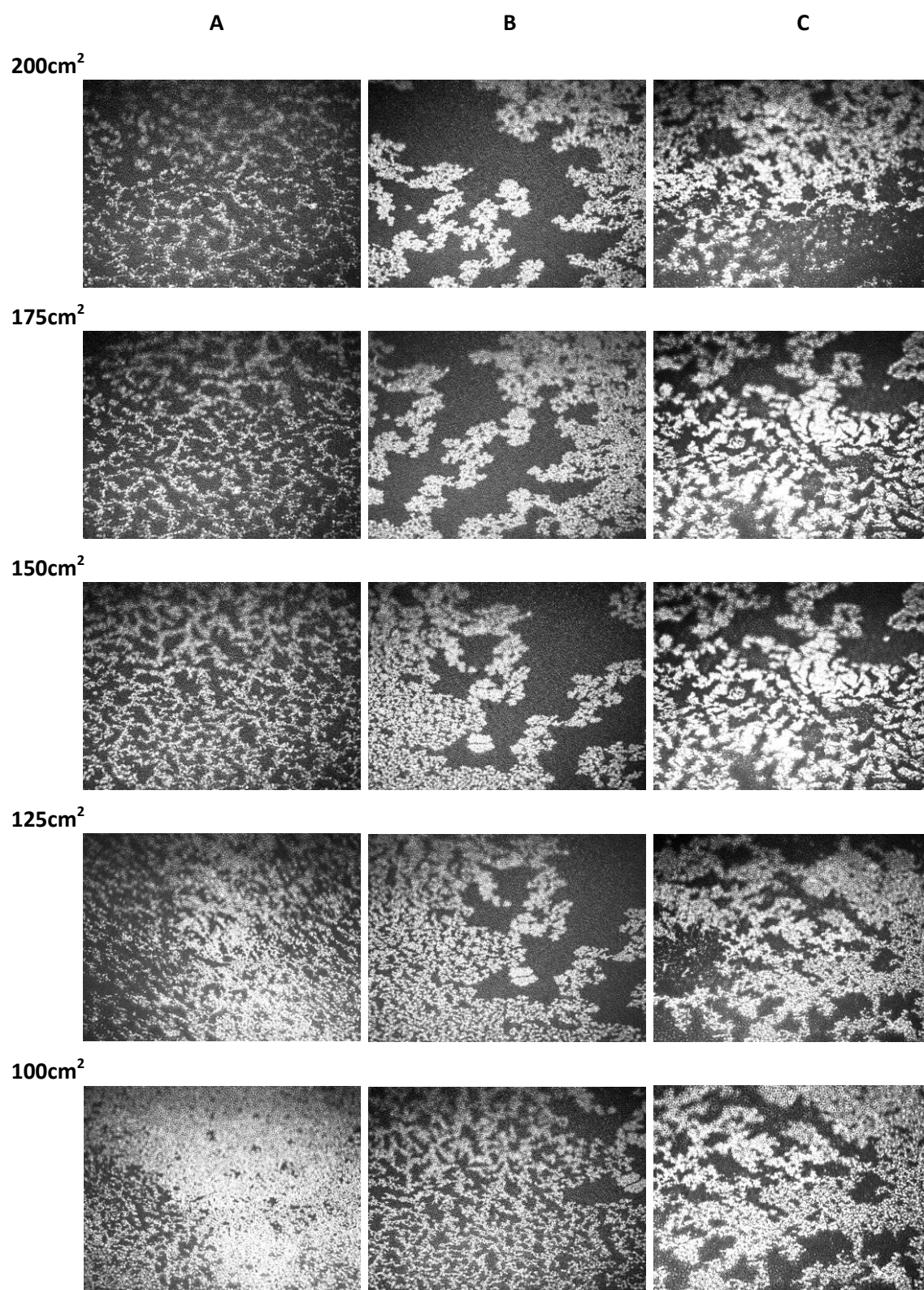


Fig 4.21 continued. BAM images taken during the π -A compression isotherm of the 500 μ l aliquot of tear sample: Px5 (column A), Px6 (column B) and Px7 (column C).

4.3.4 Contact Lens Extraction

4.3.4.1 Inter- and Intra-subject Variability

It is important to determine whether the observed surface behaviour of extracted tear samples will differ between experiments. The π -A isotherms were recorded and compared between different test samples from an extracted sample obtained from a single collected contact lens sample and from tear samples extracted from three separate contact lenses obtained from the same subject.

Inter-sample reproducibility was observed in the surface pressure-area (π -A) isotherm recorded from studies of three aliquots of the same extracted sample (Fig 4.22). Slight variances were observed in the position and shape of the π -A isotherm trace, most notably the area where transition from gaseous (G) to liquid expanded (LE) and reversibility hysteresis between compression and expansion cycles. π_{\max} for the three runs using a 200 μ l aliquot of the same tear sample was 29.7mN/m for run 1 (π_{\max} = 29.4-30.1mN/m between 175-200 μ l), 30.2mN/m for run 2 (π_{\max} = 30.1-30.2mN/m between 150-200 μ l) and 29.6mN/m for run 3 (π_{\max} = 29.4-29.7mN/m between 150-200 μ l). G-LE transition occurs over a gradual increase in surface pressure between 0-15mN/m and an wide A_t range (90-40cm²) indicative of a uniform progression of monolayer compression rather than an instantaneous transition. Hysteresis decreases as the surface concentration is increased from ~90% at loading volumes of 5-30 μ l to ~80% at the highest volume aliquot of 50 μ l.

Intra-subject reproducibility is also apparent for three different collected contact lens samples taken from the same subject (Fig 4.23). Slightly more variation in π -A isotherms for the three separately source samples is noticed, especially at lower surface concentrations. Once the critical concentration above which the maximum surface pressure does not increase significantly upon each additional aliquot (~40 μ l), the π -A isotherms tend to an equilibrium for those samples despite being extracted from separate contact lens samples. Maximum surface pressure was similar in the three experimental sample tested, with π_{\max} values of 31.6mN/m, 30.4mN/m and 29.0mN/m recorded for run 1, run 2 and run 3 respectively. These also matched with the data obtained in the π -A isotherms in Fig 4.23, as did the reversibility hysteresis between compression and expansion, and the area and surface pressure gradual increase during the G-LE phase transition.

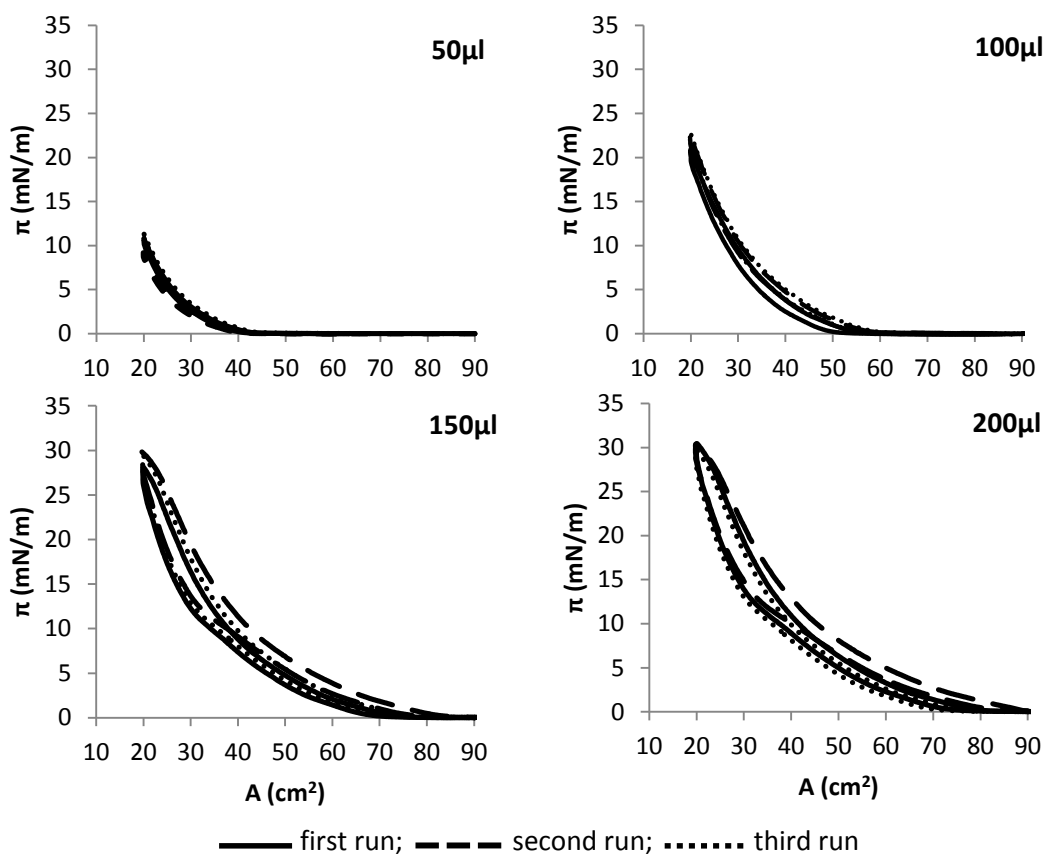


Fig 4.22. Intra-subject reproducibility of π -A isotherms from a single CL sample.

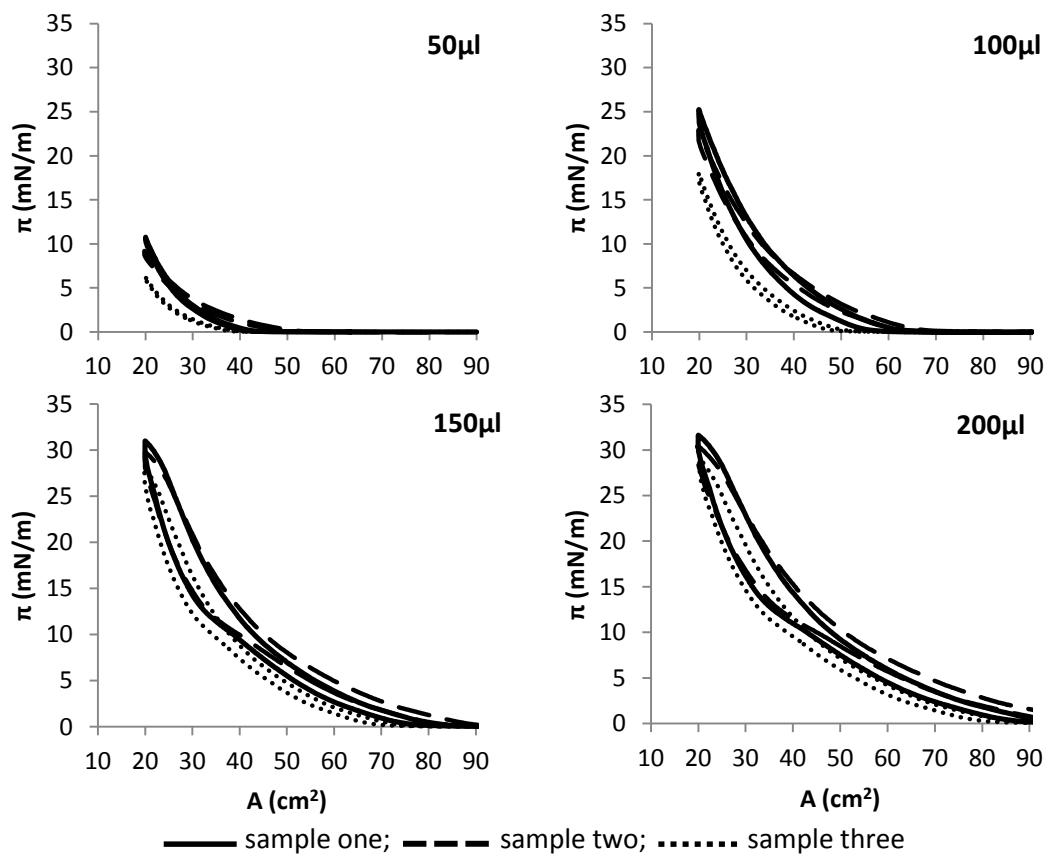


Fig 4.23. Inter-subject reproducibility of π -A isotherms from three CL samples.

4.3.4.2 Comparison of Extraction Solvents

The lenses extracted in $\text{CHCl}_3:\text{CH}_3\text{OH}$ produced π_{max} values of $\sim 28.9\text{mN/m}$ ($\pi_{\text{max}} = 28.8\text{-}29.0\text{mN/m}$ between $150\text{-}200\mu\text{l}$) and 19.6mN/m for the worn (Fig 4.24, Row 1) and control samples (Fig 4.25, Row 1) respectively. π_{init} was 0.0mN/m for both tear and control samples and the G-LE transition occurs over an increasingly gradual change in surface pressure between $0\text{-}10\text{mN/m}$ for the tear samples and $0\text{-}6\text{mN/m}$ for the control sample. This gradual change in surface pressure occurs over a large A_t range that increased as more material is introduced to the subphase surface. The reversibility for both subject and control samples was at a high value ($>90\%$) for all π -A isotherms recorded up to $200\mu\text{l}$ aliquots. For the tear sample, reversibility was high between $25\text{-}100\mu\text{l}$ with a reversibility of $\sim 99.0\%$ (range = $98.3\text{-}99.8\%$) decreasing to $\sim 94.6\%$ (range = $94.1\text{-}95.1\%$) as the surface concentration was increased to between $125\text{-}200\mu\text{l}$. For the control sample, reversibility was 99.0% (range = $98.8\text{-}99.1\%$) between $75\text{-}100\mu\text{l}$ and $\sim 97\%$ (range = $96.7\text{-}97.3\%$) over the $125\text{-}175\mu\text{l}$ volume range before decreasing significantly at the $200\mu\text{l}$ aliquot to a value of 90.72% .

The lenses extracted in C_6H_{14} produced π_{max} values of 18.9mN/m and 2.6mN/m for the worn (Fig 4.24, Row 2) and control samples (Fig 4.25, Row 2) respectively. Further increase in surface pressure would continue until reaching π_{max} at much higher loading concentrations. π_{init} was 0.0mN/m for both tear and control samples and the G-LE transition occurs at a more definable A_t with smaller transition area (A_t) ranges recorded. The reversibility between compression and expansion cycles for both subject and control samples was $\sim 99.5\%$ for all π -A isotherms recorded up to $150\mu\text{l}$ for the tear sample, decreasing to 97.0% and 94.2% for the $175\mu\text{l}$ and $200\mu\text{l}$ aliquots. The control sample produced a high reversibility of 99.8% between $150\text{-}200\mu\text{l}$ aliquots.

The lenses extracted in $\text{C}_6\text{H}_{14}:\text{CH}_3\text{OH}$ produced π_{max} values of $\sim 30.4\text{mN/m}$ and $\sim 22.5\text{mN/m}$ ($\pi_{\text{max}} = 22.2\text{-}22.8\text{mN/m}$) for the worn (Fig 4.24, Row 3) and control samples (Fig 4.25, Row 3) respectively. π_{init} was 0.0mN/m for both tear and control samples and the G-LE transition was observed except for the $200\mu\text{l}$ aliquot of the tear sample ($\pi_{\text{init}} = 0.83\text{mN/m}$). G-LE phase transition occurs over a gradual change in surface pressure between $0\text{-}10\text{mN/m}$, the A_t range for the tear samples occurring at higher areas. Reversibility for both subject and control samples was $>90\%$. Over the $25\text{-}200\mu\text{l}$ aliquot range reversibility decreased from 97.8% to 90.1% for the tear sample and from 99.9% to 94.6% for the control sample.

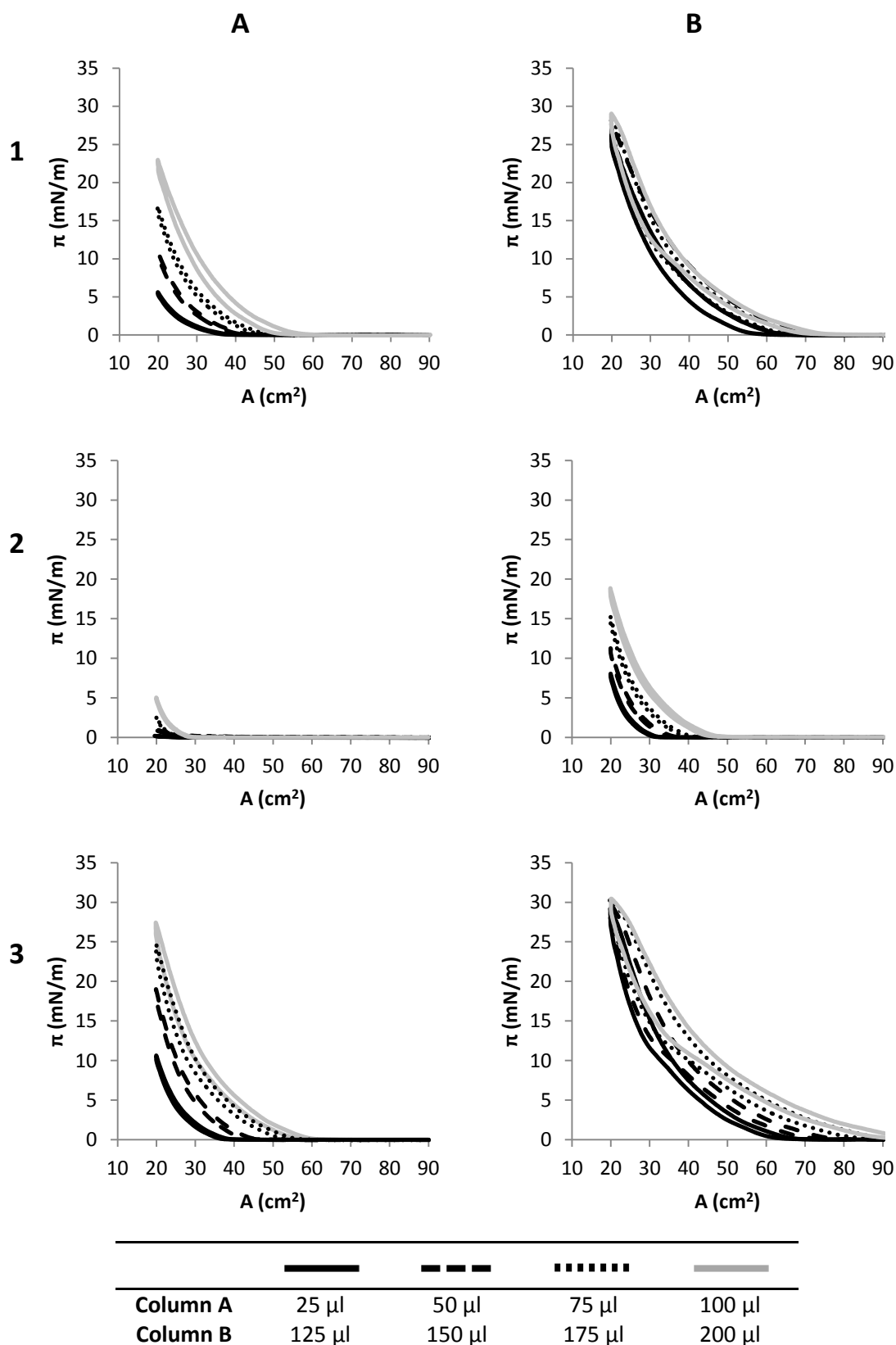


Fig 4.24. Comparison of π -A isotherms (Trough A) of tear samples obtained from worn FN+D contact lenses extracted using different solvents: $\text{CHCl}_3\text{:CH}_3\text{OH}$ (1:1 w/w; row 1); C_6H_{14} (row 2); $\text{C}_6\text{H}_{14}\text{:CH}_3\text{OH}$ (9:1 w/w; row 3).

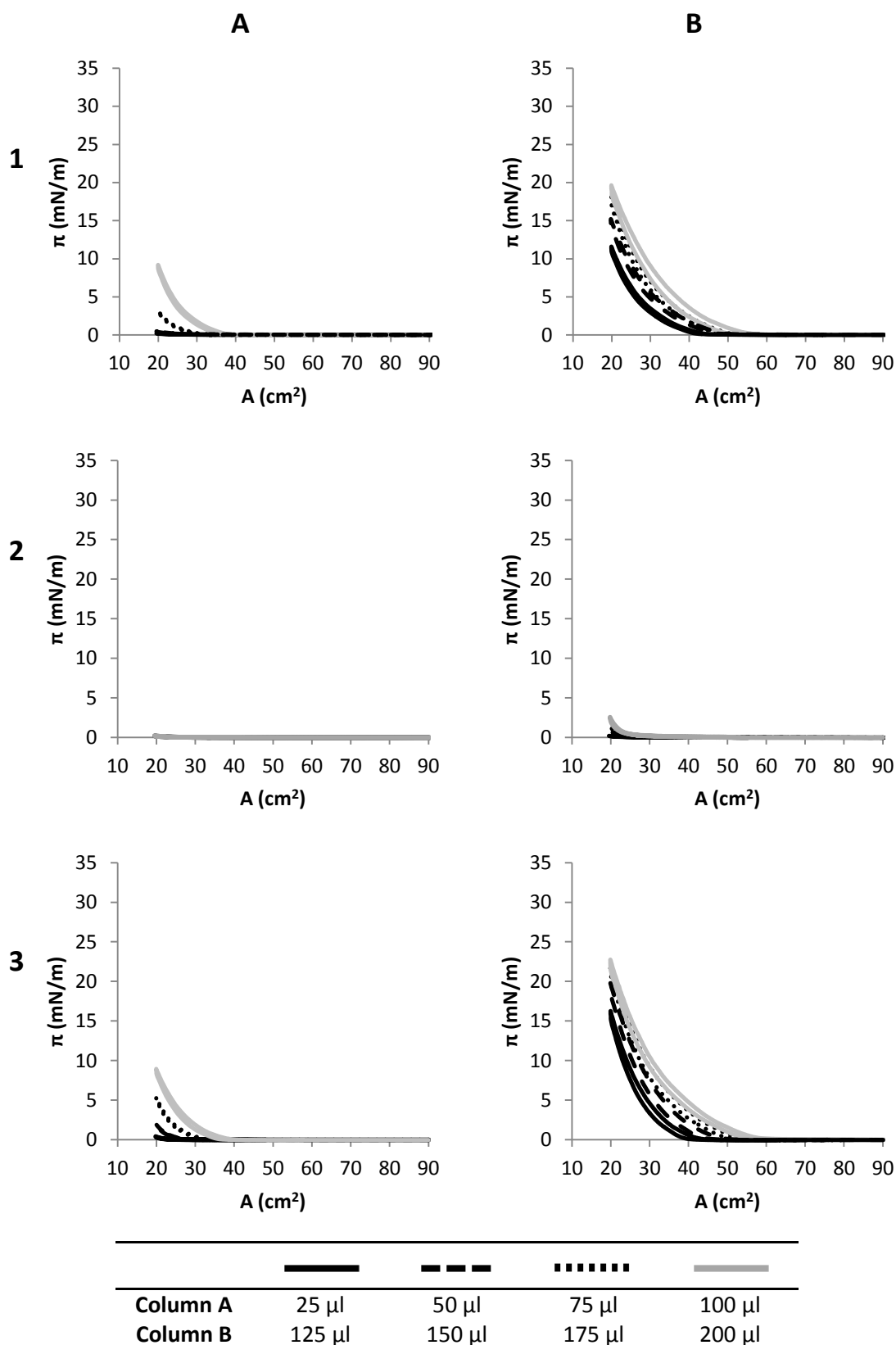


Fig 4.25. Comparison of π -A isotherms (Trough A) of samples obtained from unworn FN+D contact lenses extracted using different solvents: CHCl_3 : CH_3OH (1:1 w/w; row 1); C_6H_{14} (row 2); C_6H_{14} : CH_3OH (9:1 w/w; row 3).

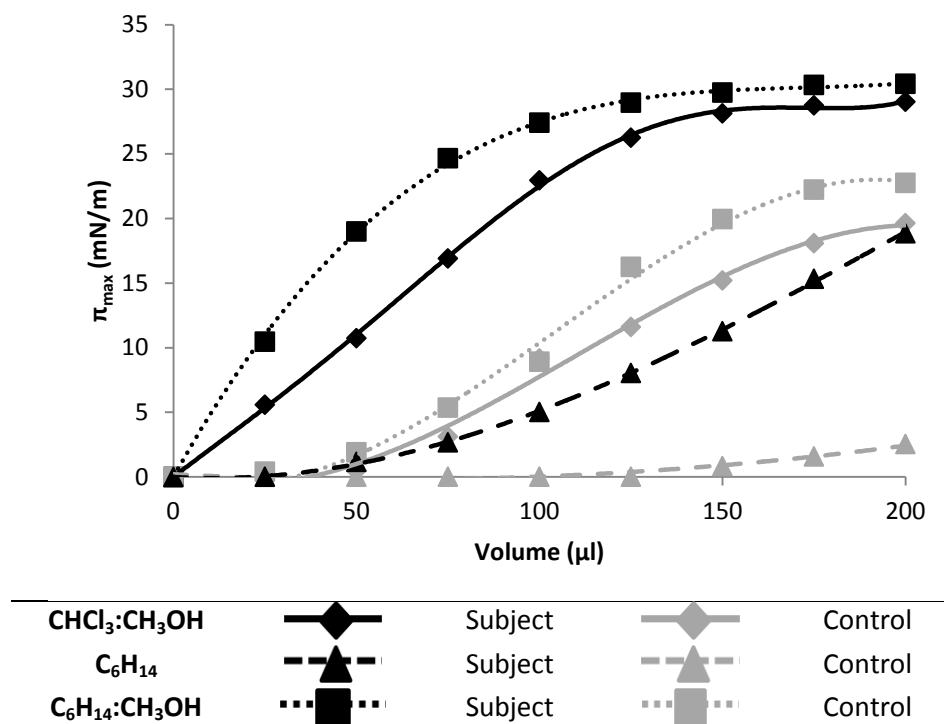


Fig 4.26. Comparison between the three solvents used to extract sample from worn and unworn FN+D contact lenses.

The $\text{CHCl}_3:\text{CH}_3\text{OH}$ and $\text{C}_6\text{H}_{14}:\text{CH}_3\text{OH}$ extractions of the worn FN+D contact lenses both attained a maximum surface pressure of $\sim 30\text{mN/m}$ which equates to those observed in other Langmuir trough based experiments of tear samples. The data obtained for the unworn samples would suggest that the incorporation of methanol in to the extraction solvent - even just 10% of the solvent - increases the extraction of lens material into the sample. Hexane could potentially achieve the same maximum value but due to the less powerful extracting nature of the solvent, it would take a volume aliquot approaching 350-400 μl to attain a π_{\max} of $\sim 30\text{mN/m}$. With a low maximum surface pressure recorded for the unworn lens extracted in hexane - and the potential small rate of increase in π_{\max} as the surface concentration is increased - hexane may be the better choice as an extracting solvent.

4.3.4.3 Trough B π -A Isotherms

The π -A isotherm data recorded on Trough B can be found in Fig 4.27-4.29. The lenses extracted in $\text{CHCl}_3\text{:CH}_3\text{OH}$ produced π_{max} values of $\sim 29.9\text{mN/m}$ ($\pi_{\text{max}} = 29.3\text{-}30.5\text{mN/m}$ between $800\text{-}1000\mu\text{l}$) and $\sim 20.6\text{mN/m}$ ($\pi_{\text{max}} = 20.2\text{-}20.9\text{mN/m}$ between $900\text{-}1000\mu\text{l}$) for the worn (Fig 4.27, Row 1) and control samples (Fig 4.28, Row 1) respectively. π_{init} was 0.0mN/m for both tear and control samples and the G-LE transition occurs at a definable A_t . Reversibility for both subject and control samples was $>95\%$ for all π -A isotherms recorded up to $1000\mu\text{l}$ aliquots. For the tear sample, reversibility was $\sim 99.5\%$ (range = $99.0\text{-}99.8\%$) between $200\text{-}600\mu\text{l}$ and decreases to $\sim 95.2\%$ at $1000\mu\text{l}$. For the control sample, reversibility was $>98\%$ (range = $98.2\text{-}99.9\%$).

The lenses extracted in C_6H_{14} produced π_{max} values of 17.1mN/m and 3.9mN/m for the worn (Fig 4.27, Row 2) and control samples (Fig 4.28, Row 2) respectively at maximum loading of $1000\mu\text{l}$. Further increase in surface pressure would continue until reaching π_{max} at much higher loading concentrations. π_{init} was 0.0mN/m for both tear and control samples and the G-LE transition occurs at a more definable A_t with smaller transition area (A_t) ranges recorded. Reversibility for the subject and control sample was $\sim 99\%$ (range = $99.8\text{-}99.4\%$) for π -A isotherms recorded for aliquots of $600\text{-}1000\mu\text{l}$. For the control sample, reversibility was only calculable for the 900 and $1000\mu\text{l}$ aliquots (reversibility = 99.9% and 96.1%).

The lenses extracted in $\text{C}_6\text{H}_{14}\text{:CH}_3\text{OH}$ produced π_{max} values of $\sim 30.4\text{mN/m}$ ($\pi_{\text{max}} = 30.1\text{-}31.1\text{mN/m}$ between $300\text{-}1000\mu\text{l}$) for the worn sample (Fig 4.27, Row 3) and 22.1mN/m at $1000\mu\text{l}$ control sample (Fig 4.28, Row 3). π_{init} was 0.0mN/m up to the $500\mu\text{l}$ aliquot and up to the $1000\mu\text{l}$ aliquot for the tear and control sample respectively. As such the transition from gaseous (G) to liquid expanded (LE) phase is observed. π_{init} increased to values $>0.0\text{mN/m}$ from the $600\mu\text{l}$ of tear. Initial reversibility at low loading concentrations began high ($\sim 99\%$) but decreased dramatically for each $100\mu\text{l}$ volume aliquot. Reversibility decreased from $\sim 96\%$ to $\sim 60\%$ for the tear sample and from $\sim 99\%$ to $\sim 73\%$ for the control sample.

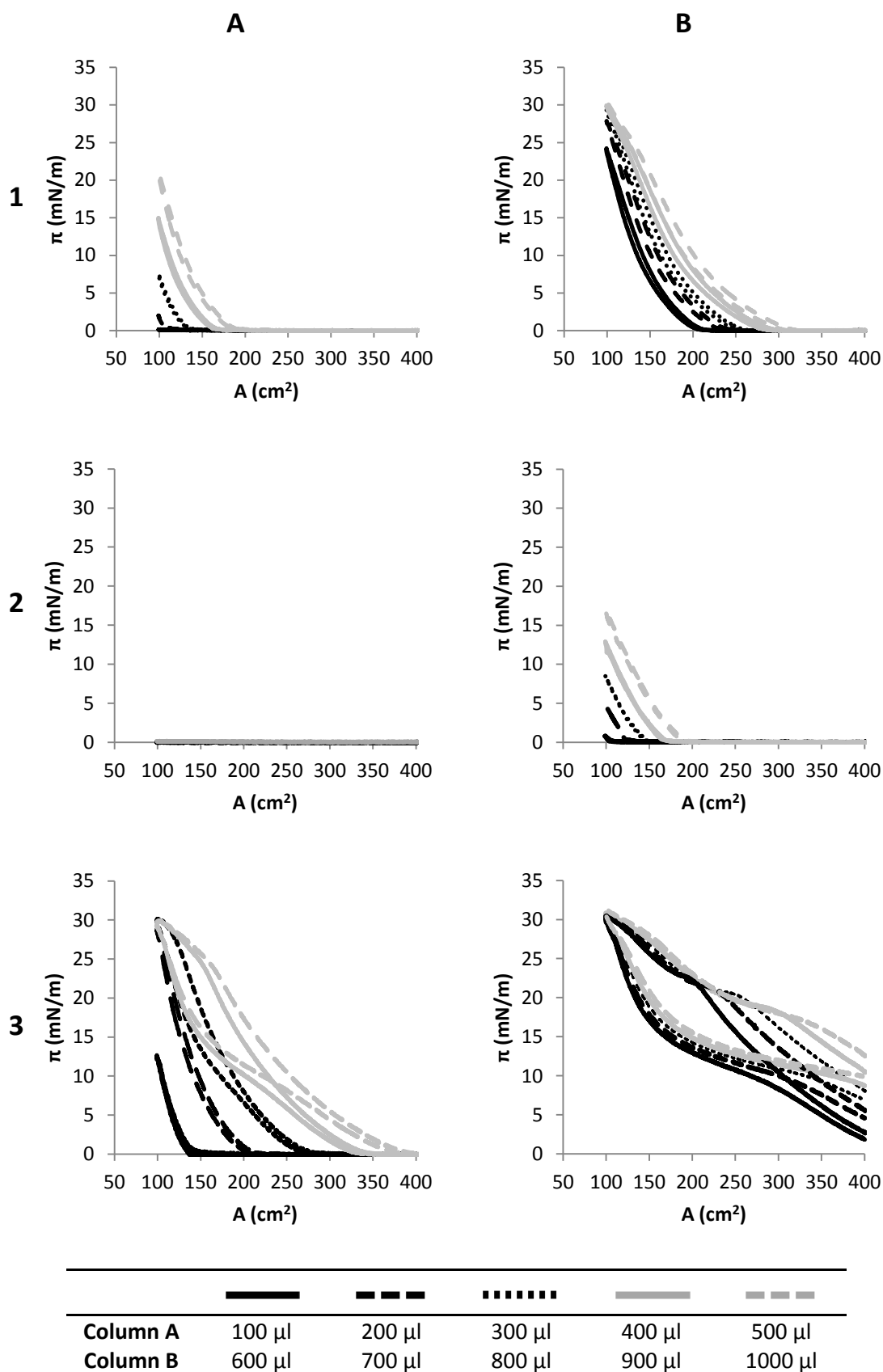


Fig 4.27. Comparison of π -A isotherms (Trough B) of tear samples obtained from worn FN+D contact lenses extracted using different solvents: CHCl_3 : CH_3OH (1:1 w/w; row 1); C_6H_{14} (row 2); C_6H_{14} : CH_3OH (9:1 w/w; row 3).

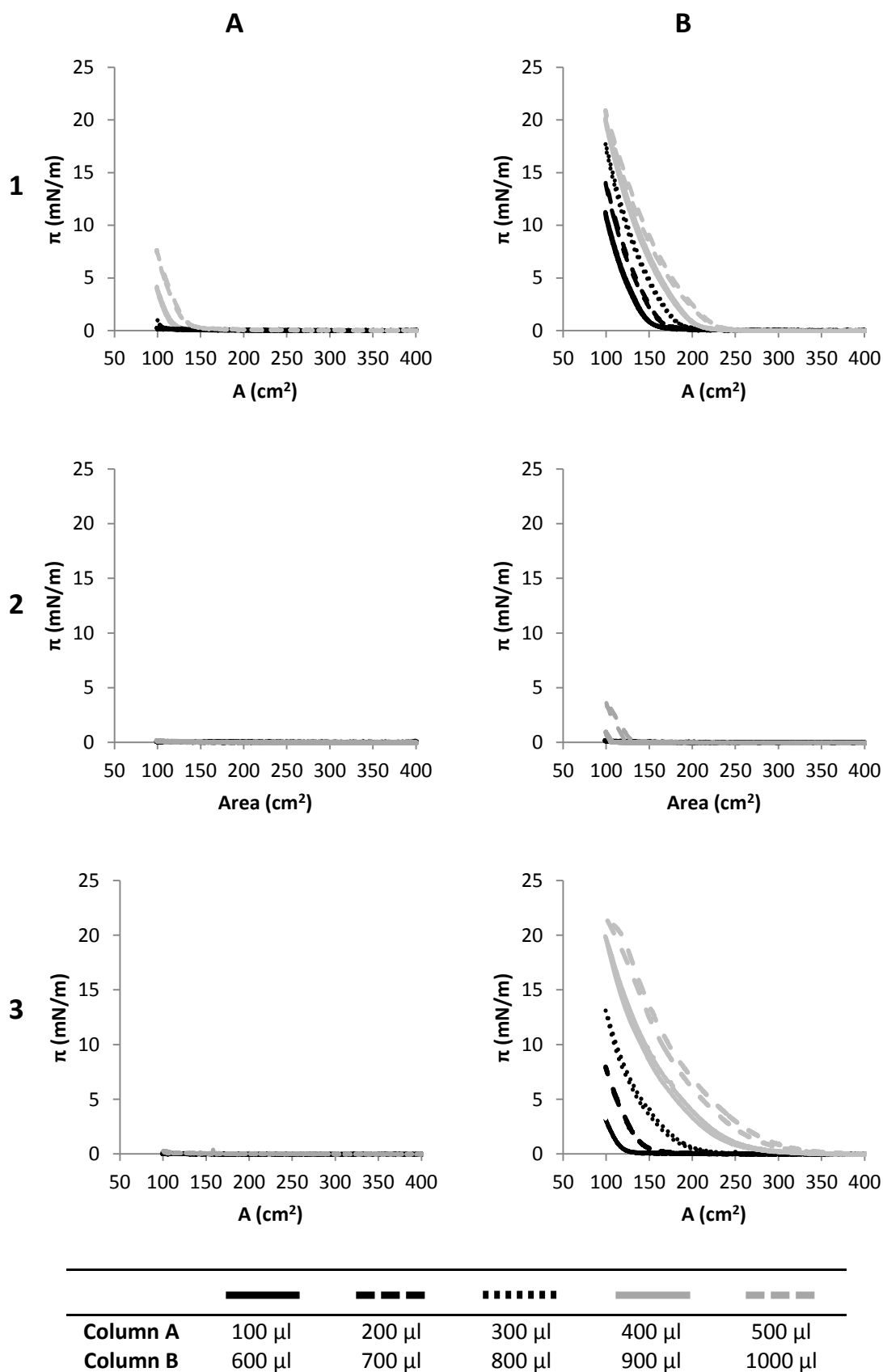


Fig 4.28. Comparison of π -A isotherms (Trough B) of samples obtained from unworn FN+D contact lenses extracted using different solvents: CHCl_3 : CH_3OH (1:1 w/w; row 1); C_6H_{14} (row 2); C_6H_{14} : CH_3OH (9:1 w/w; row 3).

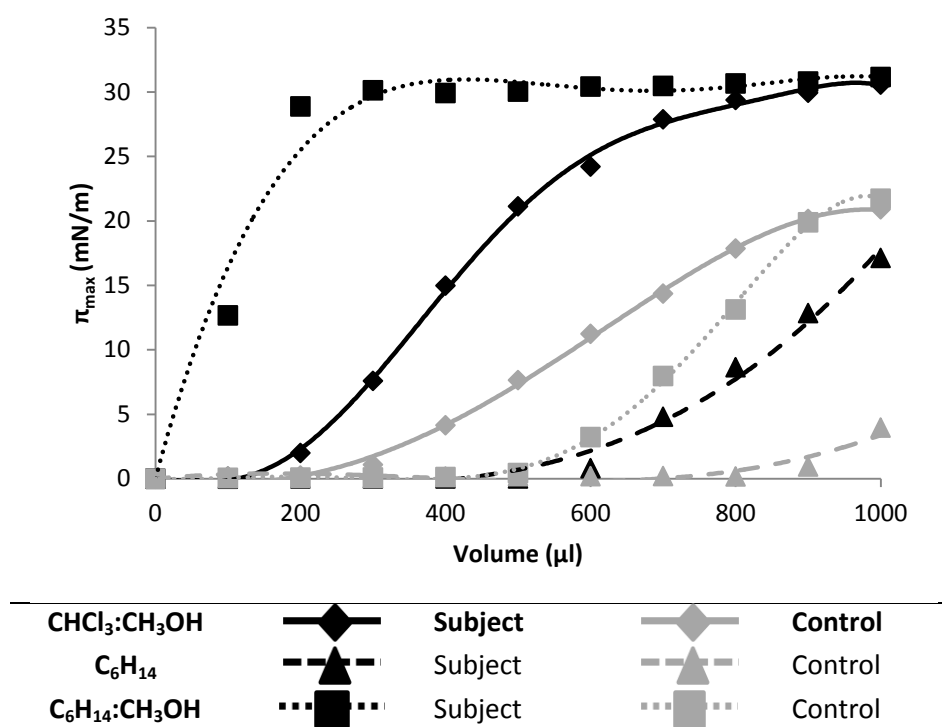


Fig 4.29. Comparison of π_{\max} as a function of the volume of sample from worn and unworn FN+D Contact lenses by three different solvents.

The comparison of maximum surface pressures as a function of the surface concentration of extracted components on Trough B show similar data to those obtained on Trough A. The $\text{CHCl}_3:\text{CH}_3\text{OH}$ and $\text{C}_6\text{H}_{14}:\text{CH}_3\text{OH}$ extractions of the worn contact lenses both attained a maximum surface pressure of $\sim 30\text{mN/m}$. Similarly, the maximum surface pressures for the control samples were also of the order observed in the Trough A π -A isotherms ($\pi_{\max} = \sim 20\text{mN/m}$ and $\sim 22\text{mN/m}$ for the $\text{CHCl}_3:\text{CH}_3\text{OH}$ and $\text{C}_6\text{H}_{14}:\text{CH}_3\text{OH}$ extractions respectively). The data obtained for the unworn samples would suggest that the incorporation of methanol in to the extraction solvent increases the extraction of lens material into the sample. Extracting samples using C_6H_{14} has been shown to be beneficial in limiting the amount of contact lens material from being extracted. However, any such benefits are negated by the need for a large volume aliquot to achieve a π_{\max} value approaching 30mN/m without affecting the concentration by the addition of more or less solvent.

4.3.4.4 Brewster Angle Microscopy

Fig 4.30 shows the BAM images recorded for a worn FN+D contact lens extracted using a $\text{CHCl}_3:\text{CH}_3\text{OH}$ (1:1w/w). These images show how lipid components can interact differently. In this case, the formation of 'plates' of material is observed. It is clear that there are regions that have different intensities that may be indicative of different lipid types or of the presence of multi-layered formation. As these BAM images were obtained for the equilibrium π -A isotherm, obtained after the sixth isocycle, it may be possible that ordered packing of the monolayer has occurred with potential overlap of layers to accommodate a stable film.

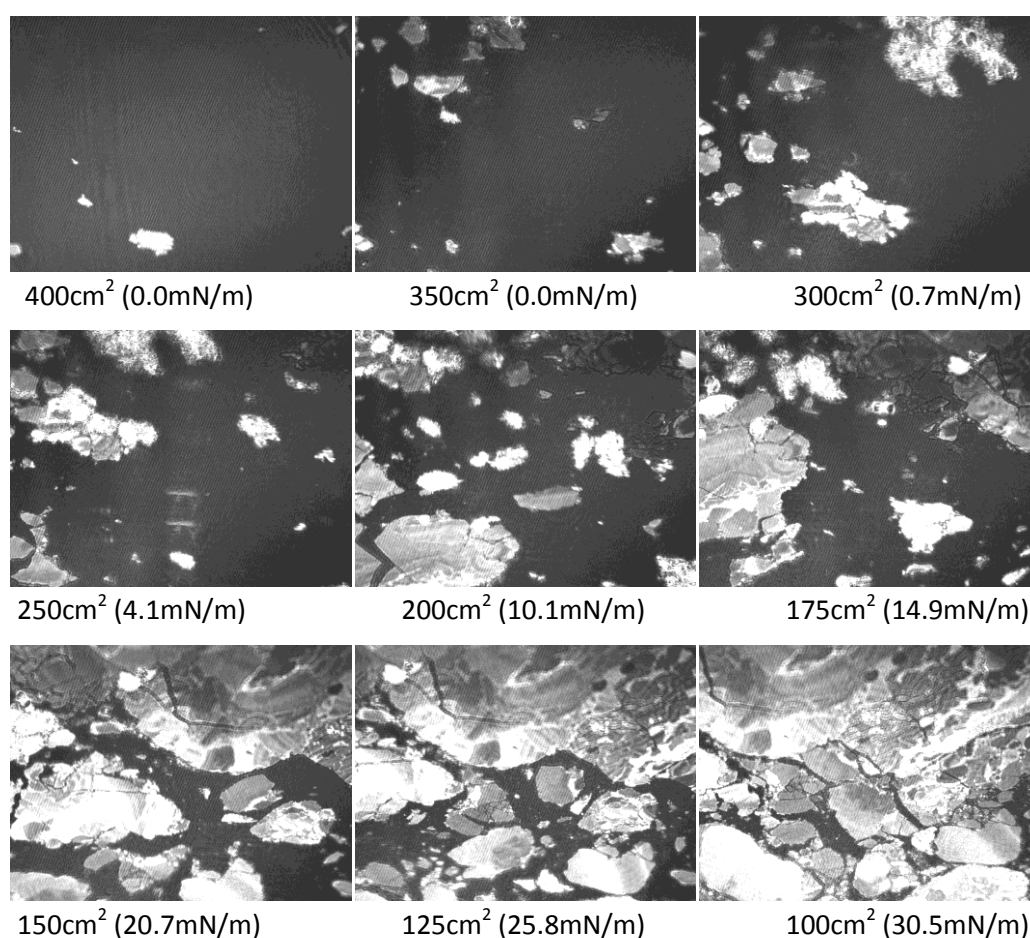


Fig 4.30. BAM images taken during the π -A compression isotherm of the sample obtained from extraction of a worn FN+D contact lens ($\text{CHCl}_3:\text{CH}_3\text{OH}$ (1:1 w/w) extraction; 1000 μl aliquot).

The presence of clear regions within the BAM images taken at low surface areas (100-150cm²) is indicative of no reflection occurring due to the absence of monolayer material. As observed in the π -A isotherm, so too is the way in which the monolayer compresses yet remaining

within the liquid expanded phase at minimum surface area. What must also be considered is the effect of lens material extracted simultaneously with the tear lipids. As the π -A isotherms of blank extractions (under similar extraction protocols) of Focus Night+Day contact lenses was observed to increase surface pressure to $\sim 20\text{mN/m}$ at maximum loading. This would seem to highlight the existence of the potentially surface active lens material that may significantly affect the π -A isotherm data obtained for worn samples.

4.4 Discussion

The surface activity of tear samples is a complex balance of interactions between lipid and protein components that affect the stability of the film system. Aspects of the behaviour of the tear sample monolayer become apparent in the π -A isotherms recorded in this chapter that can be directly related to the in-vivo behaviour of the tear film during a blink cycle.

The maximum surface pressure of the tear samples recorded from all of the collection and extraction methods utilised in this chapter was between $27\text{-}32\text{mN/m}$. This is concurrent with the surface pressures recorded by other researchers using the Langmuir trough as an instrument to measure surface behaviour of tear samples [152] [156] [217] or with combinations of Meibomian lipids and other tear film components [15] [36] [113] [226] [227] [228] [243]. This also equates to a surface tension of $41\text{-}45\text{mN/m}$, roughly analogous with the surface tension values recorded by Pandit [37] and Tiffany [11] [32] [38]. The result obtained from the studies of Zhao & Wollmer [154] [257] represented Langmuir trough data as surface tension as opposed to surface pressure, obtaining a minimum surface tension of 46.6mN/m for a healthy tear sample.

In addition to the maximum surface pressure data obtained, the π -A isotherms of tear samples also show that the monolayer forms a highly compressible liquid film that remains as such even when compressed to high surface pressures. This would indicate that the tear film is highly stable during a blink cycle under the high pressures that occur as the eyelid closes - with no collapse of the monolayer observed - and will reversibly expand as it reopens, ideal for maintaining the integrity of the tear film [2] [13]. This is due to the potential formation of a bi- or tri-layer system [13] [258]. During compression the hydrophobic regions of the Meibomian lipids are transferred over the top of hydrophilic lipids to form a multilayer film in a continuous process, with no definable transition between gaseous and liquid-expanded phase in the π -A isotherms of tear samples observed [152].

The main objective of this chapter was to evaluate the methodology for the collection, extraction and implementation of tear samples for Langmuir trough experiments. Direct quantitative comparison of the π -A isotherms of tear samples obtained from the four methods of collection is not possible. The efficacy of these collection methods are evaluated based upon four major considerations [253]:

- Collection of tear lipid samples - type and amount of lipid required;
- Patient comfort and toleration of discomfort;
- Extraction methodology - choice of solvent, extraction period;
- Experimental methodology - optimisation for Langmuir trough experiments.

In order to obtain a lipid sample ideal for analysis, the choice of sampling technique must involve an efficient method of obtaining the necessary test material whilst addressing patient-related comfort during the collection procedure. The methodology must provide lipid samples representative of the natural tear film system: therefore remain uncontaminated by lipids from other sources (such as sebaceous or cellular lipids) or obtained from stimulated/reflex tears caused by irritation by the sampling probe. The efficiency of the sampling probe in obtaining an accurate representation of the natural lipid composition of the tear film is counterbalanced by the need to collect enough material for π -A isothermal analysis. Single sample collection often produces a very small amount of material suitable for analysis and often the collection of a pool of several samples produces an adequate quantity as required for Langmuir trough experiments.

Micro-capillary tubes placed within the lower tear meniscus collect fresh tear samples as they are drawn up the tube by capillary action. It is an advantageous technique that is a relatively quick to obtain samples without any undue discomfort for the subject. However, it is a technique that has been observed to harvest low levels of lipids due to the hydrophobic affinity of these molecules to the glass surfaces of the tube. Schirmer strips are primarily used to measure the production of tears by placement inside the lower eyelid for a duration of ~5mins or until the strip is fully wetted. Irritation and reflex tear production is induced in un-anaesthetised experiments and collection of a stimulated tear sample is unavoidable [96]. Adsorbent-based methods such as ophthalmic sponges collect fresh lipids post-blink. Large volumes of un-stimulated tear sample are obtained and the technique has been used effectively for tear lipid collection. Contamination by lipids from other sources such as sebaceous and cellular lipids is possible [256].

Contact lenses produce a large volume of workable lipid material that extends itself well to analysis. However, there are more limitations with sample extraction from contact lenses than the other collection methods. It is only available to those that actually wear contact lenses which often exclude those with an intolerance to lens wear. Worn contact lenses are often collected at the end of a day's wear - usually >8hrs wear time - regardless of the wear modality. Lipoidal material that has been adsorbed to the lens surface over the course of a day/week/month becomes aged through degradation by UV and oxygen [168]. Lipid deposition depends upon the variations that naturally occur in the subjects as well as the choice of lens material, wear schedule, replacement schedule, cleaning schedule.

A commonly used methodology of obtaining Meibomian lipid samples (meibum) through hard or soft expression of the Meibomian glands and collection using a spatula. It is a method that has often been used to analyse a 'pure' sample of lipids that would form part of the tear film lipid layer after secretion [64] [67] [71] [74] [83] [259] [260] and in Langmuir trough based experiments [80] [156] [217] [227] [228] [261]. Adequate masses of meibum can be collected from a single sample for appropriate analysis and experimental study. However the methodology has its disadvantages. It is a method that induces discomfort and pain in subjects due to the process of expressing the glands to produce meibum secretions, with limited improvement when anaesthetising the eyelid. Compositional analysis has demonstrated that lipid samples obtained from the tear film lipid layer are different to those obtained from meibum [10] [74] [253]. Some lipid types with the tear film lipid layer are not exclusively sourced from the Meibomian glands [1] [2]. Meibum samples collected through expression can often be contaminated by other tear components and epithelial cells of the lid margins, conjunctiva and Meibomian glands [253]. Tear film and Meibomian lipids may also be contaminated by a small amount of sebaceous lipid [2] [10] [29] [245].

A similar consideration should be made for the solvent utilised in the extraction of test materials from the probes. The suitability of a solvent or solvent mixture is based upon the need to extract the necessary tear sample components whilst limiting the amount of unnecessary material extracted from the sampling probe. As observed in comparisons of π -A isotherms of tear and control samples, there is a varying significance in the amount of material that is extracted from the probes themselves. The microcapillary tubes produced no extractable material from the tubes themselves and were limited in the working concentration of tear lipid material. Schirmer strips and the Visispear ophthalmic sponges show extractable

cellulosic polymers and cellular lipids, with the amount of material extracted directly from the Schirmer strip nearly outweighing any tear lipid components that were adsorbed. The ophthalmic sponges also produced a significant effect on the maximum surface pressure but to a lesser extent than the Schirmer strips. The Focus Night+Day contact lenses used for this preliminary study are composed of copolymers containing the hydrophilic dimethylacrylamide (DMAA) monomer and the hydrophobic tris(trimethylsiloxy) silylpropylmethacrylate (TRIS) monomer. If a significant amount of this amphiphilic copolymer material is extracted into the solvent then it would account for the increase in surface pressure caused by adsorption to the subphase surface and interactions with lipid components [262].

In most Langmuir trough experiments, the same solvent used to extract material from the collection probe is often used for the application of the sample solution on to the subphase surface. Therefore the choice of solvent must also consider the spreading behaviour when forming an orderly structure monolayer and evaporation of solvent molecules to leave behind the adsorbed tear lipid monolayer at the surface. Chloroform is the most commonly used solvent in surface pressure based experiments due to the solubilisation of lipid molecules, rapid spreading (Harkins spreading coefficient = 13.9mN/m) and volatility of solvent (vapour pressure of chloroform = 26.2kPa). Ethanol and methanol are often utilised as part of solvent mixtures to enhance the solubility of amphiphilic/polar molecules [34] and mixtures with chloroform have often been used in the study of tear lipid and Meibomian gland secretions [64] [67] [71] [74] [83] [259] [260].

Optimisation of the extraction protocols is needed to improve the single sample collection necessary for π -A isothermal studies, especially for standard reproducibility of experiments. A solution to this would be to use a two stage solvent system. The first solvent system would be chosen based on preferred of extraction of lipid material followed by a drying stage that would remove the solvent and allow the mass of collected material to be determined. The second solvent system would be chosen based upon spreading and evaporation properties (probably CHCl_3) and would allow the concentration of lipid solution to be calculated.

4.5 Summary

The following conclusions can be observed from the experimental data within this chapter:

- The amount and type of tear lipid varies depending on the collection methodology;
- The extraction methodology also affects the amount of material extracted from the collection probe, both beneficially and detrimentally;
 - $\text{CHCl}_3:\text{CH}_3\text{OH}$ solvent mixture may provide a large sample for repeat experiments, but also shows a large degree of unwanted extractable material observed in control extractions of an unused sampling probe;
 - Using hexane as an alternative solvent limits the amount of unwanted extractable material from being obtained. However in some cases it also limited the amount of lipid material collected, meaning maximum sample surface pressures were not attainable;
- Glass microcapillary tubes are limited in the amount of material collected, which is unsuitable to attain maximum surface pressures. One advantage however is the low amount of probe material extracted from the tube, even under harsh extraction procedures;
- Schirmer strips are limited in the amount of usable material for surface pressure measurements, so that repeat experiments using the same sample may be impossible. Also the amount of cellulosic material collected during extraction present within the sample limits the effectiveness of using this method;
- Visispear™ ophthalmic sponges provide a better alternative. The amount of material collected allows repeat experiments from the same collected sample to be conducted regardless of the solvent used. The amount of extracted probe material is also limited even under harsh extraction and eliminated under weaker solvent systems;
- Contact lenses provide an insight in to the fate of lipids adsorbed onto the lens surface. A sizeable amount of material is collected that allows repeat study of the same sample can be conducted. There are however limitations that must be considered when using a contact lens as a sample probe:
 - Contact lens material that is extracted may be amphiphilic and can dominate the surface behaviour of the collected sample. This can be eliminated to some extent using hexane as a solvent;
 - They are only suitable for those that are prescribed to wear them;
 - Severe changes are induced on the chemistry of the tear film during wear.

Chapter 5

In-vitro Study of Tear Film Samples: Fate of Lipids on Extended Wear Silicone Hydrogel Contact Lenses

As established in the experimental data from Chapter 4, contact lenses provide a useful sampling probe that provides information on the fate of tear lipids during lens wear. The materials used in the development and production of contact lenses differ depending upon the manufacturers design and objective characteristics. The development of silicone hydrogel (SiHy) contact lenses overcame the low oxygen transmission within the closed eye that allows overnight wear of SiHy lenses. However, the use of these materials introduced issues of increased lipid adsorption that is detrimental to the biocompatibility of the lens within the tear film, leading to tear film disruption, loss of corrected visual acuity, discomfort and intolerance [194].

5.1 Objectives

The objectives are to determine the influence of lens material and wear modality on the deposition of lipids on to a contact lens surface. The surface behaviour profiles of deposited lipid samples extracted from two different extended wear silicone hydrogels will be recorded and compared to determine differences based on lens material and wear modality.

5.2 Experimental Design

Two SiHy contact lenses marketed for extended wear were studied: PureVision (PV; balafilcon A; Bausch & Lomb, USA) and Focus Night+Day (FN+D; lotrafilcon A; CIBA-Vision (now Alcon Laboratories), USA). Appendix 3 contains information for the contact lenses used in this study. Contact lens samples were obtained from an 18-month clinical trial conducted cooperatively between the Biomaterials Research Unit and the Vision Sciences department at Aston University.

Contact lenses were worn on a daily wear (DW) or continuous wear (CW) modality for a 30 day period. The CW group wore the contact lenses continuously for the 30 day period whereas the DW group wore the contact lens throughout the day and cleaned with Opti-Free Express multipurpose solution before reinsertion of the lens. Details of the number of subjects from

which contact lenses were collected from and the amount of each lens type and modality is found in Fig 5.1. Worn contact lenses were collected at the end of the 30-day period of prescribed wear, placed into a vial containing saline (Saline, Sauflon Pharmaceuticals Ltd, UK) to keep the lens hydrated and stored at $\sim 4^{\circ}\text{C}$ prior to analysis. Unworn contact lenses were taken from their packaging without any further modification to the lens material.

Subject and control samples were obtained by extraction of worn and unworn contact lenses respectively. Prior to extraction, lenses were removed from their storage solution - either saline (worn lenses) or packaging solution (unworn lenses) - and blotted on filter paper to remove excess liquid. Three worn lenses from each contact lens type and wear modality were collected and extracted in each of the extraction solvents (Fig 5.1). Unworn contact lenses were also extracted in the three extraction solvents. Lenses were extracted for 1hr in 1.5ml of the following extracting solvents: $\text{CHCl}_3:\text{CH}_3\text{OH}$ (1:1; w/w), C_6H_{14} or $\text{C}_6\text{H}_{14}:\text{CH}_3\text{OH}$ (9:1; w/w). Sample solutions were transferred to a clean glass vial by pipette to prevent contamination by lens material caused by swelling and breakdown of the contact lens. All samples were studied within 24hr of extraction.

The surface behaviour study of tear samples was conducted on Langmuir trough B (working surface area - $400\text{-}100\text{cm}^2$; barrier speed - $50\text{cm}^2/\text{min}$) according to the procedure described in section 2.1. HPLC-grade water was used as a subphase and kept at a constant temperature of $35.0^{\circ}\text{C} \pm 0.2^{\circ}\text{C}$. Sample solutions were applied to the subphase surface by a $50\mu\text{l}$ Hamilton syringe. Ten minutes was allowed to ensure solvent evaporation and monolayer spreading. Tear sample films were repeatedly compressed and expanded until the equilibrium surface pressure (π_{eq}) was reached. π -A isotherms were recorded for consecutive $100\mu\text{l}$ aliquots up to a total volume of $1000\mu\text{l}$.

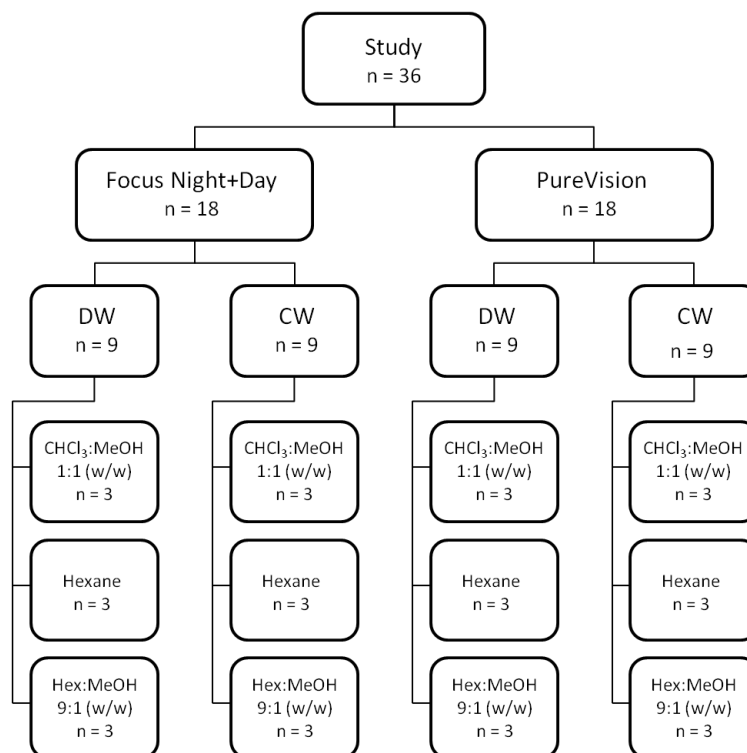


Fig 5.1. Subject sample size based on lens type, wear modality and extraction protocol.

5.3 Results

5.3.1 Focus Night+Day Contact Lenses

5.3.1.1 Chloroform : Methanol (1:1 w/w) Extraction

The π -A isothermal data for subject and control samples obtained from worn and unworn FN+D contact lenses extracted in $\text{CHCl}_3:\text{CH}_3\text{OH}$ (1:1; w/w) can be found in Fig 5.2-5.5 and Appendix 4. The extraction of a control FN+D contact lens (Fig 5.2) produced a maximum surface pressure (π_{max}) of ~ 20 - 21mN/m ($900\mu\text{l}$, $\pi_{\text{max}} = 20.2\text{mN/m}$; $1000\mu\text{l}$, $\pi_{\text{max}} = 20.9\text{mN/m}$). Higher π_{max} were recorded for the extractions of worn contact lenses under both wear modalities obtained around the same volume aliquot (800 - $1000\mu\text{l}$ region). The extraction of CW lenses (Fig 5.3) produced π_{max} of 27 - 30mN/m . Subject Px02 produced a π_{max} of 26.4mN/m obtained at the $1000\mu\text{l}$ aliquot. A further increase in the maximum surface pressure to 27.1mN/m was observed with a further $100\mu\text{l}$ aliquot ($1100\mu\text{l}$) indicates a π_{max} of $\sim 27\text{mN/m}$. Subject Px11 and Px16 produced a π_{max} of $\sim 29.5\text{mN/m}$ and $\sim 28.0\text{mN/m}$ respectively. The extraction of DW lenses (Fig 5.4) produced π_{max} in the region of 31 - 34mN/m . Subject Px05 produced a π_{max} of $\sim 33.5\text{mN/m}$, subject Px13 produced a π_{max} of $\sim 32.0\text{mN/m}$ and subject Px25 produced a π_{max} of $\sim 31.5\text{mN/m}$.

A feature of all π -A isotherms obtained from extraction of the unworn and worn contact lenses of both wear modalities in $\text{CHCl}_3:\text{CH}_3\text{OH}$ (1:1; w/w) is an Initial surface pressure (π_{init}) of 0.0mN/m up to maximum loading volume of 1000 μl and the G-LE transition was observed in all isotherm at a definable transition area (A_t). A slow transition within the LE phase as molecular orientation is optimised, with a gradual change in the rate of surface pressure increase noticeable between 0-10mN/m. As the surface concentration of sample increases during compression, ordering and packing within the monolayer can be observed in the change in the rate of surface pressure increase until a stable LE phase is obtained. A_t begins at a larger surface area for the subject samples when compared to that of the control sample at each 100 μl interval. At the 1000 μl aliquot, the A_t for the subject samples produced an the initial G-LE phase transition at A_t values in the region of 275-320 cm^2 . Ordering of the monolayer continued until a stable LE phase was obtained (indicated by no change in the rate of surface pressure increase) at an A_t of 150-200 cm^2 . The reversibility between compression and expansion cycles for the control sample was high (~99.0%). A slight decrease in reversibility was observed for the subject samples. No real difference was observable between the reversibility of the CW and DW modality lens samples at a loading volume of >600 μl (CW, Rev = ~96.1% (range = 95.8-97.0%); DW, Rev = 96.9% (range = 96.0-97.3%).

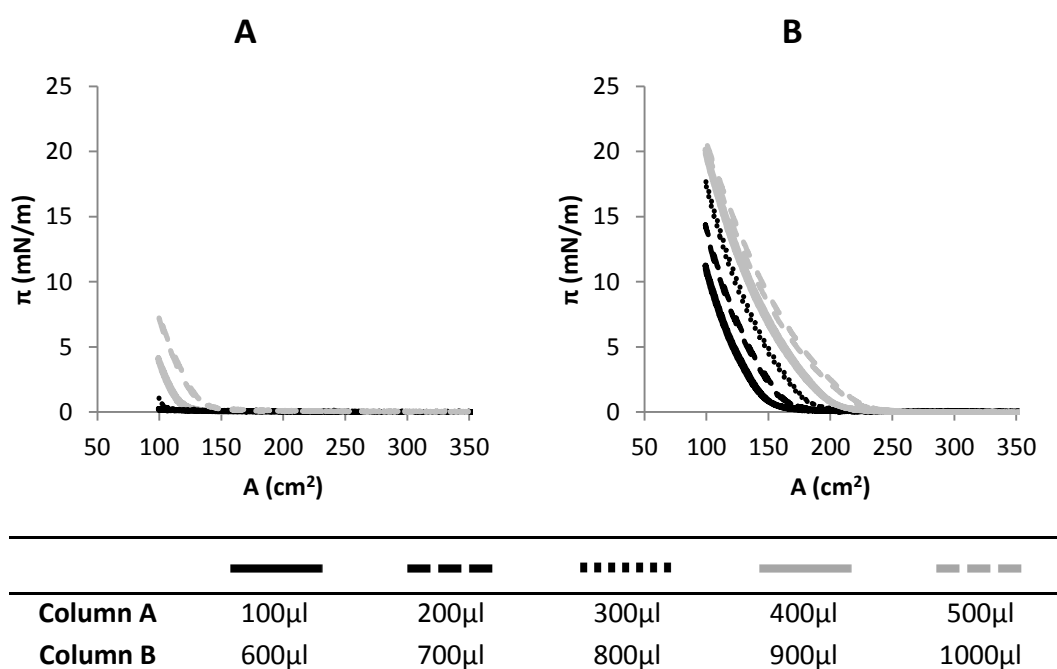


Fig 5.2. π -A isotherms of control FN+D contact lens extracted in $\text{CHCl}_3:\text{CH}_3\text{OH}$ (1:1 w/w).

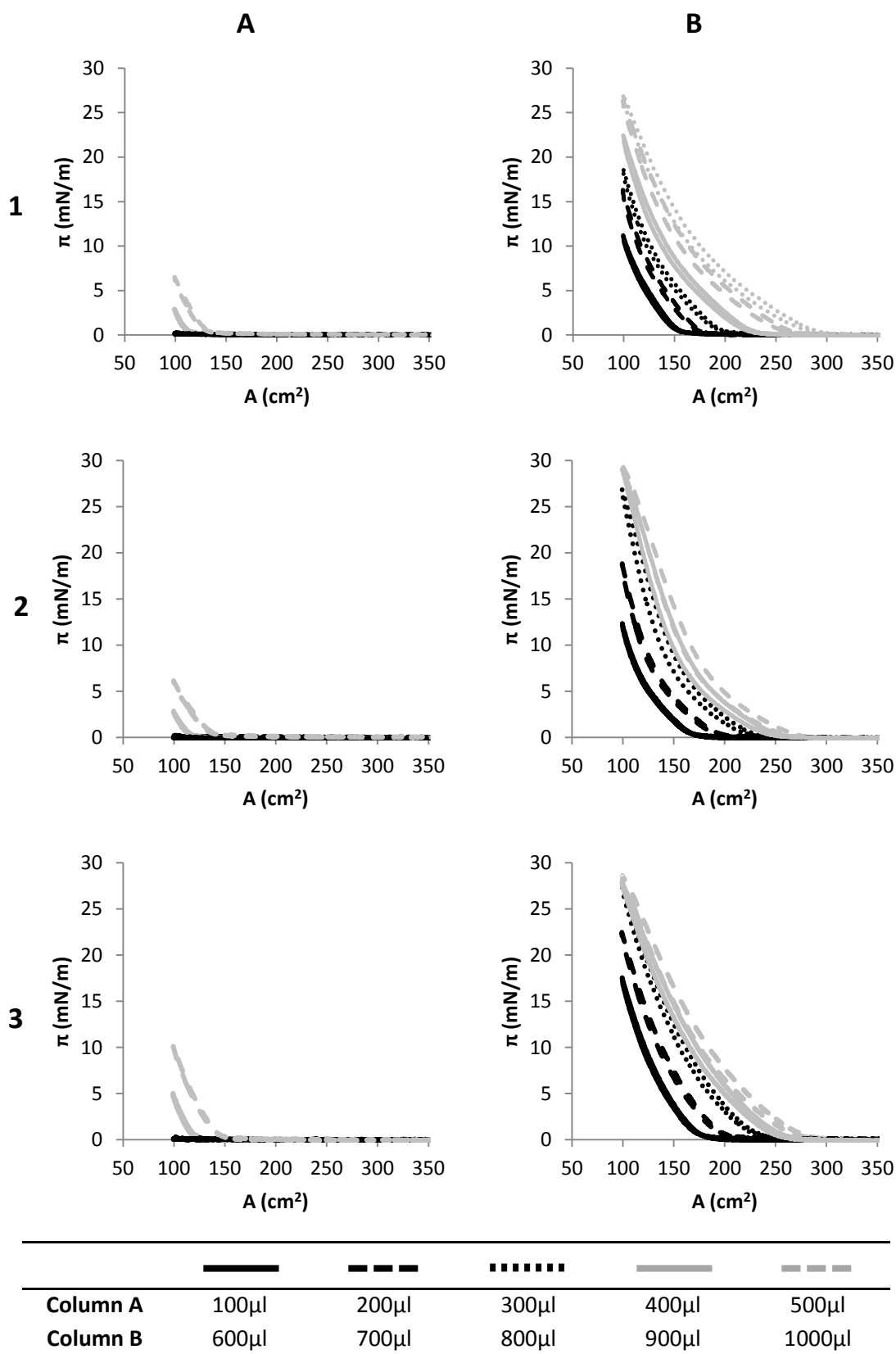
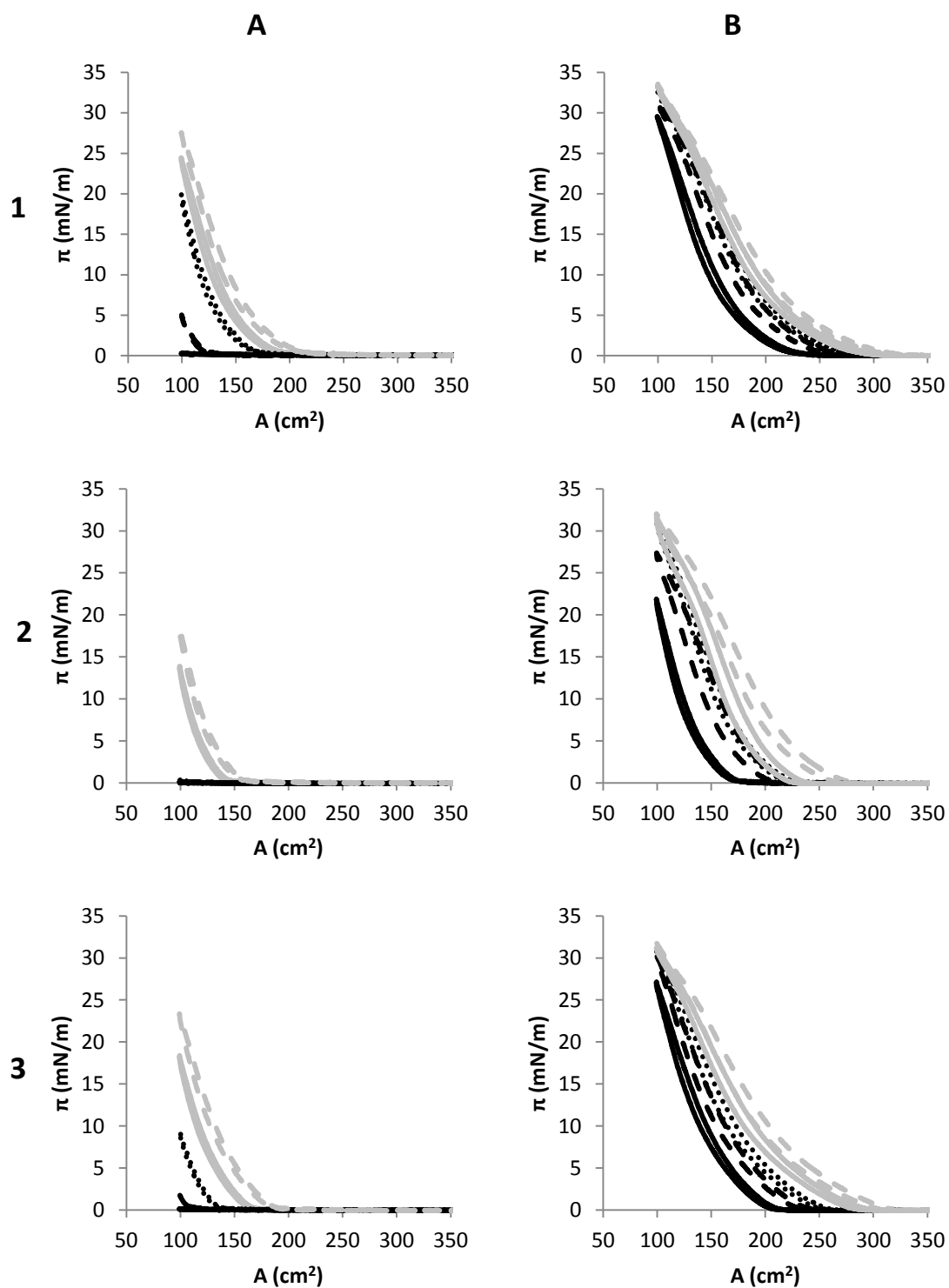


Fig 5.3. π -A isotherms of FN+D contact lens worn under a CW modality extracted in $\text{CHCl}_3:\text{CH}_3\text{OH}$ (1:1 w/w): Row 1 - Px02; Row 2 - Px11; Row 3 - Px16.



Column A	100μl	200μl	300μl	400μl	500μl
Column B	600μl	700μl	800μl	900μl	1000μl

Fig 5.4. π -A isotherms of FN+D contact lens worn under a DW modality extracted in $\text{CHCl}_3:\text{CH}_3\text{OH}$ (1:1 w/w): Row 1 - Px05; Row 2 - Px13; Row 3 - Px25.

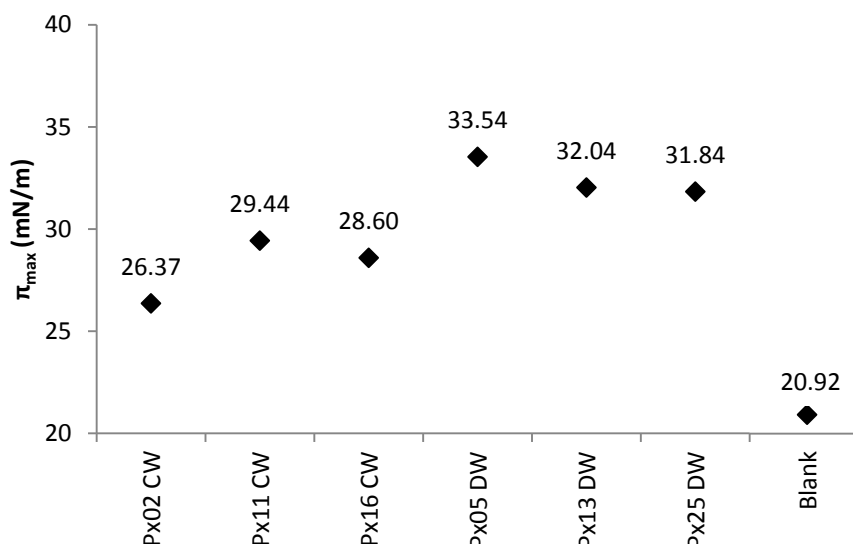


Fig 5.5. Comparison of π_{\max} as a function of wear modality of samples obtained from worn and unworn FN+D contact lenses extracted in $\text{CHCl}_3:\text{CH}_3\text{OH}$ (1:1 w/w).

5.3.1.2 Hexane Extraction

The π -A isothermal data for subject and control samples obtained from worn and unworn FN+D contact lenses extracted in C_6H_{14} can be found in Fig 5.6-5.9 and Appendix 4. The extraction of a control FN+D lens (Fig 5.6) produced no change in surface pressure from 0.0mN/m recorded for the clean subphase surface for all aliquots up to 1000 μl . None of the C_6H_{14} extracted worn samples attained a π_{\max} under either wear modality with further increases possible with a more concentrated solution.

A difference could be observed between the CW and DW wear modality samples. The extraction of CW lenses (Fig 5.7) produced surface pressures <10mN/m with values of 4.0mN/m, 3.8mN/m and 6.9mN/m recorded for Px16, Px38 and Px71 respectively at the 1000 μl aliquot. The first instance of an increase in surface pressure to >0.0mN/m at A_{\min} was observed at the 900 μl for P16 and Px17, and 800 μl for Px38. The extraction of DW lenses (Fig 5.8) produced surface pressures in the region of 13-19mN/m. Surface pressure values recorded at maximum loading (1000 μl) were 16.1mN/m, 18.7mN/m and 13.4mN/m for subject Px13, Px25 and Px62 respectively. The first instance of an increase in surface pressure to >0.0mN/m at A_{\min} was observed at the 600 μl for Px13, 300 μl for Px25 and 500 μl for Px62. In both CW and DW sample cases, further increase in surface pressure would be observable with a more concentrated sample solutions.

π_{init} of 0.0mN/m was observed for both CW and DW samples up to maximum loading volume of 1000 μ l. The G-LE transition was observed in the isotherms with a $\pi_{\text{max}} > 0.0\text{mN/m}$. As no increase in surface pressure was recorded for the control lens, it is assumed that any regions of extracted polymeric surfactant material present at the surface does not interact significantly between each other to induce an increase in surface pressure. In the π -A isotherms of subject samples obtained from worn lenses that recorded an increase in surface pressure, the transition area from G to LE phase was at a definable surface area rather than a range observed in the $\text{CHCl}_3\text{:CH}_3\text{OH}$ extracted samples. The transition indicates a clear definition between G and LE phases where the regions of extracted material begins interacting without increasing surface pressure until a critical point is attained where the monolayer transitions to a stable LE phase. The reversibility between compression and expansion cycles for the subject samples control sample was high (~98.0%). Any difference in reversibility between CW and DW samples is not comparable due to the small surface pressures recorded at highest loading volume. Without any increase in surface pressure recorded for the control sample, calculation of reversibility is not applicable.

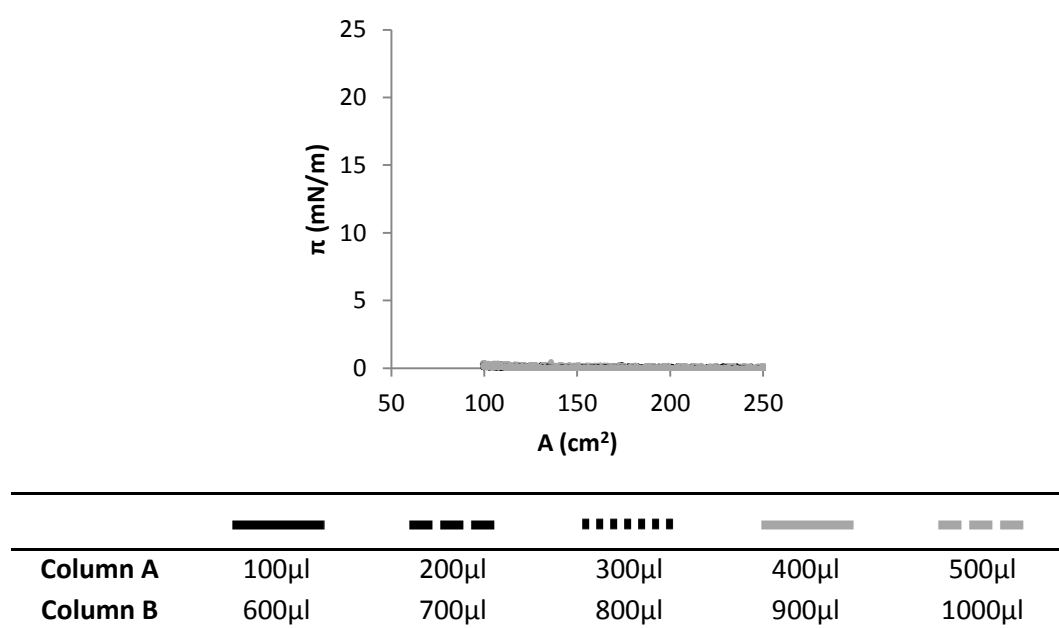


Fig 5.6. π -A isotherms of control FN+D contact lens extracted in C_6H_{14} . π -A isotherms for the 100-500 μ l aliquots not shown.

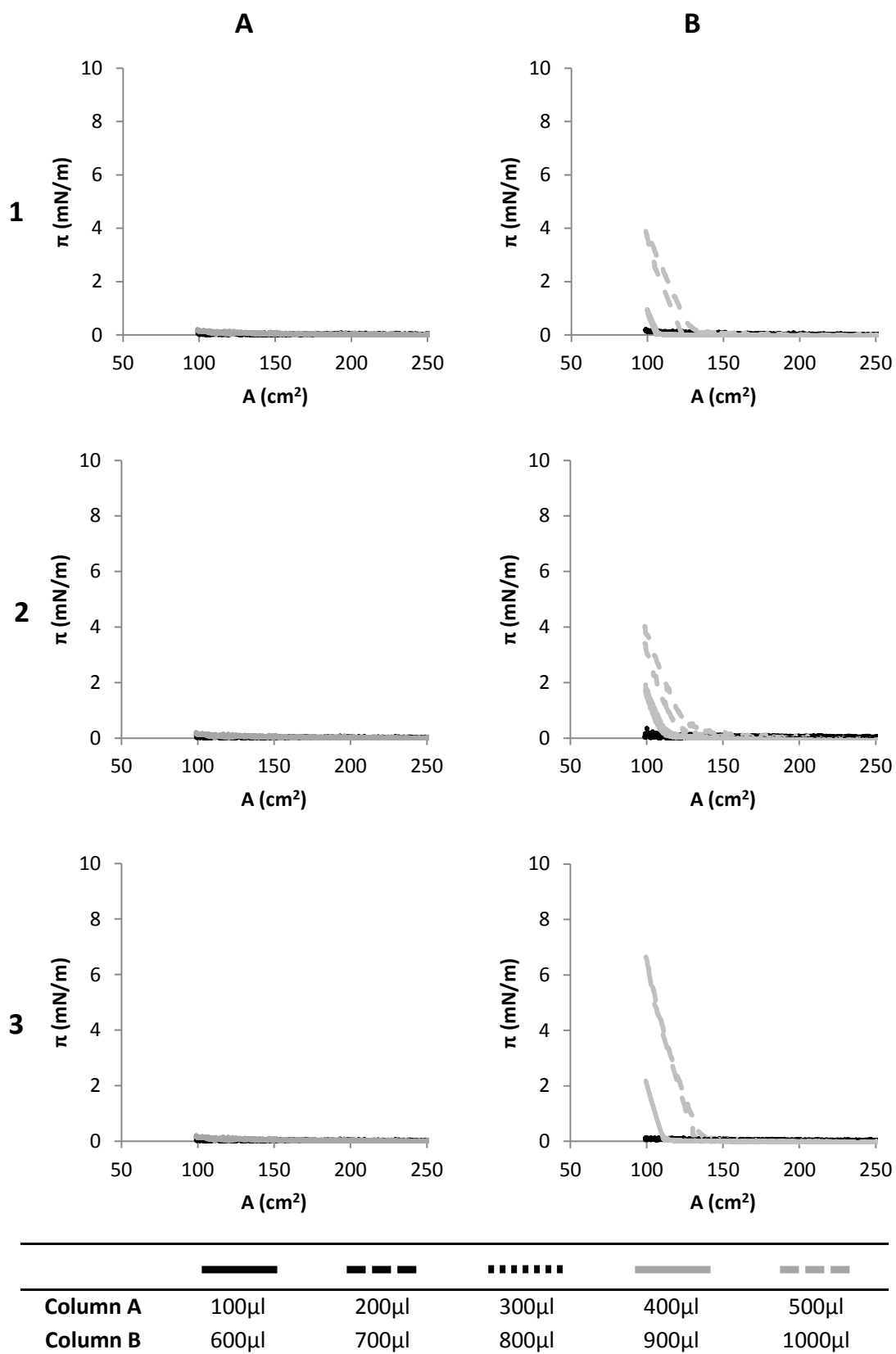


Fig 5.7. π -A isotherms of FN+D contact lens worn under a CW modality extracted in C_6H_{14} : Row 1 - Px16; Row 2 - Px38; Row 3 - Px71.

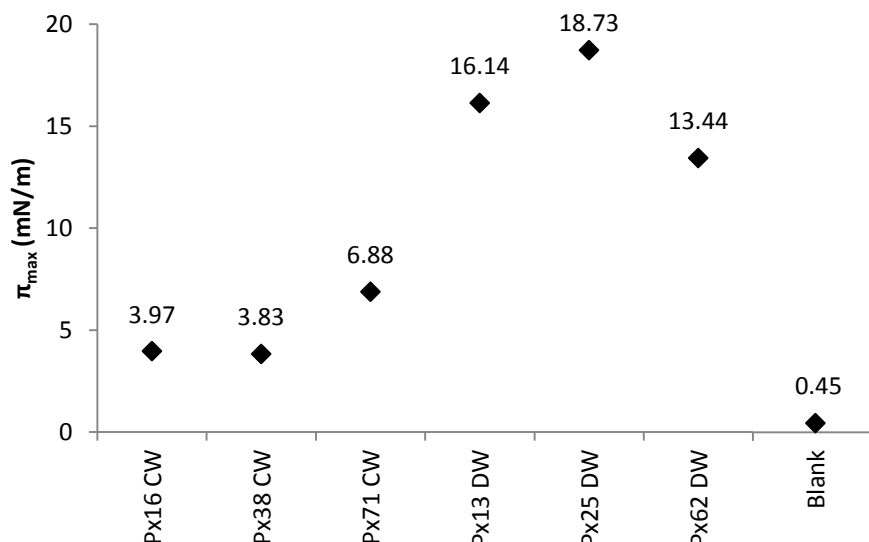


Fig 5.9. Comparison of π_{\max} as a function of wear modality of samples obtained from worn and unworn FN+D Contact lenses extracted in C_6H_{14} .

5.3.1.3 Hexane : Methanol (9:1 w/w) Extraction

The π -A isothermal data of subject and control samples obtained from worn and unworn FN+D contact lenses extracted in C_6H_{14} : CH_3OH (9:1 w/w) can be found in Fig 5.10-5.13 and Appendix 4. The control sample (Fig 5.10) produced a surface pressure of ~ 21.7 mN/m at the 1000 μ l aliquot. The extraction of CW lenses (Fig 5.11) produced surface pressures in the region of 23-26 mN/m at 1000 μ l loading volume where surface pressures of 23.5 mN/m, 23.4 mN/m and 25.3 mN/m was recorded for subjects Px11, Px12 and Px26 respectively. Further increase in surface pressure would be observable with further addition of 100 μ l aliquots to the subphase surface until attaining a maximum surface pressure. Conversely, the DW lens samples (Fig 5.12) produced a maximum surface pressure for the sample. π_{\max} values in the region of 31-35 mN/m were recorded. Subject Px05 produced a π_{\max} of ~ 31.0 mN/m attained at a small volume of sample introduced to the surface (π_{\max} attained at the 300 μ l). No significant increase was observed for each 100 μ l aliquot between 300-1000 μ l (π_{\max} range = 30.5-31.2 mN/m). Subject Px22 produced a π_{\max} of ~ 34.0 mN/m and subject Px25 produced a π_{\max} of ~ 32.0 mN/m attained at an aliquot volume of 600 μ l where no significant increase was observed for each 100 μ l aliquot between 600-1000 μ l (π_{\max} range = 31.4-32.2 mN/m).

π_{init} was 0.0 mN/m up to maximum loading volume of 1000 μ l for the control and CW subject samples. The transition from gaseous (G) to a liquid expanded (LE) phase was observable in all isotherms. For the π -A isotherms recorded for the DW subject samples, initial surface pressure

was 0.0mN/m for all isotherms up to 500 μ l aliquot for Px05 and Px22 and the 600 μ l aliquot for subject Px25 sample. The transition area was not at a definable area for all isotherm recorded for the control and CW subject samples, as well as the π -A isotherm recorded at <500 μ l aliquots for the DW subject samples where the G-LE transition was observable. The G-LE transition for these samples indicate a slow transition from G to a fully stable LE phase, with a gradual change in the rate of surface pressure increase noticeable between 0-10mN/m. There was no discernible difference in the area region where this transition occurs between the control and tear samples. At higher loading volumes, observable in the DW sample isotherm and not the CW samples, was the presence of changes within the monolayer indicated by changes in the rate of increase in surface pressure over the course of the LE phase. This would seem to indicate film behaviour that is constantly undergoing changes in packing behaviour whilst retaining stable LE monolayer structure.

The reversibility between compression and expansion cycles was \sim 97.5% for the control sample and \sim 97% (range = 95.8-97.9%) for the CW subject samples at the highest loading volume. DW samples show a significant decrease as more sample added to the subphase surface after the monolayer had achieved a maximum surface pressure. A reversibility of \sim 80% (range = 75.6-83.1%) at from the first instance where maximum surface pressure was attained decreased to a value of \sim 65% (range = 62.3-70.1%) at the maximum loading of 1000 μ l.

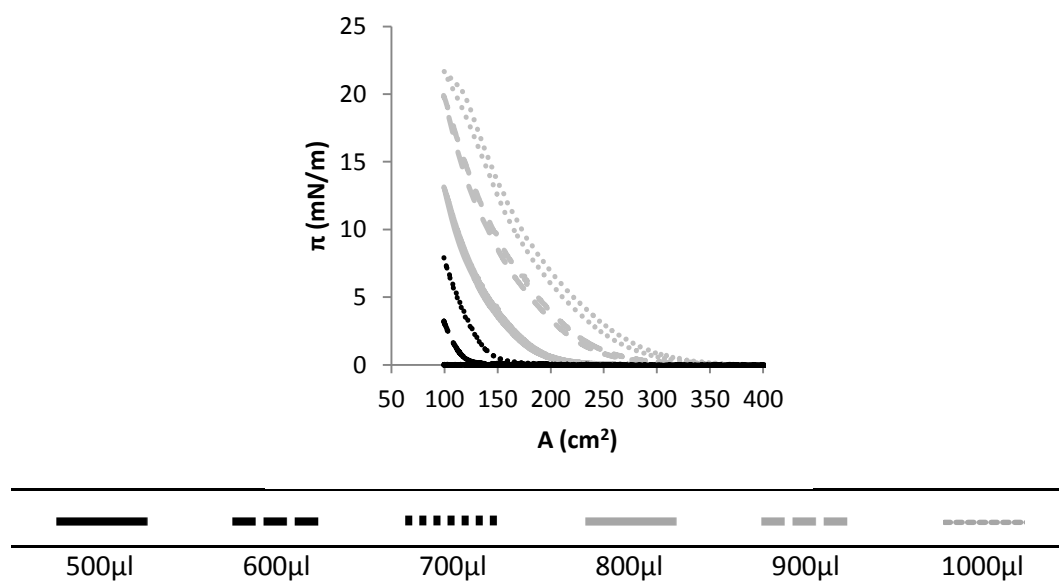


Fig 5.10. π -A isotherms of control FN+D contact lens extracted in $\text{C}_6\text{H}_{14}:\text{CH}_3\text{OH}$ (9:1 w/w). π -A isotherms for 100-400 μ l aliquots not shown.

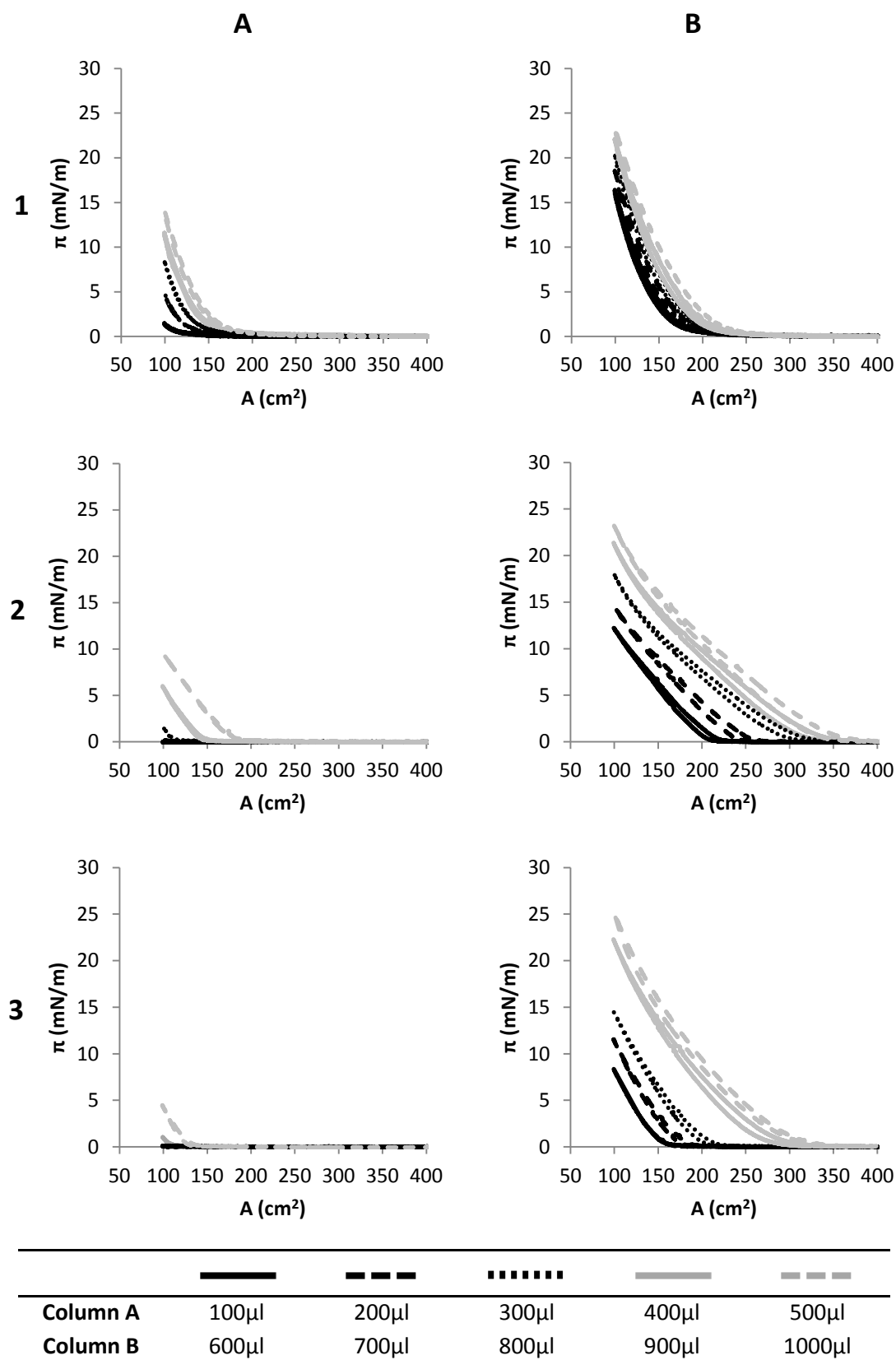


Fig 5.11. π -A isotherms of FN+D contact lens worn under a CW modality extracted in C_6H_{14} : CH_3OH (9:1 w/w): Row 1 - Px11; Row 2 - Px12; Row 3 - Px26.

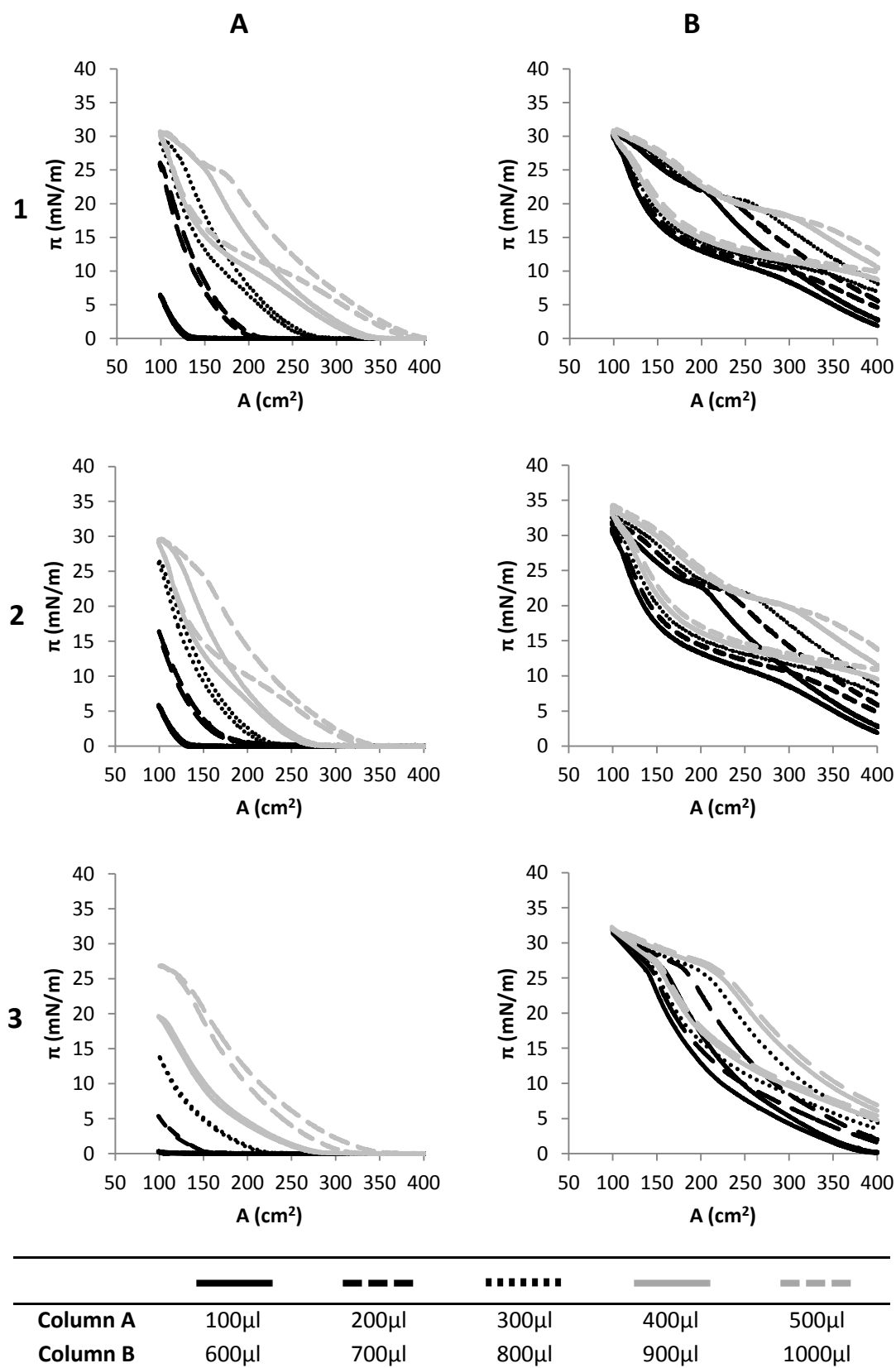


Fig 5.12. π -A isotherms of FN+D contact lens worn under a DW modality extracted in $C_6H_{14}:CH_3OH$ (9:1 w/w): Row 1 - Px5; Row 2 - Px22; Row 3 - Px25.

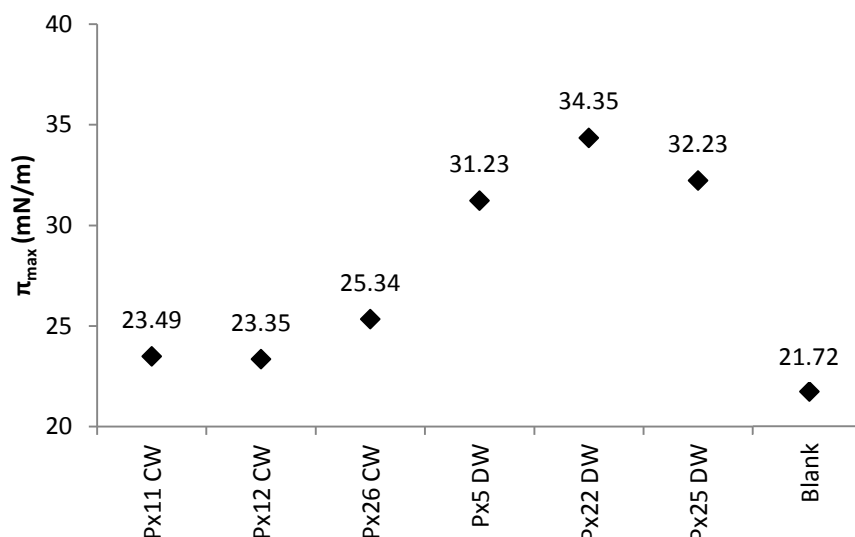


Fig 5.13. Comparison of π_{\max} as a function of wear modality of samples obtained from worn and unworn FN+D Contact lenses extracted in $\text{C}_6\text{H}_{14}:\text{CH}_3\text{OH}$ (9:1 w/w).

5.3.2 PureVision Contact Lenses

5.3.2.1 Chloroform : Methanol (1:1 w/w) Extraction

The π -A isothermal data of subject and control samples obtained from worn and unworn PureVision (PV) contact lenses extracted in $\text{CHCl}_3:\text{CH}_3\text{OH}$ (1:1 w/w) can be found in Fig 5.14-5.17 and Appendix 4. The extraction of a control PV contact lens (Fig 5.14) produced a maximum surface pressure (π_{\max}) of $\sim 23.5\text{mN/m}$ attained at the $600\mu\text{l}$ aliquot. Surface pressure does not increase significantly for each additional $100\mu\text{l}$ aliquot (π_{\max} range = 22.9 - 23.7mN/m). Higher maximum surface pressures were recorded for the extractions of worn contact lenses under both CW and DW wear modalities. These maximum values were obtained around the same volume aliquot range as the control (within the 600 - $1000\mu\text{l}$ region). The extraction of CW PV lenses (Fig 5.15) produced π_{\max} of 30 - 33mN/m : Px29 produced a π_{\max} of $\sim 32.5\text{mN/m}$ attained at the $700\mu\text{l}$ aliquot, Px41 produced a π_{\max} of $\sim 30.5\text{mN/m}$ attained at the $800\mu\text{l}$ aliquot and Px56 produced a π_{\max} of $\sim 32.5\text{mN/m}$ attained at the $800\mu\text{l}$ aliquot. The extraction of DW PV lenses (Fig 5.16) produced π_{\max} in the region of 36 - 38mN/m : Px17 and Px61 produced a π_{\max} of $\sim 37.0\text{mN/m}$, and subject Px53 produced a π_{\max} of $\sim 36.5\text{mN/m}$.

The initial surface pressure (π_{init}) was 0.0mN/m up to a loading volume of $700\mu\text{l}$ for the control samples and the transition from gaseous (G) to a liquid expanded (LE) phase was observable. For the π -A isotherms recorded for the CW subject samples, initial surface pressure was

0.00mN/m for all isotherms up to 400 μ l for Px29, 800 μ l for Px41 and 500 μ l for Px56. π_{init} was >0.0mN/m for the subsequent 100 μ l aliquot additions. Similarly, the DW subject samples also recorded a π_{init} above 0.00mN/m at the 500 μ l aliquot for Px17 and Px61 subject samples and the 600 μ l aliquot for Px53 sample. The observable G-LE transition in isotherms where π_{init} = \sim 0.0mN/m occurred over a slow transition indicated by a gradual change in the rate of surface pressure increase noticeable between 0-10mN/m. There was no discernible difference in the area region where this transition occurs between the control and tear samples.

A key feature observed in the π -A isotherms of the control sample and both CW and DW subject samples were changes in the behaviour of the film within the LE phase, even at relatively low loading volume aliquots. The stability of the monolayer is optimised through the movement of the different types of molecule, indicated by changes in the rate of surface pressure increase as the surface area is compressed. Film stability is retained throughout the course of compression due to this optimised packing behaviour. The hysteresis between compression and expansion cycles is relatively high, even at maximum loading volume, as a result of a uniformly expanding monolayer that spreads in a similar yet opposite manner to how it is compressed. Reversibility between compression and expansion cycles was \sim 98.0% for the control sample (range = 95.1-99.5%). For the subject samples, reversibility was \sim 98.5% for both CW (range = 97.9-99.1%) and DW (range = 98.0-99.5%) wear modalities.

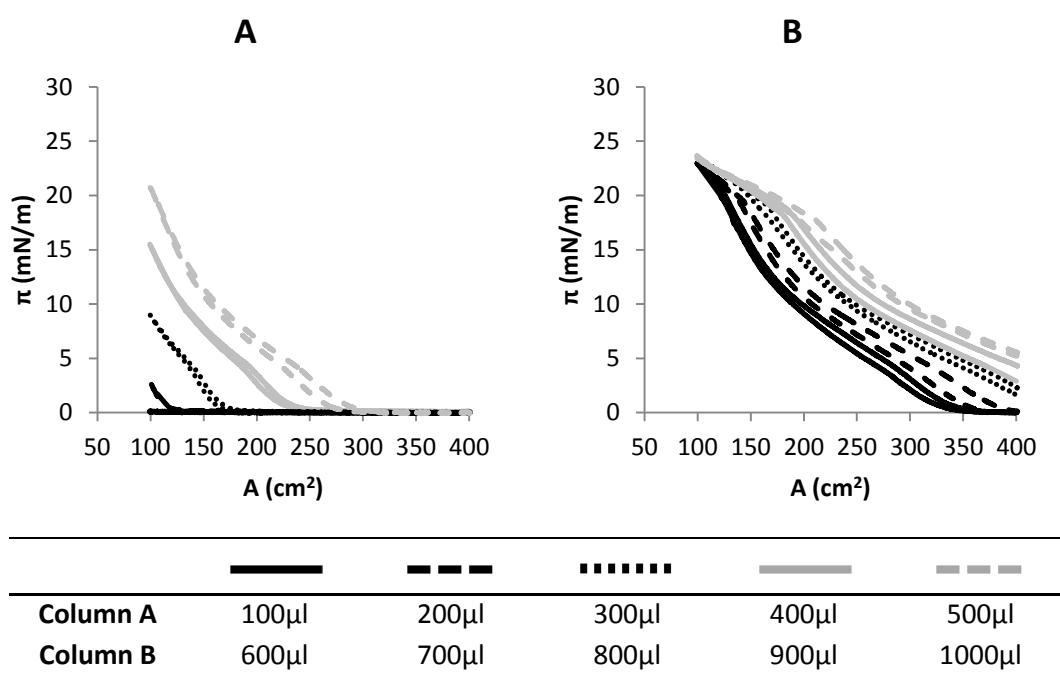


Fig 5.14. π -A isotherms of control PV contact lenses extracted in $\text{CHCl}_3\text{:CH}_3\text{OH}$ (1:1 w/w).

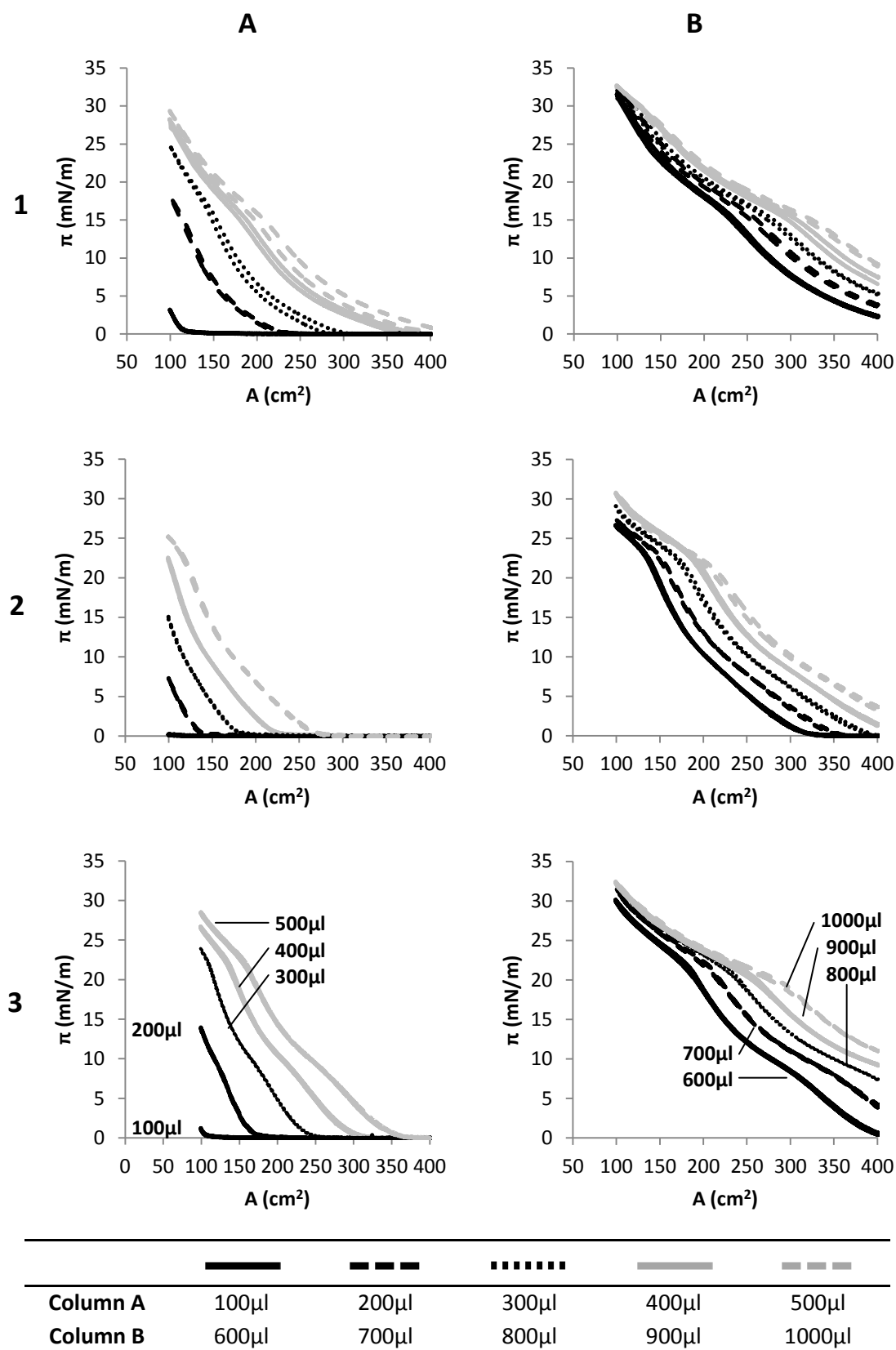


Fig 5.15. π -A isotherms of PV contact lens worn under a CW modality extracted in $\text{CHCl}_3:\text{CH}_3\text{OH}$ (1:1 w/w): Row 1 - Px29; Row 2 - Px41; Row 3 - Px56. (Annotations used for clarity)

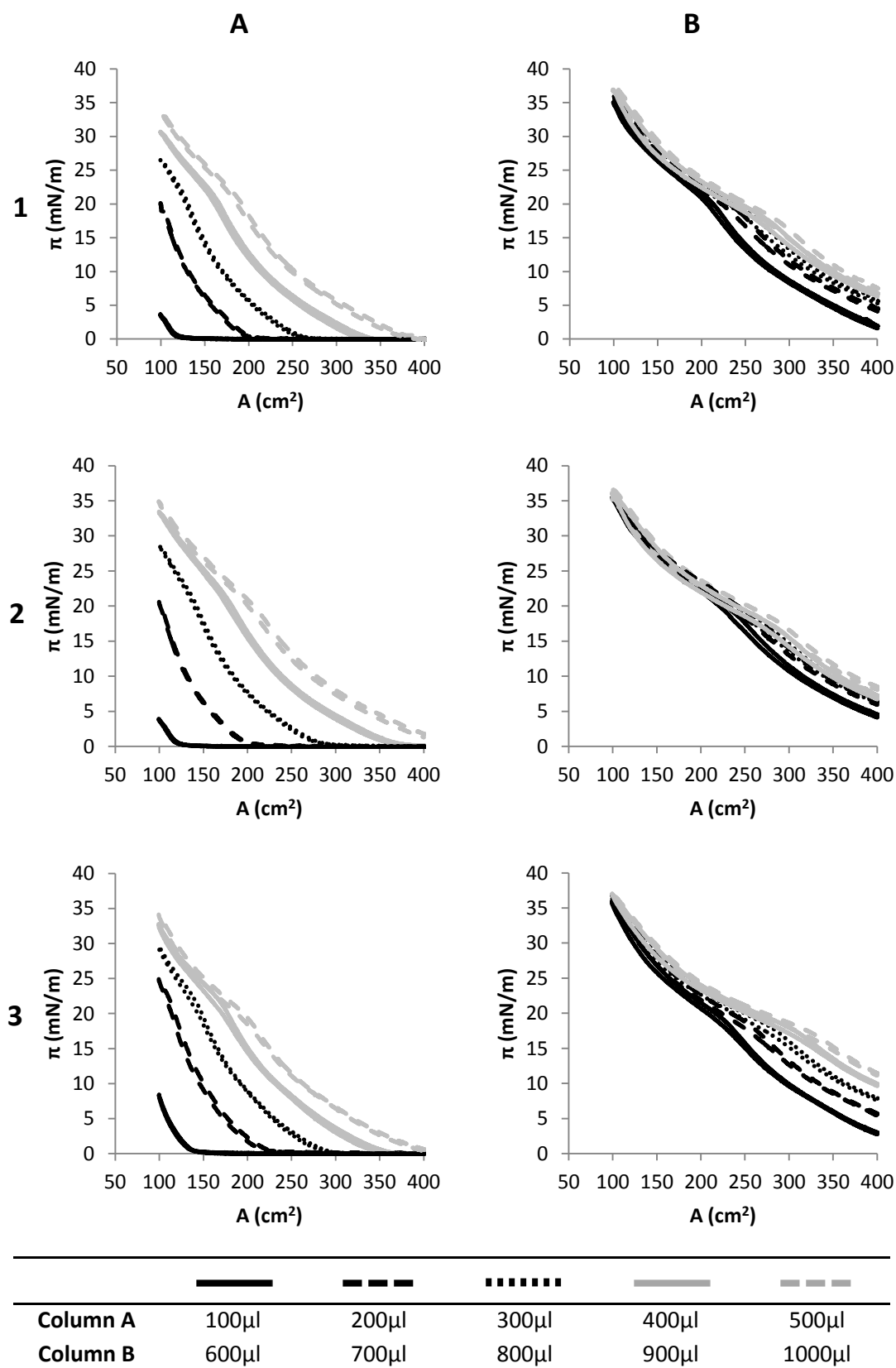


Fig 5.16. π -A isotherms of PV contact lens worn under a DW modality extracted in $\text{CHCl}_3:\text{CH}_3\text{OH}$ (1:1 w/w): Row 1 - Px17; Row 2 - Px53; Row 3 - Px61.

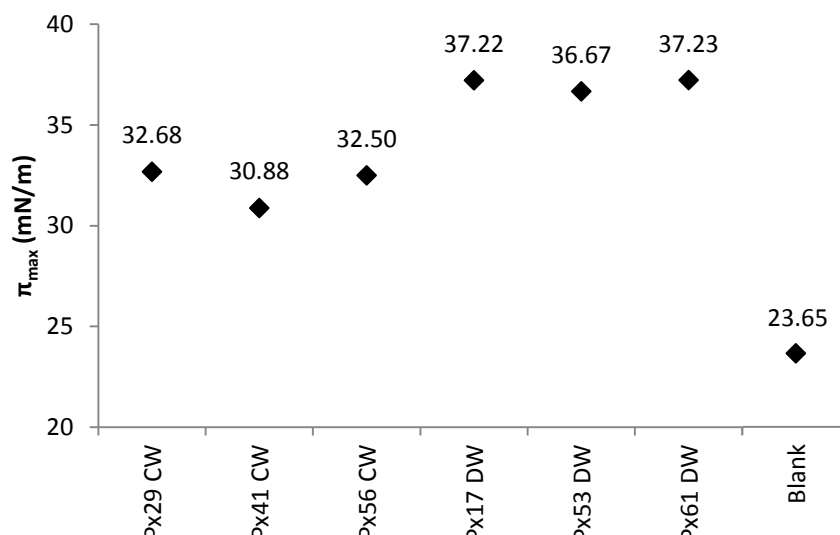


Fig 5.17. Comparison of π_{\max} as a function of wear modality of samples obtained from worn and unworn PV Contact lenses extracted in $\text{CHCl}_3:\text{CH}_3\text{OH}$ (1:1 w/w).

5.3.2.2 Hexane Extraction

The π -A isothermal data of subject and control samples obtained from worn and unworn PureVision (PV) contact lenses extracted in C_6H_{14} can be found in Fig 5.18-5.21 and Appendix 4. The extraction of a control PV contact lens (Fig 5.18) did not produce a sample maximum surface pressure, attaining a surface pressure (π_{\max}) of 17.4mN/m at the 1000 μl aliquot. Surface pressure would potentially increase significantly for additional 100 μl aliquots added to the surface. Maximum surface pressures were recorded for the extractions of worn contact lenses under both CW and DW wear modalities. The extraction of continuous wear (CW) PV lenses (Fig 5.19) produced maximum surface pressures in the region of 25-28mN/m. Subjects Px30 and Px56 produced a π_{\max} of $\sim 27.0\text{mN/m}$ attained between 800-1000 μl aliquot range. Subject Px41 did not attain a maximum surface pressure, with a π value of $\sim 25.2\text{mN/m}$ attained at the 1000 μl aliquot. The extraction of daily wear (DW) PV lenses (Fig 5.20) produced similar maximum surface pressures in the region of 24-26mN/m: Subject Px24 produced a π_{\max} of $\sim 24.5\text{mN/m}$, subject Px52 produced a π_{\max} of $\sim 25.5\text{mN/m}$ and subject Px53 produced a π_{\max} of $\sim 25.0\text{mN/m}$.

π_{init} was 0.0mN/m up to the maximum loading volume of 1000 μl for the control samples and the transition from gaseous (G) to a liquid expanded (LE) phase was observable. For the π -A isotherms recorded for the CW subject samples, initial surface pressure was 0.0mN/m for all isotherms up to 600 μl for Px30, 1000 μl for Px31 and 700 μl for Px56. π_{init} was $>0.0\text{mN/m}$ for

the subsequent 100 μ l aliquot additions. Similarly, the DW subject samples also recorded a π_{init} above 0.0mN/m at the 800 μ l aliquot for Px24 and the 900 μ l aliquot for Px53. The subject Px51 sample did not increase above 0.0mN/m for all aliquots up to the maximum loading (1000 μ l). The observable G-LE transitions in the control sample isotherms occurred at a definable A_t , indicating a clear definition between G and LE phases where the regions of extracted material begins interacting without increasing surface pressure until a critical point is attained where the monolayer transitions to a stable LE phase. The observable G-LE transition in the control sample isotherms occurs over a slow transition indicated by a gradual change in the rate of surface pressure increase noticeable between 0-10mN/m. There was no discernible difference in the area region where this transition occurs between the control and tear samples.

A key feature observed in the π -A isotherms of both CW and DW subject samples was changes in the behaviour of the film within the LE phase, even at relatively low loading volume aliquots (>300 μ l). The stability of the monolayer is optimised through the movement of the different types of molecule, indicated by changes in the rate of surface pressure increase as the surface area is compressed. Film stability is retained throughout the course of compression due to this optimised packing behaviour. Reversibility between compression and expansion cycles was \sim 97.0% for the control sample (range = 96.5-98.6%). For the subject samples, reversibility was \sim 96.5% for the CW samples (range = 95.6-97.9%) and \sim 97.0% for the DW samples (range = 95.9-98.2%) wear modalities.

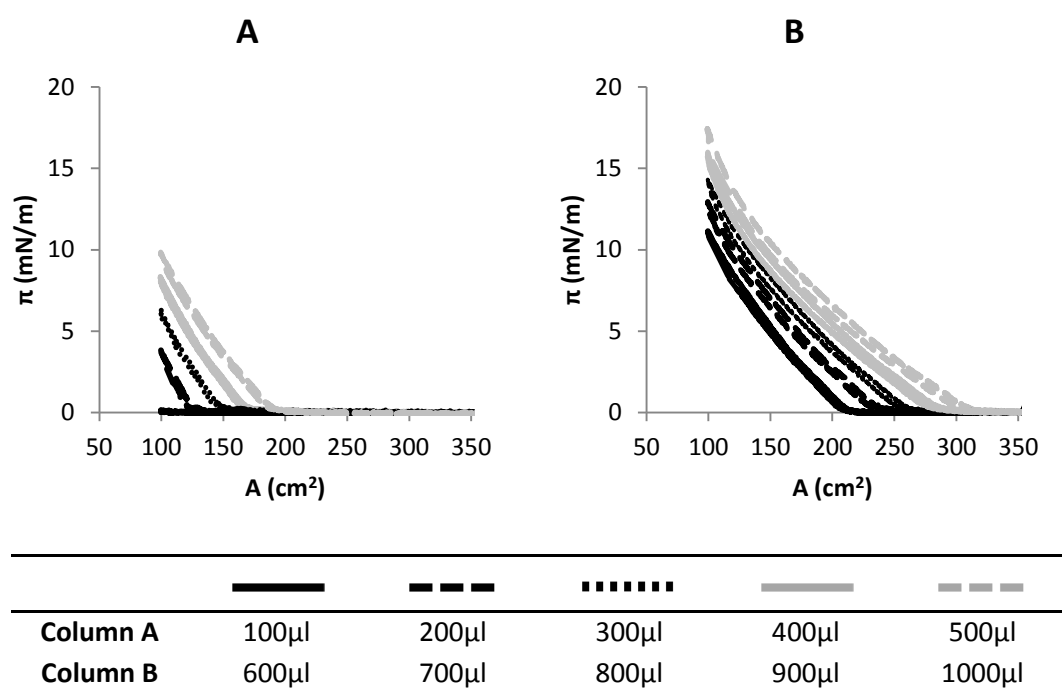


Fig 5.18. π -A isotherms of control PV contact lenses extracted in C_6H_{14} .

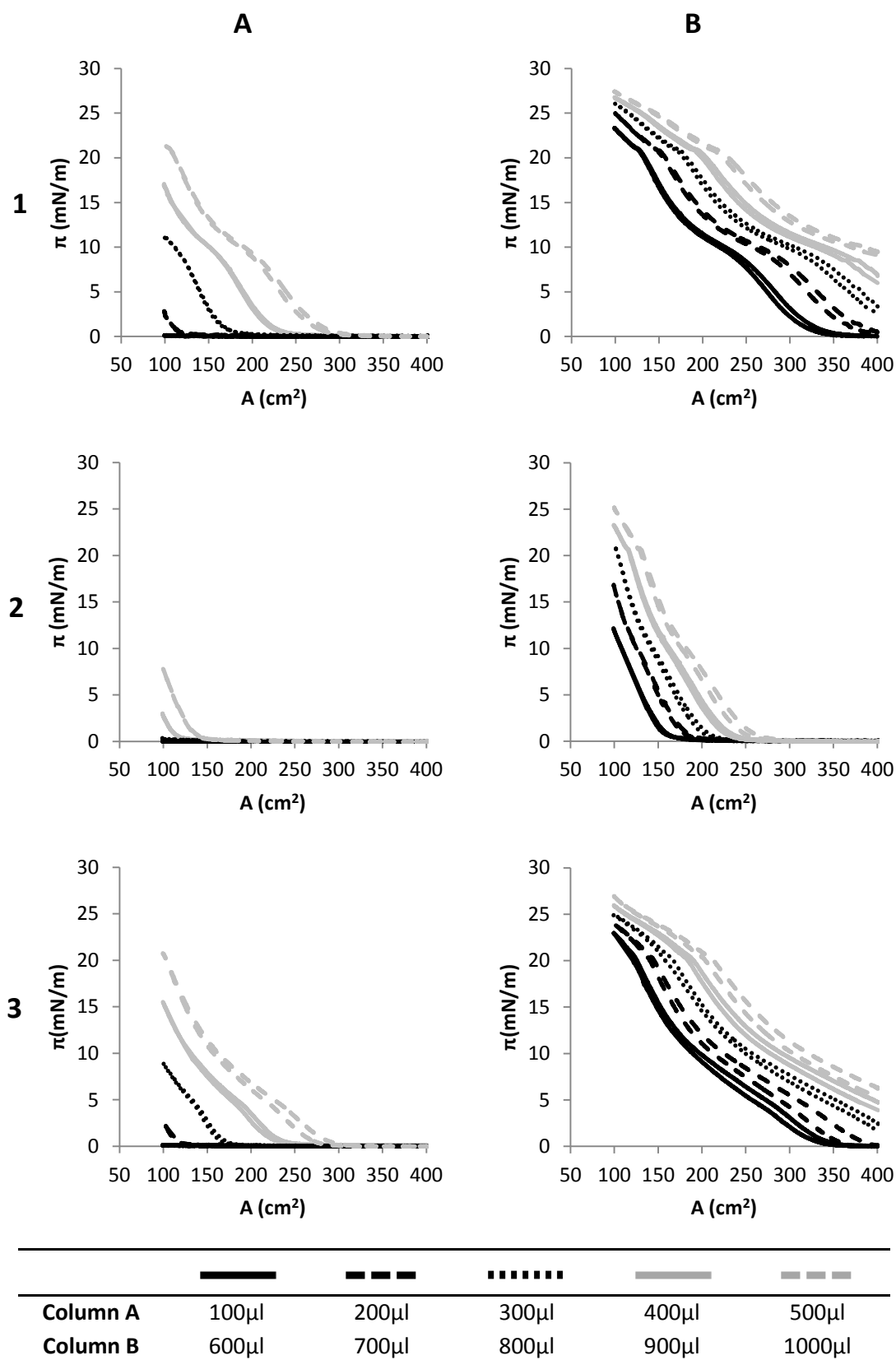


Fig 5.19. π -A isotherms of PV contact lens worn under a CW modality extracted in C_6H_{14} : Row 1 - Px30; Row 2 - Px31; Row 3 - Px56.

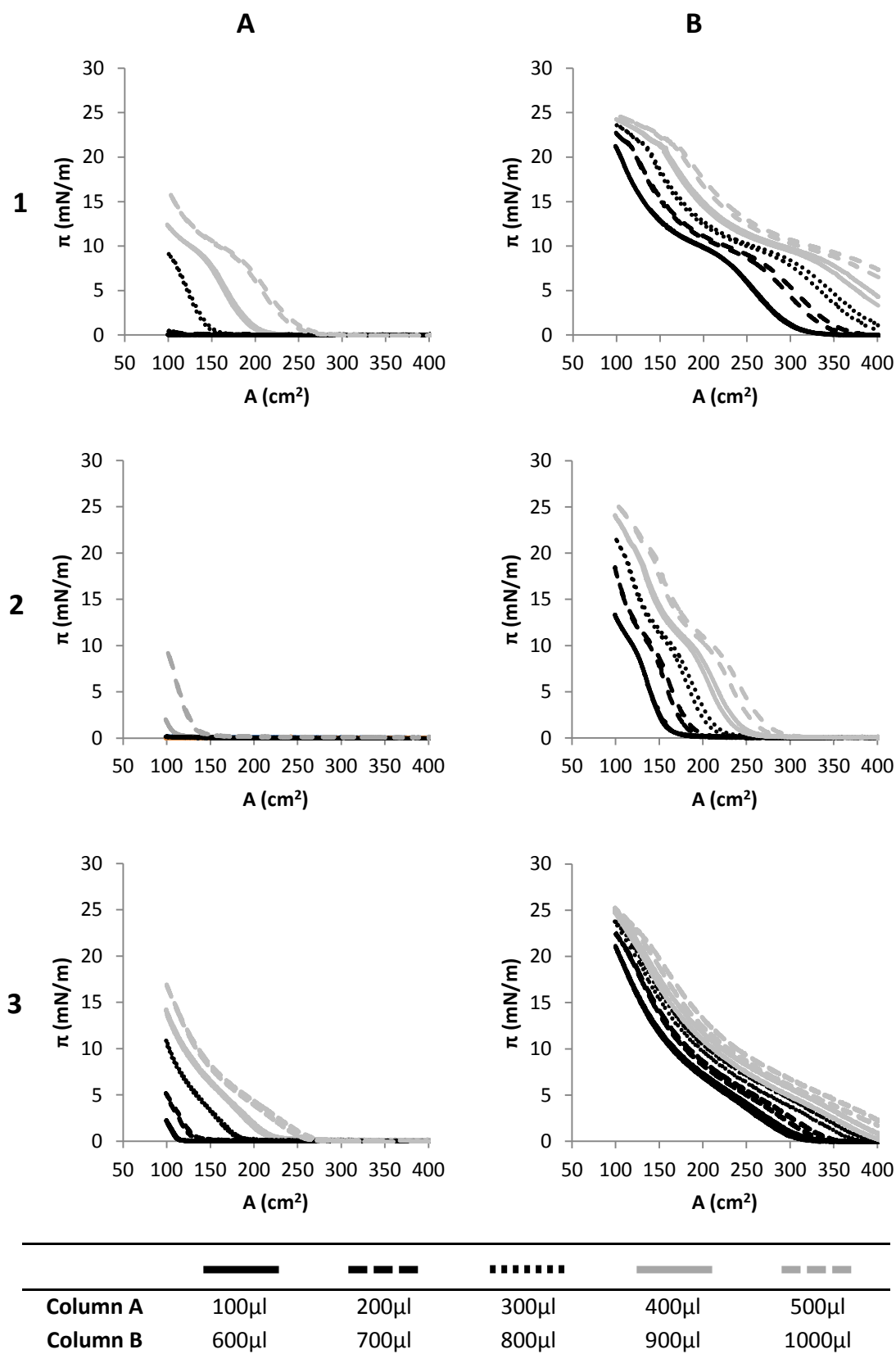


Fig 5.20. π -A isotherms of PV contact lens worn under a DW modality extracted in C_6H_{14} : Row 1 - Px24; Row 2 - Px51; Row 3 - Px53.

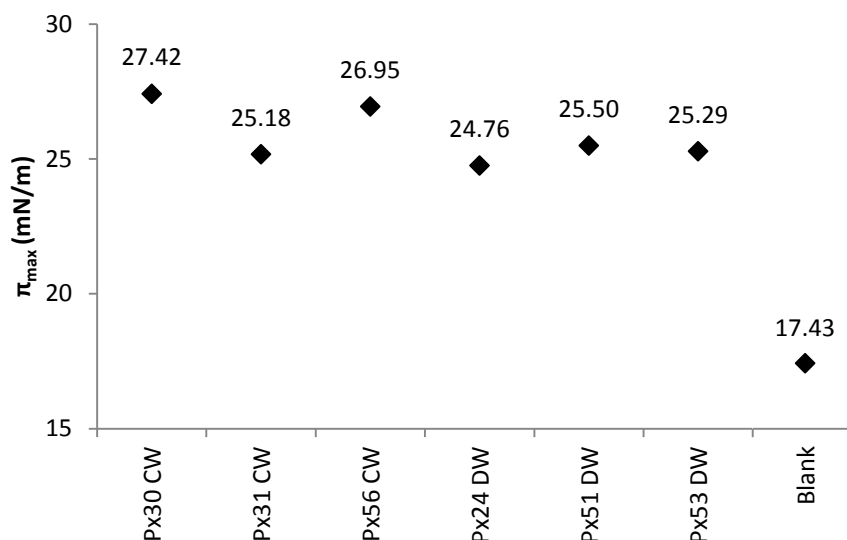


Fig 5.21. Comparison of π_{\max} as a function of wear modality of samples obtained from worn and unworn PV Contact lenses extracted in C_6H_{14} .

5.3.2.3 Hexane : Methanol (9:1 w/w) Extraction

The π -A isothermal data of worn and unworn PV contact lenses extracted with $C_6H_{14}:CH_3OH$ (9:1 w/w) can be found in Fig 5.22-5.25 and Appendix 4. The extraction of a control PV contact lens (Fig 5.22) produced a maximum surface pressure (π_{\max}) of ~ 25.0 - 25.5 mN/m attained at the 700 μ l aliquot. Surface pressure does not increase significantly for each additional 100 μ l aliquot (π_{\max} range = 24.7-25.6 mN/m). Higher π_{\max} were recorded for the extractions of worn contact lenses under both CW and DW wear modalities. These maximum values were obtained around the same volume aliquot range as the control sample (within the 700-1000 μ l region). The extraction of CW PV lenses (Fig 5.23) produced π_{\max} values of 32-35 mN/m: Px41 produced a π_{\max} of ~ 34.0 - 35.0 mN/m, Px46 produced a π_{\max} of ~ 34.0 mN/m and Px56 produced a π_{\max} of ~ 32.5 mN/m. The extraction of DW PV lenses (Fig 5.24) produced slightly higher maximum surface pressures in the region of 35-37 mN/m: Px24 produced a π_{\max} of ~ 37.0 mN/m, Px50 produced a π_{\max} of ~ 36.0 mN/m and Px61 produced a π_{\max} of ~ 35.0 mN/m.

π_{init} was 0.0 mN/m up to a loading volume of 600 μ l for the control samples and the transition from gaseous (G) to a liquid expanded (LE) phase was observable. π_{init} increased above 0.0 mN/m for the 700 μ l aliquot and increased further for each 100 μ l aliquot interval. For the π -A isotherms recorded for the CW subject samples, initial surface pressure was 0.00 mN/m for isotherms up to 300 μ l for Px41, 200 μ l for Px46 and 400 μ l for Px49 and π_{init} was >0.00 mN/m for the subsequent isotherms, increasing for each 100 μ l aliquot addition. Similarly, the DW

subject samples also recorded a π_{init} above 0.0mN/m at the 400 μl aliquot for Px24 and Px61 subject samples and the 300 μl aliquot for Px50 sample. The observable G-LE transition in control sample and both CW and DW sample π -A isotherms where $\pi_{\text{init}} = \sim 0.0\text{mN/m}$ occurred at a definable surface area. The transition indicates a clear definition between G and LE phases where the regions of extracted material begins interacting without increasing surface pressure until a critical point is attained where the monolayer transitions to a stable LE phase.

For the control and subject samples, slight relaxation of the monolayer film is observed within the LE phase as it is compressed. This is indicative of active movement of molecules within the first region of the LE phase into a preferred packing configuration. At a certain surface concentration this becomes the optimised, second region of the LE phase that results in a slight decrease in the rate of surface pressure increase. Film stability is retained throughout the course of compression due to this optimised packing behaviour. As the monolayer is expanded, the spreading behaviour as a result of repulsions between neighbouring molecules closely follows the opposite behaviour that occurs during compression. Reversibility for the control sample is $\sim 96.0\%$ (range = 94.7-95.9%). The subject samples produced similar reversibility values of $\sim 96.5\%$ for the CW samples (range = 96.0-97.8%) and $\sim 96.0\%$ for the DW subject samples (range = 95.0-96.4%) wear modalities. Reversibility in the subject samples then increases to a value of $\sim 98\%$ at very high loadings where the second region is the only one apparent on the π -A isotherm.

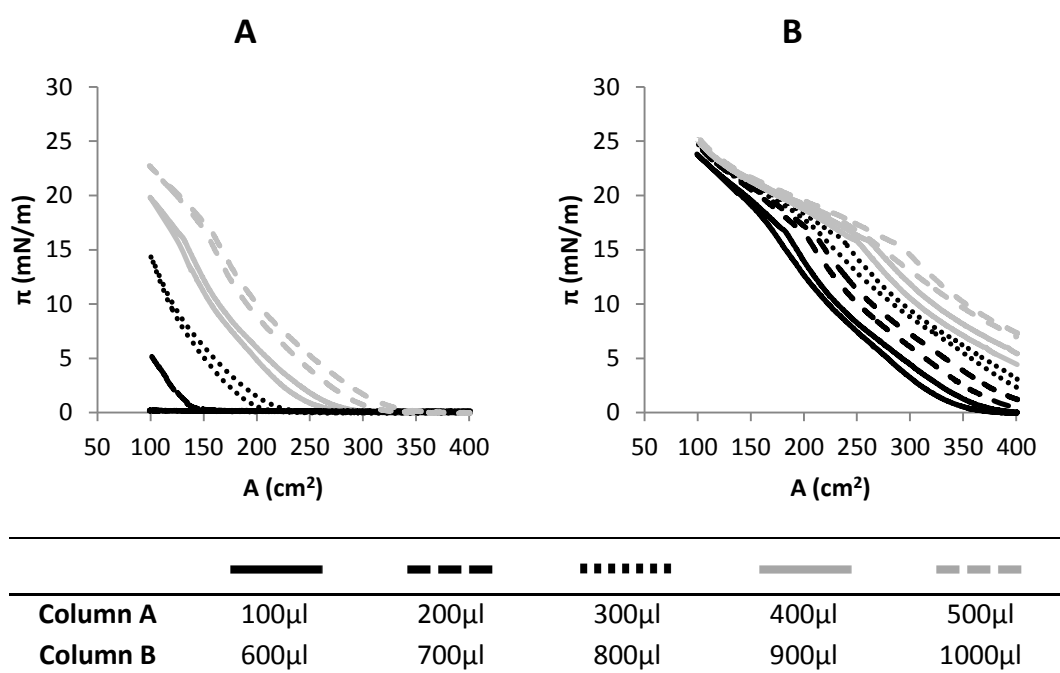


Fig 5.22. π -A isotherms of control PV contact lenses extracted in $\text{C}_6\text{H}_{14}:\text{CH}_3\text{OH}$ (9:1 w/w).

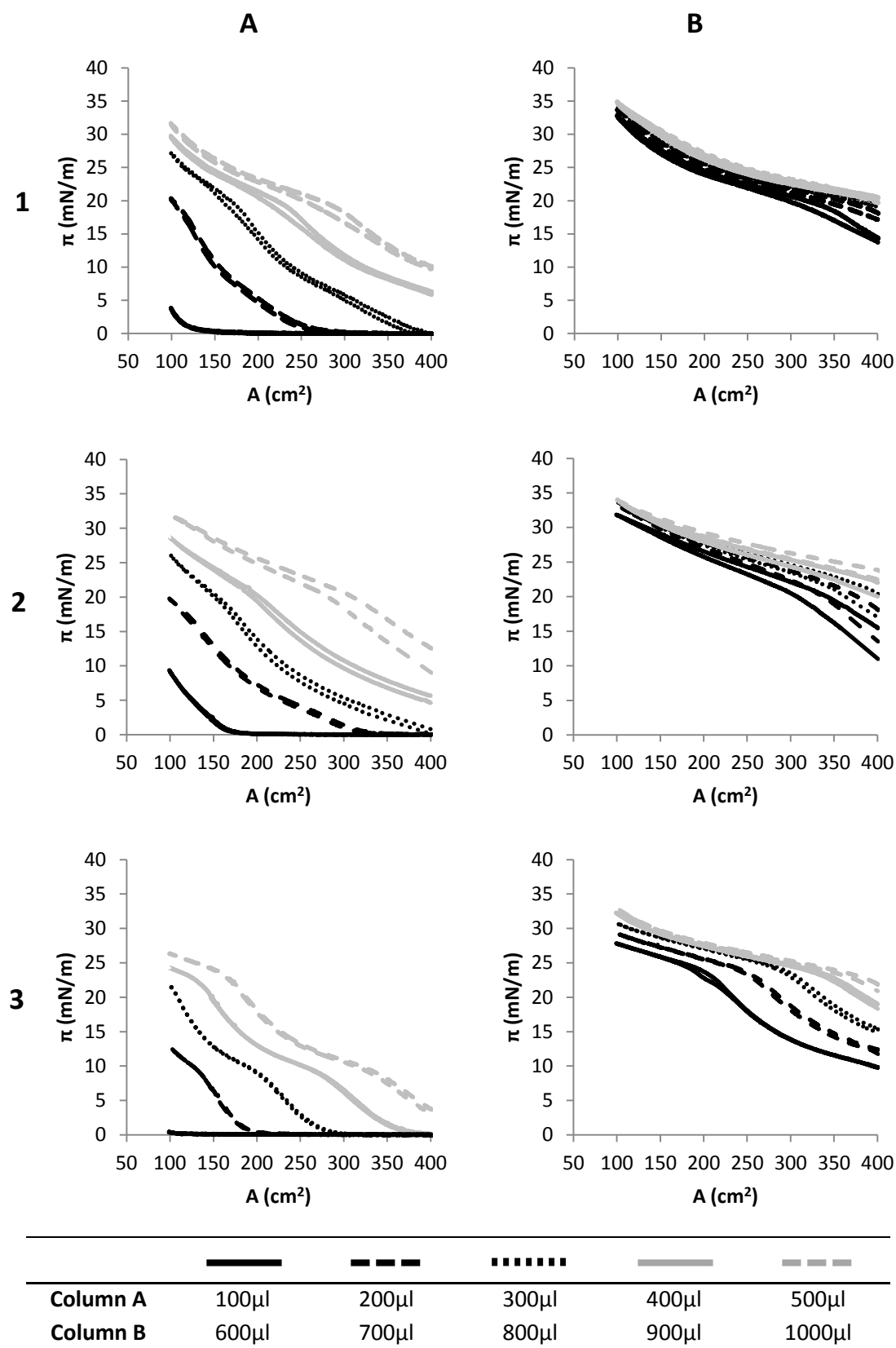


Fig 5.23. π -A isotherms of PV contact lens worn under a CW modality extracted in $C_6H_{14}:CH_3OH$ (9:1 w/w) solvent: Row 1 - Px41; Row 2 - Px46; Row 3 - Px49.

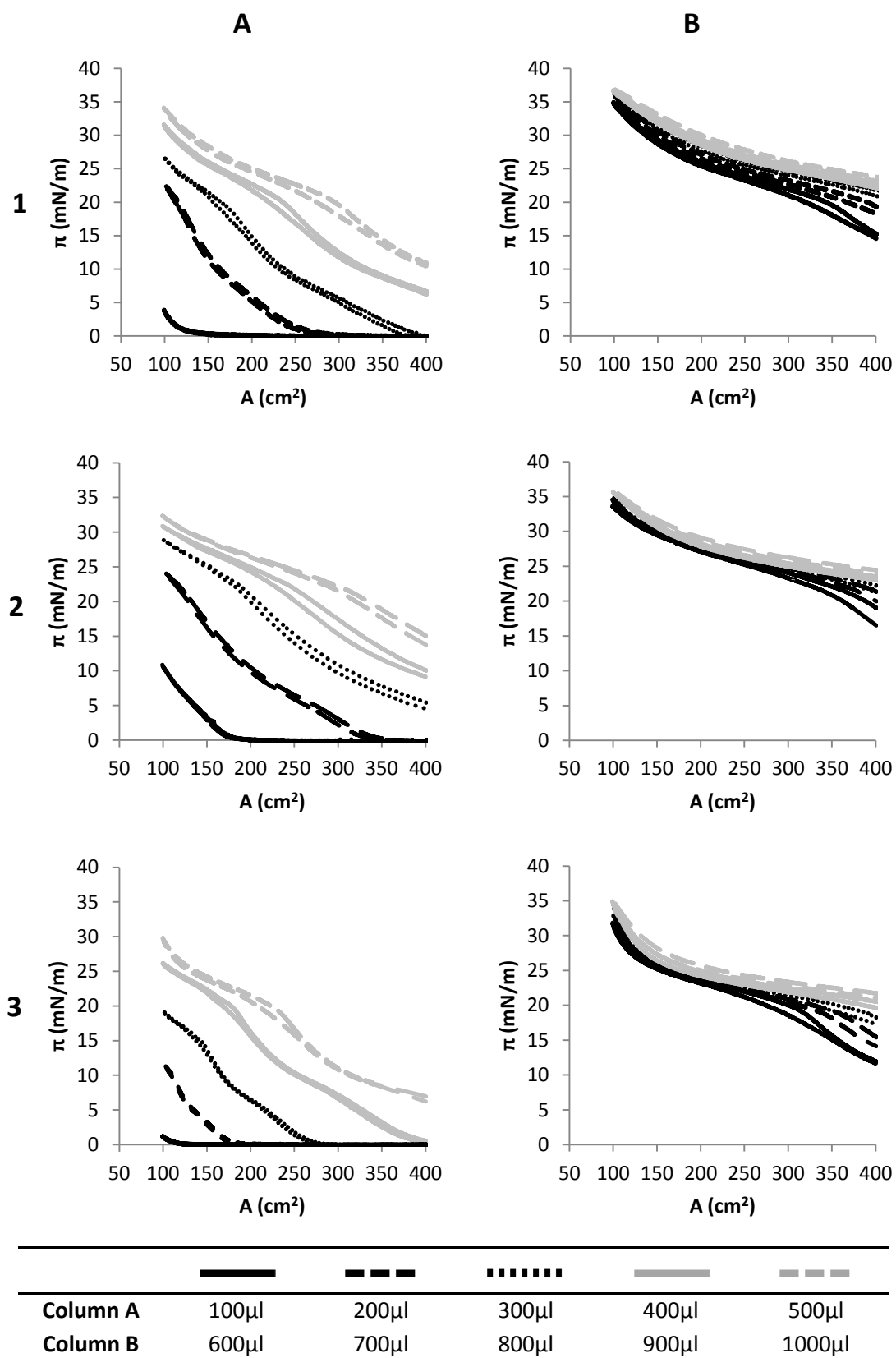


Fig 5.24. π -A isotherms of PV contact lens worn under a DW modality extracted in $C_6H_{14}:CH_3OH$ (9:1 w/w) solvent: Row 1 - Px24; Row 2 - Px50; Row 3 - Px61.

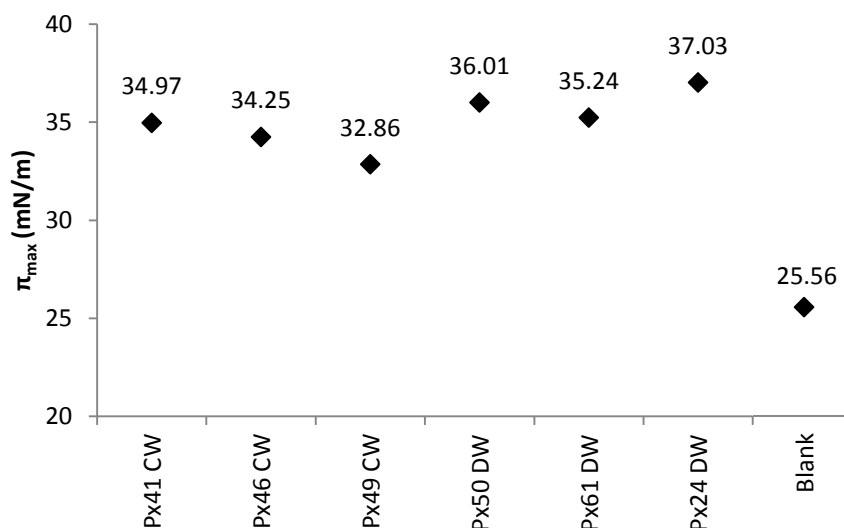


Fig 5.25. Comparison of π_{\max} as a function of wear modality of samples obtained from worn and unworn PV Contact lenses extracted in $\text{C}_6\text{H}_{14}:\text{CH}_3\text{OH}$ (9:1 w/w).

5.4 Discussion

Spoilage of contact lenses by either proteins or lipids is an important factor in the biocompatibility of contact lens materials. Such fouling may produce unfavourable effects on the function of the contact lens as well as the wearer's experience. Some of these effects may include tear film disruption, decreased vision, discomfort, intolerance, and bacterial adhesion [194]. From the π -A isotherms obtained within this study, it is apparent that the amount of tear lipid material extracted from contact lenses is dependent upon a range of variables: the individual subject tear chemistry, the material of the contact lens, the schedule of contact lens wear and the extraction methodology. Inter-subject variability was observed in the differences within the π -A isotherms of extracted subject samples obtained from the same lens type and wear schedule and the extraction procedure used to obtain the sample. The unique nature of a subjects tear film lipid profile will affect the amount and types of lipid that are deposited during contact lens wear and subsequently what will be extracted.

Differences were observed in the π -A isotherms between similar extractions of the PureVision (PV) and Focus Night+Day (FN+D) contact lenses, specifically the maximum surface pressure (π_{\max}) and initial surface pressure (π_{init}) values. PV lenses seemed to retain a larger amount of lipid material compared to FN+D lenses that, when extracted, overall produced slightly larger maximum surface pressures (Fig 5.26) that were obtained at lower loading concentrations (~ 300 - $600\mu\text{l}$ aliquots for PV compared to ~ 800 - $1000\mu\text{l}$ for FN+D). The surface pressures

attained at comparative 100 μ l aliquot intervals were higher in PV lens extractions compared to FN+D for both wear modalities and the three extraction methodologies. Initial surface pressures (Fig 5.27) only increased above 0.0mN/m for the highest loading concentrations of worn FN+D lenses under a DW modality and extracted in the hexane:methanol (9:1 w/w) solvent mixture. π_{init} increased to above 0.0mN/m commonly in the majority of PV lens extractions at lower concentrations that was independent of wear modality or the extraction solvent utilised.

The interaction between tear lipids and the contact lens begins almost immediately when the lens is placed within the tear film. Deposition of lipid molecules is a function of the characteristics of the contact lens material, specifically those within the bulk polymer matrix and at the lens surface [263]. Lipids preferentially deposit onto hydrophobic surfaces because of hydrophobic-to-hydrophobic interactions [264]. The monomers utilised to form the bulk polymer matrix affects the overall and type-specific adsorption of lipids. Certain lipid types have a greater affinity to different monomers [194] [265] [266]. Levels of lipid deposition have been observed to increase on silicone-containing contact lenses due to the greater hydrophobicity of the silicone functional groups added into the polymer matrix to increase oxygen permeability [267]. Incorporation of the N-vinylpyrrolidone (NVP) monomer has also been shown to increase lipid deposition [195]. NVP was originally added to increase the water content of the lens but it had the side effect of increasing the hydrophobic characteristics of the hydrogel material and increased the amount of lipid deposition.

Surface modification techniques are often necessarily employed to improve the biocompatibility of silicone hydrogel contact lenses within the tear film although these lenses remain relatively hydrophobic when compared to conventional hydrogel lenses [267]. FN+D lens surfaces are modified in a gas plasma reactive chamber that creates a 25nm thick hydrophilic surface [268]. PV lenses are also modified within a gas plasma reactive chamber but under a different method that transforms silicone components on the lens surface into hydrophilic silicate compounds [267]. Despite similar methods of surface modification, there are differences observed in hydrophobicity between lens types. PV lenses exhibit a higher contact angle and therefore less wettable than FN+D [269] [270] [271]. The key difference in the surface characteristics is that the plasma coating on FN+D lenses forms a homogenous layer of hydrophilicity, whereas the surface treatment of PV lenses produces a heterogeneous surface where more hydrophobic sites are exposed [267] [268].

The increased incidence of hydrophobic sites coupled with the presence of silicone and NVP monomers within the polymer matrix means that PV lenses are more susceptible to lipid deposition [195] [264] [267] [268]. This has been observed in experimental measurements of the amount of lipid deposited on PV and FN+D lenses compared to conventional hydrogels and other silicone hydrogels. Carney et al [194] compared the deposition of cholesterol and phosphatidyl- ethanolamine (PE) on to a range of silicone hydrogel contact lenses (including PV and FN+D). Cholesterol was shown to absorb more to SiHy lenses than PE over the 20 day exposure period to standard solution (25.1-fold increase compared to a 3.7-fold increase) with PV lenses absorbing approximately twice as much cholesterol than FN+D (~20µg for PV; ~10µg for FN+D). Jones et al [267] recorded a ~50-60% increase in deposition of lipids on to PV lenses compared to FN+D lenses (oleic acid: ~600µg for PV, ~400µg for FN+D; oleic acid methyl ester: ~300µg for PV, ~200µg for FN+D; cholesterol: ~120µg for PV, ~40µg for FN+D). The two SiHy lenses absorbed a much larger amount of lipid to the conventional hydrogel contact lens etafilcon A (Acuvue) which deposited no more than ~20µg of the three lipid types studied. Zhao et al [272] observed that deposition of cholesterol was increased in PV lenses compared to other SiHy lenses, with a 4-8 fold increase compared to lotrafilcon B (O2 Optix). This report studied lotrafilcon B (O2 Optix) as opposed to lotrafilcon A (FN+D). Despite comprising similar monomer components, lotrafilcon B has a higher water content (33% for lotrafilcon B; 24% for lotrafilcon A). According to Carney et al [194], lotrafilcon B deposited less cholesterol than lotrafilcon A and would therefore still be comparable to PV lenses.

The effect of material on the type and amount of lipid deposited during wear and extracted for Langmuir trough-based surface behaviour study has been discussed, but extraction of polymeric components from the lens material must also be considered. Extractions of control lenses taken directly from the packaging blisters were observed to have significant surface pressure data. An increase in surface pressure was observed in both types of lenses and under all three extraction solvents. Hexane produced minimal increases in surface pressure for FN+D ($\pi_{\max} = 0.0\text{mN/m}$ at 1000µl aliquot) but PV lens extraction produced a significant increase ($\pi_{\max} = \sim 17.5\text{mN/m}$ at 1000µl aliquot). The methanol-containing extraction solvent produced maximum surface pressures >20mN/m at maximum loading volume, with PV lenses producing initial surface pressures that increased above 0.0mN/m. Due to monomer composition or hydrophilic surface treatment, the copolymers contained within PV and FN+D may exhibit amphiphilic behaviour that, when extracted, may significantly affect the π -A isotherm of an extracted worn sample.

The second key variable studied was the wear schedule: daily wear (DW) or continuous wear (CW). The introduction of a cleaning cycle at the end of a day's wear time produced difference in surface pressure data between DW and CW modalities. For the most part, DW lens extractions produced higher maximum surface pressures, attained at lower applied volume aliquots, and an increased incidence of initial surface pressure values $>0.0\text{mN/m}$ was also observed. The observed differences in π -A isotherm between CW and DW wear modalities has more to do with the characteristics of the lipid that adsorb to the surface of the lens. With lenses worn under a DW modality, most of the lipid bearing the most anchored is removed during cleaning regimens and the sample obtained can be considered a 'fresh' sample obtained for that final days wear. Small amounts of lipid that remains immobilised within the lens matrix that are not removed by multi-purpose cleaning solutions will also be extracted.

Conversely, lenses worn under CW modalities with no cleaning regimen utilised are saturated with lipids that are adsorbed during wear and remain embedded within the surface. These lipids are immobile and are more susceptible to various degradation reactions such as oxidation, enzymatic hydrolysis or oligomerisation [168] [190]. The formation of a stable biofilm over the lens is necessary to stabilise the pre-lens tear film and allow comfortable contact lens wear. Increased deposition of hydrophobic lipids that renders the surface unwettable and degradation of immobilised lipid molecules will alter the native function of the lipid and a different pre-lens environment is created that leads to a range of problematic issues such as end of day discomfort and lens intolerance [168] [191].

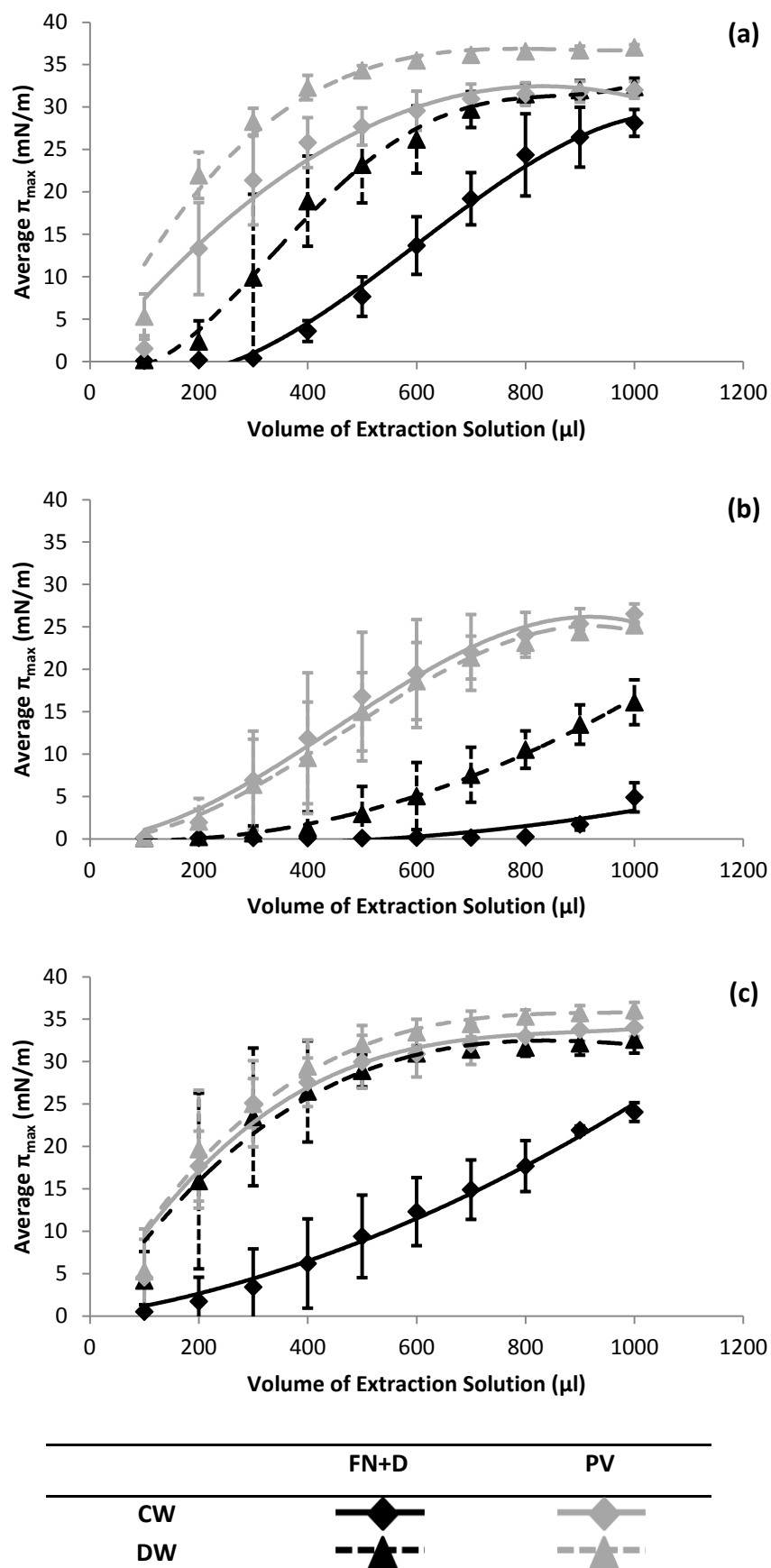


Fig 5.26. Comparison of the average maximum surface pressure at each 100 μl aliquot: (a) $\text{CHCl}_3:\text{CH}_3\text{OH}$ (1:1 w/w); (b) C_6H_{14} ; (c) $\text{C}_6\text{H}_{14}:\text{CH}_3\text{OH}$ (9:1 w/w)

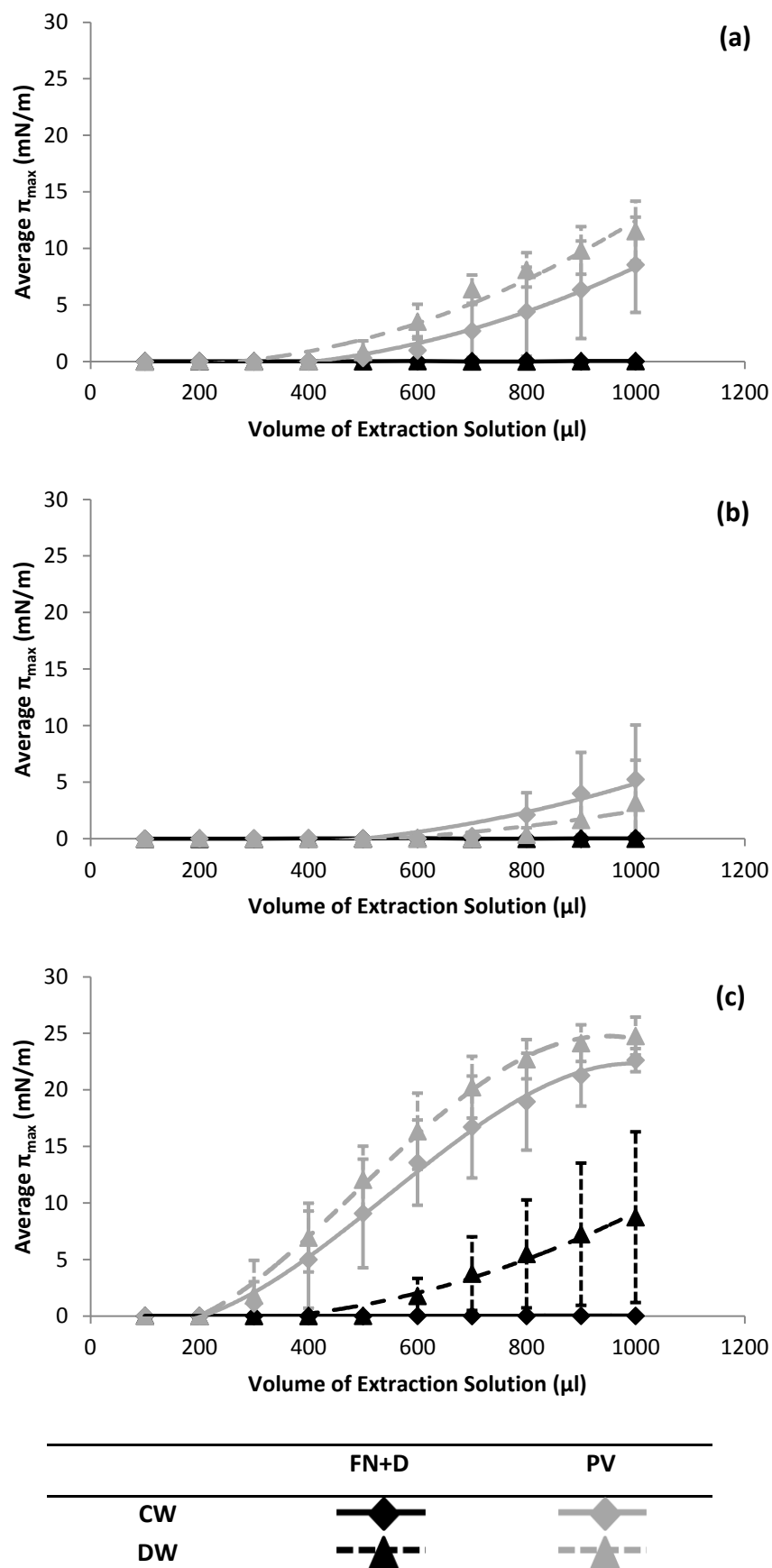


Fig 5.27. Comparison of the average initial surface pressure at each 100μl aliquot: (a) CHCl₃:CH₃OH (1:1 w/w); (b) C₆H₁₄; (c) C₆H₁₄:CH₃OH (9:1 w/w)

5.5 Summary

The following conclusions can be observed from the experimental data within this chapter.

- Individual variations between each subset of lens samples were observed. Despite the majority of samples attaining significantly similar maximum surface pressures, these were often obtained a varied volume aliquots and accompanied by significant differences in initial surface pressure or G-LE transition area;
- The effect of wear modality between daily wear (DW) and continuous wear (CW) has an effect on the surface pressure-area profiles of the samples. Generally, CW lens samples showed significantly lower maximum surface pressures obtained at larger surface concentrations:
 - As the CW modality lacks a cleaning regime, the observed differences may be indicative of changes within the lipid molecules immobilised at the lens surface that are not removed by normal tear drainage or cleaning;
 - In the DW modality, the majority of immobilised and degraded lipids are removed using multipurpose cleaning solutions and replenished with fresh lipids upon reinsertion of the lens;
- There are also significant differences observed between the samples obtained from the two lens materials. PureVision lenses extracted more material than the Focus Night&Day lenses, indicated by higher maximum surface pressures and larger G-LE transition areas or initial surface pressures for comparative volume aliquots. These differences were observed under both wear modalities;
- As with the preliminary studies of contact lens sample collection in Chapter 4, the extraction technique also plays a role in the amount of material collected and the π -A isotherm data.

Chapter 6

Effect of Daily Disposable Contact Lens Wear on the Tear Film Lipid Layer

Growing interest in daily rather than overnight wear SiHy contact lenses led to the development of daily disposable silicone hydrogel contact lenses [273]. Daily disposable lenses have significant advantages over extended wear lenses, combining the benefits of silicone hydrogel material characteristics and daily disposable wear modality. The high oxygen transmission and production of thinner and lighter materials improves comfort within the lens-wearing eye [274] [275] [276]. Improvements and simplifications to the manufacture processes of daily disposable SiHy lenses in recent years has made this mode of wear economically viable for both manufacturer and consumer. One such process simplification is the removal of a lens surface treatment, making these lenses are inherently more susceptible to lipid deposition as a result. Recently, a novel process of covering a SiHy core with a conventional hydrogel coating has been implemented in Focus Dailies Total-1 (CIBAVision) to improve biocompatibility. Streamlining of the time-consuming removal of extractable materials from the lens also has implications for residual levels of this material that are not removed by aqueous extraction.

6.1 Comparison of Daily Disposable Silicone Hydrogel Contact Lenses

6.1.1 Objective

The objective was to investigate the deposition of tear lipids on two daily disposable silicone hydrogel contact lenses by comparison of sample extraction using three different solvent extraction methods based upon existing experience. This was in order to examine the solvent extraction of lipids and the lipoidal extraction of lens material components. These factors are of clinical importance for the stability of the PLTF.

6.1.2 Experimental Design

Two silicone hydrogel (SiHy) contact lenses marketed for daily disposable wear were studied: Clariti 1day (Filcon II 3; Sauflon Pharmaceuticals, UK) and 1-Day Acuvue TruEye (TE; narafilecon A; Johnson and Johnson Vision Care, USA). TE was also tested in the narafilecon B form available in the USA. Appendix 3 contains information on the contact lens types used in this

study. Contact lens samples were obtained from a clinical trial conducted by the Vision Sciences department at Aston University. Details of the patient sample can be found in Fig 6.1. Worn contact lenses were collected at the end of a day's wear. Once removed from the eye, the contact lens was placed into a vial containing saline (Sauflon Pharmaceuticals Ltd, UK) to keep the lens hydrated, and stored at $\sim 4^{\circ}\text{C}$ prior to analysis. Unworn contact lenses were taken from their packaging without any further modification to the lens material.

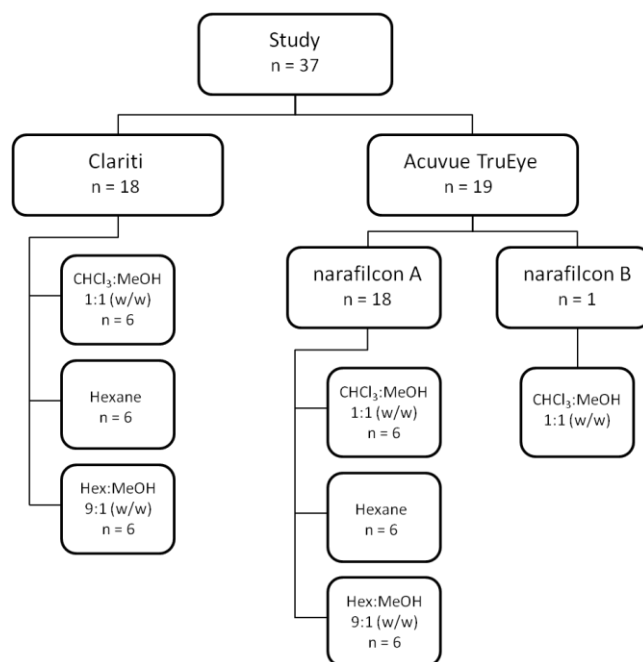


Fig 6.1. Subject sample size based on lens type and extraction protocol.

Subject and control samples were obtained by extraction of worn and unworn contact lenses respectively. Prior to extraction, lenses were removed from their storage solution - either saline (worn lenses) or packaging solution (unworn lenses) - and blotted on filter paper to remove excess liquid. Unworn contact lenses were also extracted in the three extraction solvents. Lenses were extracted for 1hr in 1.5ml of the following extracting solvents: C_6H_{14} , $\text{C}_6\text{H}_{14}:\text{CH}_3\text{OH}$ (9:1; w/w) or $\text{CHCl}_3:\text{CH}_3\text{OH}$ (1:1; w/w). Sample solutions were transferred to a clean glass vial by pipette to prevent contamination by lens material caused by swelling and breakdown of the contact lens. All samples were studied within 24hr of extraction.

The surface behaviour study of tear samples was conducted on Langmuir trough B (working surface area - $400\text{-}100\text{cm}^2$; barrier speed - $50\text{cm}^2/\text{min}$) according to the procedure described in section 2.1. HPLC-grade water was used as a subphase and kept at a constant temperature of $35.0^{\circ}\text{C} \pm 0.2^{\circ}\text{C}$. Sample solutions were applied to the subphase surface by a $50\mu\text{l}$ Hamilton

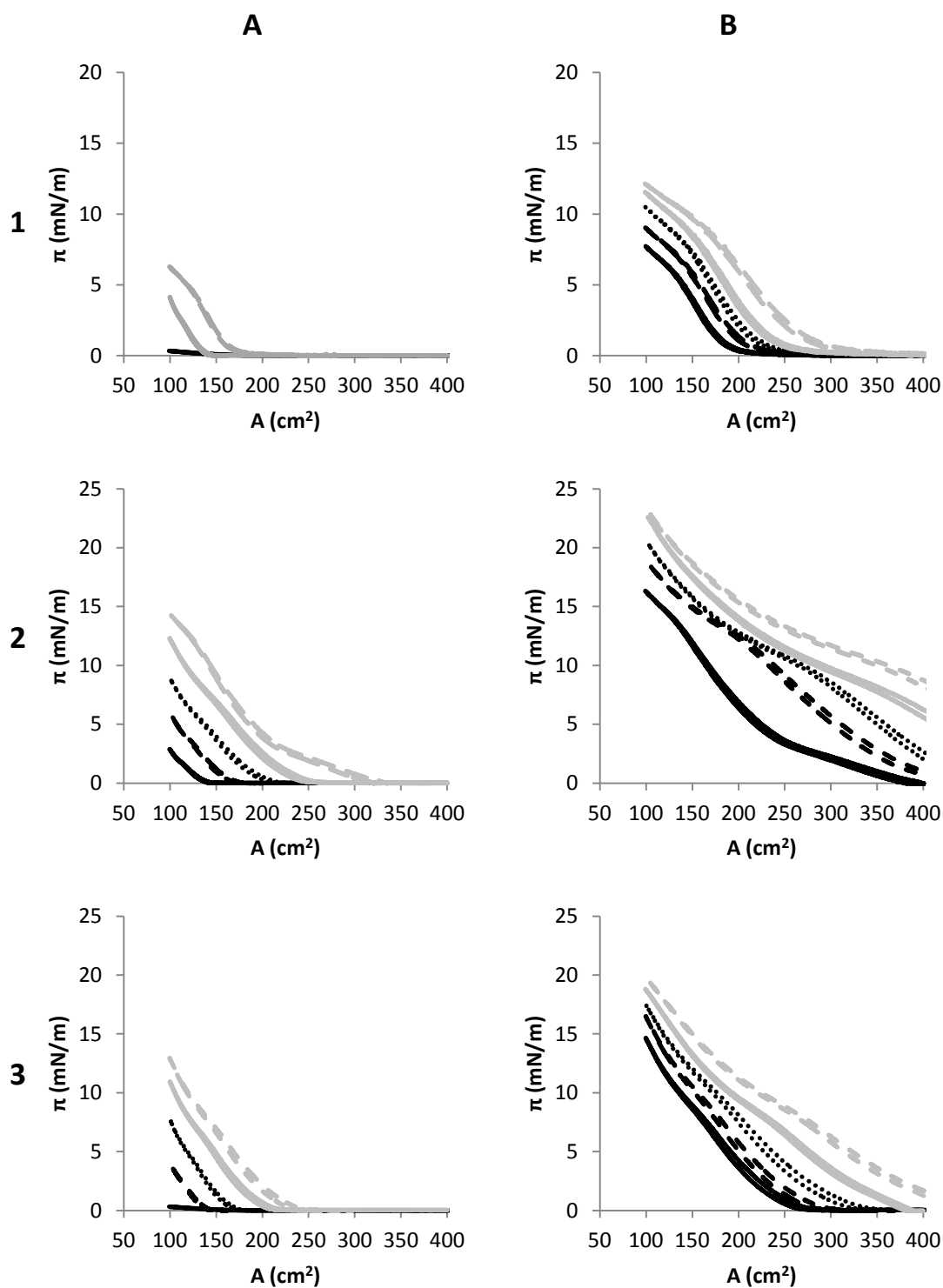
syringe. At least ten minutes was allowed to ensure full spreading of the solution, solvent evaporation and spontaneous movement and arrangement of components. Tear sample films were repeatedly compressed and expanded until the equilibrium surface pressure (π_{eq}) was reached. The choice of extraction solvent, patient variability and the volume of sample solution applied to subphase surface all have an effect on the resultant π -A isotherm data.

6.1.3 Results

6.1.3.1 Clariti 1day Contact Lenses

6.1.3.1.1 Control Lens Samples

The extraction of a control Clariti 1day lens in C_6H_{14} (Fig 6.2, Row 1) produced a π_{max} of 12.1mN/m at 1000 μ l aliquot volume. A speculative π -A isotherm with a further 100 μ l aliquot (1100 μ l) produced a negligible increase in surface pressure ($\pi_{max} = 12.2$ mN/m). The control sample recorded a π_{init} of 0.0mN/m up to the maximum loaded volume of 1000 μ l and the transition from gaseous (G) to a liquid expanded (LE) phase was observable. The phase transition occurred at relatively definable surface areas when compared to samples obtained via other extraction solvents. Reversibility was high (~98.0-99.0%) with only slight decreases in reversibility observed as loading volume was increased up to the maximum 1000 μ l volume. The control Clariti 1day lens extracted in C_6H_{14} :CH₃OH (9:1 w/w) (Fig 6.2, Row 2) produced a π_{max} of ~23.0mN/m (900 μ l, $\pi_{max} = 22.6$ mN/m; 1000 μ l, $\pi_{max} = 23.1$ mN/m). The control sample recorded a π_{init} of 0.0mN/m for 100 μ l interval aliquots up until the 600 μ l total volume with G-LE transition observed. From the 700 μ l aliquot, π_{init} increased above 0.0mN/m. Reversibility was ~98.0% at low loading volumes with insignificant decreases observed as surface concentration increased to the maximum 1000 μ l volume. The extraction of a control Clariti 1day lens in CHCl₃:CH₃OH (1:1; w/w) (Fig 6.2, Row 3) produced a π_{max} of ~19-20mN/m (900 μ l, $\pi_{max} = 18.8$ mN/m; 1000 μ l, $\pi_{max} = 19.8$ mN/m). The control sample recorded a π_{init} of 0.0mN/m for 100 μ l interval aliquots up until the 900 μ l total volume and the G-LE transition was observable. The phase transition did not occur at a definable area, taking place over a surface area range where monolayer arrangement occurs before attaining a stable LE phase. π_{init} increased to 1.7mN/m for the 1000 μ l aliquot. The reversibility between compression and expansion cycles for the control sample was high (~99.5%) with only slight decreases in reversibility observed as loading volume was increased up to the maximum 1000 μ l volume.



	—————	- - - - -	—————	- - - - -
Column A	100μl	200μl	300μl	400μl	500μl
Column B	600μl	700μl	800μl	900μl	1000μl

Fig 6.2. π -A isotherms of control Clariti 1day contact lens.
 Row 1 - C_6H_{14} ; Row 2 - $\text{C}_6\text{H}_{14}:\text{CH}_3\text{OH}$ (9:1 w/w); Row 3 - $\text{CHCl}_3:\text{CH}_3\text{OH}$ (1:1 w/w);

6.1.3.1.2 Worn Clariti 1day Lens Samples

6.1.3.1.2.1 Hexane Extraction

The π -A isothermal data of subject samples obtained from worn Clariti 1day contact lenses extracted in C_6H_{14} can be found in Fig 6.3 and Appendix 5. The worn samples produced π_{max} in the region of 22-27mN/m:

- Subject Px1 produced a π_{max} of ~22.1mN/m at 900-1000 μ l;
- Subject Px3 produced a π_{max} of ~26.0mN/m at 800-1000 μ l;
- Subject Px16 produced a π_{max} of ~22.5mN/m at 900-1000 μ l;
- Subject Px24 produced a π_{max} of 27.1mN/m at 1000 μ l aliquot ($\pi_{max} = 27.2$ mN/m recorded for a speculative isotherm with an additional 60 μ l).
- Subject Px28 produced a π_{max} of ~20.8mN/m at 900-1000 μ l;
- Subject Px36 produced a π_{max} of ~24.0mN/m at 800-1000 μ l.

Despite attaining lower maximum surface pressures than the $CHCl_3:CH_3OH$ (1:1 w/w) extracted samples, π_{init} increased above 0.0mN/m at lower sample solution volumes of sample solutions. Initial surface pressure increased above 0.0mN/m at loading volumes of 300 μ l and above for the subject samples Px1, Px16 and Px28 and at a volume of 100 μ l aliquot for Px3, Px24 and Px36 subject samples. For the isotherms that recorded an π_{init} of 0.0mN/m, the transition from gaseous (G) to a liquid expanded (LE) phase was observable. The phase transition at relatively definable surface areas when compared to samples obtained via other extraction solvents.

Similar patterns of variation were observed within the LE phase of the monolayers observed as surface pressure increased above 0.0mN/m indicative of a constant rearrangement of the monolayer when it initially enters the LE phase before the components obtain an optimum orientation where the rate of surface pressure increase over decreasing surface area becomes a linear relationship. This optimisation of molecular orientation within the monolayer produces a stable sample film. This is observed in the high reversibility between compression and expansion cycles for the control and all subject samples. Reversibility was high (~98.0-99.0%) with only slight decreases in reversibility observed as loading volume was increased up to the maximum 1000 μ l volume.

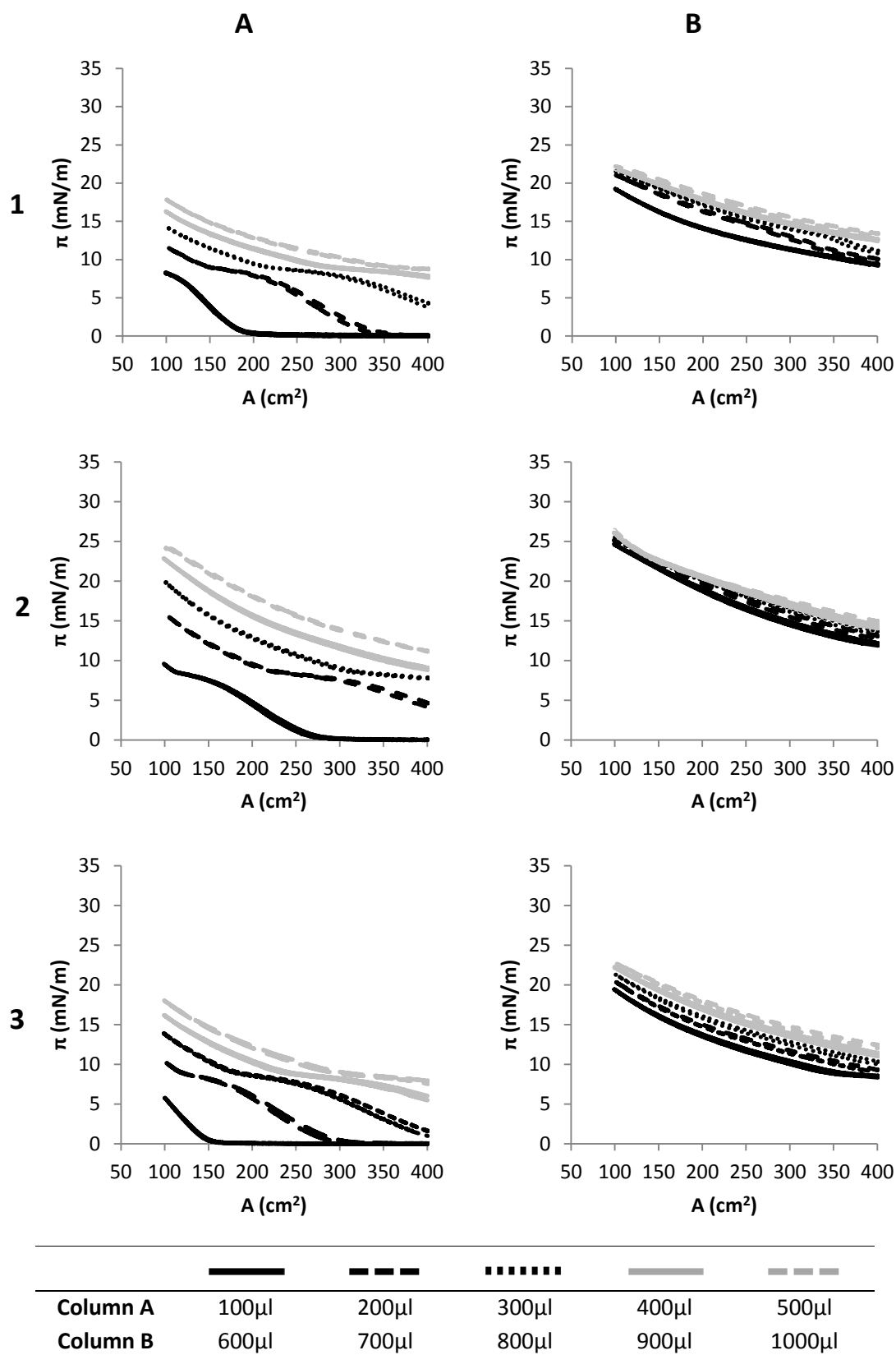


Fig 6.3a. π -A isotherms of worn Clariti 1day contact lens extracted in C_6H_{14}
 Row 1 - Px1; Row 2 - Px3; Row 3 - Px16.

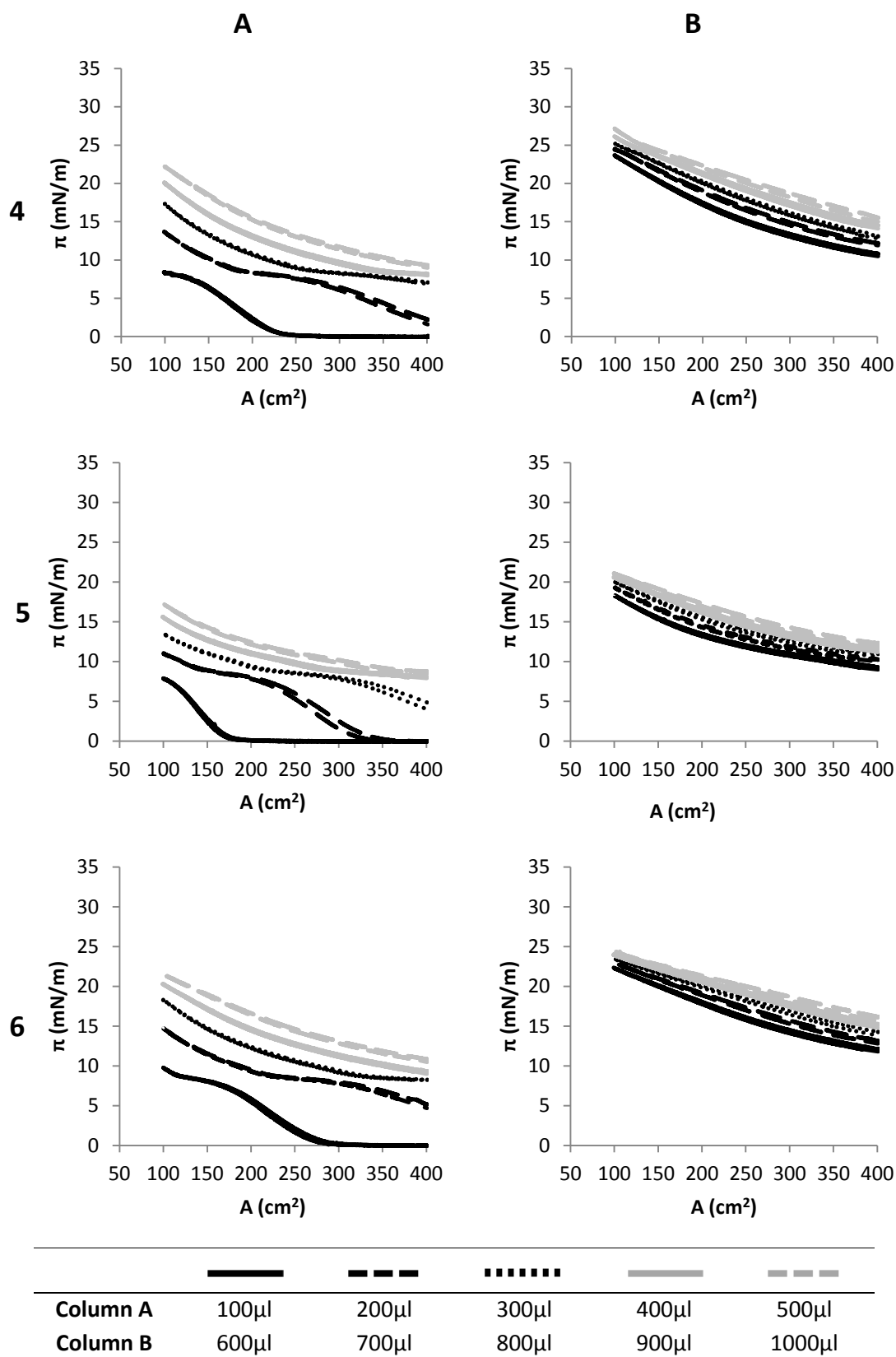


Fig 6.3b. π -A isotherms of worn Clariti 1day contact lens extracted in C_6H_{14} .
Row 4 - Px24; Row 5 - Px28; Row 6 - Px36.

6.1.3.1.2.2 Hexane : Methanol (9:1 w/w) Extraction

The π -A isothermal data of subject samples obtained from worn Clariti 1day contact lenses extracted in $C_6H_{14}:CH_3OH$ (9:1 w/w) can be found in Fig 6.4 and Appendix 5. The worn samples produced π_{max} in the region of 34-40mN/m:

- Subject Px3 produced a π_{max} of ~39.2mN/m at 900-1000 μ l;
- Subject Px16 produced a π_{max} of ~33.5mN/m at 900-1000 μ l;
- Subject Px36 produced a π_{max} of ~33.5mN/m at 700-1000 μ l;
- Subject Px19 produced a π_{max} of ~40.0mN/m at 900-1000 μ l;
- Subject Px23 produced a π_{max} of ~37.1mN/m at 900-1000 μ l;
- Subject Px40 produced a π_{max} of ~34.0mN/m at 700-1000 μ l.

Initial surface pressure (π_{init}) increased above 0.0mN/m at relatively low volume of sample solutions. π_{init} was >0.0mN/m for the 100 μ l aliquot for samples obtained from subjects Px3 and Px19. The monolayer formed at this volume is immediately concentrated enough to exist within the liquid expanded (LE) phase and as such the G-LE phase transition is not observable. Initial surface pressure was increased above 0.0mN/m at the 200 μ l aliquot for the other subject samples. A simultaneous increase in both maximum and initial surface pressures was observed before the π_{max} for the sample is attained. In the typical π -A obtained from lens extraction samples the surface pressure at minimum surface area will increase to a maximum value for the sample (π_{max}) with the surface area where the G-LE transition occurs increasing until π_{init} is greater than 0.0mN/m.

Reversibility was high (~98.0%) at higher loading volumes of control sample with only slight decrease observed from lower volumes, remaining so for Px3, Px16 and Px19 up to a volume of 1000 μ l. Px23 produced similar reversibility up to the 800 μ l aliquot, decreasing to 97.5% for the 900 μ l aliquot and 96.5% for the 1000 μ l aliquot. Px40 produced similar high hysteresis values up to the 700 μ l aliquot before a slight decrease was recorded for the 800 μ l (Rev = 97.5%), 900 μ l (Rev = 95.5%) and 1000 μ l (Rev = 94.0%) aliquots. Conversely, the sample obtained from Px36 produced significant decrease in reversibility from ~97.5% to ~88.0-93.0% between 500-1000 μ l.

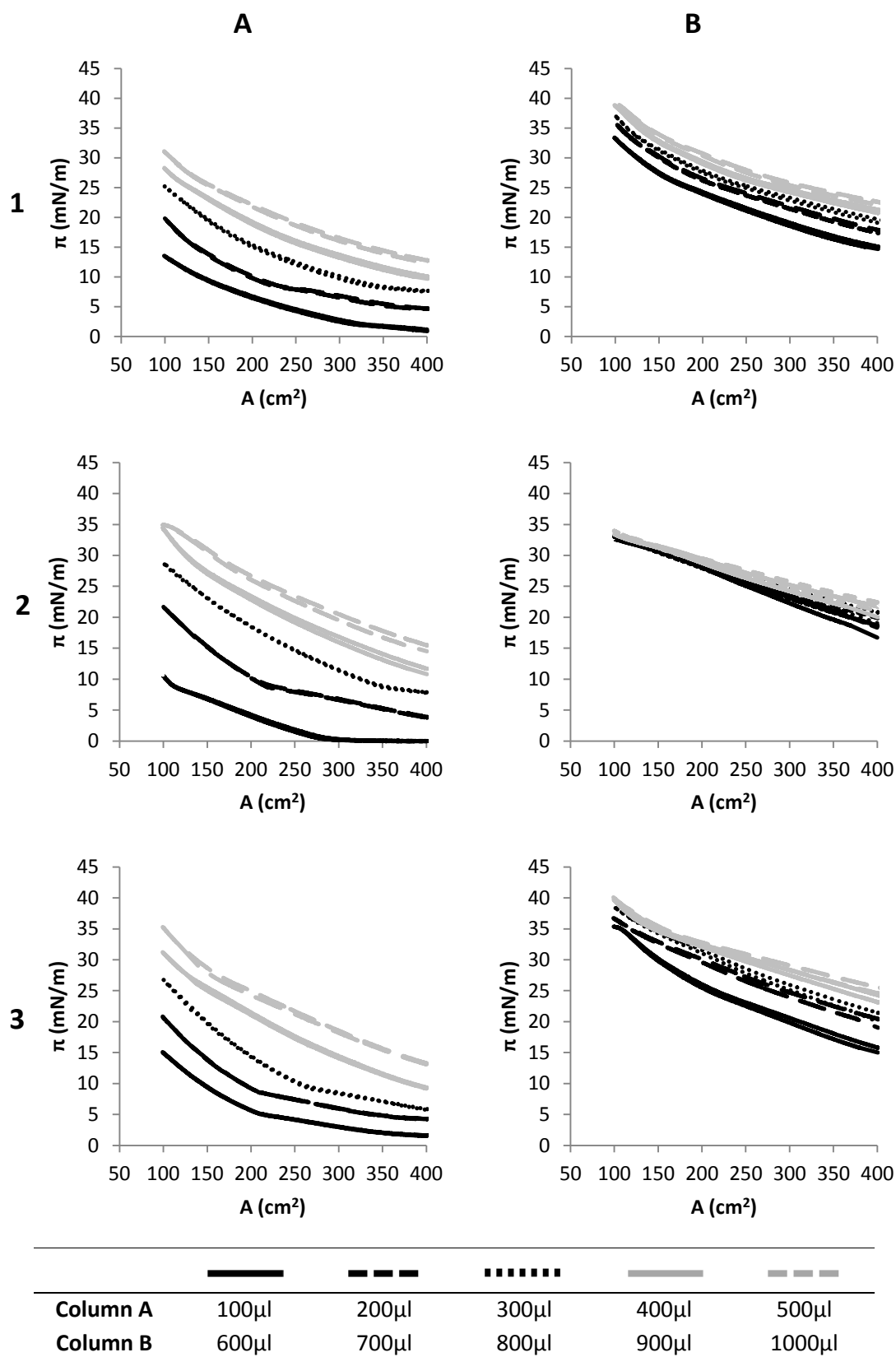


Fig 6.4a. π -A isotherms of worn Clariti 1day contact lens extracted in $C_6H_{14}:CH_3OH$ (9:1 w/w).
Row 1 - Px3; Row 2 - Px16; Row 3 - Px19

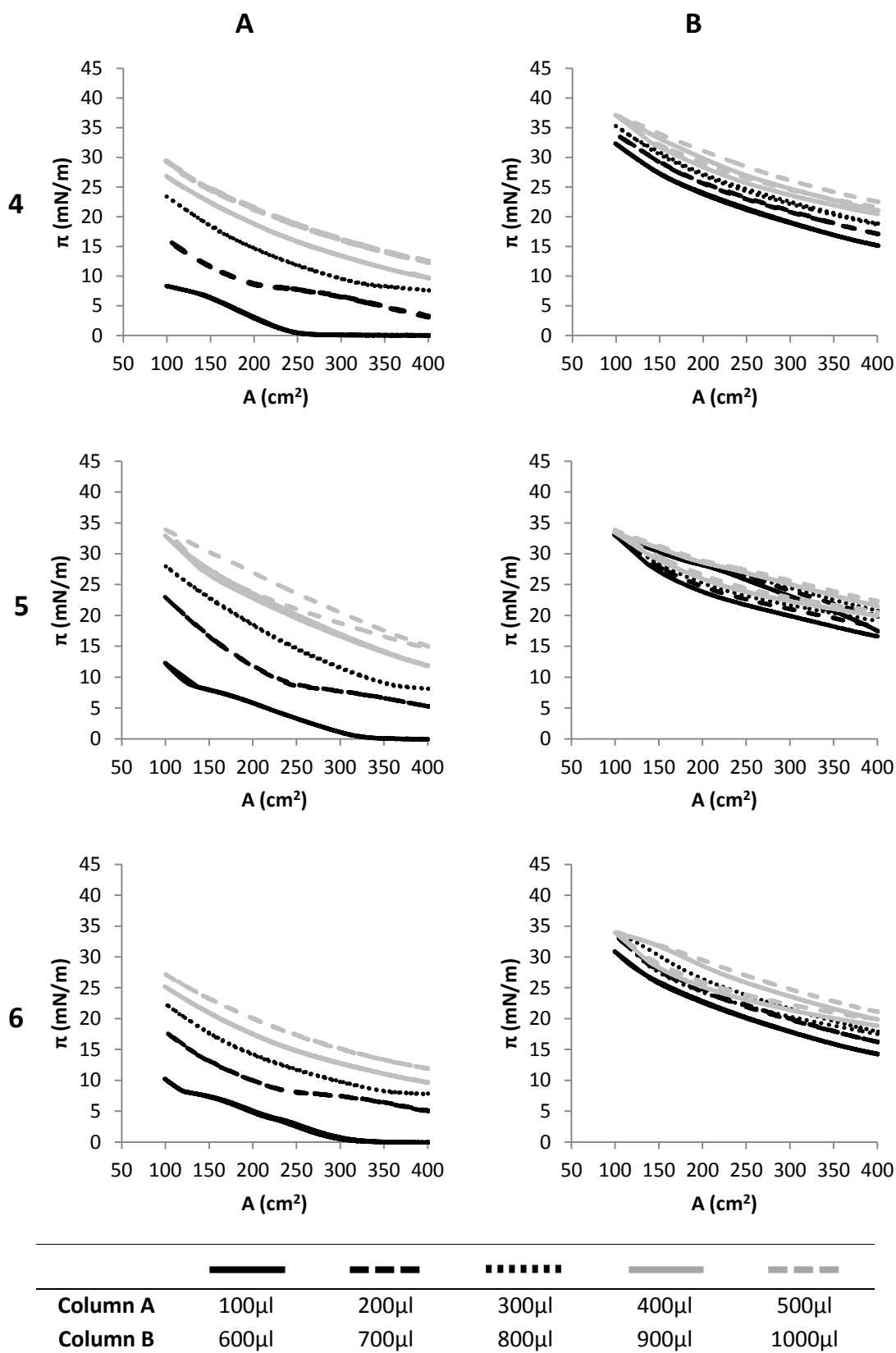


Fig 6.4b. π -A isotherms of worn Clariti 1day contact lens extracted in $C_6H_{14}:CH_3OH$ (9:1 w/w).
Row 4 - Px23; Row 5 - Px36; Row 6 - Px40.

6.1.3.1.2.3 Chloroform : Methanol (1:1 w/w) Extraction

The π -A isothermal data of subject and control samples obtained from worn and unworn Clariti 1day contact lenses extracted in $\text{CHCl}_3:\text{CH}_3\text{OH}$ (1:1; w/w) can be found in Fig 6.5 and Appendix 5. A difference in maximum surface pressure (π_{max}) between the control lens and the worn lenses was observed. The extraction of worn Clariti 1day lenses produced π_{max} of 30-36mN/m:

- Subject Px1 produced a π_{max} of 35.1mN/m at the 1000 μl aliquot;
- Subject Px19 produced a π_{max} of ~ 35.7 mN/m at 900-1000 μl ;
- Subject Px23 produced a π_{max} of ~ 33.7 mN/m at 900-1000 μl ;
- Subject Px24 produced a π_{max} of ~ 36.0 mN/m at 900-1000 μl ;
- Subject Px28 produced a π_{max} of 29.2mN/m at the 1000 μl aliquot.
- Subject Px40 produced a π_{max} of ~ 33.8 mN/m at 700-1000 μl .

Initial surface pressure (π_{init}) increased above 0.0mN/m at relatively low volume of sample solutions obtained from worn Clariti 1day lenses. Initial surface pressure was 0.00mN/m for all isotherms up to 300 μl aliquot for the subject samples Px1, Px23, Px24 and Px40, and at the 400 μl aliquot for Px19 and Px28 subject samples. For the isotherms that recorded an π_{init} of 0.0mN/m, the transition from gaseous (G) to a liquid expanded (LE) phase was observable. The phase transition did not occur at a definable area, taking place over a surface area range where monolayer arrangement occurs before attaining a stable LE phase.

Slight variations within the LE phase - observed in the π -A isotherm as surface pressure increases above 0.0mN/m to its maximum - is indicative of fluctuations occurring within the monolayer as extractable components interact. This second degree of interactions occurs after the initial interactions that produce surface pressure increase and. These changes are not as severe as the G-LE phase transition (or in fact that observed with saturated fatty acids when an LE-LC transitions occur). Components undergo constant ordering within the LE monolayer that causes slight changes in the rate of surface pressure increase until an optimum arrangement is attained. At that point the rate of surface pressure increase over decreasing surface area becomes linear. The reversibility between compression and expansion cycles for all subject samples was high ($\sim 99.5\%$) with only slight decreases in reversibility observed as loading volume was increased up to the maximum 1000 μl volume.

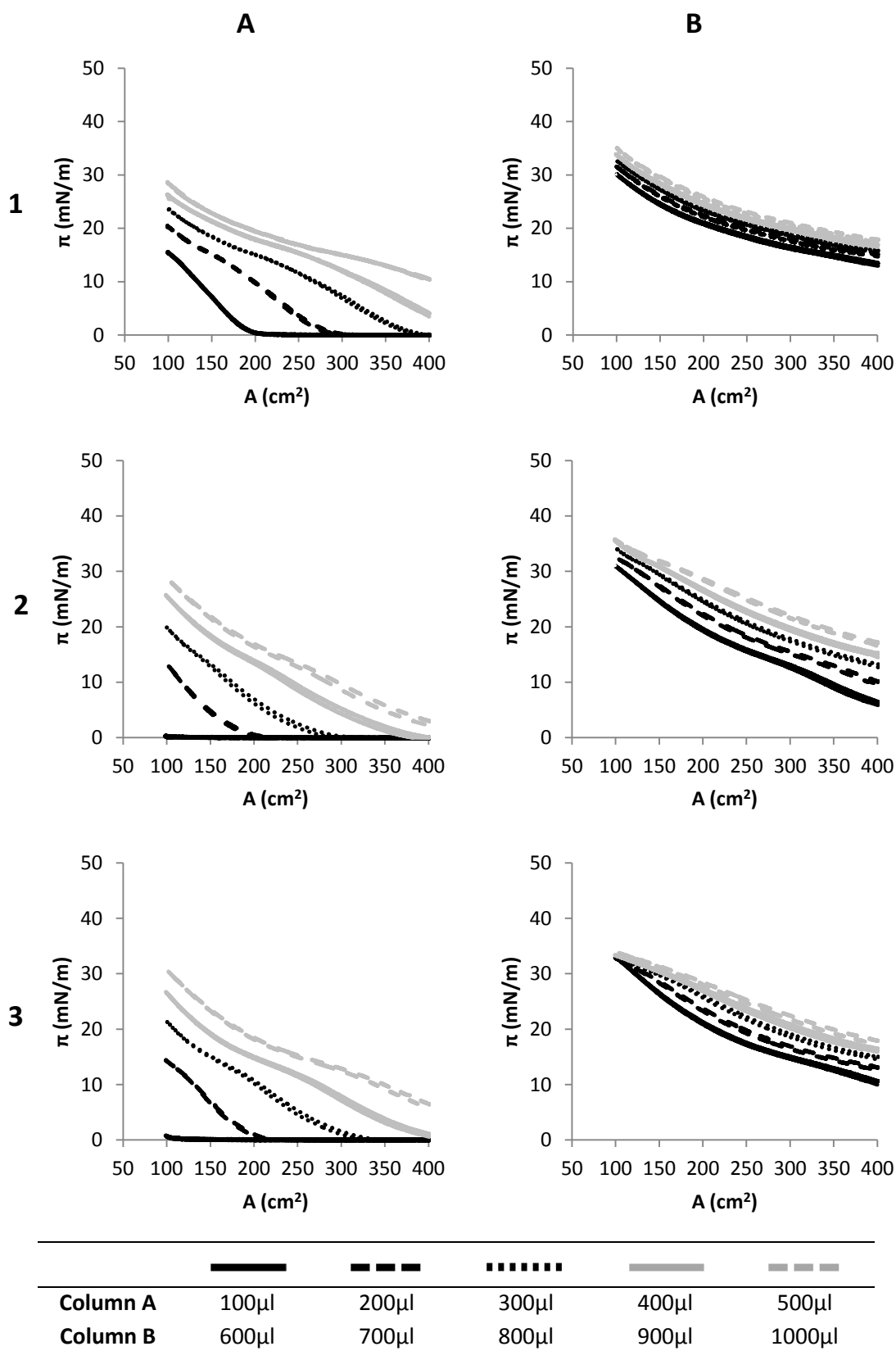


Fig 6.5a. π -A isotherms of worn Clariti 1day contact lens extracted in $\text{CHCl}_3:\text{CH}_3\text{OH}$ (1:1 w/w)
Row 1 - Px1; Row 2 - Px19; Row 3 - Px23.

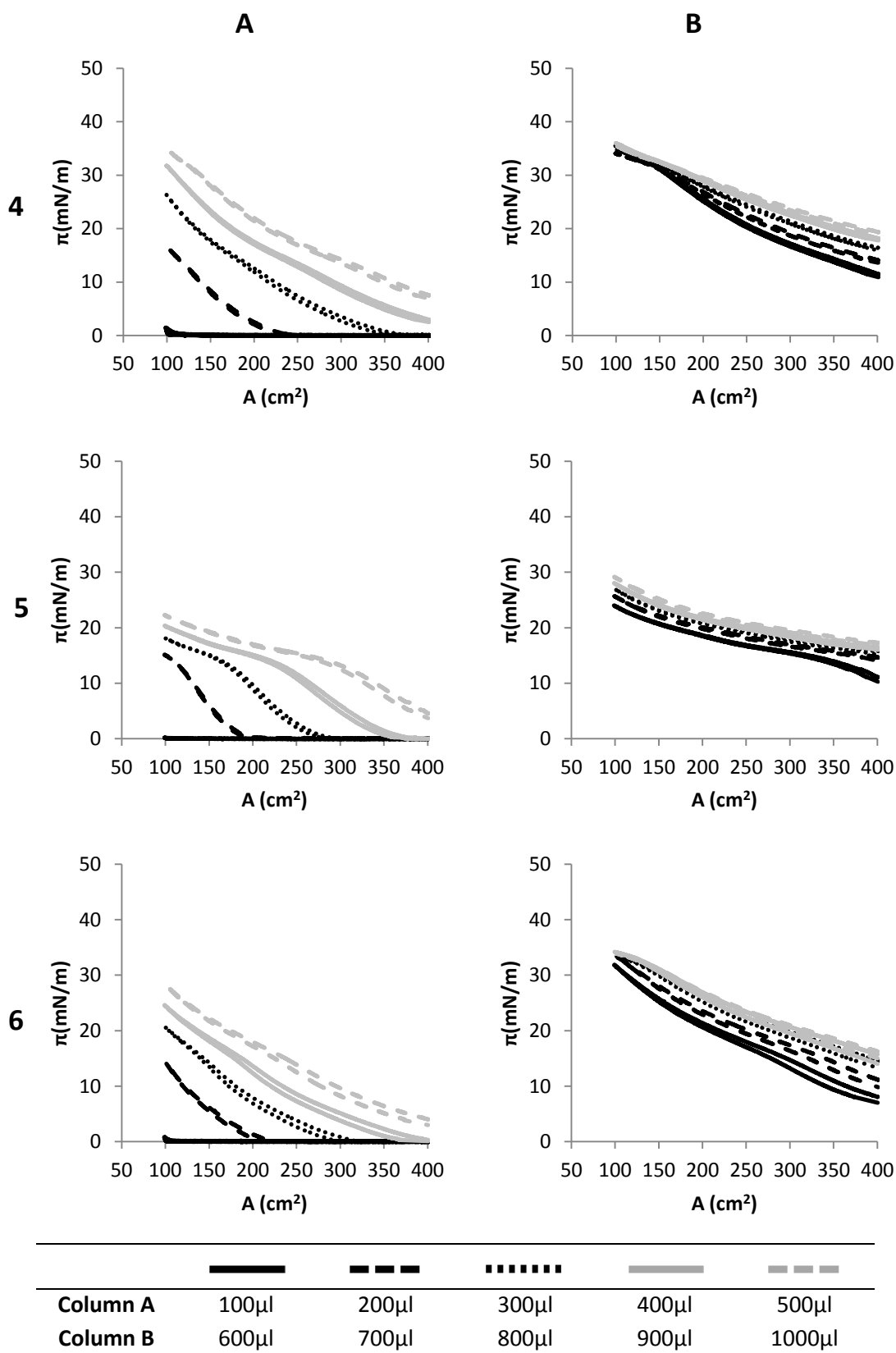


Fig 6.5b. π -A isotherms of worn Clariti 1day contact lens extracted in $\text{CHCl}_3:\text{CH}_3\text{OH}$ (1:1 w/w)
 Row 4 - Px24; Row 5 - Px28; Row 6 - Px40.

6.1.3.1.3. Comparison of Extraction Solvents

A comparison of the maximum surface pressures (π_{\max}) at the 1000 μ l aliquot of subject and control samples for the three extraction methodologies (Fig 6.6) indicate the different behaviour of the solvent in extracting tear lipid and lens material. Choice of solvent when extracting tear sampling probes is an important factor in the preparation of samples for surface behaviour studies. Samples obtained from all three solvent extractions exhibit a degree of influence from the contact lens material. C_6H_{14} solvent (Fig 6.6a) produced the smallest π_{\max} for the control sample ($\pi_{\max} = 12.1\text{mN/m}$ at 1000 μ l). However, a significant π_{\max} increase was observed between the 900 μ l and 1000 μ l aliquots that would indicate the sample had not reached a maximum value. An increase in surface concentration might present a different situation with a reduction in the difference between π_{\max} for the control and subject samples. The subject samples all attained π_{\max} values around the 800-900 μ l aliquot with no significant observed at the 1000 μ l aliquot ($\pi_{\max} = 21.1\text{-}26.4\text{mN/m}$).

The $C_6H_{14}:\text{CH}_3\text{OH}$ (9:1 w/w) solvent (Fig 6.6b) produced the highest π_{\max} values for both the subject ($\pi_{\max} = 33.9\text{-}40.1\text{mN/m}$) and control samples ($\pi_{\max} = 23.1\text{mN/m}$) at 1000 μ l. This maximum value was attained at slightly lower surface concentrations compared to C_6H_{14} (~700-800 μ l aliquot). $\text{CHCl}_3:\text{CH}_3\text{OH}$ (1:1 w/w) solvent (Fig 6.6c) also produced high surface pressure values for the subject ($\pi_{\max} = 29.2\text{-}35.5\text{mN/m}$) and control ($\pi_{\max} = 19.8\text{mN/m}$) obtained at similar surface concentrations (~800-900 μ l aliquot). These maximum values were slightly lower than the $C_6H_{14}:\text{CH}_3\text{OH}$ (9:1 w/w) solvent extraction by ~4-6mN/m for the subject samples and ~3.3mN/m for the control sample.

The π_{\max} for the control sample is proportional to the π_{\max} of the subject samples with a ~10-15mN/m decrease observed for the π_{\max} for the control sample compared to the π_{\max} for the subject samples extracted in C_6H_{14} and $\text{CHCl}_3:\text{CH}_3\text{OH}$ (1:1 w/w) solvents. A slight increase in the difference to ~11-17mN/m was observed for the samples extracted in $C_6H_{14}:\text{CH}_3\text{OH}$ (9:1 w/w). In some cases, increasing the surface concentration of the subject and control samples extracted in the solvents could increase π_{\max} significantly higher.

As two worn Clariti 1day lenses were obtained from each subject, each extracted in a separate solvent. Whilst a direct comparison between the left eye (LE) and right eye (RE) samples of a single subject does not provide enough information, a trend can be observed between three subjects per comparison (Table 6.1) that would indicate patient-to-patient variations that are detectable regardless of the extraction solvent used. The general trend is that as maximum surface pressure decreases across a range of subjects from one set of lens samples extracted in one solvent, a similar decrease is observed for samples extracted in a different solvent. Control samples also showed similar decreases in maximum surface pressure between the two solvents being compared. Although small variations exist between the tear lipids in the left eye (LE) and right eye (RE) this is not enough to cause a significant change in the π -A isotherm profiles.

	C_6H_{14}	$C_6H_{14}:CH_3OH$		C_6H_{14}	$CHCl_3:CH_3OH$
Px3	26.4	39.6	Px1	22.2	35.1
Px16	22.8	34.0	Px24	27.1	35.5
Px36	24.5	33.9	Px28	21.2	29.2
Control	12.1	23.1	Control	12.1	19.8
				$C_6H_{14}:CH_3OH$	$CHCl_3:CH_3OH$
			Px19	40.1	35.8
			Px23	37.1	34.0
			Px40	34.1	33.9
			Control	23.1	19.8

Table 6.1. Comparison of π_{max} (mN/m) between LE and RE worn Clariti 1day samples obtained using different solvent extraction methodology at the 1000 μ l aliquot.

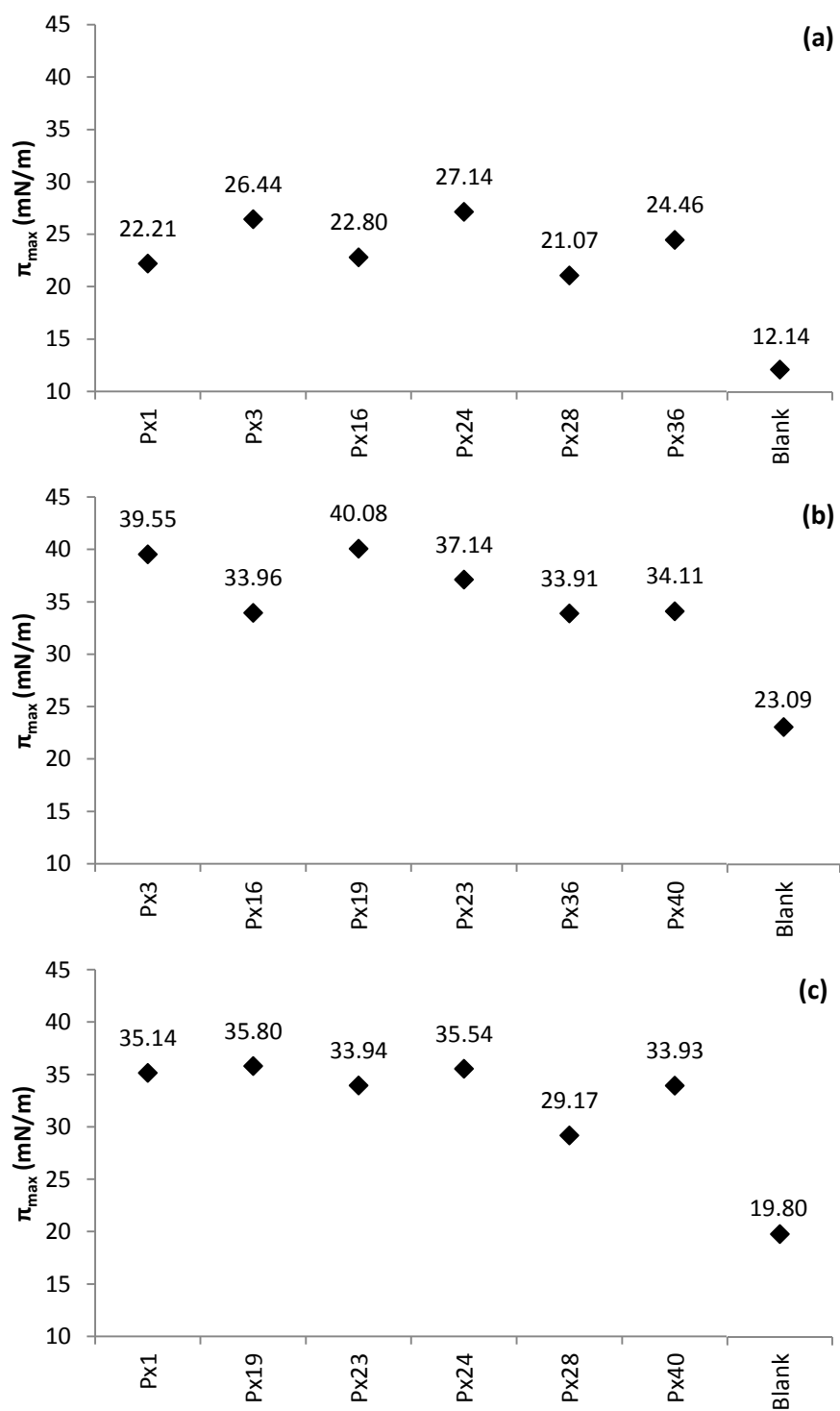


Fig 6.6. Comparison of π_{max} of samples obtained from worn and unworn Clariti 1day contact lenses at the 1000 μl aliquot.

(a) C_6H_{14} ; (b) $\text{C}_6\text{H}_{14}:\text{CH}_3\text{OH}$ (9:1 w/w); (c) $\text{CHCl}_3:\text{CH}_3\text{OH}$ (1:1 w/w).

6.1.3.2 1-Day Acuvue TruEye Contact Lenses

6.1.3.2.1 Control Lens Samples

The control 1-Day Acuvue TruEye (TE) contact lens extracted in C_6H_{14} (Fig 6.7, Row 1) produced a maximum surface pressure (π_{max}) of ~ 24.9 mN/m between 450-500 μ l. The control sample saw an increase in $\pi_{init} > 0.0$ mN/m from the 200 μ l aliquot. A gradual increase in the rate of change of surface pressure as surface area decreases is observed throughout G-LE transition. This occurs within a large area range as the monolayer attains an optimised packing structure. The control sample monolayer is relatively reversible at ~ 89 -94% for all volume aliquots up to 1000 μ l.

The control TE lens sample extracted in $C_6H_{14} : CH_3OH$ (Fig 6.7, Row 2) produced a π_{max} of ~ 34.0 -34.5 mN/m at around an aliquot volume of 450-500 μ l. π_{init} increased above 0.0 mN/m at relatively low volume and a π_{init} of > 0.0 mN was observed from the 200 μ l aliquot. The π -A isotherms for the control samples indicate several transitions of phase within the monolayer. The G-LE transition (characterised by an exponential change in the rate of change of surface pressure increase) and second transition (characterised by a plateau where rate of change of surface pressure decreases) is observed. As surface area is further decreased towards A_{min} another transition occurs and a second LE phase is observed. Despite several phase transitions, the control sample monolayer is relatively reversible (~ 91 -96%).

The control TE lens extracted in $CHCl_3 : CH_3OH$ (Fig 6.7, Row 3) produced a maximum surface pressure (π_{max}) of 32.9-33.0 mN/m around aliquot volumes of 450-500 μ l. π_{init} for the control sample increased above 0.0 mN/m at an aliquot volume of 200 μ l. Below this volume, G-LE transition can be observed indicated by a gradual increase in the rate of change of surface pressure over a large area range. Fluctuations in the rate of change of surface pressure within the LE phase indicates movement of molecules during phase transition before becoming a linear trend as orientation is optimised. At higher surface concentration, no further increase is observed in surface pressure and a plateau is observed that continues to A_{min} . Reversibility is ~ 99.8 between 100-200 cm^2 but thereafter decreases significantly to $\sim 71\%$ at highest loading (500 μ l).

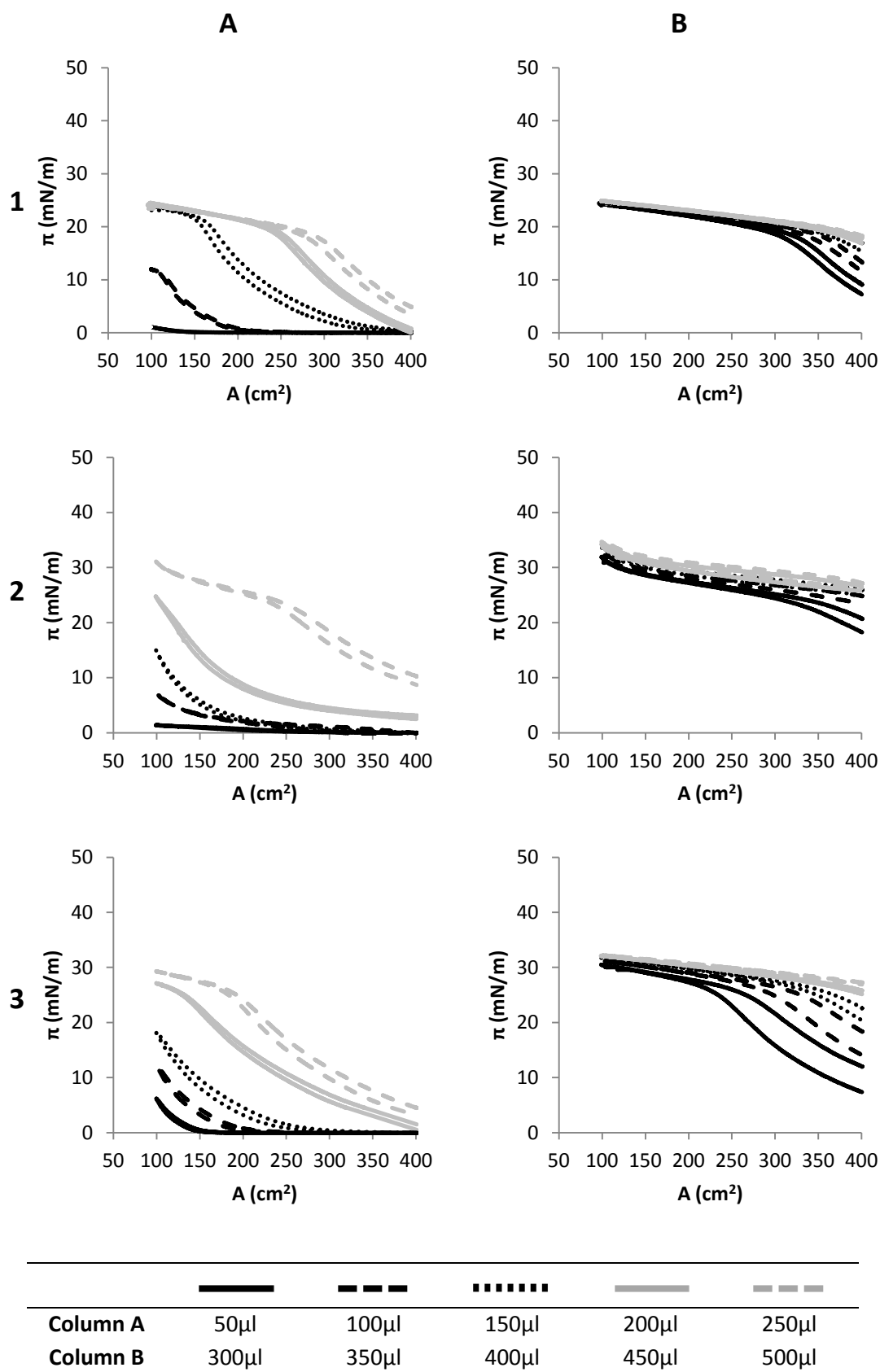


Fig 6.7. π -A isotherms of control TE contact lens samples
 Row 1 - C_6H_{14} ; Row 2 - $\text{C}_6\text{H}_{14}:\text{CH}_3\text{OH}$ (9:1 w/w); Row 3 - $\text{CHCl}_3:\text{CH}_3\text{OH}$ (1:1 w/w)

6.3.2.2 Worn 1-Day Acuvue TruEye Lens Samples

6.3.2.2.1 Hexane Extraction

The π -A isothermal data of subject samples obtained from worn TE contact lenses extracted in C_6H_{14} can be found in Fig 6.8 and Appendix 5. The extraction of worn TE lenses (Fig 6.15) produced π_{max} of ~ 31 - 35 mN/m:

- Px6 produced a π_{max} of ~ 31.8 mN/m between 450-500 μ l;
- Px7 produced a π_{max} of ~ 32.5 mN/m between 400-500 μ l;
- Px18 produced a π_{max} of ~ 35.1 mN/m between 400-500 μ l;
- Px30 produced a π_{max} of ~ 31.3 - 31.4 mN/m between 450-550 μ l;
- Px38 produced a π_{max} of ~ 34.4 mN/m between 500-600 μ l;
- Px39 produced a π_{max} of ~ 33.2 mN/m between 450-600 μ l.

π_{init} increased above 0.0 mN/m at low volumes of both worn sample solutions. In subject samples Px7, Px30, Px38 and Px39, π_{init} was >0.0 mN/m from the 100 μ l aliquot, whilst samples Px6 and Px18 produced an $\pi_{init} >0.0$ mN/m from the 150 μ l aliquot. A gradual increase in the rate of change of surface pressure as surface area decreases is observed throughout G-LE transition, occurring within a large area range. At higher surface concentrations (higher volume aliquots) a secondary phase transition occurs where a decreased rate of surface pressure change is observed (surface pressure continues to increase from the second A_t to A_{min}). Lipid components interact through the normal G-LE transition until reaching the second phase transition. Orientation of these molecules is optimised, allowing them to pack closer together without visible sign of collapse at A_{min} . As more solution is added to the subphase surface, the surface area where this maximum surface pressure is attained increases for each additional 50 μ l aliquot. At the highest loading volumes (>450 μ l) this stabilised monolayer seems to form automatically in this secondary phase transition form.

Subject samples produced a reversibility of ~ 87 - 94% . Film relaxation does not take place immediately on commencement of surface area expansion. As the surface area is increased again upon expansion, surface pressure changes at similar rates to those observed in the compression cycle. Comparing between the same surface pressure within compression and expansion cycles, a small relative difference in surface area of ~ 20 - 25 cm² is observed.

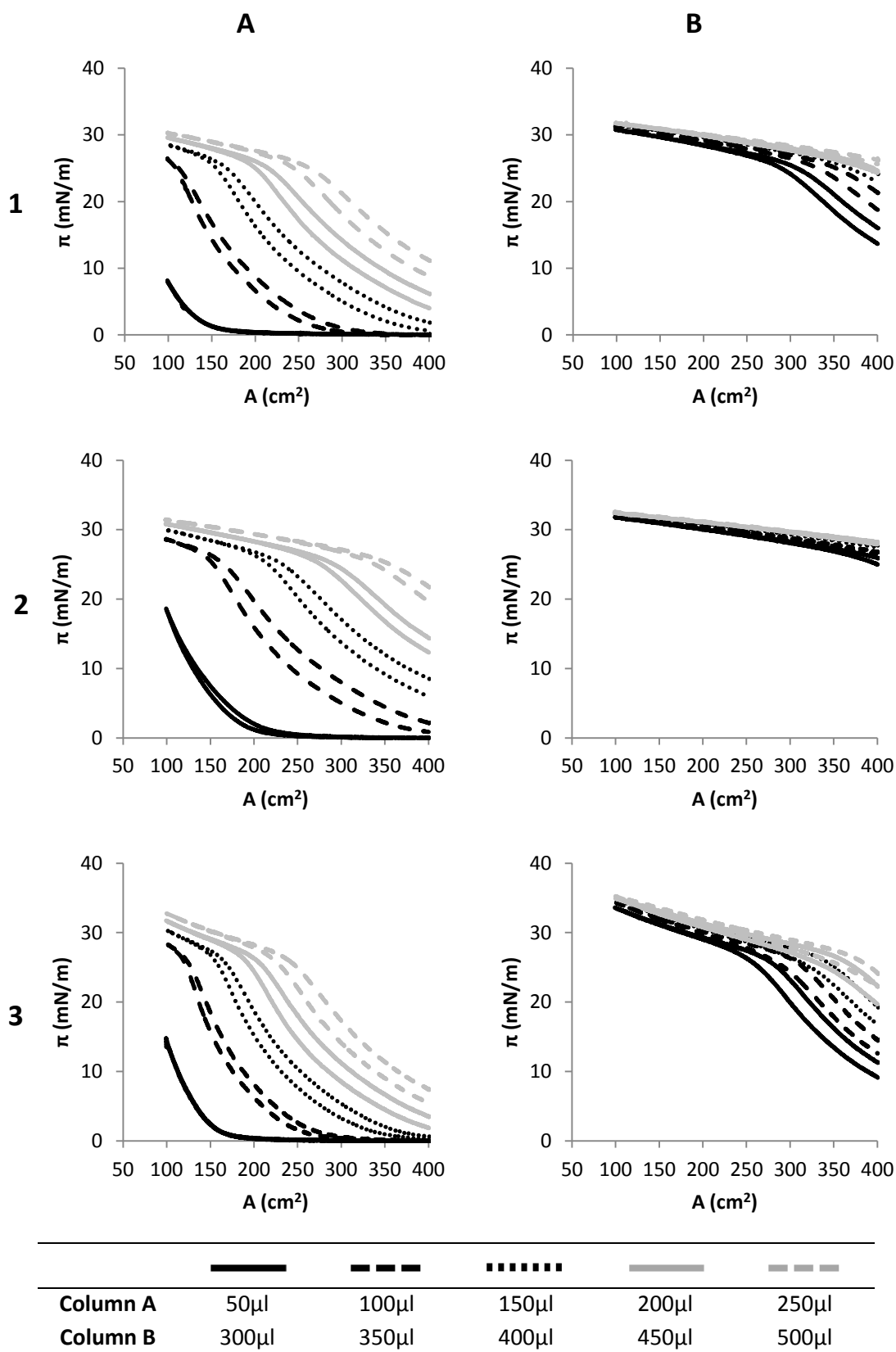


Fig 6.8a. π -A isotherms of worn TE contact lens extracted in C_6H_{14} .
Row 1 - Px6; Row 2 - Px7; Row 3 - Px18.

6.1.3.2.2.2 Hexane : Methanol (9:1 w/w) Extraction

The π -A isothermal data of subject samples obtained from worn 1-Day Acuvue TruEye (TE) contact lenses extracted in $C_6H_{14}:CH_3OH$ can be found in Fig 6.9 and Appendix 5. π_{max} in the region of ~ 42 - 47 mN/m was observed and a common feature was the low loading volumes where π_{max} for the sample is attained:

- Subject Px8 produced a π_{max} of ~ 43.0 mN/m between 200-500 μ l;
- Subject Px18 produced a π_{max} of ~ 46.2 mN/m between 150-500 μ l;
- Subject Px38 produced a π_{max} of ~ 46.1 mN/m between 100-500 μ l;
- Subject Px21 produced a π_{max} of ~ 45.0 mN/m between 350-500 μ l;
- Subject Px25 produced a π_{max} of ~ 44.6 mN/m between 400-500 μ l;
- Subject Px39 produced a π_{max} of ~ 47.0 mN/m between 200-500 μ l.

π_{init} increased above 0.0 mN/m at relatively low volume of sample solutions. In subject samples Px18, Px21 and Px38 π_{init} was >0.0 mN/m for the first 50 μ l aliquot. Samples Px8, Px25 and Px39 produced an π_{init} of >0.0 mN/m at the 100 μ l aliquot. A π_{init} of >0.0 mN was observed from the 200 μ l aliquot. The π -A isotherms for subject samples indicate several transitions of phase within the monolayer similarly observed in the control lens samples. The first transition is from gaseous (G) to liquid expanded (LE) phase where an exponential change in the rate of surface pressure increase occurs throughout the period of transition as the monolayer optimises its orientation as the rate tends to a linear relationship. At higher surface pressures (~ 30 mN/m), a second transition occurs where a decrease in the rate of change of surface pressure is observed. Orientation of molecules is optimised and compresses further with an increase in surface pressure. As the surface area is further decreased, a third transition occurs where a second LE phase is observed. The molecules at this stage begin to interact strongly with each other that are representative of the repulsion occurring between the oriented molecules.

The monolayers formed from both subject and control samples are relatively reversible with the π -A isotherms produced a reversibility of ~ 90 - 96% . Film relaxation does not take place immediately on commencement of surface area expansion. The expansion cycle closely follows the pattern of the compression cycle. As the surface area is increased again upon expansion, surface pressure changes at similar rates to those observed in the compression cycle. Comparing between the same surface pressure within compression and expansion cycles, a small relative difference in surface area of ~ 20 - 25 cm² is observed.

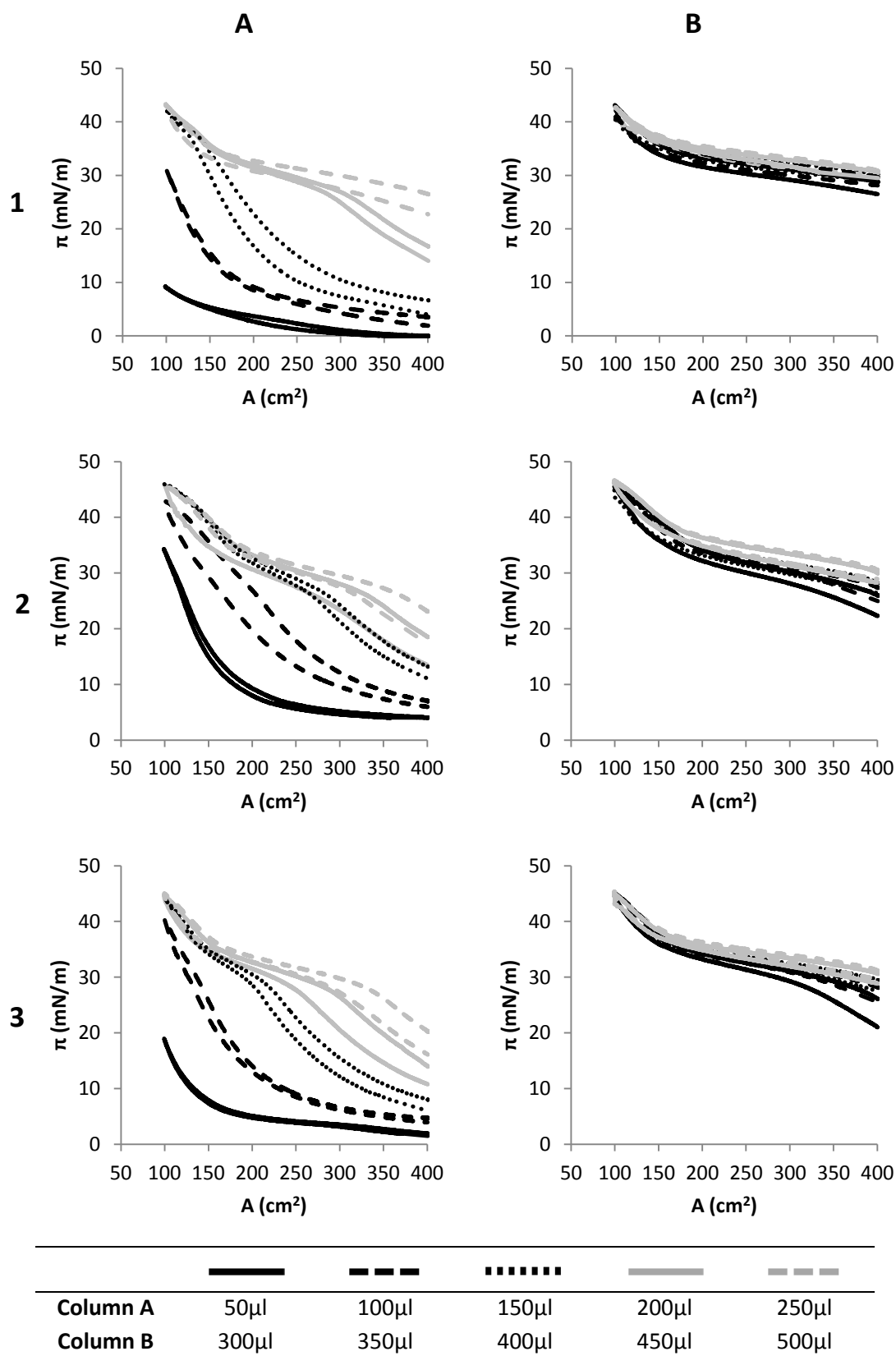


Fig 6.9a. π -A isotherms of worn TE contact lens extracted in $C_6H_{14}:CH_3OH$ (9:1 w/w).
Row 1 - Px8; Row 2 - Px18; Row 3 - Px21.

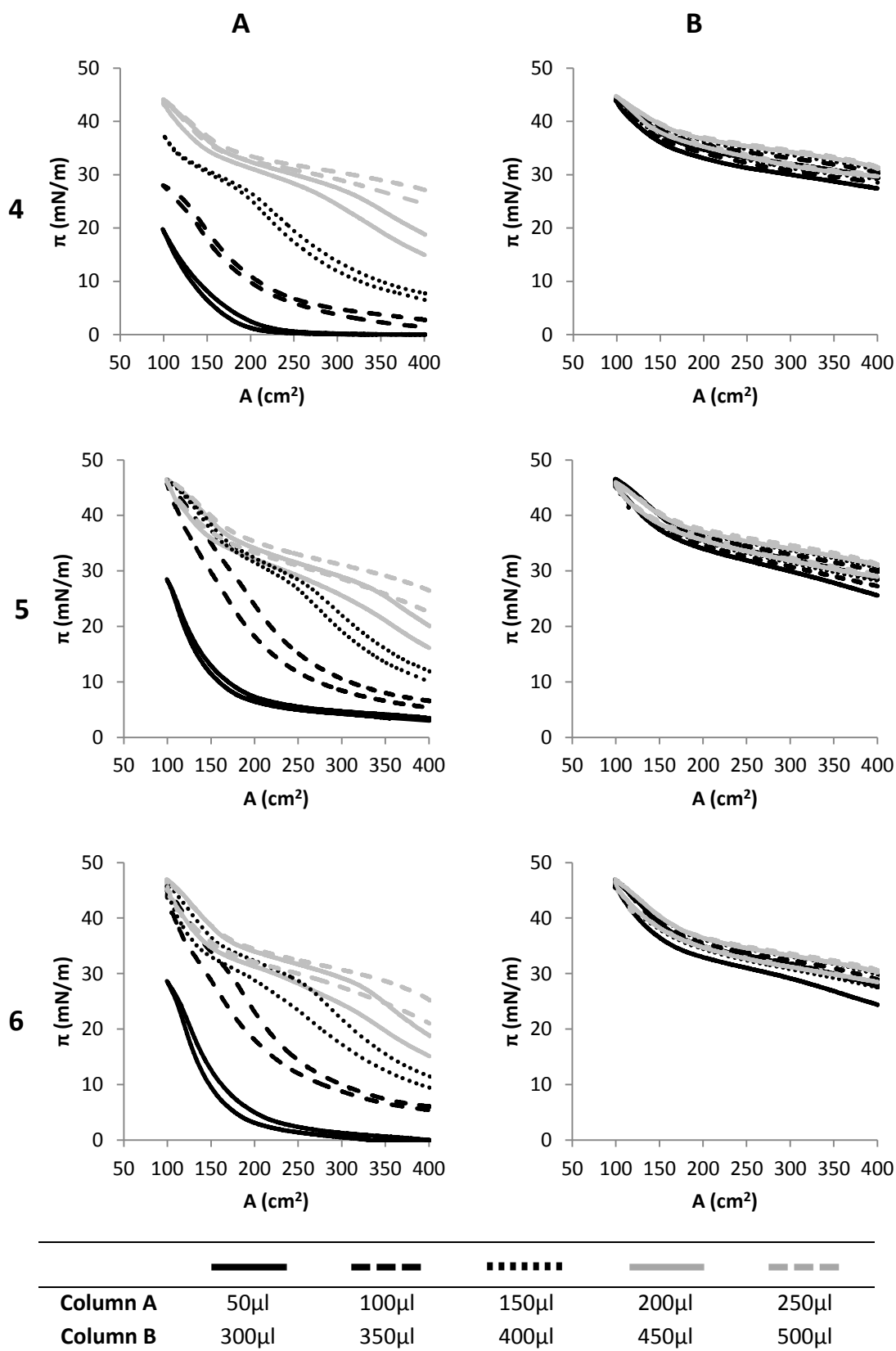


Fig 6.9b. π -A isotherms of worn TE contact lens extracted in $C_6H_{14}:CH_3OH$ (9:1 w/w).
Row 4 - Px25; Row 5 - Px38; Row 6 - Px39.

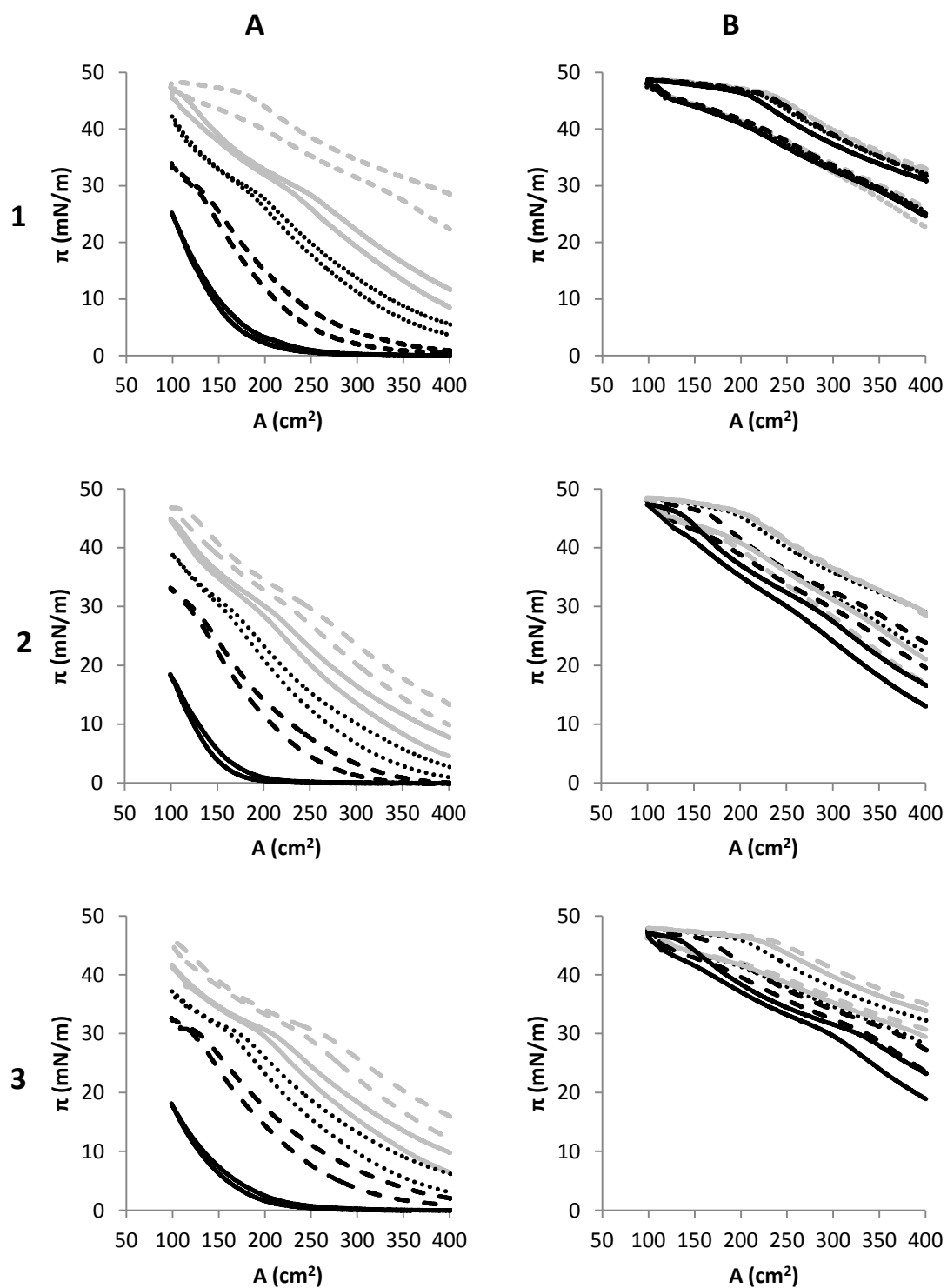
6.1.3.2.2.3 Chloroform : Methanol (1:1 w/w) Extraction

The π -A isothermal data of subject and control samples obtained from worn and unworn 1-Day Acuvue TruEye (TE) contact lenses extracted in $\text{CHCl}_3:\text{CH}_3\text{OH}$ can be found in Fig 6.10 and Appendix 5. The worn TE lens samples produced π_{max} in the region of $\sim 47\text{-}49\text{mN/m}$:

- Subject Px2 produced a π_{max} of $\sim 48.8\text{-}48.9\text{mN/m}$ between $400\text{-}500\mu\text{l}$;
- Subject Px6 produced a π_{max} of $\sim 48.5\text{-}48.6\text{mN/m}$ between $450\text{-}500\mu\text{l}$;
- Subject Px7 produced a π_{max} of $\sim 47.8\text{-}47.9\text{mN/m}$ between $400\text{-}500\mu\text{l}$;
- Subject Px8 produced a π_{max} of $\sim 48.0\text{mN/m}$ between $450\text{-}500\mu\text{l}$;
- Subject Px9 produced a π_{max} of $\sim 47.5\text{-}47.6\text{mN/m}$ between $350\text{-}500\mu\text{l}$;
- Subject Px10 produced a π_{max} of $\sim 47.2\text{-}47.3\text{mN/m}$ between $400\text{-}500\mu\text{l}$.

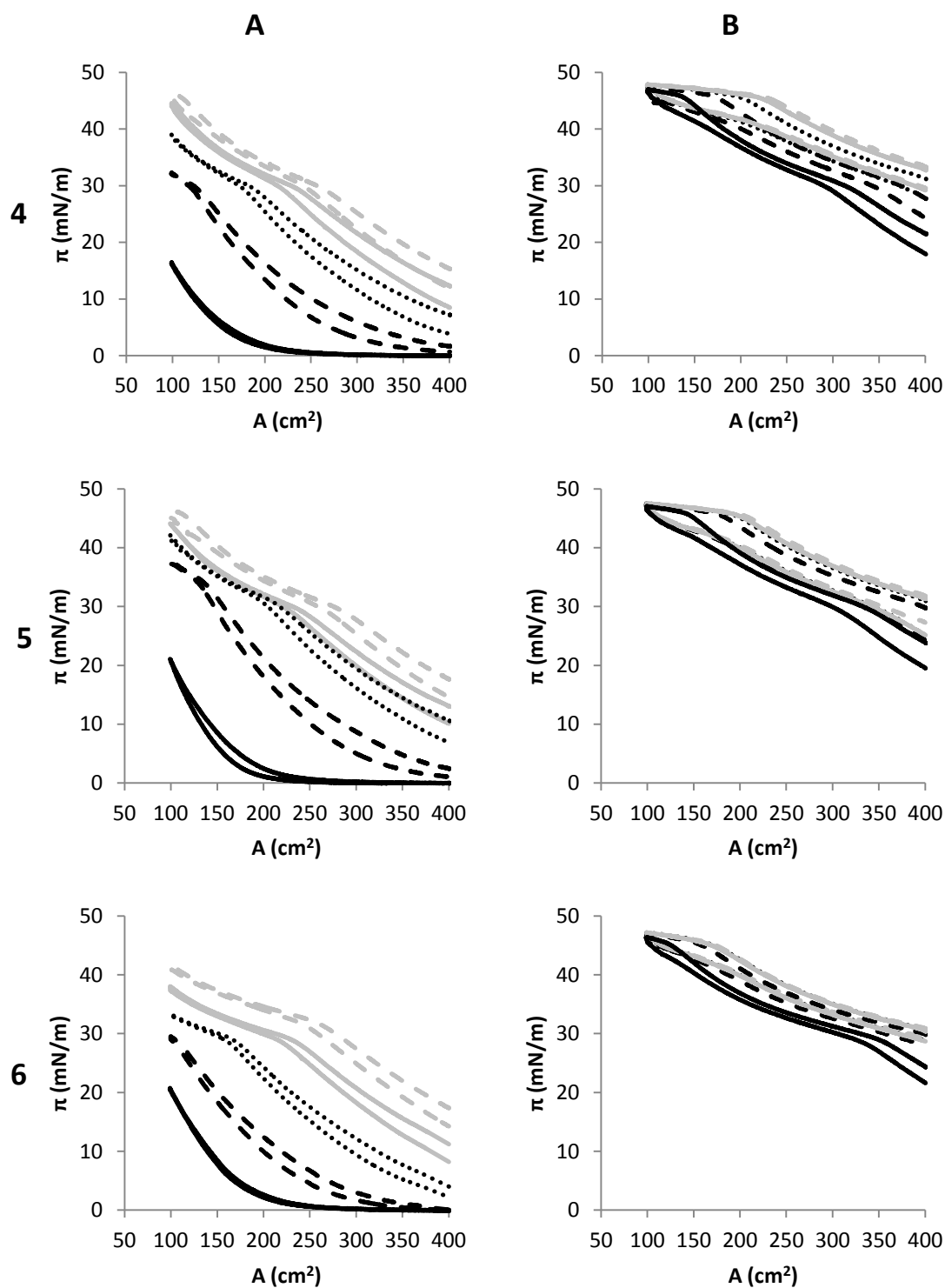
Initial surface pressure (π_{init}) increased above 0.0mN/m at relatively low sample volumes. All subject samples showed π_{init} values $>0.0\text{mN/m}$ for the $100\mu\text{l}$ aliquot except for Px6 and P10 ($\pi_{\text{init}} >0.0\text{mN/m}$ at $150\mu\text{l}$ aliquot for both samples). The G-LE transition (observable at very low surface concentrations) is characterised by a gradual increase in the rate of change of surface pressure as surface area decreases, becoming linear as the monolayer optimises molecular orientation. As more extracted material is added to the surface and π_{max} for the sample is obtained ($\sim 250\text{-}350\mu\text{l}$ of sample solutions), a plateau where no further increase in surface pressure is observed when the monolayer is compressed to A_{min} . As more solution is added to the subphase surface, the surface area where this maximum surface pressure plateau is attained increases for each additional $50\mu\text{l}$ aliquot.

This plateau is indicative of a monolayer that is highly resistant to compression. The molecules that comprise the monolayer formed from the worn lens samples interact with each other as until reaching an optimised orientation that allows them to pack closer together without visible sign of collapse. When expanded, the forces between molecules that allow it to resist compression in turn keep the molecules together enough to decrease monolayer expansion, indicated by relatively lower reversibility compared to other lens samples. The subject samples indicate high reversibility at low loading concentrations ($\sim 94\text{-}96\%$ at $50\mu\text{l}$ and $100\mu\text{l}$ aliquots) but decreases significantly as surface concentration increases, reaching a reversibility at high loading volumes of $\sim 80\text{-}85\%$ for the subject samples. This is significantly higher compared to that of the control sample at similar concentrations (Rev = $\sim 71\%$).



	—	- - -	—	- - -
Column A	50μl	100μl	150μl	200μl	250μl
Column B	300μl	350μl	400μl	450μl	500μl

Fig 6.10a. π -A isotherms of worn TE contact lens extracted in $\text{CHCl}_3:\text{CH}_3\text{OH}$ (1:1 w/w)
 Row 1 - Px6; Row 2 - Px7; Row 3 - Px8.



Column A	50μl	100μl	150μl	200μl	250μl
Column B	300μl	350μl	400μl	450μl	500μl

Fig 6.10b. π -A isotherms of worn TE contact lens extracted in $\text{CHCl}_3\text{:CH}_3\text{OH}$ (1:1 w/w).
Row 4 - Px21 ; Row 5 - Px25; Row 6 - Px30.

6.1.3.2.3. Comparison of Extraction Solvents

A comparison of the maximum surface pressures (π_{\max}) at the 500 μ l aliquot of subject and control samples for the three extraction methodologies (Fig 6.11) indicate the different behaviour of the solvent in extracting tear lipid and lens material. Choice of solvent when extracting tear sampling probes is an important factor in the preparation of samples for surface behaviour studies. Samples obtained from all three solvent extractions exhibit a degree of influence from the contact lens material. C_6H_{14} solvent (Fig 6.11a) produced the smallest π_{\max} for the control sample ($\pi_{\max} = 24.9\text{mN/m}$), with $C_6H_{14}:\text{CH}_3\text{OH}$ (Fig 6.11b) and $\text{CHCl}_3:\text{CH}_3\text{OH}$ (Fig 6.11c) producing higher π_{\max} values of 34.5mN/m and 32.3mN/m respectively.

The subject samples obtained from C_6H_{14} extraction attained π_{\max} values around the 400-450 μ l aliquot with no significant observed at the 500 μ l aliquot ($\pi_{\max} = 31.4\text{-}35.3\text{mN/m}$). The $C_6H_{14}:\text{CH}_3\text{OH}$ (9:1 w/w) solvent produced the π_{\max} values for the subject ($\pi_{\max} = 42.9\text{-}46.8\text{mN/m}$) at the 500 μ l aliquot. This maximum value was attained at much lower surface concentrations compared to C_6H_{14} (between $\sim 100\text{-}350\mu$ l aliquot). A difference was observed in the extraction of TE worn lenses using $\text{CHCl}_3:\text{CH}_3\text{OH}$ (1:1 w/w) as an extraction solvent when compared with the Clariti 1day samples. This solvent produced significantly higher maximum surface pressure compare to the $C_6H_{14}:\text{CH}_3\text{OH}$ (9:1 w/w) solvent ($\pi_{\max} = 47.3\text{-}48.9\text{mN/m}$) with the maximum surface pressure for the sample attained at $\sim 400\text{-}500\mu$ l aliquot). It is interesting to note however that the π_{\max} for the control was lower for the $\text{CHCl}_3:\text{CH}_3\text{OH}$ (1:1 w/w), opposite to that of the subject samples.

A $\sim 7\text{-}11\text{mN/m}$ decrease observed for the π_{\max} for the control sample compared to the π_{\max} for the subject samples extracted in C_6H_{14} and $C_6H_{14}:\text{CH}_3\text{OH}$ (1:1 w/w) solvents. An increase in the difference to $\sim 15\text{-}17\text{mN/m}$ was observed for the samples extracted in $C_6H_{14}:\text{CH}_3\text{OH}$ (9:1 w/w). The π_{\max} for the control sample is non-proportional to the π_{\max} of the subject samples when comparing between the $\text{CHCl}_3:\text{CH}_3\text{OH}$ (1:1 w/w) and $C_6H_{14}:\text{CH}_3\text{OH}$ (1:1 w/w) extracted samples. Comparing between each of these two solvents against C_6H_{14} does appear to be proportional.

Similarly to the Clariti 1day worn lens samples, two 1-Day Acuvue TruEye lenses were obtained from each subject and extracted in separate solvents in order to observe the trend between the left eye (LE) and right eye (RE) samples of the three worn TE samples (Table 6.2). Similar patterns that would indicate patient-to-patient variations are observable regardless of the extraction solvent used. In this case however, the general trend that maximum surface pressure decreases across a range of subjects from one set of lens samples extracted in one solvent was observable between two of the three sets of subject sample, with a discrepancy for one set of samples per comparison.

	C_6H_{14}	$C_6H_{14}:CH_3OH$		C_6H_{14}	$CHCl_3:CH_3OH$
Px18	35.3	46.6	Px6	31.8	46.6
Px38	34.4	48.0	Px7	32.6	48.0
Px39	33.2	46.8	Px30	31.4	46.8
Control	24.9	34.5	Control	24.9	32.3
				$C_6H_{14}:CH_3OH$	$CHCl_3:CH_3OH$
			Px8	42.9	48.1
			Px21	45.2	48.9
			Px25	44.7	47.6
			Control	34.5	32.3

Table 6.2. Comparison of π_{max} (mN/m) between LE and RE worn 1-Day Acuvue TruEye samples obtained using different solvent extraction methodology at the 500 μ l aliquot.

One key difference between the 1-Day Acuvue TruEye and Clariti 1day samples is the much smaller volume aliquots required to achieve a maximum surface pressure in TE subject and control samples. This may be a cause for large amounts of decanoic acid that was found to be unintentionally released from this version of TE [277] [278]. Decanoic acid (DA) is an organic acid with ten carbons within the chain, meaning it lies on boundary between forming insoluble monolayers at a surface and dissolving into the bulk subphase. As the π -A isotherm data (Fig 6.12) obtained indicates, DA can have a potential effect on surface pressure when incorporated within a monolayer obtained through worn lens extraction. At large concentrations, DA can produce surface pressure in excess of 20mN/m with high initial surface pressure that would indicate a definite effect in the samples obtained from worn TE lenses.

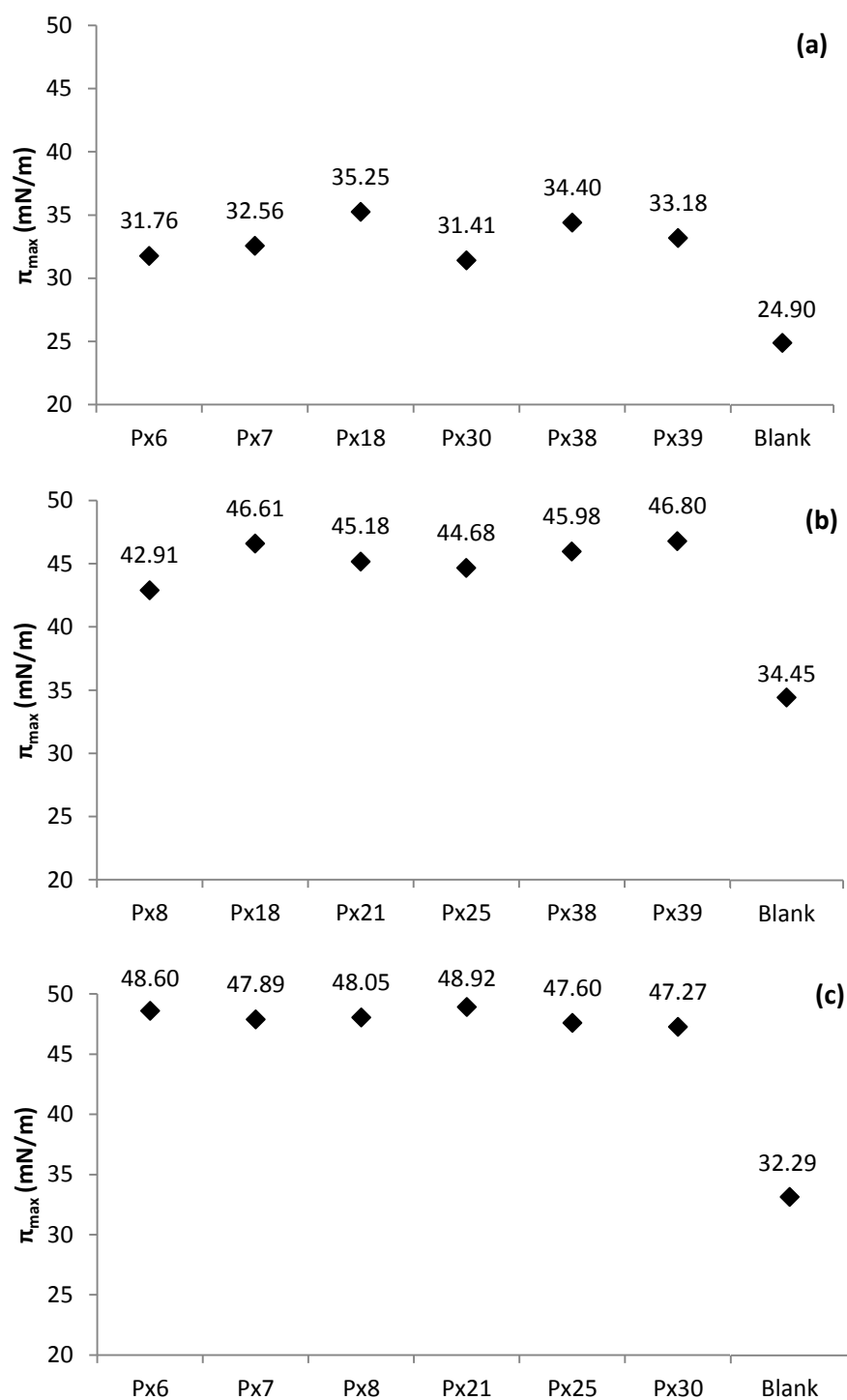


Fig 6.11. Comparison of π_{\max} of samples obtained from worn and unworn TE contact lenses at the 500 μ l aliquot

(a) C_6H_{14} ; (b) $C_3H_{14}:CH_3OH$ (9:1 w/w); (c) $CHCl_3:CH_3OH$ (1:1 w/w).

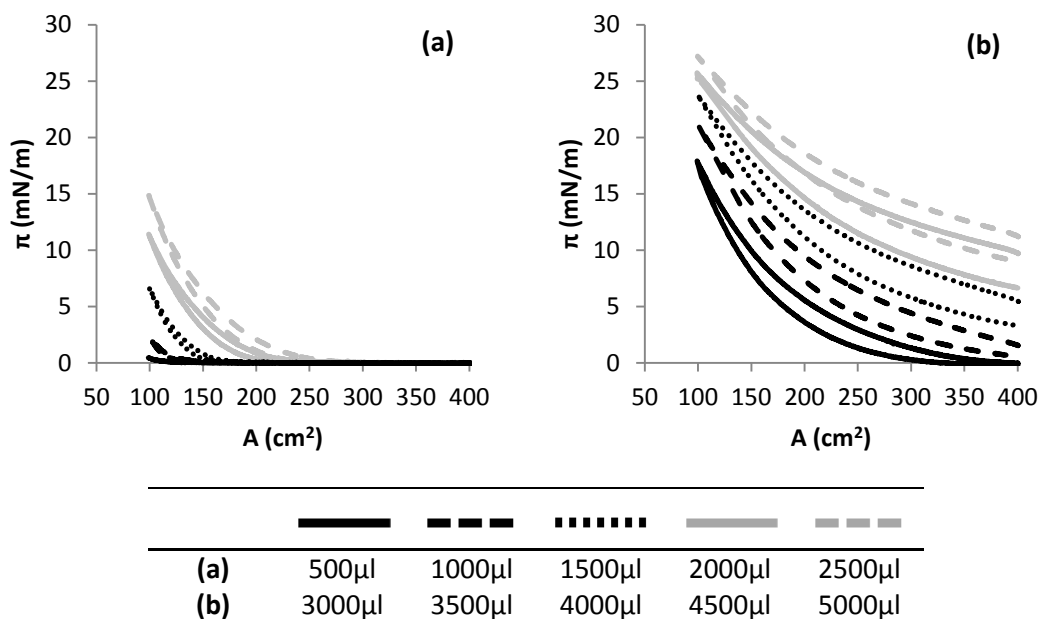


Fig 6.12. π -A isotherms of a $1.0 \times 10^{-3} \text{ moldm}^{-3}$ solution of decanoic acid (DA; 10:0).

6.1.3.2.4 Narafilcon A vs. Narafilcon B

A worn and unworn narafilcon B contact lens - marketed as Acuvue TruEye within the USA - were extracted under identical protocols to the narafilcon A lenses using $\text{CHCl}_3:\text{CH}_3\text{OH}$ (1:1 w/w). The data obtained for the worn narafilcon B lens (Fig 6.14) was compared to average values of the six worn samples of narafilcon A at the 500μl aliquot (Fig 6.13). At this volume, all samples had achieved a maximum surface pressure for that sample. The maximum surface pressure attained for the worn sample was $\sim 41.0 \text{ mN/m}$ (450-500μl aliquots). This was lower than the average value of 48.0 mN/m obtained from the six narafilcon A lenses and significantly lower than the standard deviation of those values ($\text{SD} = 0.6 \text{ mN/m}$). Similarly, the unworn narafilcon B lenses also recorded a lower maximum surface pressure compared to the unworn narafilcon A lens ($\pi_{\text{max}} = 32.5 \text{ mN/m}$ for narafilcon A and 26.5 mN/m for narafilcon B). Initial surface pressures were lower for the narafilcon B lenses compared to narafilcon A (for both worn and unworn) with an increase $> 0.0 \text{ mN/m}$ at higher surface concentrations ($> 400 \mu\text{l}$). There was no significant difference in reversibility, with narafilcon B samples showing a reversibility of $\sim 96\%$ at high loading volumes. Narafilcon B lens extractions produced stable monolayers that withstood compression and spread rapidly upon expansion.

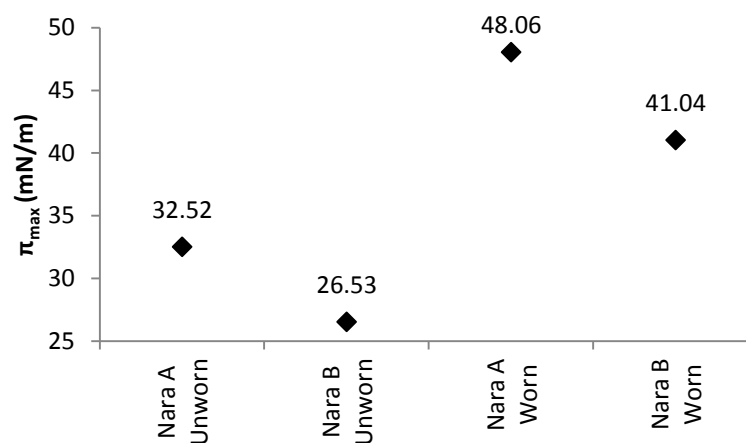


Fig 6.13. Comparison of π_{\max} of worn and unworn narafilcon A and narafilcon B samples.

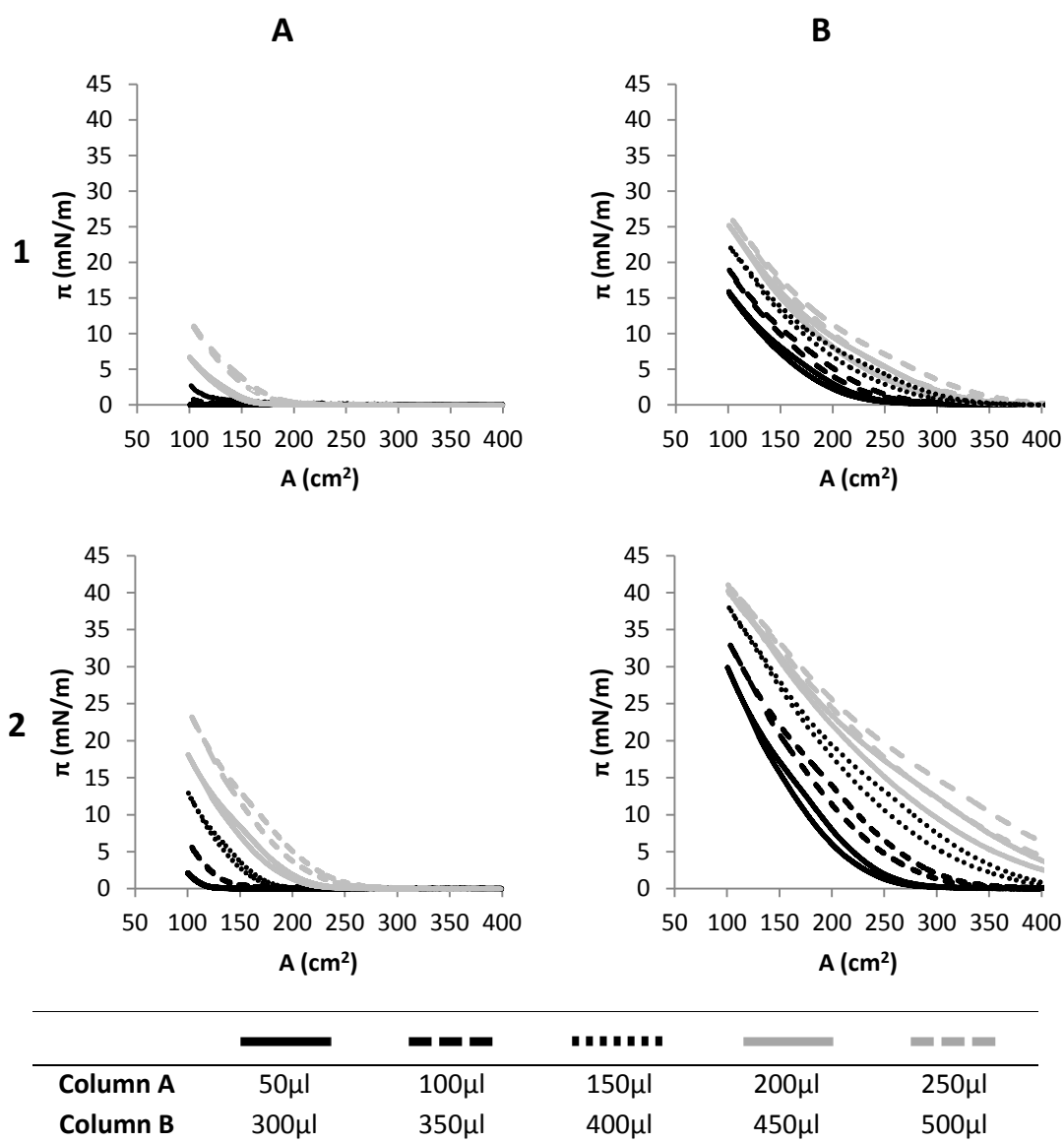


Fig 6.14. π -A isotherms of a control (Row 1) and a worn (Row 2) narafilcon B contact lens extracted in $\text{CHCl}_3:\text{CH}_3\text{OH}$ (1:1 w/w).

6.2 Focus Dailies Total-1 Contact Lenses

Contact lens-related dry eye is linked to the disruption of the tear film due to a deficiency in the phospholipid content of the lipid layer, a key component of the polar lipid sublayer necessary for TFLL stabilisation [13] [169] [176] [279]. Eye drops, eye sprays and other ointments have been utilised as dry eye treatments but were primarily designed to replenish moisture lost due to evaporation rather than lipid layer disruption [280] [281] [282]. Recent developments in therapeutic treatments have attempted to replenish the lipid layer with success in improving tear break-up time [283] [284] [285] [286], lipid layer thickness [287] [288] and patient comfort [283] [286] [289]. The efficacy and efficiency of these techniques are relatively poor due to low compliance and large amounts of instilled component lost due to the self-protective mechanisms of the eye, rapid tear turnover and spillage [290] [291]. A phospholipid delivery system that improves bioavailability, site-specific delivery and continuously releases material may benefit lipid layer stability in the lens-wearing eye. In recent years, novel techniques have been developed that use the contact lens as a release vehicle for phospholipids that could aid in dry eye treatment [280] [292] [293] [294]. One such technique - CIBA Vision's DMPC-containing Focus Dailies Total-1 - will be evaluated and discussed.

6.2.1 Objective

The subsequent aim was to investigate the desirable extraction of phospholipid molecules incorporated within a daily disposable SiHy contact lens for delivery and stabilisation of the lipid layer.

6.2.2 Experimental Design

6.2.2.1 Pre-production Contact Lenses

Prior to the public release of the clinical lenses, several batches of pre-production lenses were obtained to determine the presence of DMPC. Three batches of preliminary lenses containing DMPC were received for analytical investigation:

- Batch 1: Clinical-grade lenses with 1% DMPC and a control;
- Batch 2: DMPC-containing lenses/control lens, with/without IPC-4A;
- Batch 3: DMPC-containing lens/control lens, with/without LPEG.

6.2.2.2 Clinical Lens Trial Samples

Worn Focus Dailies Total-1 lenses (DT1, delefilcon A, CIBA Vision, USA) were obtained from two sets of clinical trials conducted by the Vision Sciences department at Aston University. Lens details can be found in Appendix 3. Trial 1 consisted of 7 subjects wearing a DT1 lens in each eye. Trial 2 consisted of 5 subjects that will compare a DT lens worn in the left eye and an 1-Day Acuvue TruEye (TE) lens worn in the right eye simultaneously. Worn contact lenses were collected at the end of a day's wear and stored in saline (Sauflon Pharmaceuticals Ltd, UK) at $\sim 4^{\circ}\text{C}$ prior to analysis. Unworn Dailies Total-1 lenses were obtained from their packaging without any further modification to the lens material. Lenses were extracted for 1hr in 1.5ml $\text{CHCl}_3:\text{CH}_3\text{OH}$ (1:1 w/w). Prior to extraction, lenses were removed from their storage solution and blotted on filter paper to remove excess liquid. Sample solutions were transferred to a clean glass vial by pipette to prevent contamination by lens material caused by swelling and breakdown of the contact lens. All samples were studied within 24hr of extraction.

6.2.2.3 Tear Samples from Lens-wearing Eye

In order to determine any measurable change in surface behaviour of the tear film caused by the potential release of DMPC, tear samples were collected from subjects during DT1 lens wear and by wiping the lenses after removal from the eye and prior to lens extraction. These were collected using Visispear™ ophthalmic sponges and extracted according to the protocol in section 7.2.1.

6.2.2.4 π -A Isotherm Measurement

The π -A isothermal study of samples worn and unworn DT1 lenses was conducted on Langmuir trough B (working surface area - $400\text{-}100\text{cm}^2$; barrier speed - $50\text{cm}^2/\text{min}$) according to the procedure described in section 2.1. HPLC-grade water was used as a subphase and kept at a constant temperature of $35.0^{\circ}\text{C} \pm 0.2^{\circ}\text{C}$. Sample solutions were applied to the subphase surface by a $50\mu\text{l}$ Hamilton syringe. At least ten minutes was allowed to ensure full spreading of the solution, solvent evaporation and spontaneous movement and arrangement of components. Tear sample films were repeatedly compressed and expanded until the equilibrium surface pressure (π_{eq}) was reached.

6.2.3 Results

6.2.3.1 Pre-production DT1 Lenses

6.2.3.1.1 Batch 1 Lenses

The π -A isotherms obtained from extraction of the Batch 1 lenses (Fig 6.15) shows the difference between the base SiHy polymer and that containing 1% DMPC. Despite a small influence from extractable lens material, the π -A isotherms obtained from extracts of the DMPC containing lenses are predominantly characterised by the effect of the phospholipid. A comparative isotherm of a 5 μ l aliquot of $1.0 \times 10^{-3} \text{ mol dm}^{-3}$ DMPC shows a similarity to the extraction of the Batch 1 lens that would confirm that this represents a significant release of DMPC. Similar maximum surface pressures were obtained from the DMPC-containing lenses ($\sim 50 \text{ mN/m}$) when compared to the pure DMPC monolayer. The presence of a stable monolayer at high compression (minimum surface area) is formed due to the plateau reached at high surface pressures. This was also observed in the pure DMPC monolayer taken to the minimum working area (100 cm^2) and is indicative of the phospholipid molecules attaining a preferred orientation at the water-air interface.

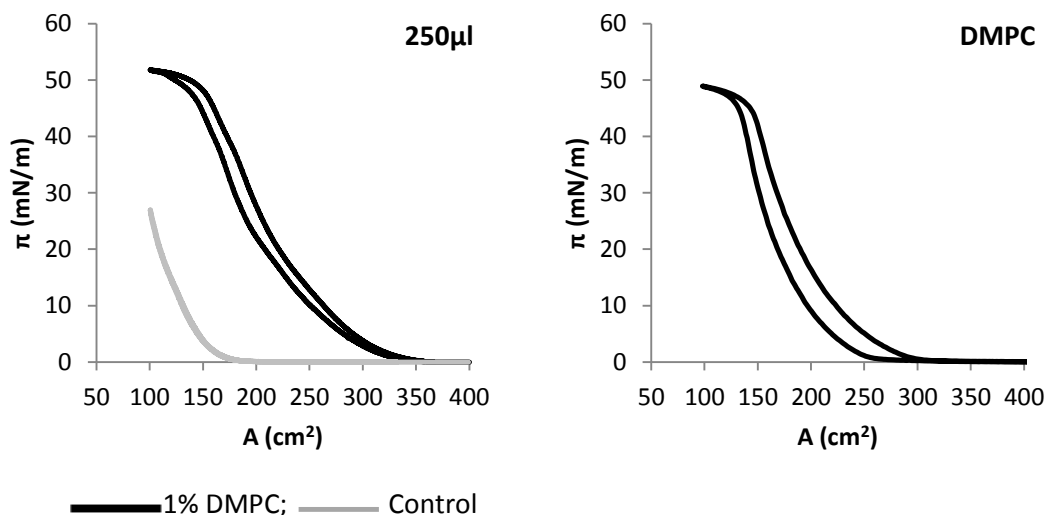


Fig 6.15. π -A isotherms for a 250 μ l aliquot of an extracted Batch 1 pre-production contact lenses and a 25 μ l aliquot of a $1.0 \times 10^{-3} \text{ mol dm}^{-3}$ DMPC solution.

6.2.3.1.2 Batch 2 Lenses

The Batch 2 lenses were designed similarly to those in Batch 1 but contained a processing aid - IPC-4A - necessary for the production of the DMPC-containing contact lenses. Fig 6.16 shows the effect that inclusion of this processing aid in extractions of non-clinical lenses can have on the π -A isotherm of the DMPC-containing lens and the control lens. There is no significant effect in the π -A isotherms that can be attributed entirely to the presence of IPC-4A processing aid within the extract. Inter-sample variability might also be a cause of the differences that can be observed in the isotherms. Similar significant differences recorded in the Batch 1 lens extractions can also be observed when comparing between the DMPC-containing and control Batch 2 lens materials. The DMPC containing lenses have the characteristic similarity to pure DMPC with a maximum surface pressure of $\sim 50\text{mN/m}$. Only a small degree of influence on the isotherm is caused by the lens material, observed with smaller maximum surface pressure and a much lower G-LE transition area.

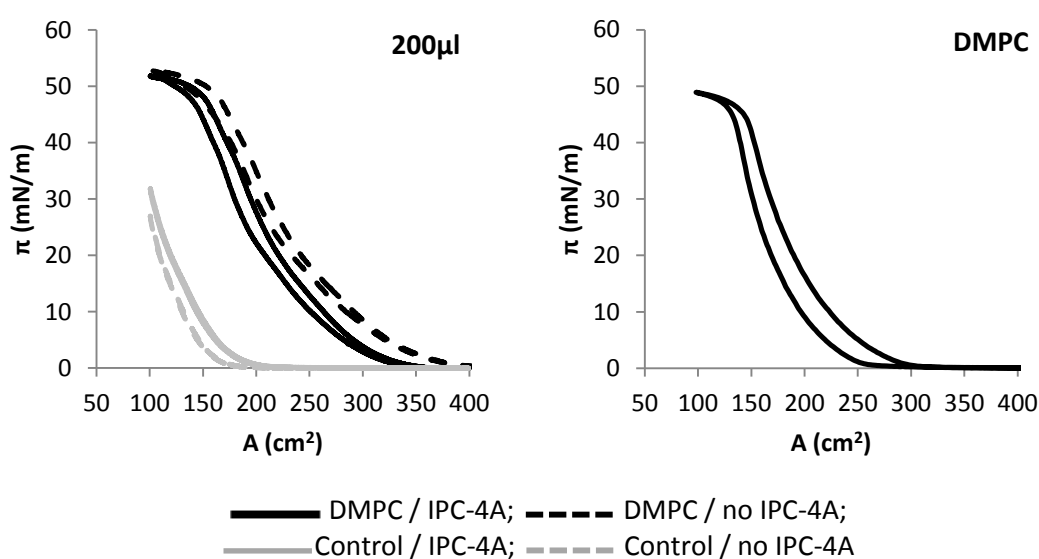


Fig 6.16. π -A isotherm for a 200 μl aliquot of the extracted Batch 2 pre-production contact lenses and a 25 μl aliquot of a $1.0 \times 10^{-3}\text{ mol dm}^{-3}$ DMPC solution.

6.2.3.1.3 Batch 3 Lenses

The Batch 3 lenses were designed similarly to those in Batch 2 but contained a different processing aid LPEG, which is a polyethylene glycol-like molecule. Fig 6.17 shows the effect that inclusion of this processing aid has on the π -A isotherm of DMPC-containing lens and the control lens extractions. Unlike IPC-4A, inclusion of LPEG has a significant effect on the π -A

isotherm of the DMPC-containing lenses. At the 100 μ l, the extract without LPEG produces a maximum surface pressure of ~ 50 mN/m, twice that of the extract that contained LPEG (~ 23.2 mN/m). At the 200 μ l aliquot volume, the lens extract that did not contain LPEG attained a maximum surface pressure of 51.9 mN/m, with the characteristic plateau of DMPC at this surface pressure attained.

At the same loading volume, the DMPC / LPEG lens extraction attains a lower maximum surface pressure of ~ 45 mN/m, just under the transition point where the plateau in surface pressure occurs. At the 300 μ l aliquot volume, both the DMPC / no LPEG and DMPC / LPEG lens extractions have attained the maximum surface pressure of ~ 50 mN/m with the transition to a plateau observed in both sets of data. The key differences therefore are the surface area where the G-LE transition and the point where the second phase transition at ~ 45 -50 mN/m occur. In this isotherm, it is possible to determine the inhibitive effect of the LPEG on the surface behaviour of the DMPC monolayer. This is possibly due to the potential competition at the subphase surface between LPEG and DMPC molecules.

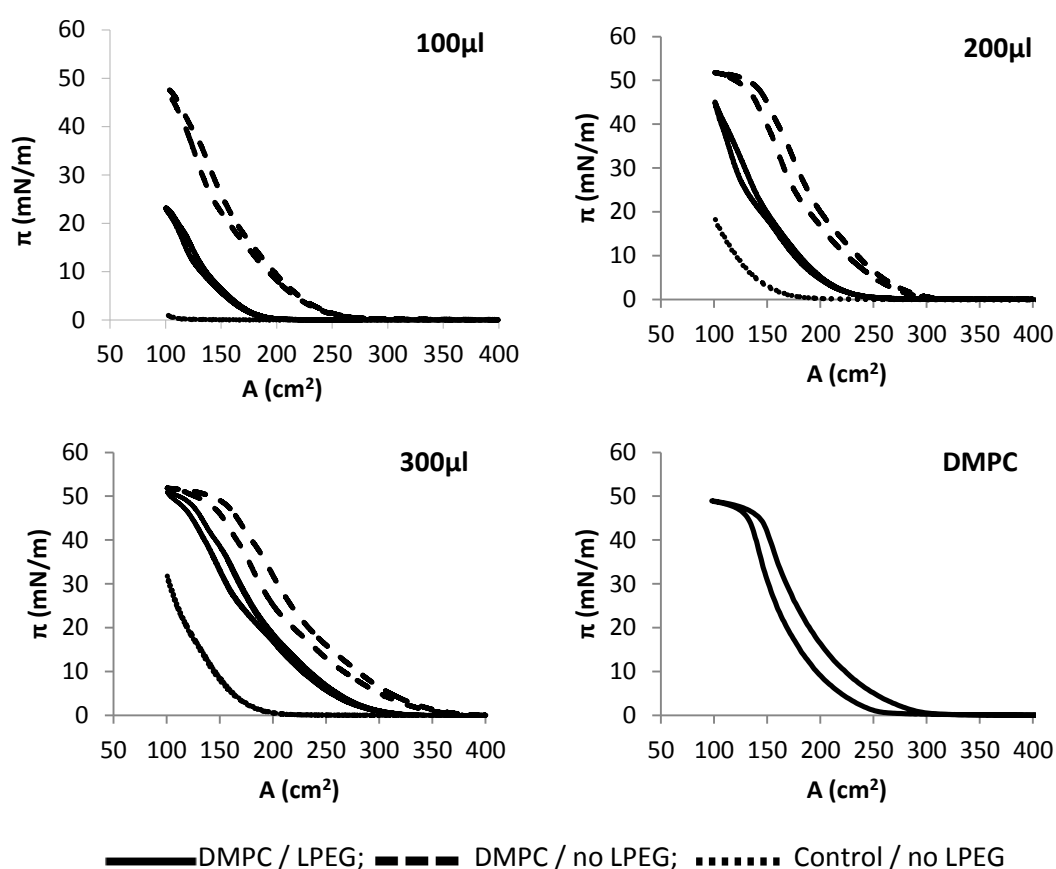


Fig 6.17. π -A isotherms for a 200 μ l aliquot of the extracted Batch 3 pre-production contact lenses and a 25 μ l aliquot of a 1.0×10^{-3} mol dm $^{-3}$ DMPC solution.

Unfortunately, a control lens that had been processed with the LPEG processing aid was not available for extraction and surface pressure-area measurement. It would have been informative to have been able to extract this lens to ascertain the surface behaviour of LPEG without the presence of DMPC.

6.2.3.2 Clinical Lens Trial Samples

6.2.3.2.1 Trial 1 Lens Extractions

The π -A isotherm data of subject and control samples obtained from worn and unworn Dailies Total-1 (DT1) lenses from Trial 1 can be found in Fig 6.18. The data obtained from compression and expansion of monolayers from the worn and unworn samples suggest that they are dominated by the behaviour of DMPC. Maximum surface pressures of ~ 50 - 51 mN/m were recorded for all tear samples. The maximum value for each sample was attained at very low volume aliquots (200 μ l for Px4, Px5 and Px14; 300 μ l for Px13, Px15 and Px20) that would indicate a large, significant amount of DMPC being extracted. With the extraction of the control lens taken from a fresh, packaged blister pack, it is possible to see that much of the DMPC will be retained by the contact lens during wear.

It is not possible to determine whether there is a small effect on the surface behaviour of the monolayer caused by the tear sample lipids. Evidence on the lack of noticeable collapse of the monolayer, common for saturated acyl chain-based phospholipids (see Chapter 3), would indicate a highly polar monolayer where the small regions of tear lipid remaining at the interface maintains a stable film at high compression would seem to suggest some sort of effect. The significant differences between subject samples from worn lenses might be caused by the usual inter-subject variability that is often found as a result of a subjects unique tear chemistry. However, the varied amounts of DMPC released from each lens cannot be dismissed as a factor in the π -A isotherm data. The low loading volumes necessary to achieve a maximum surface pressure indicates a large concentration of DMPC extracted from Dailies Total-1. This is under the influence of a strong extraction solvent mixture: in this case a 1:1 w/w mixture of chloroform and methanol.

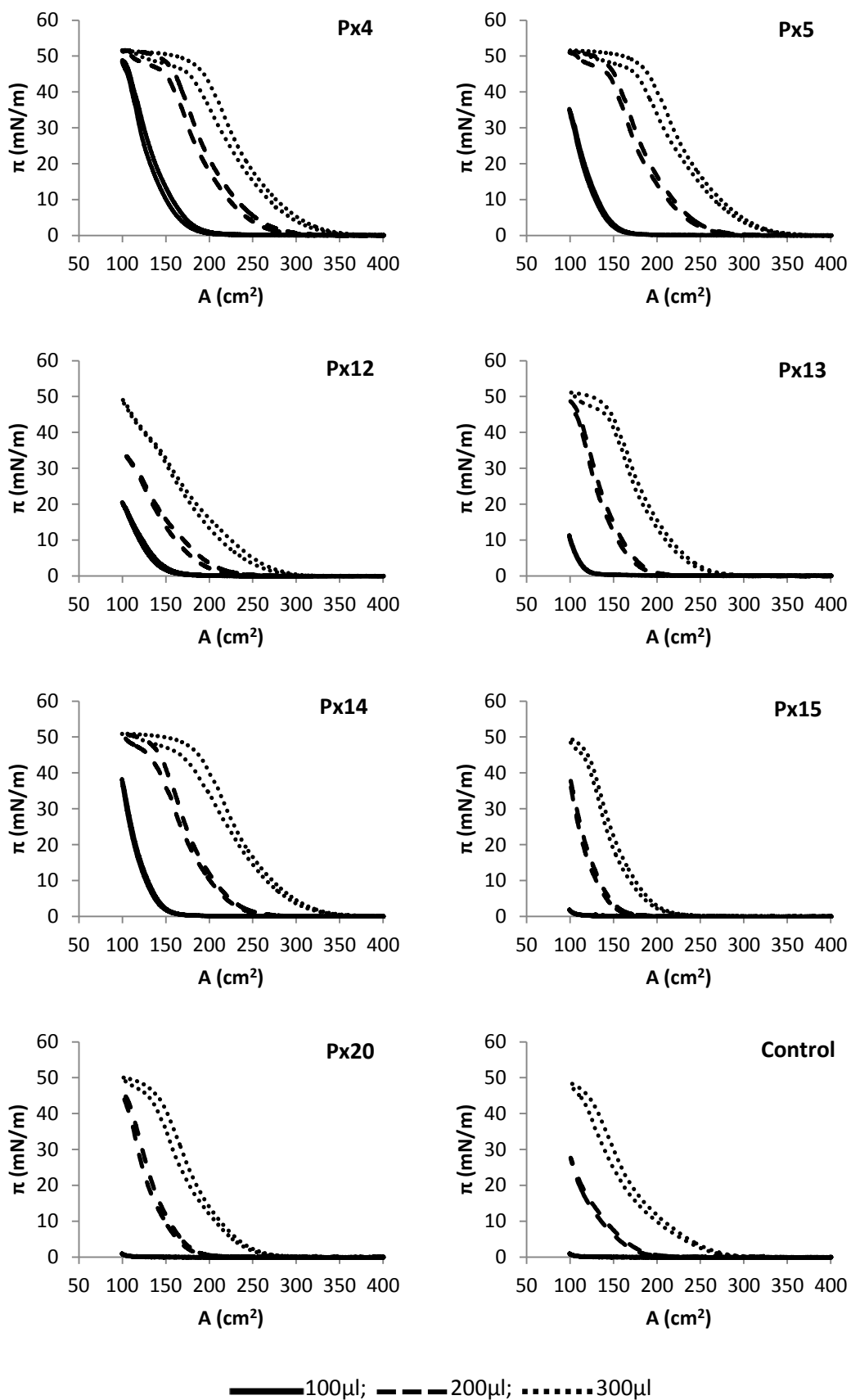


Fig 6.18. π -A isotherms for extracted Trial 1 worn and unworn DT1 contact lenses extracted in CHCl₃:CH₃OH (1:1 w/w).

6.2.3.2.2 Trial 1 Tear Samples and Lens Wipe Analysis

The harsh extraction conditions utilised on the worn DT1 lenses from Trial 1 does not indicate that any of the lipid molecules are released under natural tear conditions. Therefore, it is important to determine whether any difference can be observed and measured from tear samples collected during lens wear and a sample obtained from a lens wipe using a Visispear™ sponge after removal from the eye and before extraction. No significant difference between tear sample and lens wipe is that can be attributed solely to the release of DMPC in to the tear film. As DMPC is a significantly surface active molecule even at low concentrations (section 3.2.3.5), even a small released mass would be detectable as a significant change to the π -A isotherm. It is possible that the differences observed might be purely down to subject-to-subject and sample-to-sample variability.

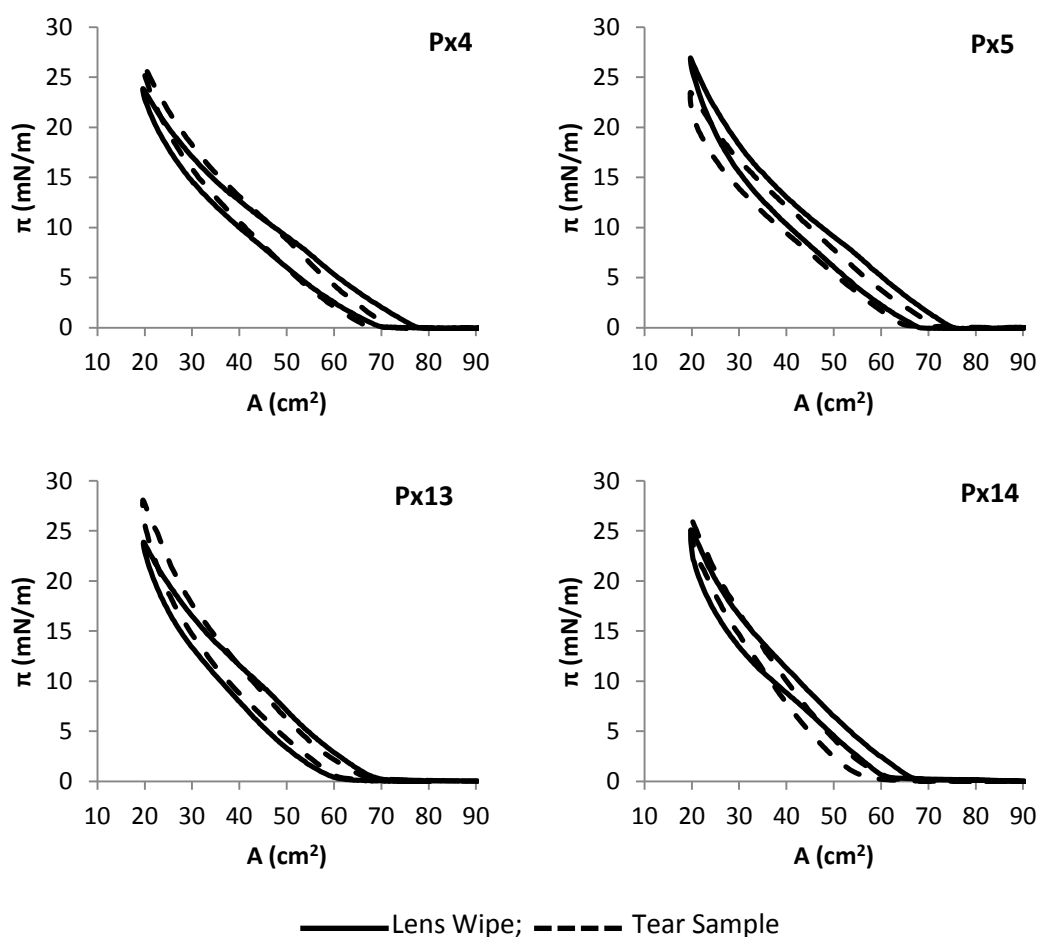


Fig 6.19. Comparative π -A isotherms of tear sample during wear and lens wipe after lens removal obtained from four subjects.

6.2.3.2.3 Trial 2 Lens Extractions

As part of Trial 2, subjects were asked to wear two different lens types simultaneously: an Acuvue TruEye lens in one eye and a Dailies Total-1 lens in the other. The π -A isotherms of extraction of these worn lenses as well as the extractions of control lenses are shown in Fig 6.20. The comparative isotherms show how much influence the lens material from both types of lenses has on the π -A isotherm of worn lens extracts. The Dailies Total-1 lens extractions show the strong influence of DMPC retained in the lens as opposed to transference into the tear film lipid layer. Acuvue TruEye has a significant amount of decanoic acid that is a part of necessary production methodologies that is retained within the lens. Similarly, Clariti 1day lenses release siloxanes and PVP that have been shown to produce surface activity. Whether this release of material is desirable, as in the case with Dailies Total-1 lenses, or undesirable, as in the case with 1-day Acuvue TruEye and Clariti 1day lenses, the material effect is significant and serves to equal or even dominate the surface behaviour of tear lipid sample collected from the lens.

The Dailies Total-1 lens showed a significant difference between the subject lens extraction and the control lens. Subject samples Px8 and Px9 obtained a plateau in surface pressure attained at $\sim 45\text{-}50\text{mN/m}$, whilst the others attained similarly high surface pressures. Compared to the control lens, the maximum surface pressure reached only $\sim 28.2\text{mN/m}$. As observed in the Trial 1 lens extractions, this difference may be purely down to differences in the DMPC content of the lens or of the extract. The Acuvue TruEye lens extractions recorded only small differences between the worn lens and the control lens. The π -A isotherms are very much characterised - in maximum surface pressure, isotherm pattern of, isothermal reversibility between compression and expansion cycle and surface areas where phase transition occurs - by the artificial material within the lens.

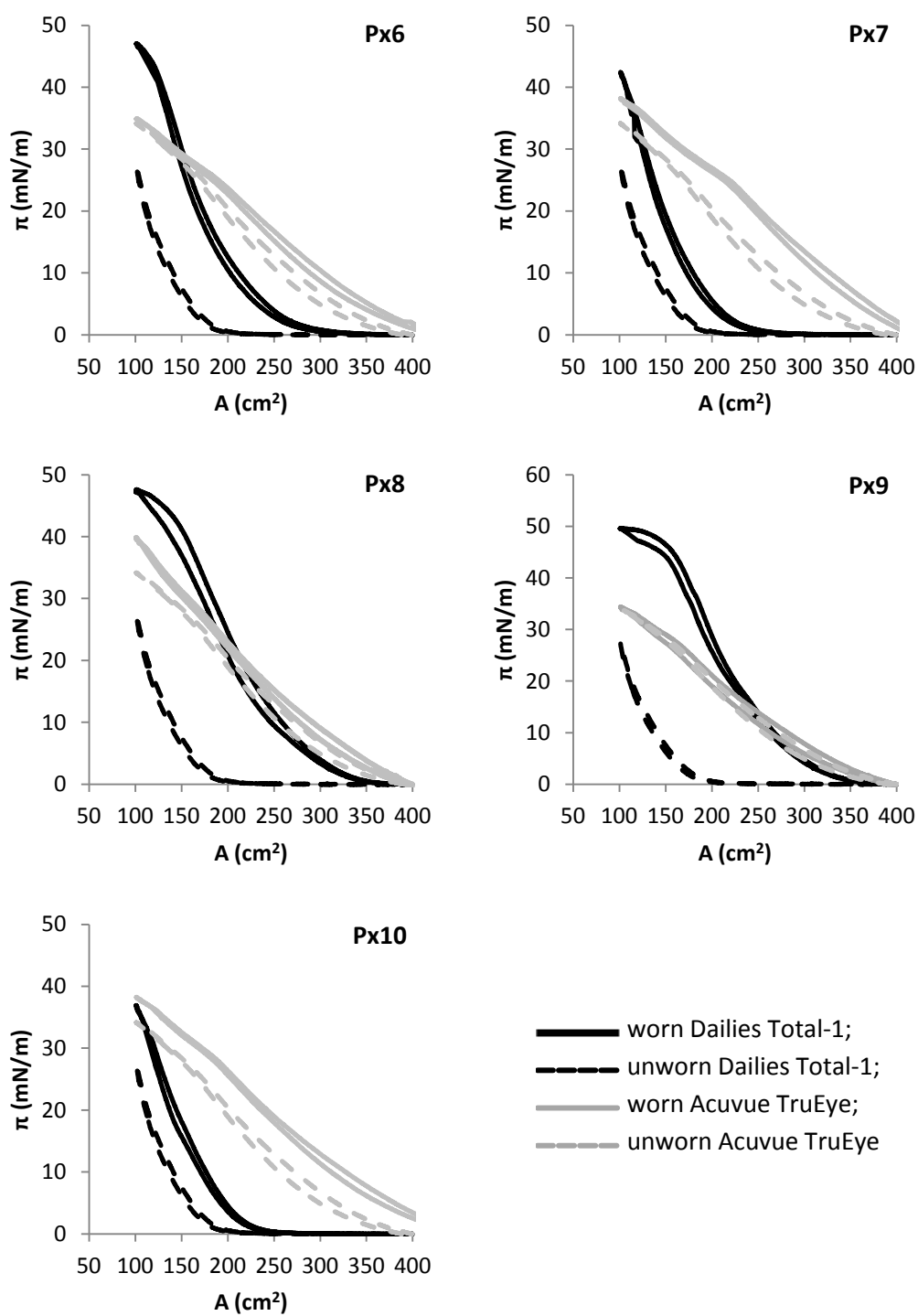


Fig 6.20. π -A isotherms for 200 μ l aliquots of extracted Trial 2 worn and unworn DT1 and TE contact lenses extracted in CHCl₃:CH₃OH (1:1 w/w)..

6.3 Discussion

6.3.1 Effect of Daily Disposable SiHy Lens Wear on the Tear Film

Daily disposable lenses forego the need for cleaning regimens whilst retaining the advantages offered by silicone hydrogel lenses (extended wear times, better end of day comfort, increased oxygen permeability). The first SiHy daily disposable lenses were often modifications to existing extended wear lenses. In order to produce cost effective lenses designed to be disposed at the end of a day's wear these lenses are often produced without surface modification utilised for extended wear lenses. Current lenses often incorporate monomers or other molecules that inherently produce a wettable surface, although these are still relatively hydrophobic compared to conventional hydrogel daily disposable lenses. As such, the surface of the lens will adsorb lipids. With the lens only being worn for a day, this is only a problem after a long day's wear.

The π -A isotherm data for the Clariti 1day lenses show higher maximum surface pressures and initial surface pressures, although data akin to the daily wear modality PureVision and Focus Night & Day lens extractions is observed. The large difference between the π_{\max} of the worn samples and the control lens would seem to indicate the limited effect of lens material extraction. The extraction of non-lipoidal materials from Clariti 1day lenses - observed in extractions of the control lenses - suggest a potential surface active behaviour for PVP and siloxane-containing compounds extracted from these lenses. This is to a lesser extent an issue as it is a common feature within extraction of SiHy lens extractions. The potential for lipid-based extraction of these compound within the lens-wearing tear film is minimal and may be comparable to the extraction using hexane.

Certainly with the Acuvue TruEye there is further evidence of increased material extraction with smaller volume aliquots of sample solution needed to achieve a maximum surface pressure for the sample. However, there may be a reason for such higher surface pressures and the minimum volume required to achieve a maximum surface pressure. In 2010, Acuvue TruEye lenses manufactured for the European and Asian markets (narafilcon A) had to be recalled due to the unexpected release of decanoic acid during wear, an acid utilised in the manufacturing process that is not fully removed. Patients reported increased levels of stinging, redness and other comfort issues upon lens insertion [277] [278]. Decanoic acid is an organic

acid with ten carbons within the chain. Normally, organic acids with twelve or less carbons are not amphiphilic due to the polar carboxylic acid group overpowering the hydrophobic carbon chain. As such, decanoic acid lies near the soluble/insoluble border and could potentially have an effect on surface pressure when incorporated within a monolayer obtained through worn lens extraction.

What we can infer from the data obtained from the π -A isotherms is that significant levels of released lens material can potentially affect the surface chemistry of extractable tear lipid molecules. Without actual data regarding the amount of decanoic acid that is retained within the lenses after production - especially in comparison to the amount of tear lipids that can absorb to the lens surface - it is not possible to know the cause of the comfort issues reported in terms of surface chemistry. But is it entirely detrimental to surface stability? From a purely surface chemical standpoint, the additional increase in surface pressure would tend to lower the surface/interfacial tension of the monolayer at the surface. Within the eye, the potential release of decanoic acid in to the tear film lipid layer may act in a similar manner to other free fatty acids thought to form a significant portion of the polar subphase. With its ten carbon chain and on the borders of solubility/insolubility, it could potentially solubilise within the lipid phases and interact favourably with other polar lipids.

6.3.2 Hildebrand Solubility Parameters

The effectiveness of a solvent depends upon the ability to selectively solubilise wanted material (such as tear lipid molecules) whilst minimising or eliminating the extraction of unwanted material (such as lens material polymers). The effectiveness of solubilisation can be defined by the Hildebrand [295] [296] [297] [298] solubility parameters (Table 6.3). The Hildebrand solubility parameter indicates the relative solvency behaviour of a specific solvent or solvent mixture derived from the cohesive energy density and heat of vaporisation. Hexane and chloroform are efficient at removing surface-bound tear lipids. Chloroform is a much better solubilising solvent than hexane according to the degree of swelling cohesion parameter within a linseed oil film (>80 times as powerful) [295] [299].

	C_6H_{14}	$C_6H_{14}:CH_3OH$ (9:1)	$CHCl_3:CH_3OH$ (1:1)
δ_t	14.90	16.38	24.20

Table 6.3. Hildebrand solubility parameters (δ_t ; MPa^{1/2}) of the three solvent mixtures.

The π -A isotherm data for the worn and unworn Clariti 1day lenses at the 1000 μ l aliquot can be found in Table 6.4. A general pattern for both worn and unworn Clariti 1day samples is observed where maximum surface pressure increases by the order $C_6H_{14} < CHCl_3:CH_3OH$ (1:1 w/w) $< C_6H_{14}:CH_3OH$ (9:1 w/w)). The ratio of worn to unworn maximum surface pressures obtained from the Clariti 1day lenses also indicate the affect of solvent solubility: C_6H_{14} (~ 2.1 x) $> CH_3Cl:CH_3OH$ 1:1 w/w (~ 1.6 x) $\approx C_6H_{14}:CH_3OH$ 9:1 w/w (~ 1.5 x). The 1-Day Acuvue TruEye (TE) hexane extracted samples produced lower π_{max} values compared to the other two solvent mixtures is observed (Table 6.4). The ratio of the π_{max} between worn and unworn is lower (~ 1.3 x). The TE unworn samples produced higher π_{max} values for the $C_6H_{14}:CH_3OH$ (9:1 w/w) samples than the $CHCl_3:CH_3OH$ (1:1 w/w) samples, a similar pattern to that observed within the Clariti samples. Conversely, the worn lens samples obtained the opposite, with π_{max} values being higher for the $CHCl_3:CH_3OH$ (1:1 w/w) samples than the $C_6H_{14}:CH_3OH$ (9:1 w/w) samples. The ratio of between for the two methanol-containing solutions were relatively similar to those observed in, although an increase was observed for the $CHCl_3:CH_3OH$ (1:1 w/w) samples (C_6H_{14} (~ 1.3 x) = $C_6H_{14}:CH_3OH$ 9:1 w/w (~ 1.3 x) $< CH_3Cl:CH_3OH$ 1:1 w/w (~ 1.5 x)).

Clariti 1day π -A isotherm data (1000 μ l aliquot)			
	δ_t (MPa $^{1/2}$)	π_{max} (mN/m)	
		Worn (SD)	Unworn
C_6H_{14}	14.90	24.02 (SD = 2.42)	12.15
$C_6H_{14}:CH_3OH$ (9:1 w/w)	16.38	36.46 (SD = 2.87)	23.09
$CH_3Cl:CH_3OH$ (1:1 w/w)	24.20	33.92 (SD = 2.45)	19.80

1-Day Acuvue TruEye isotherm data (500 μ l aliquot)			
	δ_t (MPa $^{1/2}$)	π_{max} (mN/m)	
		Worn (SD)	Unworn
C_6H_{14}	14.90	33.09 (SD = 1.50)	24.90
$C_6H_{14}:CH_3OH$ (9:1 w/w)	16.38	45.36 (SD = 1.45)	34.45
$CH_3Cl:CH_3OH$ (1:1 w/w)	24.20	48.05 (SD = 0.61)	32.29

Table 6.4. π_{max} data for Clariti 1day (1000 μ l aliquot) and 1-Day Acuvue TruEye (500 μ l aliquot) and Hildebrand solubility parameter of the three extraction solvents.

Within the worn and unworn Clariti 1day lens extracted sample data and the unworn sample data from TruEye, there is a relationship between Hildebrand solubility parameter and the maximum surface pressure. By comparing this to the relationship between swelling of a linseed oil film based on the Hildebrand solubility parameter, it is observed that there is a certain range within the parameter scale of maximum swelling and extraction [295] [296] [299]. Fig 6.21 shows the relationship between the π_{\max} data obtained for the worn and unworn samples obtained from two DD SiHy contact lenses and the calculated Hildebrand values for the three solvents (Table 6.3). The inclusion of a small percentage in methanol in hexane (10%) is shown to increase maximum surface pressure of both worn and unworn samples at, generally, smaller volume aliquots.

According to Feller et al [299], chloroform is ~80 times more powerful than hexane or methanol at swelling the linseed oil film that was tested. However, the inclusion of larger proportion methanol in the $\text{CHCl}_3:\text{CH}_3\text{OH}$ (1:1 w/w) solvent seems limit the beneficial solubilisation behaviour of chloroform. Whilst the solubility of lipid materials in methanol is low, its inclusion in the extraction solvents might potentially serve a different purpose. It is thought that the inclusion of methanol swells the lenses, aiding in the ability for the chloroform and hexane portions of the solvent to extract lipids that are immobilised within the contact lens matrix.

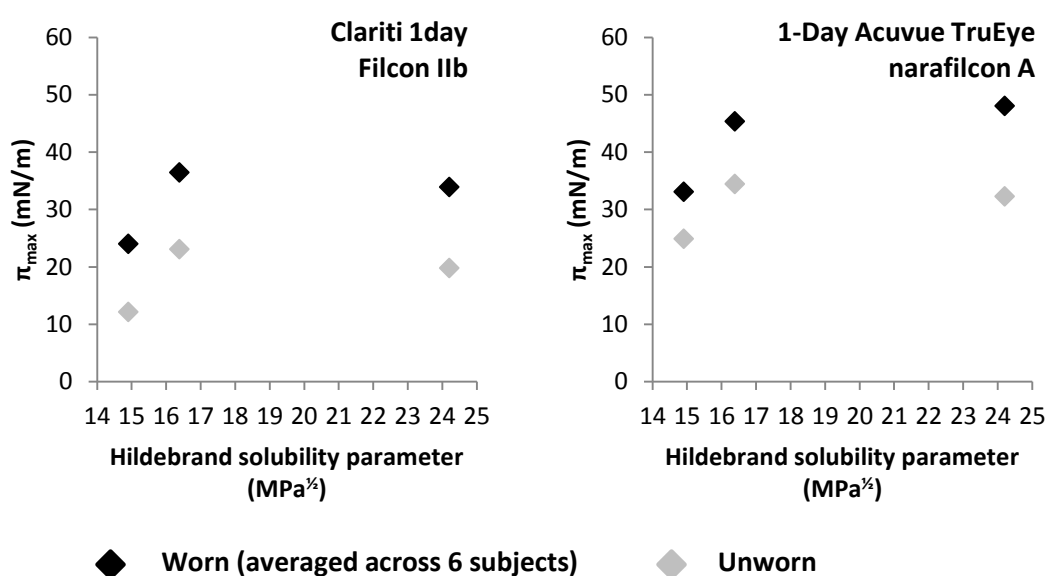


Fig 6.21. Relationship between π_{\max} and Hildebrand solubility parameter of the extracted sample data for Clariti 1day (1000 μl aliquot) and 1-Day Acuvue TruEye (500 μl aliquot).

By utilising the Hildebrand solubility parameter, it is possible to use a solvent more suited to extraction from a contact lens or to formulate a solvent mixture that will maximise the extraction of desirable test sample whilst minimising the amount of unwanted material. Whilst the Hildebrand parameter provides a good insight in to the behaviour of the solvent/solvent mixture, there are a few exceptions. Therefore, the Hansen solubility parameters may provide more information on the behaviour of the sample [295] [298]. This splits the total Hildebrand parameter of a solvent or solvent mixture in to three components: the dispersive component, the polar component and the hydrogen bonding component.

The Hildebrand parameters for contact lens polymeric components indicate a potential solubilised within the lipid film that are retained during extraction. It may be a reason why decanoic acid and small molecular weight polymer chains (e.g. PVP, mPDMS etc) are also extracted. PDMS (a common polymer in SiHy lenses) has a Hildebrand solubility of $14.93 \text{ MPa}^{1/2}$ which is relatively similar to lipid based on sample cholesterol ($18.81 \text{ MPa}^{1/2}$) and isopropyl myristate ($16.40 \text{ MPa}^{1/2}$). PHEMA (the commonest material used in conventional hydrogel materials) has a Hildebrand value of $\sim 25\text{-}27 \text{ MPa}^{1/2}$. From this data we can understand why siloxy-containing polymer chains (such as PDMS or TRIS) can be extracted in lipid and why CoHy materials are not extracted in high amounts.

6.3.3 DMPC Release from Focus Dailies Total-1 Lenses

The pre-ocular tear film contains in the region of $9\mu\text{g}$ of lipid [2] [30] and an influx of small masses of phospholipid released from DT1 lenses could affect the surface behaviour. It was important to investigate whether this release into the tear film could be detectable in the π -A isotherm data obtained from patient samples taken during lens wear. No significant release of DMPC was detectable in terms of the surface behaviour of tear samples taken from the lens-wearing eye, whether through a direct sample taken from the tear film or from the deposited lipids taken from a wipe of lens surface after removal.

Post-wear analysis of the extracts of the worn clinical lenses exhibited π -A isotherms that were comparable to similar studies of pre-production lenses, the control clinical lens and pure DMPC (see Section 3.2.3.5). The large observable release of DMPC from both pre-production and clinical lenses is a consequence of harsher extraction procedure used when compared to natural turnover of lipids within the tear film. This would indicate that the hydrophobic

interactions between phospholipid and the silicone hydrogel lens matrix material may be too strong to overcome for the lipids to diffuse spontaneously into the tear film. There is also a potential inability for the DMPC molecules to penetrate and diffuse through the conventional hydrogel surface coating utilised to improve the hydrophilicity of the lens surface.

It would therefore be beneficial to study the effect of DMPC release from the clinical lenses into a control artificial tear fluid (ATF), rather than solvent extraction, to determine any significant change detected in the π -A isotherms. Preliminary work on the pre-clinical lenses from Batch 1 showed no significant change in the data and the shape of the π -A isotherms over a 6 hour period (not published here). Only small changes were observed in maximum surface pressure ($\sim 1\text{mN/m}$ increase per hour), initial surface pressure (if $\pi_{\text{init}} > 0\text{mN/m}$ or transition area (if $\pi_{\text{init}} = 0\text{mN/m}$), and in hysteresis between compression and expansion cycles. In two separate studies, Pitt et al found that $<5\%$ of DMPC loaded onto a contact lens was released in to an ATF that contained many of the components found within the tear film - $\sim 1\text{-}4\mu\text{g}$ over a two-hour time period [280] [300]. The majority of the released phospholipid molecules eluted from the lens within a couple of hours. The slight increases observed in the π -A for each hourly interval might suggest this small amount of DMPC having some sort of interactive effect within the ATF. However, without a larger increase in levels of DMPC released in to the tear film lipid layer over the course of the day, this effect is kept at a minimum and comfort issues will remain in the in-vivo system.

6.4 Summary

The following conclusions can be observed from the experimental data within this chapter.

- The choice of solvent for extraction is important and affects the π -A isotherm data to a considerable degree based upon the Hildebrand and Hansen solubility parameters of the solvent or solvent mixture. Future design of sample extraction protocols should consider these parameters to maximise lipid material and minimise unwanted material being extracted;
- The solubilisation of lens polymeric material in the lipid phase can also be due to the similarities in Hildebrand solubility parameter values. This may contribute to the higher π_{max} values observed within the methanol-containing solutions, with larger amounts of both lens material extracted as the amount of lipid also increases;

- Significant differences were observed in the π -A isotherms of the tear samples obtained from the two lens materials:
 - The π -A isotherm data for Clariti 1day lens samples was comparable to the data obtained for the DW modality lens samples in Chapter 5 in terms of π_{\max} and surface concentration where this occurs;
 - Acuvue TruEye lens samples were shown to produce higher π_{\max} at much lower surface concentrations and larger G-LE transition areas or initial surface pressures for comparative volume aliquots;
 - Significant differences were observed between two different Acuvue TruEye lens types (narafilecon A / narafilecon B with higher maximum surface pressures recorded for both worn and unworn lenses;
- Individual subject variations between samples from both lens types worn were observed. The majority of samples attained similar π_{\max} but were often obtained at varied volume aliquots;
- The undesirable extraction of lens material has a significant effect on the π -A isotherms of extracted worn lenses.
 - Clariti 1day control lens extraction indicated significant material-based issues possibly due to extraction of siloxy material and/or PVP that may be surface;
 - Acuvue TruEye lens samples (from both narafilecon A and narafilecon B lens sample) were dominated by the unintended extraction of decanoic acid into the sample;
- Focus Dailies Total-1 DMPC-containing contact lenses;
 - The π -A isotherm data of extracted worn Dailies Total-1 lenses was shown to be dominated by DMPC that indicated a large concentration of the phospholipid remained within the lens matrix;
 - No significant observation of a change in the π -A isotherms that would indicate desirable release of DMPC into the tear film of the lens-wearing eye or within the biofilm of the lens after removal from the eye.

Chapter 7

Summary, Conclusions and Suggestions for Future Work

7.1 Summary and Conclusions

The main focus of the work described in this thesis was to evaluate the Langmuir trough method as a tool for measuring and understanding the surface chemical behaviour and stability of the tear film lipid layer, with particular reference to the usefulness in relation to contact lens wear. The Langmuir trough method allows the study of the tear film dynamics during compression and spreading in an in-vitro environment that would be impossible to replicate for in-vivo measurement. It was the intention to see how the stability of the tear film can be affected - whether beneficially or detrimentally - by various factors within the contact lens wearing eye.

7.1.1 Tear Film Lipid Component Behaviour

The surface chemistry of the lipid-aqueous interface is predominantly based upon the tear lipid content. It is important to understand how the various tear lipid types and the fatty acid content within these molecules behave at an interface [10] [12] [13] [18] [19] [41] [57]. From the data obtained in Section 3.2, the polar lipids (such as phospholipids, free fatty acids, free fatty alcohols, di- and monoacylglycerides) are highly surface active obtaining surface pressures in excess of 40mN/m with the presence of an LC phase at high surface concentrations. Cholesterol also shows high degrees of surface activity, despite the large hydrophobic 4-ring structure. The spreading conditions these surface active molecules enable the formation of a stable film that interacts favourably with the aqueous phase.

Non-polar lipids such as cholesterol esters, wax esters and triacylglycerides show no significant surface activity in themselves. Any surface activity that was observed is a possible consequence of hydrolysis of the bonds to form surface active fatty acids, fatty alcohols, cholesterol and DAGs/MAGs. As the π -A isotherms for these lipids reported in Chapter 3 were recorded after reaching equilibrium, there was ample time for these molecules to degrade into component molecules that induce surface activity. Lipids that contain unsaturated fatty acids reach a lower maximum surface pressure but no discernible collapse of the monolayer is observed. The film remains stable upon reaching the maximum surface pressure, remaining at

this level up to the minimum working area. Subsequent compression and expansion retain π -A isothermal data similar to the previous, such as initial surface pressure, transition surface pressures, transition areas and reversibility, until an equilibrium is reached. Conversely, lipids that are composed of saturated fatty acids reach a higher maximum surface pressure but continued compression induces monolayer collapse.

7.1.2 Tear Film Protein Component Behaviour

Non-lipoidal components of the tear film have been observed to have a degree interactive role in the surface behaviour at the lipid-aqueous interface that might affect the stability of the lipid layer. Aqueous layer components such as proteins and mucins have been highlighted as potential contributors to interfacial stability by interacting with the lipid layer through adsorption or by penetration [38] [217].

Evidence from Section 3.3 indicate that the analogues of tear proteins and mucins investigated have significant surface activity, but in some cases only in high concentrations far exceeding that of the tear film. The adsorption of protein and mucin analogues was shown to influence a change in surface activity that would indicate a beneficial effect on the stability of the tear film. Normal relaxation of a tear sample monolayer indicated a significant decrease from a π_{init} of 10mN/m to a π_{eq} of ~4.5mN/m. Incorporation of bovine serum mucin - as a soluble mucin analogue - produced $\pi_{eq} \approx \pi_{init}$. β 2-microglobulin (a tear lipocalin analogue) and lysozyme produced an increase in surface pressure to π_{eq} values of >20mN/m and ~13mN/m respectively, indicating an active role on decreasing the surface tension of the tear sample monolayer between these protein analogues and the tear sample components. Changes were also observed to the π -A isotherm of the tear sample monolayer before and after the injection of protein/mucin analogues with increases in π_{max} and G-LE transition area and a decrease in reversibility observed.

The data obtained in Section 3.3 correlates with similar literature data that used extracted protein or mucins from the tear film or by utilising similar analogues. Tear lipocalin has been shown to have surface activity in both apo- and holo-lipocalin forms upon a clean subphase and limited adsorption to prepared monolayer of Meibomian lipids or tear sample [226] [227] [301]. The release characteristics of lipids would not be detected at the pH of the subphase utilised in the Langmuir trough experiments. Similarly, lysozyme has also been shown to have

surface activity, although the adsorption to at Meibomian lipid and tear sample monolayer is limited compared to tear lipocalin [38] [113] [217] [301]. Evidence suggests that the antibacterial activity of lysozyme is a function of interaction with negatively charged phospholipids. Within the tear film, lysozyme is thought to act as a more type-specific lipid binder that acts similarly to lipocalin in transportation and/or removal of lipids [113] [114]. Surface pressure studies have indicated that mucins have surface activity but only at concentrations far larger than that found within the tear film [38] [217] [228] [301]. Despite this fact, ocular mucins are likely to be present at the surface of the tear film where they will have an effect in lowering surface tension of the lipid-aqueous interface through reorganisation of the lipids and alteration to the viscoelastic properties of the lipid layer [38] [228].

7.1.3 Tear Sampling Methodology

The collection of tear samples for in-vitro surface pressure measurements in order to gain an understanding of the in-vivo system of stabilisation through surface chemistry. Four commonly utilised tear analysis probes - glass microcapillary tubes, Schirmer strips, Visispear™ ophthalmic sponges and Focus Night&Day contact lenses - were tested to determine the efficacy of each sample probe technique. The three main considerations that must be made in order to determine the efficacy of the method are: amount of sample collected/extracted, types of material collected and the influence of extractable probe material.

The preliminary sample extraction and preparation work in Chapter 4 indicated differences in the amount of surface active molecules obtained. The glass microcapillary tubes (Section 4.3.1) provide small concentrations of extractable material. Even at maximum loading volumes, samples did not achieve a maximum surface pressure and repeatable experiments using the same sample was not possible. Samples collected using Schirmer strips (Section 4.3.2) and Visispear™ ophthalmic sponges (Section 4.3.3) provided π -A data at an equilibrium for sample, with the sponges requiring less of the extraction solution to achieve maximum surface pressures. As both of these methods are based upon the flow of tears and adsorption of the probe material, the extraction procedure should reflect the choice of sample required: variations based upon lipid composition or amount of sample collected. Extraction of control probes was observed to contaminate the sample with extractable cellulosic material shown by the large influence on the maximum surface pressure.

Extraction of contact lenses also provides a large amount of usable extracted material based on the amount of lipids adsorbed to the surface (Section 4.3.4). It has been shown, regardless of the choice of extracting solvent, that the methods that produce surface activity with small volumes of utilised solvent also show an influence from the probe material. The inclusion of methanol as part of a solvent mixture, even at 10% of the total volume, increases the amount of probe material extracted. It is important that the materials used in the fabrication of these sampling probes do not interfere directly in surface pressure measurements when extracted alongside tear samples. Collection of samples extracted from contact lenses are limited to those that wear them and is dependent upon lens material and wear modality. Samples are not reflective of the natural tear film due to the alterations wrought upon it by the lens.

The most commonly used collection technique used in Langmuir surface pressure balance experiments has been the direct collection of lipid material from the Meibomian glands [152] [156] [217] [227]. This method requires the mechanical expression of the glands to produce Meibomian lipids to be collected by a small spatula. This will involve a degree of trauma, regardless of the 'gentle' massage often employed, and can often contaminate the Meibomian lipid sample with those of other sources. Compositional analysis of aqueous tears and meibum show the lipids found within tears are more complex than those collected from the Meibomian glands [22]. Whilst the Meibomian glands produce the majority of the lipids found within the tear film lipid layer, other sources of lipid such as the glands of Moll and Zeiss, the conjunctival and corneal surfaces and from lipid produced by lacrimal glands and found within the aqueous tears [22] [38] [74] [76].

Comparisons between the π -A isotherms of samples collected directly from the Meibomian glands and from the collection methods utilised in this thesis (Chapter 4) indicate similarities in the data: maximum surface pressure values are ~ 25 - 35 mN/m with a smooth transition from gaseous to liquid expanded phase is observed. Reversibility denoted by the hysteresis between compression and expansion isotherms is high, with similar molecular interaction observed when the molecules are compressed together and then spread during the expansion cycle.

7.1.4 The Fate of Lipids on Contact Lenses

The study of samples obtained from adsorbed lipid material on contact lenses based upon lens material and wear modality was the main focus of this thesis (Chapter 5 and 6). The fate of lipid adsorbed onto the lens surface during wear is an important indicator to the biocompatibility of the lens over the course of a day or an extended period of wear. The lens material also has an effect on the amounts and types of lipids deposited. Within silicone hydrogel contact lenses, deposition will depend on the silicone monomers included within the lens matrix and whether any surface treatment or internal wetting agents are present. Differences in the amount of lipid and lens material extracted were observed between the four different contact lenses extracted.

Significant differences observed between the samples obtained from the two extended wear lens materials (Chapter 5). PureVision lenses (Section 5.3.2) extracted more material than the Focus Night&Day lenses (Section 5.3.1) indicated by higher maximum surface pressures and larger G-LE transition areas or initial surface pressures for comparative aliquot volumes. Significant differences were observed in the surface pressure-area profiles of the samples obtained from the two daily disposable lens materials (Chapter 6). The π -A isotherm data for Clariti 1day lens samples (Section 6.3.1) was comparable to the data obtained for the extended wear lenses in Chapter 5. Acuvue TruEye lens samples (Section 6.3.2) were shown to have much higher amounts extracted, indicated by higher maximum surface pressures and larger G-LE transition areas or initial surface pressures for comparative volume aliquots. Significant differences were observed between two different Acuvue TruEye lens types - narafilcon A (UK/Europe market lens) and narafilcon B (US market lens). Although only slight differences in water content and oxygen permeability is present, narafilcon A produced higher maximum surface pressures for both worn and unworn lenses.

Maximum surface pressures were attained at lower sample solution volumes for the two daily disposable lenses (Acuvue TruEye and Clariti 1day) as a result of no surface treatment. PureVision worn wear lens samples required similar volumes to attain a maximum surface pressure due to the documented movement of surface polymers after treatment to produce more regions of hydrophobicity. Samples obtained from Focus Night&Day worn lenses required slightly higher volumes to be applied to the surface to attain a maximum surface

pressure of the sample (therefore higher surface concentrations) that indicates less lipid deposition upon the lens surface.

Upon insertion of a contact lens, the interaction between tear lipids and the lens material begins almost immediately. Deposition of lipid molecules is a function of the characteristics of the contact lens material, specifically those within the bulk polymer matrix and at the lens surface [263]. Lipids preferentially deposit onto hydrophobic surfaces because of hydrophobic-to-hydrophobic interactions [264]. The monomers utilised to form the bulk polymer matrix affects the overall and type-specific adsorption of lipids. Certain lipid types have a greater affinity to different monomers [194] [265] [266]. Levels of lipid deposition have been observed to increase on silicone-containing contact lenses due to the greater hydrophobicity of the silicone functional groups added into the polymer matrix to increase oxygen permeability [267]. Incorporation of the N-vinylpyrrolidone (NVP) monomer has also been shown to increase lipid deposition [195].

Surface modification techniques are often necessarily employed to improve the biocompatibility of silicone hydrogel contact lenses within the tear film although these lenses remain relatively hydrophobic when compared to conventional hydrogel lenses [267]. FN+D lens surfaces are modified in a gas plasma reactive chamber that creates a 25nm thick hydrophilic surface [268]. PV lenses are also modified within a gas plasma reactive chamber but under a different method that transforms silicone components on the lens surface into hydrophilic silicate compounds [267]. Despite similar methods of surface modification, there are differences observed in hydrophobicity between lens types. PV lenses exhibit a higher contact angle and therefore less wettable than FN+D [269] [270] [271]. The key difference in the surface characteristics is that the plasma coating on FN+D lenses forms a homogenous layer of hydrophilicity, whereas the surface treatment of PV lenses produces a heterogeneous surface where more hydrophobic sites are exposed [267] [268].

The effect of wear modality between daily wear (DW) and continuous wear (CW) has an effect on the surface pressure-area profiles of the samples, observed in both Focus Night&Day (Section 5.3.1) and PureVision (Section 5.3.2) lenses. Generally, CW lens samples showed significantly lower maximum surface pressures obtained at larger surface concentrations. This is a result of the inclusion of a cleaning regime that may. It suggests that the lipids on DW lenses are fresher compared to the immobilised lipids on CW lenses. The π -A isotherm data for

Clariti 1day lens samples (Section 6.3.1) was comparable to the data obtained for the daily wear lenses in Chapter 5. Lipids deposit upon the lens surface immediately upon insertion and builds up throughout the day. In DW modality, these lipids are removed by cleaning regimes and multipurpose solutions, assuming a good compliance. However on CW modality lenses these lipids become immobilised and not removed through normal tear drainage which are increasingly susceptible to degradation by oxidation and hydrolysis [168] [174]. Daily disposable contact lenses do not suffer from either a lack of compliance for cleaning or prolonged immobilisation and degradation of lipids.

7.1.5 Tear Film Supplementation

The end-of-day issues of comfort and the commonly reported contact lens-related dry eye disease are major causes for discontinuation of contact lens use. It is thought that depletion of polar lipid is the predominant reason for a loss in tear film stability, quicker lipid layer break up [2] [42] [71] [191] and evaporation of the aqueous phase [41] [302]. Polar lipids have been used as components in pharmaceutical artificial tear solutions that have been developed to replenish the tear film lipid layer.

The beneficial effect on the surface activity of a tear sample monolayer through supplementation with DMPC or DPPC has led to their inclusion in new, novel techniques for introducing these molecules into the lens-wearing eye. Alterations to the π -A isotherm behaviour and monolayer properties of Meibomian lipids was observed with additions of DPPC [303] and free fatty acids such as oleic and linoleic acid [304] to monolayers of Meibomian lipids collected from human samples. The addition of free fatty acids, specifically unsaturated fatty acids (e.g. oleic acid, linoleic acid), was shown to increase maximum surface pressure. Addition of cholesterol and ceramides seem to have a deleterious effect to the stability of Meibomian lipid films [305]. In vivo studies of supplementation have demonstrated that these solutions produce a significant increase in the non-invasive break-up time of the tear film [283] [286] [287].

The results from this research indicate that Focus Dailies Total-1 contact lenses do not work as a phospholipid release device within the lens-wearing tear film (Section 7.3.2). Extraction of lenses, both worn and unworn, in commonly utilised extraction solvents obtains a large amount of DMPC. This overloads the monolayer and allows only a very minimal (if any) effect

from tear sample components to be detected in the π -A isotherms. Analysis of the tear samples should allow drastic changes caused by the release of DMPC to be detected. From the data obtained in the π -A isotherms of lens wipes and tear samples indicate that any DMPC from the lens is in a minute amount that does not significantly affect surface pressure. Despite the relatively small amounts (1-3 μ l) of DMPC that was released into an artificial tear film in studies by Pitt et al [280] [300], this may still be a significant amount that could alter the surface behaviour of the lipid layer beneficially. Further research of in-vivo samples will provide beneficial data in order to determine the efficacy of direct release of DMPC over the course of a day's contact lens wear in terms of a surface behaviour consideration.

7.2 Suggestions for Future Work

The study of the surface behaviour of the tear film lipid layer is still very much in its infancy. Further work is necessary to gather more information on the surface behaviour of the tear film lipid layer and what can affect the stability of this layer. The following points are suggestions for future work to further develop the Langmuir trough method and the application to tear film studies.

1) Component studies:

- Artificial lipid layers based upon the composition of the tear film lipid layer in various healthy or unhealthy states - verified by compositional analysis of lipid type and fatty acid content detailed in the literature - may provide a better model;
- The study of other common tear protein components, using either extracted components from tears or analogues, to determine whether other aqueous proteins have a beneficial or detrimental effect to lipid-aqueous interface stability;
- The presence of the surfactant proteins A, B, C and D have been identified within the tear film as potential significant components of the tear film [120] [121] [122] [123]. Surfactant proteins B (SP-B) and C (SP-C) are embedded within the lipid component of the tear film orientated due to the amphiphilic characteristics and are thought to fulfil a role in aiding the stability of the lipid-aqueous interface [122] [125] [126] [127].

2) Make refinements to the tear lipid collection and extraction methodology, and optimisation of Langmuir trough surface pressure measurements of tear samples:

- Developing the application of methods such as the Schirmer strip, Visispear™ sponges and microcapillary tubes to ensure that we are looking at the correct type of sample - the amount or composition of the lipid;
- Tests of other solvents for sample probe extraction to maximise amount of lipid but minimise extractable probe materials based upon Hildebrand and Hansen solubility parameters;
- Utilisation of the two stage sample preparation using separate solvent systems for extraction from probe and application to the Langmuir trough discussed in section 4.4;
- Development of a model subphase solution that models the protein, electrolyte, metabolite and pH of the tear aqueous layer;
- Development of the methodology for a smaller Langmuir trough with a working surface area of $\sim 2\text{cm}^2$ that models the palpebral aperture of the cornea with a depth of $\sim 0.2\text{cm}^2$ to better replicate the thickness of the tear film;

3) Comprehensive clinical studies of tear samples obtained from a wide sample of the population to observe and measure surface behaviour due to alterations in lipid amount/composition as a consequence of different individual factors:

- Study of the lipid layer altered by changes to the biochemistry caused by ocular diseases and/or dysfunctional states. For example, Meibomian gland dysfunction (MGD) alters the quality of the tear lipid that is more viscous and less fluid than normal meibum that would impede delivery to the lid margin [76] [155] [259] [306] [307].
- Age-related alterations in the stability of the tear film as age increases. Research has indicated a decline in the production of key tear film components as a result of the loss of function of the lacrimal glands, Meibomian glands and goblet cells throughout life [308] [309] [310] [311];
- Comparison of the alterations in surface behaviour between the pre-ocular and pre-lens tear film might give indications to contact lens tolerance/intolerance. This would require collection of samples from a wide range of subjects that show different degrees of lens tolerance by taking samples prior to and during lens wear alongside commonly used ophthalmic comfort surveys and questionnaires;

- Further study of the fate of lipids adsorbed upon the surface of the contact lens should be to include a wider range of conventional and silicone hydrogel lens types, and wear modality, including single week or fortnight wear in addition to daily disposable and monthly wear.

4) Incorporate additional techniques can be run concurrently with Langmuir trough experiments or separate to the surface pressure measurement but using the same sample material:

- The fluidity of the lipid layer varies due to the change in forces over the course of a blink. Interfacial rheology measures the viscoelastic properties of a tear lipid monolayer. An interfacial stress rheometer (ISR) [312] [313] can be run alongside π -A isotherm measurement and allows the measurement of the interfacial viscoelasticity of lipid monolayers at various surface pressures;
- Surface potential of a monolayer is the difference between the clean subphase surface and a monolayer-covered surface [224] due to dipole moments of the monolayer components, reorientation of water molecules at the surface and interaction between the head-groups of surfactants and the subphase. Surface potential can be measured by the vibrating capacitor technique or the ionising electrode technique [224];
- The use of analytical techniques such as gas chromatography mass spectroscopy (GCMS) and high pressure liquid chromatography (HPLC) can provide information on the fatty acid content of and the amount of each lipid class.

5) Supplementation of the tear film, especially within the pre-lens tear film during contact lens wear, is important to improve the stability and health of the ocular system. Contact lens delivery systems require location-specific delivery and timed release of lipids.

- Further study of the efficacy of tear aqueous-extractable lipid compounds that can aid in improving the structure of the lipid layer;
- Further experimentation of the release capability of DPPC from PSMA-based Astosome conjugates. The surface active polymer micelle would adsorb at the lipid-aqueous interface, the polymer chains would unravel due to interactions with the lipid layer and release the DPPC molecule into the polar lipid sublayer [314].
- Dietary supplementation of omega-3 and omega-6 fatty acids may improve lipid layer stability either as a source of polar lipids or to improve the expression of lipids from the Meibomian glands. Omega-3 fatty acid supplementation is likely to be more

beneficial due to its ability to reduce inflammation of eyelids and Meibomian glands that could alleviate blepharitis, MGD and dry eye-associated issues in contact lens wear [315] [316] [317] [318] [319].

6) Multipurpose solutions (MPS) used in contact lens care regimens include surfactant polymer components designed to clean lipids and proteins adsorbed to the lens surface. The surfactant poloxamer (Pluronic™) and poloxamine (Tetronic™) molecules are amphiphilic copolymers of hydrophilic polyethylene oxide (PEO) and hydrophobic polypropylene oxide (PPO) chains [320] [321] [322]. These molecules are surface active and absorb at an interface between two dissimilar phases [323] [324] [325] [326] [327] [328] [329] [330] [331].

- In addition to the study of the fate of lipids on different types of lenses, it would also be prudent to evaluate the effect of different MPS in cleaning lenses;
- Whilst there may be a beneficial consequence of adsorbed surfactants in improving the hydrophilicity of the lens surface, these surfactant molecules may be released in to the tear film when the lens is worn after cleaning. The small amounts loosely bound to a lens surface and carried from cleaning vessel into the tear film is enough to provide significant surface activity that could disrupt the lipid-aqueous interface stability:
 - Persistence tests of MPS and surfactant molecules on different lens types by replicating normal lens cleaning regimes in lens cases;
 - Potential simulated release from lenses in to an artificial tear film to determine any significant release of surfactant molecules over time;

References

- [1] J. P. Craig, "Structure and function of the precorneal tear film," in *The tear film: structure, function and clinical examination*, Oxford, Butterworth-Heinemann, 2002, pp. 18-50.
- [2] A. J. Bron, J. M. Tiffany, S. M. Gouviea, N. Yokoi and L. W. Voon, "Functional aspects of the tear film lipid layer," *Exp Eye Res*, vol. 78, pp. 347-360, 2004.
- [3] J. I. Prydal, P. Artal, H. Woon and F. W. Campbell, "Study of human precorneal tear film thickness and structure using laser interferometry," *IOVS*, vol. 33, pp. 2006-2011, 1992.
- [4] J. I. Prydal and F. W. Campbell, "Study of precorneal tear film thickness and structure by interferometry and confocal microscopy," *IOVS*, vol. 33, pp. 1996-2005, 1992.
- [5] P. E. King-Smith, B. A. Fink, N. Fogt, K. K. Nichols, R. M. Hill and G. S. Wilson, "The thickness of the human precorneal tear film: Evidence from reflection spectra," *IOVS*, vol. 41, pp. 3348-3359, 2000.
- [6] J. Wang, D. Fonn, T. L. Simpson and L. Jones, "Pre-corneal and pre- and postlens tear film thickness measured indirectly with optical coherence tomography," *IOVS*, vol. 44, pp. 2524-2528, 2003.
- [7] M. A. Lemp and H. J. Blackman, "Ocular surface defense mechanisms," *Ann Ophthalmol*, vol. 13, no. 1, pp. 61-63, 1981.
- [8] G. Smolin, R. A. Thoft and D. W. Lamberts, "Physiology of the tear film," in *The Cornea: Scientific Foundations and Clinical Practice*, London, Little Brown, 1994, pp. 439-456.
- [9] E. Wolff, "Muco-cutaneous junction of the lid margin and the distribution of tear fluid," *Trans Ophthalmol Soc UK*, vol. 104, pp. 351-354, 1946.
- [10] J. M. Tiffany, "The lipid secretion of the meibomian glands," *Adv Lipid Res*, vol. 22, pp. 1-62, 1987.
- [11] J. M. Tiffany, "Tear film stability and contact lens wear," *J BCLA*, vol. 11, pp. 35-38, 1988.
- [12] J. P. McCulley and W. E. Shine, "A compositional based model for the tear film lipid layer," *Trans Am Ophthalmol Soc*, vol. 95, pp. 79-93, 1997.
- [13] J. P. McCulley and W. E. Shine, "The lipid layer: The outer surface of the ocular surface tear film," *Biosci Reports*, vol. 21, no. 4, pp. 407-418, 2001.
- [14] R. J. Braun, "Dynamics of the tear film," *Ann Rev Fluid Mech*, vol. 44, pp. 267-297, 2012.
- [15] F. J. Holly, "Formation and stability of the tear film," *Int Ophthalmol Clin*, vol. 13, pp. 73-96, 1973.
- [16] D. R. Korb, J. V. Greiner, J. P. Herman, E. Hebert, V. M. Finnemore, J. M. Exford, T. Glonek and M. C. Olson, "Lid-wiper epitheliopathy and dry-eye symptoms in contact lens wearers," *Contact Lens Assoc Ophthalmol*, vol. 28, no. 4, pp. 211-216, 2002.
- [17] Y. Ohashi, M. Dogru and K. Tsubota, "Laboratory findings in tear fluid analysis," *Clin Chim Acta*, vol. 78, pp. 17-28, 2006.
- [18] I. A. Butovich, T. J. Millar and B. M. Ham, "Understanding and analyzing Meibomian lipids," *Curr Eye Res*, vol. 33, pp. 405-420, 2008.
- [19] J. P. McCulley and W. E. Shine, "Meibomian gland function and the tear lipid layer," *The Ocular Surface*, vol. 1, no. 3, pp. 97-106, 2003.
- [20] J. P. Craig, K. Blades and S. Patel, "Tear lipid layer structure and stability following expression of the meibomian glands," *Ophthalm Phys Opt*, vol. 15, no. 6, pp. 569-574, 1995.
- [21] A. J. Bron and J. M. Tiffany, "The meibomian glands and tear film lipids: Structure, function, and control," *Adv Exp Med Biol*, vol. 438, pp. 281-295, 1998.

- [22] I. A. Butovich, "On the lipid composition of human meibum and tears: Comparative analysis of nonpolar lipids," *IOVS*, vol. 49, no. 9, pp. 3779-3789, 2008.
- [23] J. E. Josephson, "Appearance of the precorneal tear film lipid layer," *Am J Optom Physiol Optics*, vol. 60, pp. 883-887, 1983.
- [24] N. Yokoi, A. J. Bron, J. M. Tiffany and S. Kinoshita, "Reflective meniscometry: a new field of dry eye assessment," *Cornea*, vol. 19, pp. s37-s43, 2000.
- [25] D. R. Korb, D. F. Baron, J. P. Herman, V. M. Finnemore, J. M. Exford, J. L. Hermosa, C. D. Leahy, T. Glonek and J. V. Greiner, "Tear film lipid layer thickness as a function of blinking," *Cornea*, vol. 13, pp. 354-359, 1994.
- [26] G. Foulks and A. J. Bron, "A clinical description of meibomian gland dysfunction," *Ocular Surface*, vol. 1, pp. 107-126, 2003.
- [27] M. Norn, "Meibomian orifices and Marx's line studied by triple staining," *Acta Ophthalmol*, vol. 63, pp. 698-700, 1985.
- [28] M. S. Norn, "Semiquantitative interference study of fatty layer of precorneal film," *Acta Ophthalmol*, vol. 57, pp. 766-774, 1979.
- [29] M. S. Norn, "Natural fat in external eye. Vital-stained by Sudan III," *Acta Ophthalmol*, vol. 58, pp. 331-336, 1980.
- [30] C. K. S. Chew, P. G. Hykin, C. Jansweijer, S. Dikstein, J. M. Tiffany and A. J. Bron, "The casual level of meibomian lipids in humans," *Curr Eye Res*, vol. 12, pp. 255-259, 1993.
- [31] G. N. Foulks, "The correlation between the tear film lipid layer and dry eye disease," *Surv Ophthalmol*, vol. 52, no. 4, pp. 369-374, 2007.
- [32] J. M. Tiffany, N. Winter and G. Bliss, "Tear film stability and tear surface tension," *Curr Eye Res*, vol. 8, no. 5, pp. 507-515, 1989.
- [33] J. M. Tiffany, "Surface tension in tears," *Arch Soc Esp Ophthalmol*, vol. 81, pp. 363-366, 2006.
- [34] G. T. Barnes and I. R. Gentle, *Interfacial Science: An Introduction*, 1st ed., Oxford: Oxford University Press, 2005.
- [35] D. J. Shaw, *Introduction to Colloid & Surface Chemistry*, 4th ed., Oxford: Butterworth-Heinemann, 1992.
- [36] F. J. Holly, "Surface chemistry of tear film component analogs," *J Coll Interface Sci*, vol. 59, no. 2, pp. 221-231, 1974.
- [37] J. C. Pandit, B. Nagyova, A. J. Bron and J. M. Tiffany, "Physical properties of the stimulated and unstimulated tears," *Exp Eye Res*, vol. 68, pp. 247-253, 1999.
- [38] B. Nagyova and J. M. Tiffany, "Components responsible for the surface tension of human tears," *Curr Eye Res*, vol. 19, pp. 4-11, 1999.
- [39] S. Mishima, "Some physiological aspects of the precorneal tear film," *Arch Ophthalmol*, vol. 73, pp. 233-241, 1965.
- [40] S. Mishima and D. M. Maurice, "The oily layer of the tear film and evaporation from the corneal surface," *Exp Eye Res*, vol. 1, pp. 39-45, 1961.
- [41] W. D. Mathers and J. A. Lane, "Meibomian gland lipids, evaporation, and tear film stability," *Adv Exp Med Biol*, vol. 438, pp. 349-360, 1998.
- [42] J. P. Craig and A. Tomlinson, "Importance of the lipid layer in human tear film stability and evaporation," *Optom Vis Sci*, vol. 74, pp. 8-13, 1997.
- [43] W. D. Mathers and T. E. Daley, "Tear flow and evaporation in patients with and without dry eye," *Ophthalmology*, vol. 103, no. 4, pp. 664-669, 1996.

- [44] M. Yamada and K. Tsubota, "Measurement of tear evaporation from ocular surface," *Nippon Ganka Gakkai Zasshi*, vol. 94, no. 11, pp. 1061-1070, 1990.
- [45] J. P. Craig, I. Singh, A. Tomlinson, P. B. Morgan and N. Efron, "The role of tear physiology in ocular surface temperature," *Eye*, vol. 14, pp. 635-641, 2000.
- [46] W. Mathers, "Evaporation from the ocular surface," *Exp Eye Res*, vol. 78, pp. 389-394, 2004.
- [47] M. A. Lemp, "The definition and classification of dry eye disease," *The Ocular Surface*, vol. 5, no. 2, pp. 75-92, 2007.
- [48] J. M. Tiffany, "The viscosity of human tears," *Int Ophthalmol*, vol. 15, no. 6, pp. 371-376, 1991.
- [49] S. M. Gouviea and J. M. Tiffany, "Human tear viscosity: An interactive role for proteins and lipids," *Biochim Biophys Acta*, vol. 1753, pp. 155-163, 2005.
- [50] J. M. Tiffany and J. K. G. Dart, "Normal and abnormal functions of meibomian secretions," *R Soc Med Int Congr Symp Ser*, vol. 40, pp. 1061-1064, 1981.
- [51] J. M. Tiffany and B. Nagyova, "The role of lipocalin in determining the physical properties of tears," *Adv Exp Med Biol*, vol. 506, pp. 581-585, 2002.
- [52] B. J. Glasgow, A. R. Abduragimov, Z. T. Farahbakhsh, K. F. Faull and W. L. Hubbell, "Tear lipocalins bind a broad array of lipid ligands," *Curr Eye Res*, vol. 14, no. 5, pp. 363-372, 1995.
- [53] O. K. Gasymov, A. R. Abduragimov, T. N. Yusifov and B. J. Glasgow, "Structural changes in human tear lipocalins associated with lipid binding," *Biochim Biophys Acta*, vol. 1386, no. 1, pp. 145-156, 1998.
- [54] F. J. Holly, "Formation and rupture of the tear film," *Exp Eye Res*, vol. 15, pp. 515-525, 1973.
- [55] J. M. Tiffany, "Refractive index of meibomian and other lipids," *Curr Eye Res*, vol. 5, no. 11, pp. 887-889, 1986.
- [56] N. Nicolaides, J. K. Kaitaranta, T. N. Rawdah, J. I. Macy, F. M. Boswell 3rd and R. E. Smith, "Meibomian gland studies: comparison of steer and human lipids," *IOVS*, vol. 20, pp. 522-536, 1981.
- [57] N. Nicolaides, "Recent findings on the chemical composition of the lipids of steer and human meibomian glands," in *The Preocular Tear Film: In Health, Disease and Contact Lens Wear*, F. J. Holly, Ed., Lubbock, Dry Eye Institute, 1986, pp. 570-596.
- [58] T. J. Millar, "A mechanism to explain the behaviour of spread films of meibomian lipids," *Curr Eye Res*, vol. 38, no. 1, pp. 220-223, 2013.
- [59] S. M. Lam, L. Tong, S. S. Yong, B. Li, S. S. Chaurasia, G. Shui and M. R. Wenk, "Meibum lipid composition in Asians with dry eye disease," *PLoS ONE*, vol. 6, no. 10, p. e24339, 2011.
- [60] J. Chen, K. B. Green-Church and K. K. Nichols, "Shotgun lipidomic analysis of human Meibomian gland secretions with electrospray ionization tandem mass spectrometry," *IOVS*, vol. 51, pp. 6220-6231, 2010.
- [61] A. W. Dean and B. J. Glasgow, "Mass spectrometric identification of phospholipids in human tears and tear lipocalin," *Invest Ophthalmol Vis Sci*, vol. 53, no. 4, pp. 1773-1782, 2012.
- [62] J. M. Dougherty and J. P. McCulley, "Analysis of the free fatty acid component of meibomian secretions in chronic blepharitis," *IOVS*, vol. 27, pp. 52-56, 1986.
- [63] W. E. Shine and J. P. McCulley, "Association of meibum oleic acid with Meibomian seborrhea," *Cornea*, vol. 19, pp. 72-74, 2000.

- [64] K. K. Nichols, B. M. Ham, J. J. Nichols, C. Ziegler and K. B. Green-Church, "Identification of fatty acids and fatty acid amides in human Meibomian gland secretions," *IOVS*, vol. 48, pp. 34-39, 2007.
- [65] D. R. Whikehart, *Biochemistry of the Eye*, 2nd ed., Butterworth Heinemann, 2003.
- [66] I. A. Butovich, "Lipidomic analysis of human meibum using HPLC-MS," in *Lipidomics, Methods in Molecular Biology*, D. Armstrong, Ed., Humana Press, 2009, pp. 221-246.
- [67] I. A. Butovich, E. Uchiyama, M. A. Di Pascuale and J. P. McCulley, "Liquid chromatography-mass spectrometric analysis of lipids present in human Meibomian gland secretions," *Lipids*, vol. 42, pp. 765-776, 2007.
- [68] I. A. Butovich, J. C. Wojtowicz and M. Molai, "Human tear film and meibum. Very long chain wax esters and (O-acyl)-omega-hydroxy fatty acids of meibum," *J Lipid Res*, vol. 50, pp. 2471-2485, 2009.
- [69] I. A. Butovich, "Cholesteryl esters as a depot for very long chain fatty acids in human meibum," *J Lipid Res*, vol. 50, pp. 501-513, 2009.
- [70] I. A. Butovich, "Fatty acid composition of cholesteryl esters of human Meibomian gland secretions," *Steroids*, vol. 75, pp. 726-733, 2010.
- [71] W. E. Shine and J. P. McCulley, "Polar lipids in human Meibomian gland secretions," *Curr Eye Res*, vol. 26, pp. 89-94, 2003.
- [72] J. V. Greiner, T. Glonek, D. R. Korb, R. Booth and C. D. Leahy, "Phospholipids in meibomian gland secretion," *Ophthalmic Res*, vol. 28, pp. 44-49, 1996.
- [73] N. Nicolaides, "Skin Lipids II: Lipid class composition of samples from various species and anatomical sites," *J Am Oil Chem*, vol. 42, pp. 691-702, 1965.
- [74] D. Borchman, G. N. Foulks, M. C. Yappert, D. Tang and D. V. Ho, "Spectroscopic evaluation of human tear lipids," *Chem Phys Lipids*, vol. 147, pp. 87-102, 2007.
- [75] I. A. Butovich, "Lipidomics of human Meibomian gland secretions: Chemistry, biophysics and physiological role of Meibomian lipids," *Pro Lipid Res*, vol. 50, pp. 278-301, 2011.
- [76] D. Borchman, G. N. Foulks, M. C. Yappert and D. V. Ho, "Temperature-induced conformational changes in human tear lipids hydrocarbon chains," *Biopolymers*, vol. 87, pp. 124-133, 2007.
- [77] D. Campbell, G. Griffiths and B. J. Tighe, "Tear analysis and lens-tear interactions 2: Ocular lipids - nature and fate of meibomian gland phospholipids," *Cornea*, vol. 30, no. 3, pp. 325-332, 2011.
- [78] N. Nicolaides and E. C. Santos, "The di- and triesters of the lipids of steer and human meibomian glands," *Lipids*, vol. 20, no. 7, pp. 454-467, 1985.
- [79] I. A. Butovich, "On the presence and role of polar lipids in meibum," *IOVS*, vol. 51, no. 12, pp. 6908-6910, 2010.
- [80] D. L. Leiske, C. E. Miller, L. Rosenfeld, C. Cerretani, A. Ayzner, B. Lin, M. Meron, M. Senchyna, H. A. Ketelson, D. Meadows, S. Srinivasan, L. Jones, C. J. Radke, M. F. Toney and G. G. Fuller, "Molecular structure of interfacial human meibum films," *Langmuir*, vol. 28, pp. 11858-11865, 2012.
- [81] I. A. Butovich, J. C. Arciniega, H. Lu and M. Molai, "Evaluation and quantification of intact wax esters of human meibum by gas-liquid chromatography-ion trap mass spectrometry," *Biochem Mol Biol*, vol. 53, pp. 3766-3781, 2012.
- [82] I. A. Butovich, "On the presence of (O-acyl)-omega-hydroxy fatty acids and of their esters in human meibomian gland secretions," *IOVS*, vol. 52, no. 1, pp. 639-641, 2011.
- [83] W. E. Shine, J. P. McCulley and A. G. Pandya, "Minocycline effect on Meibomian gland lipids in meibomianitis patients," *Exp Eye Res*, vol. 76, pp. 417-420, 2003.

- [84] W. E. Shine and J. P. McCulley, "Meibomian gland triglyceride fatty acid differences in chronic blepharitis patients," *Cornea*, vol. 15, pp. 340-346, 1996.
- [85] L. A. Wickham, J. Gao, I. Toda, E. M. Rocha, M. Ono and D. A. Sullivan, "Identification of androgen, estrogen and progesterone receptor mRNAs in the eye," *Acta Ophthalmol Scand*, vol. 78, pp. 146-153, 2000.
- [86] E. M. Rocha, L. A. Wickham, L. A. da Silveira, K. L. Krenzer, F. S. Yu, I. Toda, B. D. Sullivan and D. A. Sullivan, "Identification of androgen receptor protein and 5alpha-reductase mRNA in human ocular tissue," *Br J Ophthalmol*, vol. 84, pp. 76-84, 2000.
- [87] M. Souchier, C. Joffre, S. Gregoire, L. Bretillon, A. Muselier, N. Acar, J. Beynat, A. J. Bron, P. D'Athis and C. Creuzot-Garcher, "Changes in meibomian fatty acids and clinical signs in patients with meibomian gland dysfunction after minocycline treatment," *Br J Ophthalmol*, vol. 92, pp. 819-822, 2008.
- [88] J. M. Tiffany, "Individual variations in human meibomian lipid composition," *Exp Eye Res*, vol. 27, no. 3, pp. 289-300, 1978.
- [89] P. N. Dilly, "Structure and function of the tear film," *Adv Exp Med Biol*, vol. 350, pp. 239-247, 1994.
- [90] I. Fatt and B. Weissman, *Physiology of the eye: An introduction to the vegetative functions*, 2nd ed., Boston: Butterworth-Heinemann, 1992.
- [91] A. M. Gachon, P. Verelle, G. Betail and B. Dastugue, "Immunological and electrophoretic studies of human tear proteins," *Exp Eye Res*, vol. 29, pp. 539-553, 1979.
- [92] N. Li, N. Wang, J. Zheng, X. M. Liu, O. W. Lever, P. M. Erickson and L. Li, "Characterization of human tear proteome using multiple proteomic analysis techniques," *J Proteome Res*, vol. 4, no. 6, pp. 2051-2061, 2005.
- [93] K. B. Green-Church, K. K. Nichols, N. M. Kleinholz, L. Zhang and J. J. Nichols, "Investigation of the human tear film proteome using multiple proteomic approaches," *Mol Vis*, vol. 14, pp. 456-470, 2008.
- [94] B. Milder, "The lacrimal apparatus," in *Adler's Physiology of the Eye*, R. A. Moses and W. M. Hart, Eds., St Louis, Mosby, 1987, pp. 15-35.
- [95] J. I. McGill, G. M. Liakos, N. Goulding and D. V. Seal, "Normal tear protein profiles and age-related changes," *Br J Ophthalmol*, vol. 68, pp. 316-320, 1984.
- [96] R. J. Fullard and C. Snyder, "Protein levels in non-stimulated and stimulated tears of normal human subjects," *IOVS*, vol. 31, pp. 1119-1126, 1990.
- [97] R. J. Fullard and D. L. Tucker, "Changes in human tear protein levels with progressively increasing stimulus," *IOVS*, vol. 32, no. 8, pp. 2290-2301, 1991.
- [98] A. M. Bright and B. J. Tighe, "The composition and interfacial properties of tears, tear substitutes and tear models," *CLAE*, vol. 16, pp. 57-66, 1993.
- [99] A. Kijlstra and A. Kuizenga, "Analysis and function of the human tear proteins," *Adv Exp Med Biol*, vol. 350, pp. 299-308, 1994.
- [100] K. M. Saari, E. Aine, A. Posz and M. Klockars, "Lysozyme content of tears in normal subjects and in patients with external eye infections," *Graefe's Arch Clin Exp Ophthalmol*, vol. 221, pp. 86-88, 1983.
- [101] R. N. Stuchell, R. L. Farris and I. D. Mandell, "Basal and reflex human tear analysis II. Chemical analysis: lactoferrin and lysozyme," *Ophthalmol*, vol. 88, pp. 858-861, 1983.
- [102] R. J. Fullard and D. M. Kissner, "Purification of the isoforms of tear specific prealbumin," *Curr Eye Res*, vol. 10, pp. 613-628, 1991.
- [103] B. H. McClellan, C. H. Whitney, L. P. Newman and M. R. Allansmith, "Immunoglobulins in tears," *Am J Ophthalmol*, vol. 76, no. 1, pp. 89-101, 1973.

- [104] O. K. Gasymov, A. R. Abduragimov, T. N. Yusifov and B. J. Glasgow, "Binding studies of tear lipocalin: The role of the conserved tryptophan in maintaining structure stability and ligand affinity," *Biochim Biophys Acta*, vol. 1433, pp. 307-320, 1999.
- [105] B. J. Glasgow, G. Marshall, O. K. Gasymov, A. R. Abduragimov, N. Taleh, T. N. Yusifov and C. M. Knobler, "Tear lipocalins: Potential lipid scavengers for the corneal surface," *IOVS*, vol. 40, no. 13, pp. 3100-3107, 1999.
- [106] D. A. Dartt, "Tear lipocalin: Structure and function," *Ocular Surface*, vol. 9, no. 3, pp. 126-138, 2011.
- [107] B. Redl, "Human tear lipocalin," *Biochim Biophys Acta*, vol. 1482, no. 1-2, pp. 241-248, 1998.
- [108] R. D. Schoenwald, S. Vidvauns, D. E. Wurster and C. F. Barfknecht, "The role of tear proteins in tear film stability in the dry eye patient and in the rabbit," in *Lacrimal Gland, Tear Film and Dry Eye Syndromes 2*, vol. 438, D. A. Sullivan, D. A. Dartt and M. A. Meneray, Eds., New York, Plenum Press, 1998, pp. 391-400.
- [109] O. K. Gasymov, A. R. Abduragimov, P. Prasher, T. N. Yusifov and B. J. Glasgow, "Tear lipocalin: Evidence for a scavenging function to remove lipids from the human corneal surface," *IOVS*, vol. 46, no. 10, pp. 3589-3596, 2005.
- [110] M. Lechner, P. Wojnar and B. Redl, "Human tear lipocalin acts as an oxidative stress-induced scavenger of potentially harmful lipid peroxidation products in a cell culture system," *Biochim J*, vol. 356, pp. 129-135, 2001.
- [111] D. V. Seal, J. I. McGill, I. A. Mackie, G. M. Liakos, P. Jacobs and N. J. Goulding, "Bacteriology and tear protein profiles of the dry eye," *Br J Ophthalmol*, vol. 70, pp. 122-125, 1986.
- [112] U. Pleyer and H. Baatz, "Antibacterial protection of the ocular surface," *Ophthalmologica*, vol. 211, no. 1, pp. 2-8, 1997.
- [113] P. Mudgil, M. Torres and T. J. Millar, "Adsorption of lysozyme to phospholipid and meibomian lipid monolayer films," *Coll Surf B: Biointerfaces*, vol. 48, no. 2, pp. 128-137, 2006.
- [114] K. Arnold, D. Hoekstra and S. Ohki, "Association of lysozyme to phospholipid surfaces and vesicle formation," *Biochim Biophys Acta*, vol. 1124, no. 1, pp. 88-94, 1992.
- [115] R. R. Arnold, M. F. Cole and J. R. McGhee, "A bactericidal effect for human lactoferrin," *Science*, vol. 197, pp. 263-265, 1977.
- [116] R. L. Farris, "Tear analysis in contact lens wearers," *Trans Am Ophthalmol Soc*, vol. 83, pp. 501-545, 1985.
- [117] K. Yamauchi, M. Tomita, T. J. Giehl and R. R. Ellison, "Antibacterial activity of lactoferrin and a pepsin-derived lactoferrin peptide fragment," *Infection & Immunity*, vol. 61, no. 2, pp. 719-728, 1993.
- [118] P. Aisen and A. Leibman, "Lactoferrin and transferrin: A comparative study," *Biochim Biophys Acta*, vol. 257, pp. 314-323, 1972.
- [119] J. F. Heremans, "Immunoglobulin formation and function in different tissues," *Curr Top Microbiol Immunol*, vol. 45, pp. 131-203, 1968.
- [120] L. Brauer, C. Kindler, K. Jager, S. Sel, B. Nolle, U. Pleyer, M. Ochs and F. P. Paulsen, "Detection of surfactant proteins A and D in human tear fluid and the human lacrimal system," *Invest Ophthalmol Vis Sci*, vol. 48, no. 9, pp. 3945-3953, 2007.
- [121] L. Brauer, M. Johl, J. Borgermann, U. Pleyer, M. Tsokos and F. P. Paulsen, "Detection and localization of the hydrophobic surfactant proteins B and C in human tear fluid and the human lacrimal system," *Curr Eye Res*, vol. 11, no. 931-938, p. 32, 2007.

- [122] L. Brauer and F. P. Paulsen, "Tear film and ocular surface surfactants," *J Epithelial Biol & Pharm*, vol. 1, pp. 62-67, 2008.
- [123] K. B. Green-Church, I. Butovich, M. Willcox, D. Borchman, F. Paulsen, S. Barabino and B. J. Glasgow, "The international workshop on Meibomian gland dysfunction: Report of the subcommittee on tear film lipids and lipid-protein interactions in health and disease," *Invest Ophthalmol Vis Sci*, vol. 52, no. 4, pp. S1979-S1993, 2011.
- [124] M. Ni, D. J. Evans, S. Hawgood, E. M. Anders, R. A. Sack and S. M. Fleiszig, "Surfactant protein D is present in human tear fluid and the cornea and inhibits epithelial cell invasion by *Pseudomonas aeruginosa*," *Infect Immun*, vol. 73, pp. 2147-2156, 2005.
- [125] S. Schurch, M. Lee and P. Gehr, "Pulmonary surfactant: Surface properties and function of alveolar and airway surfactant," *Pure & Appl Chem*, vol. 64, no. 11, pp. 1745-1750, 1992.
- [126] F. Possmayer, K. Nag, K. Rodriguez, R. Qanbar and S. Schurch, "Surface activity in vitro: role of surfactant proteins," *Comparative Biochem Physiol - Part A*, vol. 129, no. 1, pp. 209-220, 2001.
- [127] R. Wustneck, J. Perez-Gil, N. Wustneck, A. Cruz, V. B. Fainerman and U. Pison, "Interfacial properties of pulmonary surfactant layers," *Adv Coll Int Sci*, vol. 117, pp. 33-58, 2005.
- [128] L. Chen, L. Zhou, E. C. Y. Chan, J. Neo and R. W. Beuerman, "Characterization of the human tear metabolome by LC-MS/MS," *J Proteome Res*, vol. 10, pp. 4876-4882, 2011.
- [129] N. J. van Haeringen and E. Glasius, "Collection method dependant concentrations of some metabolites in human tear fluid, with special reference to glucose in hyperglycaemic conditions," *Albrecht von Graefes Arch Klin Exp Ophthalmol*, vol. 202, no. 1, pp. 1-7, 1977.
- [130] M. Nakatsukata, C. Sotozono, K. Shimbo, N. Ono, H. Miyano, A. Okana, J. Hamuro and S. Kinoshita, "Amino acid profiles in human tear fluids analysed by High-Performance Liquid Chromatography and Electrospray Ionization Tandem Mass Spectroscopy," *Am J Ophthalmol*, vol. 151, no. 5, pp. 799-808, 2011.
- [131] J. J. Nichols and L. T. Sinnott, "Tear film, contact lens, and patient-related factors associated with contact lens-related dry eye," *IOVS*, vol. 47, no. 4, pp. 1319-1328, 2006.
- [132] J. P. Craig and A. Tomlinson, "Effect of age on tear osmolality," *Optom Vis Sci*, vol. 72, no. 10, pp. 713-717, 1995.
- [133] J. P. Craig, P. A. Simmons, S. Patel and A. Tomlinson, "Refractive index and tear osmolality," *Optom Vis Sci*, vol. 72, no. 10, pp. 718-724, 1995.
- [134] J. P. Gilbard, "Human tear film electrolyte concentrations in health and dry-eye disease," *Int Ophthalmol Clin*, vol. 34, no. 1, pp. 27-36, 1994.
- [135] N. J. van Haeringen, "Clinical biochemistry of tears," *Surv Ophthalmol*, vol. 26, pp. 84-96, 1981.
- [136] D. Mirejovsky, A. S. Patel, D. D. Rodriguez and T. J. Hunt, "Lipid adsorption onto hydrogel contact lens materials. Advantages of Nile red over oil red O in visualisation of lipids," *Optom Vis Sci*, vol. 68, pp. 858-864, 1991.
- [137] D. W. Lamberts, "Physiology of the tear film," in *The Cornea: Scientific Foundations and Clinical Practice*, G. Smolin and R. A. Thoft, Eds., London, Little Brown, 1994, pp. 439-456.
- [138] B. A. Cowell, M. D. P. Willcox and R. P. Schneider, "A relatively small change in sodium chloride concentration has a strong effect in adhesion of ocular bacteria to contact lenses," *J App Microbiol*, vol. 84, pp. 950-958, 1998.
- [139] S. J. Gendler and A. P. Spicer, "Epithelial mucin genes," *Ann Rev Physiol*, vol. 57, pp. 607-634, 1995.

- [140] N. Moniaux, F. Escande, N. Porchet, J. P. Aubert and S. K. Batra, "Structural organization and classification of the human mucin genes," *Front Biosci*, vol. 6, pp. D1192-D1206, 2001.
- [141] D. A. Dartt, "Physiology of tear production," in *The Dry Eye. A Comprehensive Guide*, M. A. Lemp and R. Marquandt, Eds., Berlin, Springer-Verlag, 1992, pp. 65-99.
- [142] D. A. Dartt, "Regulation of tear secretion," *Adv Exp Med Biol*, vol. 350, pp. 1-9, 1994.
- [143] F. J. Holly and M. A. Lemp, "Wettability and wetting of corneal epithelium," *Exp Eye Res*, vol. 11, no. 2, pp. 239-250, 1971.
- [144] P. Argueso and I. K. Gipson, "Epithelial mucins of the ocular surface: Structure, biosynthesis and function," *Exp Eye Res*, vol. 73, pp. 281-289, 2001.
- [145] I. K. Gipson, "Distribution of mucins at the ocular surface," *Exp Eye Res*, vol. 78, pp. 379-388, 2004.
- [146] M. M. Jumblatt, R. W. McKenzie and J. E. Jumblatt, "MUC5AC mucin is a component of the human precorneal tear film.," *IOVS*, vol. 40, no. 1, pp. 43-49, 1999.
- [147] J. W. Rohen and E. Lutjen-Drecoll, "Functional morphology of the conjunctiva," in *The Dry Eye: A Comprehensive Guide*, M. A. Lemp and R. Marquandt, Eds., Berlin, Springer-Verlag, 1992, pp. 35-63.
- [148] F. M. Fowkes, "Attractive forces at interfaces," *Ind Eng Chem*, vol. 56, no. 12, pp. 40-52, 1964.
- [149] N. Ehlers, "The precorneal film. Biomicroscopical, histological and chemical investigations," *Acta Ophthalmol*, vol. 81, pp. 79-136, 1965.
- [150] H. Owens and J. Philips, "Spreading of tears after a blink: velocity and stabilisation time in healthy eyes," *Cornea*, vol. 20, pp. 484-487, 2001.
- [151] W. D. Mathers and T. E. Daley, "In vivo observation of the human tear film by tandem scanning confocal microscopy," *Scanning*, vol. 16, pp. 316-319, 1994.
- [152] P. Mudgil and T. J. Millar, "Surfactant properties of human Meibomian lipids," *IOVS*, vol. 52, pp. 1661-1670, 2011.
- [153] J. M. Tiffany, "The normal tear film," in *Surgery for the Dry Eye*, vol. 41, G. Geerling and H. Brewitt, Eds., Basel, Karger, 2008, pp. 1-20.
- [154] J. Zhao and P. Wollmer, "Surface activity of tear fluid in normal subjects," *Acta Ophthalmol Scand*, vol. 76, pp. 438-441, 1998.
- [155] J. P. McCulley and W. E. Shine, "The lipid layer of tears: dependant on Meibomian gland function," *Exp Eye Res*, vol. 78, pp. 361-365, 2004.
- [156] D. L. Leiske, S. R. Raju, H. A. Ketelson, T. J. Millar and G. G. Fuller, "The interfacial viscoelastic properties and structures of human and animal Meibomian lipids," *Exp Eye Res*, vol. 90, pp. 598-604, 2010.
- [157] H. Owens and J. R. Philips, "Tear spreading rates: post-blink," *Adv Exp Med Biol*, vol. 506, pp. 1201-1204, 2002.
- [158] M. G. Doane, "Interaction of eyelid and tears in corneal wetting and the dynamics of the normal human eyeblink," *Am J Ophthalmol*, vol. 89, pp. 507-516, 1980.
- [159] F. Miano, M. Calcara, F. Giuliano, T. J. Millar and V. Enea, "Effect of meibomian lipid layer on evaporation of tears," *J Phys: Condensed Matter*, vol. 16, pp. 2461-2467, 2004.
- [160] K. K. Nichols, G. N. Foulks, A. J. Bron, B. J. Glasgow, M. Dogru, K. Tsubota, M. A. Lemp and D. A. Sullivan, "The international workshop on Meibomian gland dysfunction: Executive summary," *Invest Ophthalmol Vis Sci*, vol. 52, no. 4, pp. 1922-1929, 2011.

- [161] G. N. Foulks, K. K. Nichols, A. G. Kabat, P. M. Karpecki and J. J. Nichols, "Meibomian Gland Dysfunction: Understanding and implementing the new consensus definition and treatment regimens into your optometric practice," *Review of Optometry*, 2012.
- [162] P. J. Driver and M. A. Lemp, "Meibomian gland dysfunction," *Surv Ophthalmol*, vol. 40, no. 5, pp. 343-367, 1996.
- [163] F. J. Holly and M. A. Lemp, "Tear physiology and dry eye," *Surv Ophthalmol*, vol. 22, no. 2, pp. 69-87, 1977.
- [164] M. E. Johnson and P. J. Murphy, "Changes in the tear film and ocular surface from dry eye syndrome," *Prog Retinal Eye Res*, vol. 23, pp. 449-474, 2004.
- [165] M. Guillon, E. Styles, J.-P. Guillon and C. Maissa, "Preocular tear film characteristics nonwearers and soft contact lens wearers," *Optom Vis Sci*, vol. 74, no. 5, pp. 273-279, 1997.
- [166] K. A. Kinney, "Detecting dry eye in contact lens wearers," *Contact Lens Spectrum*, vol. 13, pp. 21-28, 1998.
- [167] E. Fahy, "A comprehensive classification system for lipids," *J Lipid Res*, vol. 46, pp. 839-862, 2005.
- [168] A. Panaser and B. J. Tighe, "Function of lipids - their fate in contact lens wear: an interpretive review," *CLAE*, vol. 35, pp. 100-111, 2012.
- [169] M. Yamada, H. Mochizuki, M. Kawashima and S. Hata, "Phospholipids and their degrading enzyme in the tear of soft contact lens wearers," *Cornea*, vol. 25, no. 10, pp. S68-S72, 2006.
- [170] V. V. Aho, V. Paavilainen, T. J. Nevelainen, H. Peuravouri and K. M. Saari, "Diurnal variation in group IIa phospholipase A(2) content in tears of contact lens wearers and normal controls," *Graefes Arch Clin Exp Ophthalmol*, vol. 241, no. 2, pp. 85-88, 2003.
- [171] S. Shimmura, M. Suematsu, M. Shimoyama, K. Tsubota, Y. Oguchi and Y. Ishimura, "Subthreshold UV radiation-induced peroxide formation in cultured corneal epithelial cells: the protective effects of lactoferrin," *Exp Eye Res*, vol. 63, pp. 519-526, 1996.
- [172] R. C. Rose, S. P. Richer and A. M. Bode, "Ocular oxidants and antioxidant protection," *Proc Soc Exp Biol Med*, vol. 217, pp. 397-407, 1998.
- [173] B. Halliwell and J. M. C. Gutteridge, *Free Radicals in Biology and Medicine*, 3rd ed., Oxford: Oxford University Press, 1999.
- [174] A. J. Augustin, M. Spitznas, N. Kaviani, D. Meller, F. H. J. Koch, F. Grus and M. J. Gobbels, "Oxidative reactions in the tear fluid of patients suffering from dry eyes," *Graefes Arch Clin Exp Ophthalmol*, vol. 233, pp. 694-698, 1995.
- [175] E. N. Frankel, *Lipid Oxidation*, California: The Oily Press, 2002.
- [176] M. J. Glasson, F. Stapleton and M. D. P. Willcox, "Lipid, lipase and lipocalin differences between tolerant and intolerant contact lens wearers," *Curr Eye Res*, vol. 25, no. 4, pp. 227-235, 2002.
- [177] R. Gogia, S. P. Richer and R. C. Rose, "Tear fluid content of electrochemically active components including water soluble antioxidants," *Curr Eye Res*, vol. 17, pp. 257-263, 1998.
- [178] C. K. M. Choy, P. Cho, W.-Y. Chung and I. F. F. Benzie, "Water-soluble antioxidant in human tears: Effect of the collection method," *Invest Ophthalmol Vis Sci*, vol. 42, no. 13, pp. 3130-3134, 2001.
- [179] C. K. M. Choy, I. F. F. Benzie and P. Cho, "Ascorbic acid concentration and total antioxidant activity of human tear fluid measured using the FRASC assay," *Invest Ophthalmol Vis Sci*, vol. 41, no. 11, pp. 3293-3298, 2000.

- [180] C. A. Paterson and M. C. O'Rourke, "Vitamin C levels in human tears," *Arch Ophthalmol*, vol. 105, pp. 376-377, 1987.
- [181] R. Dreyer and R. C. Rose, "Lacrimal gland uptake and metabolism of ascorbic acid," *Proc Soc Exp Biol Med*, vol. 202, pp. 212-216, 1993.
- [182] A. Kuizenga, N. J. van Haeringen and A. Kijlstra, "Inhibition of hydroxyl radical formation by human tears," *Invest Ophthalmol Vis Sci*, vol. 28, pp. 305-313, 1987.
- [183] C. K. M. Choy, I. F. F. Benzie and P. Cho, "Antioxidants in tears and plasma: Inter-relationships and effect of vitamin C supplementation," *Curr Eye Res*, vol. 27, no. 1, pp. 55-60, 2003.
- [184] BCLA, "Facts and stats on the UK contact lens market: Consumer guide to contact lenses," 2011. [Online]. Available: <http://www.bcla.org.uk/en/consumers/consumer-guide-to-contact-lenses/facts-and-stats-on-the-uk-len-market.cfm>. [Accessed 20 9 2012].
- [185] J. J. Nichols, "Contact Lens 2012: Annual Report," 1 January 2013. [Online]. Available: <http://www.clspectrum.com/articleviewer.aspx?articleID=107853>. [Accessed 18 January 2013].
- [186] D. R. Korb, "Tear film-contact lens interactions," *Adv Exp Med Biol*, vol. 350, pp. 403-410, 1994.
- [187] K. Richdale, L. T. Sinnott, E. Skadahl and J. J. Nichols, "Frequency of and factors associated with contact lens dissatisfaction and discontinuation," *Cornea*, vol. 26, no. 2, pp. 168-174, 2007.
- [188] G. Young, J. Veys, N. Pritchard and S. Coleman, "A multi-centre study of lapsed contact lens wear," *Ophthalm Phys Optics*, vol. 22, no. 6, pp. 516-527, 2002.
- [189] B. A. Holden and G. W. Mertz, "Critical oxygen levels to avoid corneal edema for daily and extended wear contact lenses," *Invest Ophthalmol Vis Sci*, vol. 25, no. 10, pp. 1161-1167, 1984.
- [190] J. T. Jacobs, "Biocompatibility in the development of silicone-hydrogel lenses," *Eye & Contact Lens*, vol. 39, no. 1, pp. 13-19, 2013.
- [191] D. R. Korb, J. V. Greiner and T. Glonek, "Tear film lipid layer formation: Implications for contact lens wear," *Optom Vis Sci*, vol. 73, no. 3, pp. 189-192, 1996.
- [192] E. Faber, T. R. Golding, R. Lowe and N. A. Brennan, "Effect of hydrogel lens wear on tear film stability," *Optom Vis Sci*, vol. 68, no. 5, pp. 380-384, 1991.
- [193] J. J. Nichols, G. L. Mitchell and P. E. King-Smith, "Thinning rate of precorneal and pre-lens tears films," *Invest Ophthalmol Vis Sci*, vol. 46, pp. 2353-2361, 2005.
- [194] F. P. Carney, W. L. Nash and K. B. Sentell, "The adsorption of major tear film lipids in vitro to various silicone hydrogels over time," *IOVS*, vol. 49, no. 1, pp. 120-124, 2008.
- [195] C. Maissa, V. Franklin, M. Guillon and B. Tighe, "Influence of contact lens material surface characteristics and replacement frequency on protein and lipid deposition," *Optom Vis Sci*, vol. 75, no. 9, pp. 697-705, 1998.
- [196] M. J. Doughty, D. Fonn, D. Richter, T. Simpson, B. Caffery and K. Gordon, "A patient questionnaire approach to estimating the prevalence of dry eye symptoms in patients presenting to optometric practices across Canada," *Optom Vis Sci*, vol. 74, pp. 624-631, 1997.
- [197] J. J. Nichols, G. L. Mitchell, K. K. Nichols, R. Chalmers and C. Begley, "The performance of the Contact Lens Dry Eye Questionnaire as a screening survey for contact lens-related dry eye," *Cornea*, vol. 21, pp. 469-475, 2002.

- [198] C. G. Begley, R. L. Chalmers, G. L. Mitchell, K. K. Nichols, B. Caffery, T. Simpson, R. Du Toit, J. Portello and L. Davis, "Characterization of ocular surface symptoms from optometric practices in North America," *Cornea*, vol. 20, pp. 610-618, 2001.
- [199] C. G. Begley, B. Caffery, K. K. Nichols and R. Chalmers, "Responses of contact lens wearers to a dry eye survey," *Optom Vis Sci*, vol. 77, pp. 40-46, 2000.
- [200] M. Guillon and C. Maissa, "Dry eye symptomatology of soft contact lens wearers and non-wearers," *Optom Vis Sci*, vol. 82, no. 9, pp. 829-834, 2005.
- [201] J.-P. Guillon, "Tear film structure and contact lenses," in *The Preocular Tear Film in Health, Disease and Contact Lens Wear*, F. J. Holly, Ed., Lubbock, Dry Eye Institute, 1986, pp. 914-939.
- [202] M. J. Glasson, F. Stapleton, L. Keay and M. D. P. Willcox, "The effect of short term contact lens wear on the tear film and ocular surface characteristics of tolerant and intolerant wearers," *CLAE*, vol. 29, pp. 41-47, 2006.
- [203] M. A. Lemp and J. R. Hamill, "Factors affecting tear breakup in normal eyes," *Arch Ophthalmol*, vol. 89, pp. 103-105, 1973.
- [204] P. Cho and W. Douthwaite, "The relation between invasive and non-invasive tear break-up time," *Optom Vis Sci*, vol. 72, no. 1, pp. 17-22, 1995.
- [205] L. S. Mengher, A. J. Bron, S. R. Tonge and D. J. Gilbert, "Effect of fluorescein instillation on the pre-corneal tear film stability," *Curr Eye Res*, vol. 4, pp. 9-12, 1985.
- [206] J. J. Nichols and P. E. King-Smith, "Thickness of the pre- and post-contact lens tear film measured in vivo by interferometry," *IOVS*, vol. 44, no. 1, pp. 68-77, 2003.
- [207] P. E. King-Smith, J. J. Nichols, K. K. Nichols, B. A. Fink and R. J. Braun, "Contributions of evaporation and other mechanisms to tear film thinning and break-up," *Optom Vis Sci*, vol. 85, no. 8, pp. 623-630, 2008.
- [208] M. J. Glasson, F. Stapleton, L. Keay, D. Sweeney and M. D. P. Willcox, "Differences in clinical parameters and tear film of tolerant and intolerant contact lens wearers," *IOVS*, vol. 44, no. 12, pp. 5116-5124, 2003.
- [209] M. Elliott, H. Fandrich, T. Simpson and D. Fonn, "Analysis of the repeatability of tear break-up time measurement techniques on asymptomatic subjects before, during and after contact lens wear," *Contact Lens Anterior Eye*, vol. 21, pp. 98-103, 1998.
- [210] M. J. Doughty, V. Jalota, E. Bennett, T. Naase and E. Oblak, "Use of a high molecular weight fluorescein (fluorexon) ophthalmic strip in assessments of tear film break-up time in contact lens wearers and non-contact lens wearers," *Ophthalmol Phys Optics*, vol. 25, no. 2, pp. 119-127, 2005.
- [211] J.-P. Guillon and M. Guillon, "Tear film examination of the contact lens patient," *Optician*, vol. 206, pp. 21-29, 1993.
- [212] K. B. Bjerrum, "Tear fluid analysis in patients with primary Sjogren's syndrome using lectin probes," *Acta Ophthalmol Scand*, vol. 77, pp. 1-8, 1999.
- [213] G. Young and N. Efron, "Characteristics of the pre-lens tear film during hydrogel contact lens wear," *Ophthalmic Physiol Opt*, vol. 11, pp. 53-58, 1991.
- [214] G. L. Gaines, "On the use of filter paper Wilhelmy plates with insoluble monolayers," *J Coll Int Sci*, vol. 62, no. 1, pp. 191-192, 1977.
- [215] D. R. Lide, Ed., "Laboratory solvents and other liquid reagents," in *Handbook of Chemistry and Physics*, Boca Raton, FL, USA, CRC Press, 2008-2009, pp. 13-22.
- [216] H. E. Ries, "Monomolecular films," *Sci Am*, vol. 204, no. 3, pp. 152-165, 1961.

- [217] S. T. Tragoulias, P. J. Anderton, G. R. Dennis, F. Miano and T. J. Millar, "Surface pressure measurements of human tears and individual tear film components indicate that proteins are major contributors to the surface pressure," *Cornea*, vol. 24, no. 2, pp. 189-200, 2005.
- [218] P. Martin and M. Szablewski, *Langmuir-Blodgett Trough: Operating Manual*, 6th ed., F. Grunfeld, Ed., 2002.
- [219] S. Henon and J. Meunier, "Microscope at the Brewster angle: Direct observation of first-order phase transitions in monolayers," *Rev Scientific Instruments*, vol. 62, no. 4, pp. 936-939, 1991.
- [220] D. Honig and D. Moebius, "Direct visualization of monolayers at the air-water interface by Brewster angle microscopy," *J Phys Chem*, vol. 95, no. 12, pp. 4590-4592, 1991.
- [221] L. A. Laxhuber and H. Mohwald, "Thermodesorption spectroscopy of Langmuir-Blodgett films," *Langmuir*, vol. 3, pp. 837-845, 1987.
- [222] V. M. Kaganer, H. Mohwald and P. Dutta, "Structure and phase transitions in Langmuir monolayers," *Rev Mod Phys*, vol. 71, no. 3, pp. 779-819, 1999.
- [223] M. Losche and H. Mohwald, "Electrostatic interactions in phospholipid membranes: II. Influence of divalent ions on monolayer structure," *J Colloid Interface Sci*, vol. 131, pp. 56-67, 1989.
- [224] P. Dynarowicz-Latka, A. Dhanabalan and O. N. Oliveira Jr, "Modern physicochemical research on Langmuir monolayers," *Adv Colloid Interface Sci*, vol. 91, pp. 221-293, 2001.
- [225] S. Kundu and D. Langevin, "Fatty acid monolayer dissociation and collapse: Effect of pH and cations," *Colloids & Surfaces A: Physicochem*, vol. 325, pp. 81-85, 2008.
- [226] P. Mudgil and T. J. Millar, "Adsorption of apo- and holo-tear lipocalin to a bovine Meibomian lipid film," *Exp Eye Res*, vol. 86, pp. 622-628, 2008.
- [227] T. J. Millar, P. Mudgil, I. A. Butovich and C. K. Palaniappan, "Adsorption of human tear lipocalin to human Meibomian lipid films," *IOVS*, vol. 50, pp. 140-151, 2009.
- [228] T. J. Millar, S. T. Tragoulias, P. J. Anderton, M. S. Ball, F. Miano, G. R. Dennis and P. Mudgil, "The surface activity of purified ocular mucin at the air-liquid interface and interactions with Meibomian lipids," *Cornea*, vol. 25, pp. 91-100, 2006.
- [229] G. Thakur, C. Wang and R. M. Leblanc, "Surface chemistry and in situ spectroscopy of a lysozyme Langmuir monolayer," *Langmuir*, vol. 24, pp. 4888-4893, 2008.
- [230] S. A. Roberts, I. W. Kellaway, K. M. G. Taylor, B. Warburton and K. Peters, "Combined surface pressure-interfacial shear rheology study of the effect of pH on the adsorption of proteins at the air-water interface," *Int J Pharm*, vol. 300, pp. 48-55, 2005.
- [231] C. Postel, O. Abillon and B. Desbat, "Structure and denaturation of adsorbed lysozyme at the air-water interface," *J Coll Int Sci*, vol. 266, no. 1, pp. 74-81, 2003.
- [232] A. Sharma and E. Ruckenstein, "The role of lipid abnormalities, aqueous and mucus deficiencies in the tear film breakup, and implications for tear substitutes and contact lens tolerances," *J Coll Interface Sci*, vol. 111, no. 1, pp. 8-34, 1986.
- [233] J. R. Kanicky and D. O. Shah, "Effect of degree, type and position of unsaturation on the pKa of long-chain fatty acids," *J Colloid Interface Sci*, vol. 256, no. 1, pp. 201-207, 2002.
- [234] I. A. Butovich, "The Meibomian puzzle: Combining pieces together," *Prog Retinal & Eye Res*, vol. 28, pp. 483-498, 2009.
- [235] P. Somerharju, J. A. Virtanen and K. H. Cheng, "Lateral organization of membrane lipids: the superlattice view," *Biochim Biophys Acta*, vol. 1440, pp. 32-48, 1999.

- [236] P. Somerharju, J. A. Virtanen, K. H. Cheng and M. Hermansson, "The superlattice model of lateral organisation of membranes and its implications on membrane lipid homeostasis," *Biochim Biophys Acta*, vol. 1788, pp. 12-23, 2009.
- [237] P. B. Morgan, A. B. Tullo and N. Efron, "Infrared thermography of the tear film in dry eye," *Eye*, vol. 9, pp. 615-618, 1995.
- [238] P. Chen, Z. Policova, C. R. Pace-Asciak and A. W. Neumann, "Study of molecular interactions between lipid and proteins using dynamic surface tension measurements: a review," *Coll Surf B: Biointerfaces*, vol. 15, pp. 313-324, 1999.
- [239] S. Y. Nishimura, G. M. Magana, H. A. Ketelson and G. G. Fuller, "Effect of lysozyme adsorption on the interfacial rheology of DPPC and cholesteryl myristate films," *Langmuir*, vol. 24, pp. 11728-11733, 2008.
- [240] F. Miano, X. Zhao, J. R. Lu and J. Penfold, "Coadsorption of human milk lactoferrin into the dipalmitoylglycerolphosphatidylcholine phospholipid monolayer spread at the air/water interface," *Biophys J*, vol. 92, pp. 1254-1262, 2007.
- [241] H. Wong, I. Fatt and C. J. Radke, "Deposition and thinning of the human tear film," *J Coll Interface Sci*, vol. 184, pp. 44-51, 1996.
- [242] A. Sharma, S. Tiwari, R. Khanna and J. M. Tiffany, "Hydrodynamics of meniscus-induced thinning of the tear film," in *Lacrimal Gland, Tear Film, and Dry Eye Syndromes 2*, D. A. Sullivan, D. A. Dartt and M. A. Meneray, Eds., New York, Plenum, 1998, pp. 425-431.
- [243] F. Holly and M. Lemp, "Surface chemistry of the tear film: Implications for dry eye syndromes, contact lenses and ophthalmic polymers," *J Contact Lens Soc Am*, vol. 5, pp. 12-19, 1971.
- [244] J. M. Tiffany and R. G. Marsden, "The influence of composition on physical properties of meibomian secretions," in *The Preocular Tear Film in Health, Disease and Contact Lens Wear*, F. J. Holly, Ed., Lubbock, Dry Eye Institute, 1986, pp. 597-608.
- [245] B. L. Ong and J. R. Larke, "Meibomian gland dysfunction: some clinical, biochemical and physical observations," *Ophthalmol Physiol Opt*, vol. 10, pp. 144-148, 1990.
- [246] S. I. Brown and D. G. Dervichian, "The oils of the Meibomian glands: Physical and surface characteristics," *Arch Ophthalmol*, vol. 82, pp. 527-540, 1969.
- [247] J. S. Andrews, "The meibomian secretion," *Int Ophthalmol Clin*, vol. 13, pp. 23-28, 1973.
- [248] G. Gabrielli, G. Caminati and M. Puggelli, "Interactions and reactions of monolayers and Langmuir-Blodgett multilayers with compounds in the bulk phase," *Adv Coll Interface Sci*, vol. 87, pp. 75-111, 2000.
- [249] H. Mohwald, "Surfactant layers at water surfaces," *Rep Prog Phys*, vol. 56, pp. 653-685, 1993.
- [250] M. Yamada, H. Mochizuki, M. Kawai, M. Yoshino and Y. Masima, "Fluorophotometric measurement of pH of human tears in vivo," *Exp Eye Res*, vol. 16, no. 5, pp. 482-486, 1997.
- [251] A. Jyoti, R. M. Prokop, J. Li, D. Vollhardt, D. Y. Kwok, R. Miller, H. Mohwald and A. W. Neumann, "An investigation of the compression rate dependence on the surface pressure-surface area isotherm for a dipalmitoylphosphatidylcholine monolayer at the air/wat interface," *Coll & Surf A: Physicochem Eng Asp*, vol. 116, pp. 173-180, 1996.
- [252] K. Nag, C. Boland, N. Rich and K. M. W. Keough, "Epifluorescence microscopic observation of monolayers of dipalmitoylphosphatidylcholine: dependence of domain size on compression rates," *Biochim Biophys Acta*, vol. 1068, no. 2, pp. 157-160, 1991.

- [253] K. M. Haworth, J. J. Nichols, M. Thangavelu, L. T. Sinnott and K. K. Nichols, "Examination of human meibum collection and extraction techniques," *Optom Vis Sci*, vol. 88, no. 4, pp. 525-533, 2011.
- [254] R. N. Stuchell, J. J. Feldman, R. L. Farris and I. D. Mandel, "The effect of collection technique on tear composition," *Invest Ophthalmol Vis Sci*, vol. 25, pp. 374-377, 1984.
- [255] A. M. Mann and B. J. Tighe, "Tear analysis and lens-tear interactions I: Protein fingerprinting with microfluidic technology," *CLAE*, vol. 30, pp. 163-173, 2007.
- [256] C. A. Maissa, Biochemical markers and contact lens wear, Birmingham: Aston University, 1999.
- [257] J. Zhao, R. Manthorpe and P. Wollmer, "Surface activity of tear fluid in patients with primary Sjogren's syndrome," *Clin Phys Func Im*, vol. 22, no. 1, pp. 24-27, 2002.
- [258] P. G. Petrov, J. M. Thompson, I. B. Abdul Rahman, R. E. Ellis, E. M. Green, F. Miano and C. P. Winlove, "Two-dimensional order in mammalian pre-ocular tear film," *Exp Eye Res*, vol. 84, no. 6, pp. 1140-1146, 2007.
- [259] W. E. Shine and J. P. McCulley, "Keratoconjunctivitis sicca associated with meibomian secretion polar lipid abnormality," *Arch Ophthalmol*, vol. 116, no. 7, pp. 849-852, 1998.
- [260] I. A. Butovich, E. Uchiyama and J. P. McCulley, "Lipids of human meibum: mass-spectrometric analysis and structural elucidation," *J Lipid Res*, vol. 48, pp. 2220-2235, 2007.
- [261] F. Miano, M. G. Mazzone, A. Giannetto, V. Enea, P. McCauley, A. Bailey and P. C. Winlove, "Interface properties of simplified tear-like fluids in relations to lipid and aqueous layers composition," *Adv Exp Med Biol*, vol. 506, pp. 405-417, 2002.
- [262] Y. Ogata, M. Iwano, T. Mogi and Y. Makita, "Aggregation behavior of amphiphilic random copolymer of 2-(acrylamido)-2-methylpropanesulfonic acid and tris(trimethylsiloxy)silylpropylmethacrylate in aqueous solution," *J Polymer Sci B: Polymer Phys*, vol. 49, no. 23, pp. 1651-1659, 2011.
- [263] H. Lorentz and L. Jones, "Lipid deposition on hydrogel contact lenses: How history can help us today," *Optom Vis Sci*, vol. 84, no. 4, pp. 286-295, 2007.
- [264] L. Jones, A. Mann, K. Evans, V. Franklin and B. Tighe, "An in vivo comparison of the kinetics of protein and lipid deposition on group II and IV frequent replacement contact lenses," *Optom Vis Sci*, vol. 77, no. 10, pp. 503-510, 2000.
- [265] A. R. Bontempo and J. Rapp, "Protein and lipid deposition onto hydrophilic contact lenses in vivo," *Contact Lens Assoc Ophthalmol*, vol. 27, no. 2, pp. 75-80, 2001.
- [266] L. Jones, K. Evans, R. Sariri, V. Franklin and B. Tighe, "Lipid and protein deposition of N-vinyl pyrrolidone-containing group II and group IV frequent replacement contact lenses," *CLAO J*, vol. 23, pp. 122-126, 1997.
- [267] L. Jones, M. Senchyna, M.-A. Glasier, J. Schickler, I. Forbes, D. Louie and C. May, "Lysozyme and lipid deposition on silicone hydrogel contact lens materials," *Eye & Contact Lens*, vol. 29, no. 18, pp. 75-79, 2003.
- [268] B. Tighe, "Silicone hydrogel materials: how do they work?," in *Silicone Hydrogels: The Rebirth of Continuous Wear Contact Lenses*, D. Sweeney, Ed., Oxford, UK, Butterworth-Heinemann, 2000, pp. 1-21.
- [269] S. L. Willis, J. L. Court, R. P. Redman, J.-H. Wang, S. W. Leppard, V. J. O'Byrne, S. A. Small, A. L. Lewis, S. A. Jones and P. W. Stratford, "A novel phosphocholine-coated contact lens for extended wear use," *Biomaterials*, vol. 22, no. 24, pp. 3261-3272, 2001.

- [270] G. M. Bruinsma, H. C. van der Mei and H. J. Busscher, "Bacterial adhesion to surface hydrophilic and hydrophobic contact lenses," *Biomaterials*, vol. 22, no. 24, pp. 3217-3224, 2001.
- [271] C. Maldonado-Codina and P. B. Morgan, "In vitro water wettability of silicone hydrogel contact lenses determined using the sessile drop and captive bubble techniques," *J Biomed Mat Res A*, vol. 83A, no. 2, pp. 496-502, 2007.
- [272] Z. Zhao, N. A. Carnt, Y. Aliwarga, X. Wei, T. Naduvilath, Q. Garrett, J. Korth and M. D. P. Willcox, "Care regimen and lens material influence on silicone hydrogel contact lens deposition," *Optom Vis Sci*, vol. 86, no. 3, pp. 251-259, 2009.
- [273] B. J. Tighe, "A decade of silicone hydrogel development: Surface properties, mechanical properties, and ocular compatibility," *Eye & Contact Lens*, vol. 39, pp. 4-12, 2013.
- [274] E. Papas, "The daily disposable takeover," *Contact Lens Update*, 9 January 2013.
- [275] L. Jones and C. Woods, "Compromises' End? The introduction of a silicone hydrogel daily disposable lens," *Silicone Hydrogels*, June 2008.
- [276] E. B. Papas, N. Carnt, M. D. P. Willcox and B. A. Holden, "Complications associated with care product use during silicone daily wear of hydrogel contact lens," *Eye Contact Lens*, vol. 33, no. 6 pt 2, pp. 392-393, 2007.
- [277] Johnson & Johnson Vision Care, "Medical Device Alert: Contact Lenses, 1-Day Acuvue TruEye (narafilecon A)," 01 December 2010. [Online]. Available: <http://www.mhra.gov.uk/home/groups/dts-bs/documents/medicaldevicealert/con102765.pdf>.
- [278] Vistakon, "Vistakon 1 Day Acuvue TruEye narafilecon A soft contact lens," MAUDE Adverse Event Report, 2010.
- [279] K. Peters and T. J. Millar, "The role of different phospholipids on tear break-up time using a model eye," *Curr Eye Res*, vol. 25, no. 1, pp. 55-60, 2002.
- [280] W. G. Pitt, D. R. Jack, Y. Zhao, J. L. Nelson and J. D. Pruitt, "Loading and release of a phospholipid from contact lenses," *Optom Vis Sci*, vol. 88, no. 4, pp. 502-506, 2011.
- [281] J. P. Craig, C. Purslow, P. J. Murphy and J. S. W. Wolffsohn, "Effect of a liposomal spray on the pre-ocular tear film," *Contact Lens and Anterior Eye*, vol. 33, no. 2, pp. 83-87, 2010.
- [282] H. Pult, F. Gill and B. H. Riede-Pult, "Effect of three different liposomal eye sprays on ocular comfort and tear film," *Contact Lens and Anterior Eye*, vol. 35, no. 5, pp. 203-207, 2012.
- [283] D. Dausch, S. Lee, S. Dausch, J. C. Kim, G. Schwert and W. Michelson, "Comparative study of treatment of the dry eye syndrome due to disturbances of the tear film lipid layer with lipid-containing tear substitutes," *Klin Monatsbl Augenheilkd*, vol. 223, pp. 974-983, 2006.
- [284] G. W. Ousler, C. Michaelson and M. T. Christensen, "An evaluation of tear film breakup time extension and ocular protection index scores among three marketed lubricant eye drops," *Cornea*, vol. 26, pp. 949-952, 2007.
- [285] R. Solomon, H. D. Perry, E. D. Donnenfeld and H. E. Greenman, "Slitlamp biomicroscopy of the tear film of patients using topical Restasis and Refresh Endura," *J Cataract Refract Surg*, vol. 31, pp. 661-663, 2005.
- [286] S. Lee, S. Dausch, G. Maierhofer and D. Dausch, "A new therapy concept for the treatment of dry eye - the usefulness of phospholipid liposomes," *Klin Monatsbl Augenheilkd*, vol. 221, pp. 825-836, 2004.

- [287] D. R. Korb, R. C. Scaffidi, J. V. Greiner, K. R. Kenyon, J. P. Herman, C. A. Blackie, T. Glonek, C. L. Case, V. M. Finnemore and T. Douglass, "The effect of two novel lubricant eye drops on tear film lipid layer thickness in subjects with dry eye symptoms," *Optom Vis Sci*, vol. 82, pp. 594-601, 2005.
- [288] M. A. Di Pascuale, E. Goto and S. C. Tseng, "Sequential changes of lipid tear film after the instillation of a single drop of a new emulsion eye drop in dry eye patients," *Ophthalmology*, vol. 111, pp. 783-791, 2004.
- [289] S. Dinslage, W. Stoffel, M. Diestelhorst and G. K. Kriegelstein, "Tolerability and safety of two new preservative-free tear film substitutes," *Cornea*, vol. 21, pp. 352-355, 2002.
- [290] K. Jarvinen, T. Jarvinen and A. Urtti, "Ocular adsorption following topical delivery," *Adv Drug Delivery Rev*, vol. 16, pp. 3-19, 1995.
- [291] J. C. Lang, "Ocular drug-delivery conventional ocular formulations," *Adv Drug Deliv*, vol. 16, pp. 39-43, 1995.
- [292] D. Gulsen, C.-C. Li and A. Chauhan, "Dispersion of DMPC liposomes in contact lenses in ophthalmic drug delivery," *Curr Eye Res*, vol. 30, pp. 1071-1080, 2005.
- [293] C. L. Bourlais, L. Acar, H. Zia, P. A. Sado, T. Needham and R. Leverge, "Ophthalmic drug delivery systems," *Prog Retin Eye Res*, vol. 17, no. 1, pp. 33-58, 1998.
- [294] J. L. Creech, A. Chauhan and C. J. Radke, "Dispersive mixing in the posterior tear film under a soft contact lens," *IEC Res*, vol. 40, pp. 3015-3026, 2001.
- [295] J. Burke, "Solubility Parameters: Theory and Application," Book and Paper Group, 1984. [Online]. Available: <http://cool.conversion-us.org/coolaic.sg.bpg/annual/v03/bp03-04.html>. [Accessed 17 July 2013].
- [296] J. H. Hildebrand, *The Solubility of Non-Electrolytes*, New York, USA: Reinhold, 1936.
- [297] A. F. M. Barton, *Handbook of Solubility Parameters and Other Cohesion Parameters*, Boca Raton, USA: CRC Press Inc, 1983.
- [298] C. M. Hansen, "The universality of the solubility parameter concept," *I&EC Prod Res Dev*, vol. 8, no. 1, pp. 2-11, 1969.
- [299] R. L. Feller, N. Stolow and E. H. Jones, *On Picture Varnishes and Their Solvents*, Cleveland, USA: The Press of Case Western Reserve University, 1971.
- [300] W. G. Pitt, D. R. Jack, Y. Zhao, J. L. Nelson and J. D. Pruitt, "Transport of phospholipid in silicone hydrogel contact lenses," *J Biomaterial Sci*, vol. 23, pp. 527-541, 2012.
- [301] F. Miano, M. Calcara, T. J. Millar and V. Enea, "Insertion of tear proteins into a Meibomian lipids film," *Coll Surf B: Biointerfaces*, vol. 44, pp. 49-55, 2005.
- [302] W. D. Mathers, "Ocular evaporation in meibomian gland dysfunction and dry eye," *Ophthalmol*, vol. 100, pp. 347-451, 1993.
- [303] G. A. Georgiev, E. Kutsarova, A. Jordanova, R. Krastev and Z. Lalchev, "Interactions of Meibomian gland secretion with polar lipids in Langmuir monolayers," *Coll Surf B: Biointerfaces*, vol. 78, pp. 317-327, 2010.
- [304] J. C. Arciniega, E. J. Nadji and I. A. Butovich, "Effects of free fatty acids on meibomian lipid films," *Exp Eye Res*, vol. 93, no. 4, pp. 452-459, 2011.
- [305] J. C. Arciniega, E. Uchiyama and I. A. Butovich, "Disruption and destabilisation of Meibomian lipid films caused by increasing amounts of ceramides and cholesterol," *Invest Ophthalmol Vis Sci*, vol. 54, no. 2, pp. 1352-1360, 2013.
- [306] Y. Oshima, H. Sato, A. Zaghloul, G. N. Foulks, M. C. Yappert and D. Borchman, "Characterization of human meibum lipid using Raman spectroscopy," *Curr Eye Res*, vol. 34, pp. 824-835, 2009.

- [307] C. Joffre, M. Souchier, S. Gregoire, S. Viau, L. Bretillon, N. Acar, A. J. Bron and C. Creuzot-Garcher, "Differences in meibomian fatty acid composition in patients with meibomian gland dysfunction and aqueous-deficient dry eye," *Br J Ophthalmol*, vol. 92, pp. 116-119, 2008.
- [308] W. D. Mathers, J. A. Lane and M. B. Zimmerman, "Tear film changes associated with normal aging," *Cornea*, vol. 15, no. 3, pp. 229-234, 1996.
- [309] S. Patel and J. C. Farrell, "Age-related changes in precorneal tear film stability," *Optom Vis Sci*, vol. 66, no. 3, pp. 175-178, 1989.
- [310] J. P. Craig and A. Tomlinson, "Age and gender effects on the normal tear film," *Adv Exp Med Biol*, vol. 438, pp. 411-415, 1998.
- [311] C. Maissa and M. Guillon, "Tear film dynamics and lipid layer characteristics - Effect of age and gender," *Contact Lens & Anterior Eye*, vol. 33, no. 4, pp. 176-182, 2010.
- [312] C. F. Brooks, G. G. Fuller, C. W. Frank and C. R. Robertson, "An interfacial stress rheometer to study rheological transitions in monolayers at the air-water interface," *Langmuir*, vol. 15, pp. 2450-2459, 1999.
- [313] S. Reynaert, C. F. Brooks, P. Moldenaers, J. Vermant and G. G. Fuller, "Analysis of the magnetic rod interfacial stress rheometer," *J Rheol*, vol. 52, pp. 261-285, 2008.
- [314] S. R. Tonge and B. J. Tighe, "Lipid-containing Compositions and Uses Thereof". UK Patent WO99/09955, 22 August 1997.
- [315] M. S. Macsai, "The role of omega-3 dietary supplementation in blepharitis and Meibomian gland dysfunction (an AOS thesis)," *Trans Am Ophthalmol Soc*, vol. 106, pp. 336-356, 2008.
- [316] K. H. Kokke, J. A. Morris and J. G. Lawrenson, "Oral omega-6 essential fatty acid treatment in contact lens associated dry eye," *Contact Lens & Anterior Eye*, vol. 31, no. 3, pp. 141-146, 2008.
- [317] D. Hwang, "Fatty acids and immune responses - A new perspective in searching for clues to mechanism," *Ann Rev Nutr*, vol. 20, pp. 431-456, 2000.
- [318] R. J. Ambrosia, S. K. Stelzner Jr, C. F. Boerner, P. R. Honan and D. J. McIntyre, "Nutrition and dry eye: the role of lipids," *Rev Refract Surg*, vol. 1, pp. 29-32, 2002.
- [319] S. Viau, M.-A. Maire, B. Pasquis, S. Gregoire, N. Acar, A. M. Bron, L. Bretillon, C. P. Creuzot-Garcher and C. Joffre, "Efficacy of a 2-month dietary supplementation with polyunsaturated fatty acids in dry eye induced by scopolamine in a rat model," *Graefes Arch Clin Exp Ophthalmol*, vol. 247, pp. 1039-1050, 2009.
- [320] X. Xin, G. Xu, Z. Zhang, Y. Chen and F. Wang, "Aggregation behaviour of star-like PEO-PPO-PEO block copolymer in aqueous solution," *European Poly J*, vol. 43, pp. 3106-3111, 2007.
- [321] P. Alexandridis and T. A. Hatton, "Poly(ethylene oxide) - poly(propylene oxide) - poly(ethylene oxide) block copolymer surfactants in aqueous solutions and at interfaces: thermodynamics, structure, dynamics, and modeling," *Coll Surf A: Physicochem End Asp*, vol. 96, no. 1-2, pp. 1-46, 1995.
- [322] P. Alexandridis, V. Athanassiou, S. Fukuda and T. A. Hatton, "Surface activity of poly(ethylene oxide)-block-poly(propylene oxide)-block-poly(ethylene oxide) copolymers," *Langmuir*, vol. 10, no. 8, pp. 2604-2612, 1994.
- [323] S. Stolnik, N. C. Felumb, C. R. Heald, M. C. Garnett, L. Illum and S. S. Davis, "Adsorption behaviour and conformation of selected poly(ethylene oxide) copolymers on the surface of a model colloidal drug carrier," *Coll Surf A: Physicochemical and Engineering Aspects*, vol. 122, pp. 151-159, 1997.

- [324] R. Nagajaran, "Solubilisation of hydrocarbons and resulting aggregate shape transitions in aqueous solutions of Pluronic (PEO-PPO-PEO) bloc copolymers," *Coll Surf B: Biointerfaces*, vol. 16, pp. 55-72, 1999.
- [325] J. James, C. Ramalechume and A. B. Mandala, "Two-dimensional surface properties of PEO-PPO-PEO triblock copolymer film at the air-water interface in the absence and presence of Tyr-Phe dipeptide, Val-Tyr-Val tripeptide, SDS and stearic acid," *Coll Surf B: Biointerfaces*, vol. 82, no. 2, pp. 345-353, 2011.
- [326] J. Eastoe and J. S. Dalton, "Dynamic surface tension and adsorption mechanisms of surfactants at the air-water interface," *Adv Coll Int Sci*, vol. 85, pp. 103-144, 2000.
- [327] M. G. Munoz, F. Monroy, F. Ortega, R. G. Rubio and D. Langevin, "Monolayers of symmetric triblock copolymers at the air-water interface 1: Equilibrium properties," *Langmuir*, vol. 16, no. 3, pp. 1083-1093, 2000.
- [328] M. G. Munoz, F. Monroy, F. Ortega, R. G. Rubio and D. Langevin, "Monolayers of symmetric triblock copolymers at the air-water interface. 2. Adsorption kinetics," *Langmuir*, vol. 16, no. 3, pp. 1094-1101, 2000.
- [329] C. R. E. Mansur, S. P. Barboza, G. Gonzalez and E. F. Lucas, "Pluronic x Tetronic polyols: study of their properties and performance in the destabilisation of emulsions formed in the petroleum industry," *J Coll Int Sci*, vol. 271, pp. 232-240, 2004.
- [330] L. Caseli, T. M. Nobro, D. A. K. Silva, W. Loh and M. E. D. Zaniquelli, "Flexibility of the triblock copolymers modulating their penetration and expulsion mechanism in Langmuir monolayers of dihexadecyl phosphoric acid," *Coll Surf B: Biointerfaces*, vol. 22, pp. 309-321, 2001.
- [331] M. J. Newman, M. Balusubramanian and C. W. Todd, "Development of adjuvant-active nonionic block copolymers," *Adv Drug Delivery Rev*, vol. 32, pp. 199-223, 1998.

Appendices

Appendix 1 - Lipid Concentration and Surface Concentration

		Concentration (mol/dm ³)			
		0.5 x 10 ⁻³	1.0 x 10 ⁻³	1.5 x 10 ⁻³	2.0 x 10 ⁻³
Volume (μl)	5	(a) 2.50 x 10 ⁻⁹	(a) 5.00 x 10 ⁻⁹	(a) 7.50 x 10 ⁻⁹	(a) 1.00 x 10 ⁻⁸
		(b) 1.51 x 10 ¹⁵	(b) 3.01 x 10 ¹⁵	(b) 4.52 x 10 ¹⁵	(b) 6.02 x 10 ¹⁵
	10	(a) 5.00 x 10 ⁻⁹	(a) 1.00 x 10 ⁻⁸	(a) 1.50 x 10 ⁻⁸	(a) 2.00 x 10 ⁻⁸
		(b) 3.01 x 10 ¹⁵	(b) 6.02 x 10 ¹⁵	(b) 9.03 x 10 ¹⁵	(b) 1.20 x 10 ¹⁶
	15	(a) 7.50 x 10 ⁻⁹	(a) 1.50 x 10 ⁻⁸	(a) 2.25 x 10 ⁻⁸	(a) 3.00 x 10 ⁻⁸
		(b) 4.52 x 10 ¹⁵	(b) 9.03 x 10 ¹⁵	(b) 1.35 x 10 ¹⁶	(b) 1.81 x 10 ¹⁶
	20	(a) 1.00 x 10 ⁻⁸	(a) 2.00 x 10 ⁻⁸	(a) 3.00 x 10 ⁻⁸	(a) 4.00 x 10 ⁻⁸
		(b) 6.02 x 10 ¹⁵	(b) 1.20 x 10 ¹⁶	(b) 1.81 x 10 ¹⁶	(b) 2.41 x 10 ¹⁶
	25	(a) 1.25 x 10 ⁻⁸	(a) 2.50 x 10 ⁻⁸	(a) 3.75 x 10 ⁻⁸	(a) 5.00 x 10 ⁻⁸
		(b) 7.53 x 10 ¹⁵	(b) 1.50 x 10 ¹⁶	(b) 2.26 x 10 ¹⁶	(b) 3.01 x 10 ¹⁶

Fig A1.1. Number of moles of lipid molecules in aliquot volume (mol): (a) Number of molecules in aliquot volume (b) x 6.022 x 10²³

		Concentration (mol/dm ³)			
		0.5 x 10 ⁻³	1.0 x 10 ⁻³	1.5 x 10 ⁻³	2.0 x 10 ⁻³
Volume (μl)	5	(a) 2.77 x 10 ⁻¹¹	(a) 5.55 x 10 ⁻¹¹	(a) 8.33 x 10 ⁻¹¹	(a) 1.11 x 10 ⁻¹⁰
		(b) 1.25 x 10 ⁻¹⁰	(b) 2.50 x 10 ⁻¹⁰	(b) 3.75 x 10 ⁻¹⁰	(b) 5.00 x 10 ⁻¹⁰
	10	(a) 5.55 x 10 ⁻¹¹	(a) 1.11 x 10 ⁻¹⁰	(a) 1.66 x 10 ⁻¹⁰	(a) 2.22 x 10 ⁻¹⁰
		(b) 2.50 x 10 ⁻¹⁰	(b) 5.00 x 10 ⁻¹⁰	(b) 7.50 x 10 ⁻¹⁰	(b) 1.00 x 10 ⁻⁹
	15	(a) 8.33 x 10 ⁻¹¹	(a) 1.66 x 10 ⁻¹⁰	(a) 2.50 x 10 ⁻¹⁰	(a) 3.33 x 10 ⁻¹⁰
		(b) 3.75 x 10 ⁻¹⁰	(b) 7.50 x 10 ⁻¹⁰	(b) 1.125 x 10 ⁻⁹	(b) 1.50 x 10 ⁻⁹
	20	(a) 1.11 x 10 ⁻¹⁰	(a) 2.22 x 10 ⁻¹⁰	(a) 3.33 x 10 ⁻¹⁰	(a) 4.44 x 10 ⁻¹⁰
		(b) 5.00 x 10 ⁻¹⁰	(b) 1.00 x 10 ⁻⁹	(b) 1.50 x 10 ⁻⁹	(b) 2.00 x 10 ⁻⁹
	25	(a) 1.38 x 10 ⁻¹⁰	(a) 2.77 x 10 ⁻¹⁰	(a) 4.17 x 10 ⁻¹⁰	(a) 5.55 x 10 ⁻¹⁰
		(b) 6.25 x 10 ⁻¹⁰	(b) 1.25 x 10 ⁻⁹	(b) 1.875 x 10 ⁻⁹	(b) 2.50 x 10 ⁻⁹

Fig A1.2. Surface concentration per unit area (mol/cm²) at: (a) maximum area (90cm²); (b) at minimum area (20cm²).

Appendix 2 - Additional Condition Test Data

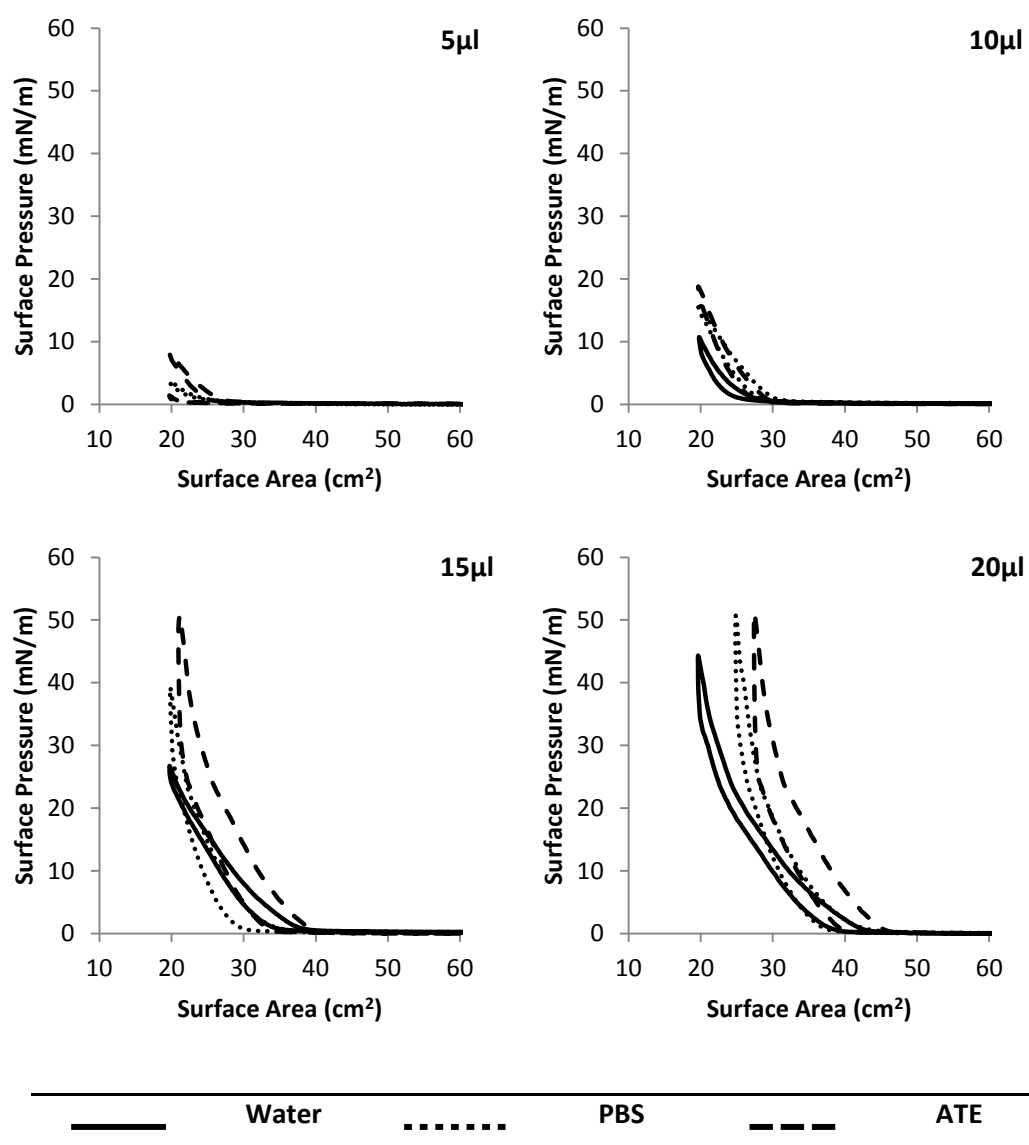


Fig A2.1. Additional π -A isotherms of SA monolayer on three types of subphase

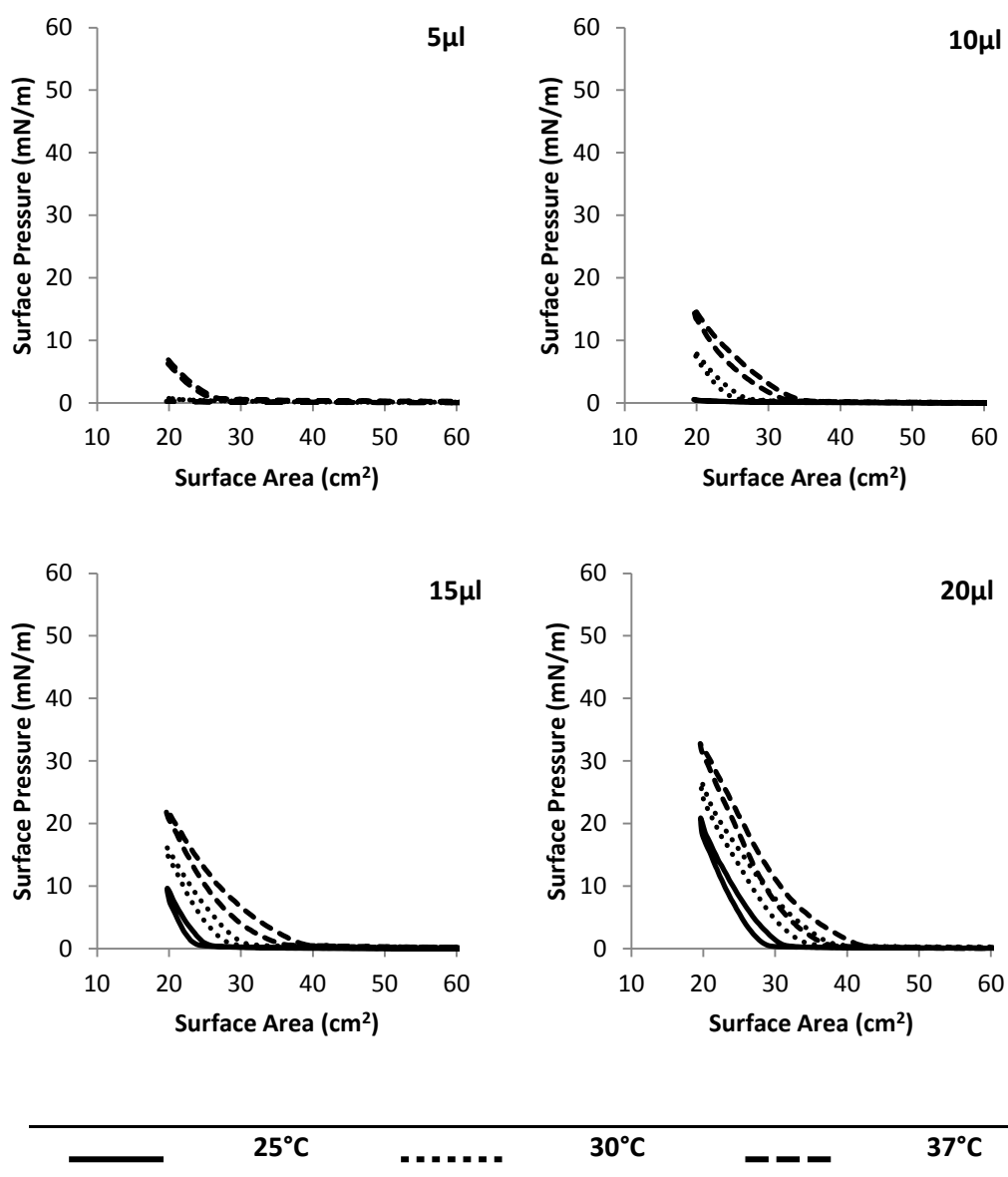


Fig A2.2. Additional π -A isotherms of SA monolayer on three types of subphase

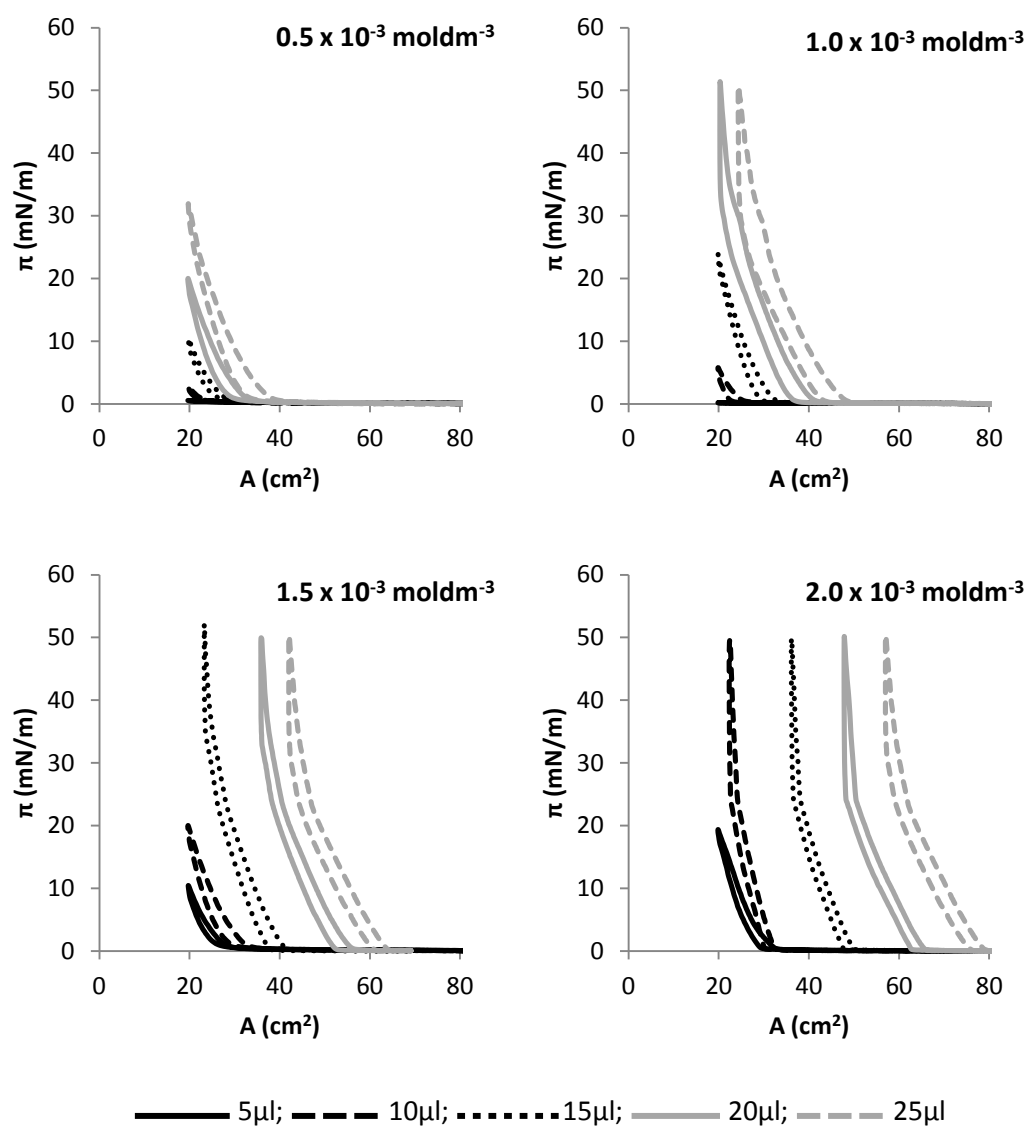


Fig A2.3. Additional π -A isotherms of increasing concentrations of SA at different aliquot volumes:

Appendix 3 - Contact Lens Information

Lens Type (USAN)	balafilcon A	lotrafilcon A
Brand Name	PureVision	Focus Night & Day
Manufacturer	Bausch & Lomb	CIBA Vision
FDA Group	I	III
Water Content (%)	36	24
Dk (barrers)	91	140
Modulus (MPa)	1.06	1.50
Principle Monomers	NVP, TPVC, NVA, PBVC	DMA, TRIS, fluorine-containing siloxane macromer
Surface treatment	Plasma oxidation	25nm Plasma coating

Table A3.1. Information for extended wear SiHy contact lenses.

Lens Type (USAN)	Filcon II 3	narafilcon A	narafilcon B	delefilcon A
Brand Name	Clariti 1day	1-Day Acuvue TruEye (UK)	1-Day Acuvue TruEye (USA)	Dailies Total-1
Manufacturer	Sauflon	Johnson & Johnson	Johnson & Johnson	CIBA Vision
FDA Group	-	I	I	II
Water Content (%)	56	46	48	33 (Core) 80 (Surface)
Dk (barrers)	60	101	55	140
Modulus (MPa)	0.50	0.66	0.66	0.70
Principle Monomers	Alkyl methacrylates, silicon acrylates, siloxane monomers, NVP	Hydroxy-functionalised mPDMS, DMA, HEMA, TEGDMA, PVP	Hydroxy-functionalised mPDMS, DMA, HEMA, TEGDMA, PVP	silicone macromers, phosphatidylcho line
Surface treatment	None (inherently wettable)	None (internal wetting agent, PVP)	None (internal wetting agent, PVP)	None (CoHy surface)

Table A3.2. Information for daily disposable SiHy contact lenses.

PVP: poly(vinyl pyrrolidone); mPDMS: monofunctional methacryloxypropyl terminated polydimethylsiloxane; DMA: N,N-dimethylacrylamide; HEMA: hydroxyethyl methacrylate; EGDMA: ethyleneglycol dimethacrylate; TEGDMA: tetraethyleneglycol dimethacrylate; TRIS: methacryloxypropyl tris(trimethyl siloxy)silane; NVP: N-vinyl pyrrolidone; TPVC: tris-(trimethyl siloxysilyl) propylvinyl carbamate; NVA: N-vinyl amino acid; PBVC: poly(dimethylsiloxo) di (silylbutanol) bis (vinyl carbamate); MMA: methyl methacrylate

Appendix 4 - Extended Wear Extraction Data

		Control	CW			DW	
			Px02	Px11	Px16	Px05	Px13 Px25
100	(a)	0.01	(a) 0.01	(a) 0.01	(a) 0.02	(a) 0.04	(a) 0.00 (a) 0.02
	(b)	0.21	(b) 0.13	(b) 0.04	(b) 0.14	(b) 0.28	(b) 0.11 (b) 0.17
200	(a)	0.08	(a) 0.04	(a) 0.01	(a) 0.00	(a) 0.02	(a) 0.00 (a) 0.05
	(b)	0.26	(b) 0.22	(b) 0.22	(b) 0.11	(b) 5.00	(b) 0.19 (b) 1.92
300	(a)	0.06	(a) 0.01	(a) 0.00	(a) 0.03	(a) 0.04	(a) 0.00 (a) 0.03
	(b)	1.09	(b) 0.36	(b) 0.31	(b) 0.50	(b) 19.99	(b) 0.40 (b) 9.37
400	(a)	0.01	(a) 0.01	(a) 0.01	(a) 0.02	(a) 0.02	(a) 0.02 (a) 0.03
	(b)	4.16	(b) 2.89	(b) 2.88	(b) 5.02	(b) 24.47	(b) 13.88 (b) 18.39
500	(a)	0.01	(a) 0.00	(a) 0.02	(a) 0.02	(a) 0.00	(a) 0.06 (a) 0.02
	(b)	7.65	(b) 6.52	(b) 6.12	(b) 10.34	(b) 27.56	(b) 18.57 (b) 23.48
600	(a)	0.01	(a) 0.00	(a) 0.02	(a) 0.06	(a) 0.10	(a) 0.00 (a) 0.02
	(b)	11.25	(b) 11.20	(b) 12.28	(b) 17.55	(b) 29.57	(b) 21.84 (b) 27.13
700	(a)	0.02	(a) 0.01	(a) 0.01	(a) 0.05	(a) 0.01	(a) 0.01 (a) 0.02
	(b)	14.38	(b) 16.32	(b) 18.82	(b) 22.45	(b) 31.51	(b) 27.87 (b) 30.25
800	(a)	0.01	(a) 0.02	(a) 0.03	(a) 0.08	(a) 0.01	(a) 0.02 (a) 0.01
	(b)	17.87	(b) 18.78	(b) 26.90	(b) 27.42	(b) 32.85	(b) 30.81 (b) 30.93
900	(a)	0.05	(a) 0.00	(a) 0.02	(a) 0.01	(a) 0.07	(a) 0.00 (a) 0.05
	(b)	20.12	(b) 22.44	(b) 29.09	(b) 27.83	(b) 33.28	(b) 31.55 (b) 31.19
1000	(a)	0.04	(a) 0.03	(a) 0.03	(a) 0.01	(a) 0.09	(a) 0.02 (a) 0.02
	(b)	20.92	(b) 26.37	(b) 29.44	(b) 28.60	(b) 33.54	(b) 32.04 (b) 31.54

Table A4.1. (a) π_{init} and (b) π_{max} values (mN/m) for the control and subject samples extracted from FN+D contact lenses extracted with $\text{CHCl}_3:\text{CH}_3\text{OH}$ (1:1 w/w).

		Control	CW			DW	
			Px16	Px38	Px71	Px13 Px25	Px62
100	(a)	0.03	(a) 0.01	(a) 0.00	(a) 0.00	(a) 0.00	(a) 0.01 (a) 0.01
	(b)	0.14	(b) 0.06	(b) 0.13	(b) 0.10	(b) 0.10	(b) 0.21 (b) 0.07
200	(a)	0.00	(a) 0.00	(a) 0.00	(a) 0.00	(a) 0.00	(a) 0.00 (a) 0.02
	(b)	0.11	(b) 0.16	(b) 0.09	(b) 0.10	(b) 0.09	(b) 0.44 (b) 0.17
300	(a)	0.00	(a) 0.00	(a) 0.01	(a) 0.02	(a) 0.01	(a) 0.00 (a) 0.00
	(b)	0.08	(b) 0.13	(b) 0.10	(b) 0.11	(b) 0.18	(b) 1.67 (b) 0.14
400	(a)	0.01	(a) 0.01	(a) 0.00	(a) 0.01	(a) 0.06	(a) 0.03 (a) 0.00
	(b)	0.10	(b) 0.11	(b) 0.09	(b) 0.07	(b) 0.20	(b) 3.48 (b) 0.20
500	(a)	0.01	(a) 0.03	(a) 0.00	(a) 0.00	(a) 0.02	(a) 0.05 (a) 0.00
	(b)	0.10	(b) 0.10	(b) 0.08	(b) 0.09	(b) 0.21	(b) 6.51 (b) 2.13
600	(a)	0.02	(a) 0.01	(a) 0.01	(a) 0.01	(a) 0.03	(a) 0.11 (a) 0.04
	(b)	0.15	(b) 0.10	(b) 0.19	(b) 0.14	(b) 1.47	(b) 9.30 (b) 4.37
700	(a)	0.00	(a) 0.04	(a) 0.01	(a) 0.01	(a) 0.00	(a) 0.01 (a) 0.01
	(b)	0.13	(b) 0.11	(b) 0.20	(b) 0.14	(b) 4.82	(b) 11.14 (b) 6.72
800	(a)	0.00	(a) 0.07	(a) 0.00	(a) 0.04	(a) 0.00	(a) 0.00 (a) 0.01
	(b)	0.17	(b) 0.15	(b) 0.46	(b) 0.16	(b) 9.30	(b) 13.07 (b) 9.19
900	(a)	0.01	(a) 0.00	(a) 0.01	(a) 0.02	(a) 0.01	(a) 0.07 (a) 0.00
	(b)	0.24	(b) 0.95	(b) 1.93	(b) 2.24	(b) 12.91	(b) 16.03 (b) 11.49
1000	(a)	0.02	(a) 0.14	(a) 0.02	(a) 0.00	(a) 0.00	(a) 0.04 (a) 0.01
	(b)	0.18	(b) 3.97	(b) 3.83	(b) 6.88	(b) 16.14	(b) 18.73 (b) 13.44

Table A4.2. (a) π_{init} and (b) π_{max} values (mN/m) for the control and subject samples extracted from FN+D contact lenses extracted with C_6H_{14} .

		Control	CW			DW	
			Px11	Px12	Px26	Px05	Px22 Px25
100	(a)	0.00	(a) 0.00	(a) 0.01	(a) 0.00	(a) 0.00	(a) 0.10 (a) 0.01
	(b)	0.04	(b) 1.48	(b) 0.08	(b) 0.09	(b) 6.50	(b) 5.82 (b) 0.30
200	(a)	0.04	(a) 0.00	(a) 0.01	(a) 0.01	(a) 0.00	(a) 0.00 (a) 0.01
	(b)	0.07	(b) 5.03	(b) 0.10	(b) 0.08	(b) 26.06	(b) 16.38 (b) 5.36
300	(a)	0.00	(a) 0.02	(a) 0.03	(a) 0.03	(a) 0.02	(a) 0.02 (a) 0.04
	(b)	0.09	(b) 8.55	(b) 1.63	(b) 0.11	(b) 29.50	(b) 26.71 (b) 14.25
400	(a)	0.00	(a) 0.00	(a) 0.00	(a) 0.00	(a) 0.00	(a) 0.03 (a) 0.04
	(b)	0.13	(b) 11.57	(b) 6.00	(b) 1.05	(b) 30.48	(b) 29.34 (b) 19.64
500	(a)	0.02	(a) 0.00	(a) 0.00	(a) 0.02	(a) 0.04	(a) 0.04 (a) 0.02
	(b)	0.44	(b) 14.18	(b) 9.59	(b) 4.45	(b) 30.45	(b) 29.53 (b) 26.80
600	(a)	0.04	(a) 0.05	(a) 0.01	(a) 0.01	(a) 2.65	(a) 2.71 (a) 0.17
	(b)	3.23	(b) 16.38	(b) 12.22	(b) 8.36	(b) 30.50	(b) 31.09 (b) 31.38
700	(a)	0.02	(a) 0.01	(a) 0.03	(a) 0.01	(a) 5.50	(a) 5.77 (a) 1.95
	(b)	7.97	(b) 18.53	(b) 14.67	(b) 11.53	(b) 30.54	(b) 31.96 (b) 31.84
800	(a)	0.05	(a) 0.03	(a) 0.00	(a) 0.01	(a) 7.97	(a) 8.53 (a) 4.40
	(b)	13.13	(b) 20.47	(b) 18.10	(b) 14.50	(b) 30.71	(b) 32.76 (b) 31.53
900	(a)	0.02	(a) 0.00	(a) 0.00	(a) 0.07	(a) 10.40	(a) 11.33 (a) 6.12
	(b)	19.89	(b) 22.11	(b) 21.36	(b) 22.30	(b) 30.86	(b) 33.64 (b) 31.99
1000	(a)	0.00	(a) 0.05	(a) 0.01	(a) 0.04	(a) 12.47	(a) 13.71 (a) 6.89
	(b)	21.72	(b) 23.49	(b) 23.35	(b) 25.34	(b) 31.23	(b) 34.35 (b) 32.23

Table A4.3. (a) π_{init} and (b) π_{max} values (mN/m) for the control and subject samples extracted from FN+D contact lenses extracted with C₆H₁₄:CH₃OH (9:1 w/w).

		Control	CW			DW	
			Px29	Px41	Px56	Px17	Px53 Px61
100	(a)	0.00	(a) 0.01	(a) 0.00	(a) 0.00	(a) 0.00	(a) 0.00 (a) 0.00
	(b)	0.16	(b) 3.19	(b) 0.19	(b) 1.21	(b) 3.64	(b) 3.90 (b) 8.38
200	(a)	0.03	(a) 0.00	(a) 0.00	(a) 0.02	(a) 0.04	(a) 0.04 (a) 0.02
	(b)	2.88	(b) 18.29	(b) 7.53	(b) 14.14	(b) 20.12	(b) 20.68 (b) 25.10
300	(a)	0.04	(a) 0.00	(a) 0.03	(a) 0.00	(a) 0.00	(a) 0.00 (a) 0.00
	(b)	9.04	(b) 24.89	(b) 15.33	(b) 23.89	(b) 26.55	(b) 28.69 (b) 29.62
400	(a)	0.06	(a) 0.05	(a) 0.00	(a) 0.00	(a) 0.00	(a) 0.10 (a) 0.00
	(b)	15.52	(b) 28.24	(b) 22.54	(b) 26.67	(b) 30.68	(b) 33.45 (b) 32.77
500	(a)	0.00	(a) 0.77	(a) 0.00	(a) 0.09	(a) 0.00	(a) 1.74 (a) 0.58
	(b)	20.75	(b) 29.35	(b) 25.21	(b) 28.55	(b) 33.82	(b) 34.91 (b) 34.28
600	(a)	0.04	(a) 2.34	(a) 0.02	(a) 0.63	(a) 1.96	(a) 4.61 (a) 2.89
	(b)	22.95	(b) 31.54	(b) 27.03	(b) 30.14	(b) 35.06	(b) 35.53 (b) 35.92
700	(a)	0.06	(a) 3.83	(a) 0.00	(a) 4.15	(a) 4.44	(a) 6.32 (a) 5.64
	(b)	23.08	(b) 32.28	(b) 28.99	(b) 31.64	(b) 36.44	(b) 35.56 (b) 36.49
800	(a)	2.28	(a) 5.29	(a) 0.02	(a) 7.44	(a) 5.59	(a) 6.50 (a) 7.86
	(b)	23.56	(b) 32.42	(b) 29.98	(b) 32.20	(b) 36.75	(b) 36.21 (b) 36.77
900	(a)	4.29	(a) 7.46	(a) 1.43	(a) 9.21	(a) 6.63	(a) 7.15 (a) 9.86
	(b)	23.46	(b) 32.60	(b) 30.37	(b) 32.41	(b) 36.90	(b) 36.13 (b) 37.05
1000	(a)	5.49	(a) 9.16	(a) 3.63	(a) 11.02	(a) 7.50	(a) 8.43 (a) 11.39
	(b)	23.65	(b) 32.68	(b) 30.88	(b) 32.50	(b) 37.22	(b) 36.67 (b) 37.23

Table A4.4. (a) π_{init} and (b) π_{max} values (mN/m) for the control and subject samples extracted from PV contact lenses extracted with CHCl₃:CH₃OH (1:1 w/w).

		Control	CW			DW	
			Px30	Px31	Px56	Px24	Px51 Px53
100	(a)	0.01	0.01	0.01	0.01	0.00	0.01 0.07
	(b)	0.17	0.15	0.09	0.16	0.09	0.17 0.14
200	(a)	0.00	0.00	0.00	0.00	0.06	0.07 0.07
	(b)	3.84	2.81	0.14	2.88	0.80	0.18 5.17
300	(a)	0.04	0.04	0.04	0.04	0.00	0.03 0.02
	(b)	6.31	11.34	0.35	9.04	9.28	0.19 9.69
400	(a)	0.05	0.05	0.05	0.05	0.00	0.01 0.02
	(b)	8.36	17.07	2.99	15.52	12.41	2.03 14.21
500	(a)	0.03	0.03	0.03	0.03	0.02	0.07 0.03
	(b)	9.86	21.54	8.03	20.75	16.54	9.79 18.62
600	(a)	0.00	0.00	0.00	0.00	0.01	0.01 0.03
	(b)	11.16	23.36	12.14	22.96	22.22	13.35 21.23
700	(a)	0.02	0.47	0.02	0.02	0.00	0.03 0.02
	(b)	12.96	25.05	16.85	24.04	22.78	18.45 22.88
800	(a)	0.04	3.35	0.04	2.42	1.07	0.03 0.02
	(b)	14.37	26.07	21.06	25.04	23.68	21.75 23.95
900	(a)	0.01	6.92	0.01	4.73	4.28	0.02 0.69
	(b)	15.98	26.77	23.36	25.96	24.31	24.11 24.71
1000	(a)	0.02	9.45	0.02	6.26	7.34	0.03 2.22
	(b)	17.43	27.42	25.18	26.95	24.76	25.50 25.29

Table A4.5. (a) π_{init} and (b) π_{max} values (mN/m) for the control and subject samples extracted from PV contact lenses extracted with C_6H_{14} .

		Control	CW			DW	
			Px41	Px46	Px49	Px24	Px50 Px61
100	(a)	0.06	0.00	0.01	0.05	0.00	0.00 0.00
	(b)	0.21	3.86	9.38	0.47	3.87	10.84 1.19
200	(a)	0.05	0.00	0.04	0.01	0.00	0.00 0.01
	(b)	5.41	20.32	19.80	12.93	22.81	24.54 11.72
300	(a)	0.00	0.04	3.34	0.00	0.04	5.41 0.02
	(b)	14.51	27.28	26.23	21.85	26.81	28.99 19.31
400	(a)	0.04	6.78	8.11	0.10	6.89	10.01 3.93
	(b)	19.84	29.69	28.71	24.31	31.60	30.87 25.87
500	(a)	0.00	11.06	12.57	3.60	11.34	15.32 9.52
	(b)	22.74	31.70	31.87	26.38	34.14	32.32 9.79
600	(a)	0.02	16.00	15.49	9.23	16.55	19.61 12.89
	(b)	23.82	32.92	31.99	27.82	34.90	33.65 31.85
700	(a)	1.23	20.36	18.12	11.68	21.09	22.44 17.19
	(b)	24.71	33.67	33.30	29.30	35.92	34.53 32.91
800	(a)	3.21	22.36	20.37	14.15	23.30	24.08 20.76
	(b)	24.88	34.30	33.84	30.75	36.21	35.03 34.74
900	(a)	5.87	23.50	22.04	18.27	24.55	25.51 22.35
	(b)	25.16	34.85	34.13	32.26	36.65	35.66 34.92
1000	(a)	8.04	23.14	23.29	21.45	24.49	26.56 23.25
	(b)	25.56	34.97	34.25	32.86	37.03	36.01 35.24

Table A4.6. (a) π_{init} and (b) π_{max} values (mN/m) for the control and subject samples extracted from PV contact lenses extracted with $\text{C}_6\text{H}_{14}:\text{CH}_3\text{OH}$ (9:1 w/w).

Appendix 5 - Daily Disposable Extraction Data

	Control	Px1	Px19	Px23	Px24	Px28	Px40
100	(a) 0.01 (b) 0.33	(a) 0.08 (b) 15.57	(a) 0.09 (b) 0.28	(a) 0.01 (b) 0.79	(a) 0.02 (b) 1.44	(a) 0.08 (b) 0.19	(a) 0.03 (b) 0.75
200	(a) 0.01 (b) 4.14	(a) 0.07 (b) 20.46	(a) 0.05 (b) 13.47	(a) 0.10 (b) 14.38	(a) 0.07 (b) 16.76	(a) 0.03 (b) 15.15	(a) 0.04 (b) 14.48
300	(a) 0.02 (b) 7.78	(a) 0.11 (b) 23.90	(a) 0.02 (b) 20.07	(a) 0.04 (b) 21.58	(a) 0.06 (b) 26.39	(a) 0.05 (b) 18.18	(a) 0.08 (b) 20.76
400	(a) 0.02 (b) 10.95	(a) 4.03 (b) 26.36	(a) 0.04 (b) 25.78	(a) 1.11 (b) 26.71	(a) 2.94 (b) 31.77	(a) 0.05 (b) 20.37	(a) 0.27 (b) 24.62
500	(a) 0.03 (b) 12.95	(a) 10.43 (b) 28.63	(a) 2.96 (b) 28.90	(a) 6.40 (b) 30.72	(a) 7.51 (b) 35.18	(a) 4.54 (b) 22.31	(a) 4.00 (b) 28.32
600	(a) 0.03 (b) 14.64	(a) 13.40 (b) 30.13	(a) 6.47 (b) 31.06	(a) 10.56 (b) 32.86	(a) 11.40 (b) 35.52	(a) 11.07 (b) 23.99	(a) 8.05 (b) 31.85
700	(a) 0.04 (b) 16.49	(a) 15.06 (b) 31.56	(a) 10.04 (b) 32.60	(a) 13.05 (b) 32.76	(a) 14.03 (b) 34.08	(a) 14.60 (b) 25.71	(a) 11.14 (b) 33.58
800	(a) 0.04 (b) 17.52	(a) 15.78 (b) 32.78	(a) 13.18 (b) 34.22	(a) 14.96 (b) 33.06	(a) 16.37 (b) 34.78	(a) 15.71 (b) 27.04	(a) 14.61 (b) 33.52
900	(a) 0.00 (b) 18.81	(a) 16.80 (b) 33.87	(a) 15.10 (b) 35.59	(a) 16.35 (b) 33.38	(a) 18.16 (b) 36.01	(a) 16.39 (b) 28.08	(a) 15.71 (b) 34.19
1000	(a) 1.68 (b) 19.80	(a) 17.73 (b) 35.14	(a) 17.15 (b) 35.80	(a) 17.88 (b) 33.94	(a) 19.36 (b) 35.54	(a) 17.23 (b) 29.17	(a) 16.24 (b) 33.93

Table A5.1. (a) π_{init} and (b) π_{max} values (mN/m) for the control and subject samples extracted from Clariti 1day contact lenses extracted with $\text{CHCl}_3:\text{CH}_3\text{OH}$ (1:1 w/w).

	Blank	Px1	Px3	Px16	Px24	Px28	Px36
100	(a) 0.00 (b) 0.33	(a) 0.01 (b) 8.30	(a) 0.02 (b) 9.59	(a) 0.03 (b) 5.76	(a) 0.14 (b) 8.41	(a) 0.06 (b) 7.88	(a) 0.06 (b) 9.76
200	(a) 0.00 (b) 0.33	(a) 0.04 (b) 11.72	(a) 4.62 (b) 16.01	(a) 0.00 (b) 10.34	(a) 2.21 (b) 13.71	(a) 0.08 (b) 11.06	(a) 5.13 (b) 14.77
300	(a) 0.00 (b) 0.33	(a) 4.27 (b) 14.31	(a) 7.76 (b) 19.99	(a) 1.58 (b) 13.88	(a) 7.01 (b) 17.40	(a) 4.86 (b) 13.57	(a) 8.22 (b) 18.37
400	(a) 0.00 (b) 4.14	(a) 7.83 (b) 16.31	(a) 9.08 (b) 22.87	(a) 6.04 (b) 16.19	(a) 8.09 (b) 20.10	(a) 7.96 (b) 15.63	(a) 9.29 (b) 20.28
500	(a) 0.01 (b) 6.30	(a) 8.71 (b) 17.94	(a) 10.83 (b) 23.96	(a) 7.87 (b) 18.05	(a) 9.27 (b) 22.19	(a) 8.69 (b) 17.26	(a) 10.80 (b) 21.49
600	(a) 0.01 (b) 7.73	(a) 9.32 (b) 19.23	(a) 12.14 (b) 24.65	(a) 8.50 (b) 19.43	(a) 10.76 (b) 23.67	(a) 9.24 (b) 18.31	(a) 12.05 (b) 22.34
700	(a) 0.01 (b) 9.04	(a) 10.01 (b) 21.09	(a) 13.06 (b) 25.16	(a) 9.28 (b) 20.50	(a) 12.14 (b) 24.50	(a) 10.22 (b) 19.29	(a) 13.12 (b) 22.97
800	(a) 0.01 (b) 10.49	(a) 11.14 (b) 21.54	(a) 13.65 (b) 25.55	(a) 10.29 (b) 21.39	(a) 13.05 (b) 25.18	(a) 10.95 (b) 20.05	(a) 14.17 (b) 23.49
900	(a) 0.01 (b) 11.57	(a) 12.65 (b) 21.92	(a) 14.39 (b) 26.10	(a) 11.39 (b) 22.23	(a) 14.48 (b) 26.15	(a) 11.59 (b) 20.61	(a) 15.21 (b) 23.98
1000	(a) 0.01 (b) 12.15	(a) 13.33 (b) 22.21	(a) 14.90 (b) 26.44	(a) 12.35 (b) 22.80	(a) 15.47 (b) 27.14	(a) 12.23 (b) 21.07	(a) 16.11 (b) 24.46

Table A5.2. (a) π_{init} and (b) π_{max} values (mN/m) for the control and subject samples extracted from Clariti 1day contact lenses extracted with C_6H_{14} .

	Blank	Px3	Px16	Px19	Px23	Px36	Px40
100	(a) 0.01 (b) 2.89	(a) 1.06 (b) 13.55	(a) 0.04 (b) 10.69	(a) 1.59 (b) 15.08	(a) 0.04 (b) 8.37	(a) 0.09 (b) 12.33	(a) 0.12 (b) 10.23
200	(a) 0.01 (b) 6.02	(a) 4.62 (b) 19.92	(a) 3.77 (b) 21.86	(a) 4.26 (b) 20.83	(a) 3.20 (b) 16.24	(a) 5.25 (b) 23.04	(a) 5.02 (b) 18.03
300	(a) 0.02 (b) 8.92	(a) 7.62 (b) 25.21	(a) 7.82 (b) 28.91	(a) 5.87 (b) 26.87	(a) 7.55 (b) 23.46	(a) 8.13 (b) 28.17	(a) 7.76 (b) 22.45
400	(a) 0.03 (b) 12.31	(a) 10.02 (b) 28.33	(a) 11.68 (b) 34.45	(a) 9.30 (b) 31.21	(a) 9.66 (b) 26.89	(a) 11.83 (b) 32.98	(a) 9.62 (b) 25.22
500	(a) 0.01 (b) 14.46	(a) 12.72 (b) 31.10	(a) 15.44 (b) 34.95	(a) 13.18 (b) 35.28	(a) 12.36 (b) 29.41	(a) 14.97 (b) 33.92	(a) 11.91 (b) 27.33
600	(a) 0.01 (b) 16.34	(a) 15.04 (b) 33.39	(a) 18.62 (b) 32.71	(a) 15.76 (b) 35.37	(a) 15.09 (b) 32.37	(a) 17.45 (b) 33.10	(a) 14.20 (b) 30.92
700	(a) 0.72 (b) 18.76	(a) 17.34 (b) 35.97	(a) 19.89 (b) 33.06	(a) 20.33 (b) 36.73	(a) 17.04 (b) 34.04	(a) 19.82 (b) 33.05	(a) 16.23 (b) 33.60
800	(a) 1.98 (b) 20.40	(a) 19.04 (b) 37.31	(a) 20.75 (b) 33.11	(a) 21.35 (b) 38.56	(a) 18.79 (b) 35.30	(a) 20.68 (b) 33.20	(a) 17.86 (b) 33.76
900	(a) 4.66 (b) 22.61	(a) 20.73 (b) 38.84	(a) 21.72 (b) 33.42	(a) 23.07 (b) 39.69	(a) 21.06 (b) 37.11	(a) 21.50 (b) 33.52	(a) 19.85 (b) 33.96
1000	(a) 6.86 (b) 23.09	(a) 22.03 (b) 39.55	(a) 22.38 (b) 33.96	(a) 24.55 (b) 40.08	(a) 22.49 (b) 37.14	(a) 22.22 (b) 33.91	(a) 21.09 (b) 34.11

Table A5.3. (a) π_{init} and (b) π_{max} values (mN/m) for the control and subject samples extracted from Clariti 1day contact lenses extracted with C₆H₁₄:CH₃OH (9:1 w/w).

	Control	Px2	Px6	Px7	Px8	Px9	Px10
50	(a) 0.01 (b) 6.18	(a) 0.01 (b) 25.22	(a) 0.02 (b) 18.48	(a) 0.02 (b) 16.45	(a) 0.01 (b) 18.11	(a) 0.04 (b) 17.56	(a) 0.04 (b) 20.72
100	(a) 0.02 (b) 12.37	(a) 0.91 (b) 33.91	(a) 0.02 (b) 33.15	(a) 1.66 (b) 32.32	(a) 2.03 (b) 32.64	(a) 2.50 (b) 32.76	(a) 0.07 (b) 31.62
150	(a) 0.04 (b) 18.28	(a) 5.47 (b) 42.39	(a) 2.70 (b) 39.13	(a) 7.16 (b) 39.03	(a) 6.19 (b) 37.35	(a) 10.53 (b) 40.22	(a) 4.01 (b) 36.50
200	(a) 1.53 (b) 27.13	(a) 11.75 (b) 46.90	(a) 7.76 (b) 44.88	(a) 12.23 (b) 44.57	(a) 9.76 (b) 41.71	(a) 13.03 (b) 44.10	(a) 11.22 (b) 41.58
250	(a) 4.49 (b) 29.29	(a) 28.48 (b) 48.46	(a) 13.36 (b) 46.82	(a) 15.27 (b) 46.26	(a) 15.91 (b) 46.10	(a) 17.61 (b) 46.42	(a) 17.33 (b) 45.16
300	(a) 12.05 (b) 30.49	(a) 30.83 (b) 48.66	(a) 16.54 (b) 47.38	(a) 21.44 (b) 47.01	(a) 23.19 (b) 47.08	(a) 23.75 (b) 47.04	(a) 24.32 (b) 46.37
350	(a) 18.35 (b) 31.23	(a) 31.82 (b) 48.75	(a) 23.82 (b) 47.96	(a) 27.71 (b) 47.58	(a) 27.19 (b) 47.58	(a) 29.74 (b) 47.48	(a) 29.88 (b) 47.05
400	(a) 22.56 (b) 31.71	(a) 32.06 (b) 48.83	(a) 29.01 (b) 48.37	(a) 31.17 (b) 47.81	(a) 32.29 (b) 47.88	(a) 30.92 (b) 47.57	(a) 30.55 (b) 47.21
450	(a) 25.82 (b) 32.07	(a) 32.97 (b) 48.81	(a) 28.88 (b) 48.49	(a) 32.73 (b) 47.86	(a) 33.85 (b) 47.96	(a) 31.30 (b) 47.51	(a) 30.35 (b) 47.16
500	(a) 27.23 (b) 32.29	(a) 32.22 (b) 48.92	(a) 28.41 (b) 48.60	(a) 33.27 (b) 47.89	(a) 34.99 (b) 48.05	(a) 31.75 (b) 47.60	(a) 30.85 (b) 47.27

Table A5.4. (a) π_{init} and (b) π_{max} values (mN/m) for the control and subject samples extracted from TE contact lenses extracted with CHCl₃:CH₃OH (1:1 w/w).

	Control	Px6	Px7	Px18	Px30	Px38	Px39
50	(a) 0.01 (b) 1.07	(a) 0.04 (b) 8.13	(a) 0.02 (b) 18.64	(a) 0.02 (b) 14.80	(a) 0.02 (b) 17.92	(a) 0.04 (b) 28.45	(a) 0.53 (b) 22.19
100	(a) 0.02 (b) 11.97	(a) 0.01 (b) 26.43	(a) 2.20 (b) 28.63	(a) 0.01 (b) 28.42	(a) 2.23 (b) 27.33	(a) 4.07 (b) 30.74	(a) 0.53 (b) 29.29
150	(a) 0.51 (b) 24.02	(a) 1.86 (b) 28.57	(a) 8.51 (b) 29.90	(a) 0.63 (b) 30.38	(a) 7.38 (b) 28.77	(a) 11.66 (b) 31.85	(a) 3.66 (b) 30.63
200	(a) 0.71 (b) 24.54	(a) 6.13 (b) 29.60	(a) 14.35 (b) 30.88	(a) 3.46 (b) 31.70	(a) 11.82 (b) 29.65	(a) 18.62 (b) 32.65	(a) 9.05 (b) 31.41
250	(a) 4.85 (b) 24.11	(a) 11.13 (b) 30.30	(a) 21.73 (b) 31.47	(a) 7.34 (b) 32.76	(a) 16.79 (b) 30.18	(a) 24.13 (b) 33.25	(a) 14.29 (b) 32.00
300	(a) 9.09 (b) 24.37	(a) 16.02 (b) 30.84	(a) 25.87 (b) 31.80	(a) 11.32 (b) 33.53	(a) 21.46 (b) 30.54	(a) 26.76 (b) 33.58	(a) 20.00 (b) 32.45
350	(a) 13.23 (b) 24.57	(a) 21.32 (b) 31.22	(a) 26.71 (b) 32.14	(a) 14.61 (b) 34.37	(a) 24.15 (b) 30.76	(a) 26.83 (b) 33.73	(a) 23.11 (b) 33.12
400	(a) 16.89 (b) 24.79	(a) 24.09 (b) 31.52	(a) 27.75 (b) 32.39	(a) 19.23 (b) 34.84	(a) 25.16 (b) 31.05	(a) 28.07 (b) 33.97	(a) 24.19 (b) 32.77
450	(a) 17.87 (b) 24.91	(a) 24.54 (b) 31.79	(a) 28.17 (b) 32.46	(a) 22.30 (b) 34.92	(a) 26.32 (b) 31.26	(a) 28.61 (b) 34.10	(a) 24.22 (b) 32.85
500	(a) 18.22 (b) 24.90	(a) 26.17 (b) 31.76	(a) 28.15 (b) 32.56	(a) 24.11 (b) 35.25	(a) 27.02 (b) 31.41	(a) 29.00 (b) 34.40	(a) 26.41 (b) 33.18

Table A5.5. (a) π_{init} and (b) π_{max} values (mN/m) for the control and subject samples extracted from TE contact lenses extracted with C₆H₁₄.

	Control	Px8	Px18	Px21	Px25	Px38	Px39
50	(a) 0.01 (b) 1.42	(a) 0.01 (b) 9.15	(a) 3.98 (b) 34.29	(a) 1.86 (b) 18.95	(a) 0.01 (b) 19.76	(a) 3.40 (b) 28.49	(a) 0.00 (b) 28.66
100	(a) 0.02 (b) 7.30	(a) 3.51 (b) 31.47	(a) 7.09 (b) 42.95	(a) 4.70 (b) 40.70	(a) 2.74 (b) 28.03	(a) 6.55 (b) 45.75	(a) 6.05 (b) 45.41
150	(a) 0.03 (b) 15.02	(a) 6.64 (b) 42.33	(a) 13.22 (b) 45.99	(a) 8.04 (b) 43.17	(a) 7.71 (b) 37.66	(a) 11.89 (b) 46.46	(a) 11.46 (b) 45.54
200	(a) 3.14 (b) 24.79	(a) 16.72 (b) 43.32	(a) 18.49 (b) 45.83	(a) 13.94 (b) 43.77	(a) 18.77 (b) 44.14	(a) 20.06 (b) 46.52	(a) 18.77 (b) 47.02
250	(a) 10.24 (b) 31.16	(a) 26.45 (b) 42.97	(a) 23.14 (b) 46.08	(a) 20.19 (b) 44.00	(a) 27.14 (b) 44.26	(a) 26.44 (b) 46.62	(a) 25.19 (b) 46.74
300	(a) 20.68 (b) 31.93	(a) 28.77 (b) 43.11	(a) 25.97 (b) 46.00	(a) 26.12 (b) 44.17	(a) 29.42 (b) 44.31	(a) 28.50 (b) 46.56	(a) 27.53 (b) 46.84
350	(a) 24.83 (b) 33.09	(a) 29.62 (b) 42.85	(a) 27.42 (b) 46.26	(a) 28.09 (b) 44.59	(a) 30.22 (b) 44.38	(a) 29.85 (b) 46.40	(a) 28.77 (b) 46.96
400	(a) 25.95 (b) 33.67	(a) 30.15 (b) 42.88	(a) 28.14 (b) 46.48	(a) 29.46 (b) 44.88	(a) 30.70 (b) 44.65	(a) 30.37 (b) 46.16	(a) 29.72 (b) 46.99
450	(a) 26.51 (b) 34.26	(a) 30.60 (b) 42.81	(a) 29.94 (b) 46.67	(a) 30.27 (b) 45.01	(a) 31.09 (b) 44.59	(a) 30.97 (b) 46.00	(a) 30.29 (b) 46.82
500	(a) 27.10 (b) 34.45	(a) 30.86 (b) 42.91	(a) 30.42 (b) 46.61	(a) 31.12 (b) 45.18	(a) 31.36 (b) 44.68	(a) 31.16 (b) 45.98	(a) 30.57 (b) 46.80

Table A5.6. (a) π_{init} and (b) π_{max} values (mN/m) for the control and subject samples extracted from TE contact lenses extracted with C₆H₁₄:CH₃OH (9:1 w/w).